"A New Method for Determining Condensed and Uncondensed Structures in Lignin"

A thesis

submitted in partial fulfillment

of the requirements for the degree

of

Doctor of Philosophy in Chemistry

at the

University of Waikato

by

Ruben Smit

University of Waikato
2000

Abstract

This thesis describes a new analytical method to determine the levels of uncondensed (protonated C5) and condensed (bonded through C5 to other phenyl propane units) guaiacyl (G) units in lignin.

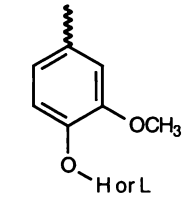

Uncondensed

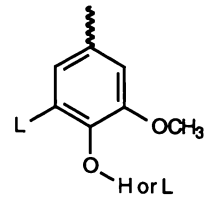

Condensed

This method is important because the proportion of condensed and uncondensed units in lignin determines, in part, how the lignin will behave during mechanical and chemical processing. Currently there are few analytical techniques that can simultaneously determine the proportions of condensed and uncondensed units in isolated lignins and even fewer that can elucidate this information for lignin *in situ* in wood.

The method combines two well-accepted techniques, thioacidolysis and quantitative ^{31}P NMR spectroscopy. Thioacidolysis involves depolymerisation of lignin with ethanethiol and boron trifluoride at elevated temperatures. This leads to an organic-solvent soluble product in which almost all the phenylpropane units are phenolic. Subsequent quantitative ^{31}P NMR spectroscopic analysis, of the thioacidolysis product derivatised with 2-chloro-4,4,5,5-teramethyl-1,3,2-dioxaphospholane gave the total amount of condensed and uncondensed units in the lignin.

The method proved highly successful at determining the amounts of uncondensed G, condensed G, syringyl (S) and *p*-hydroxyphenyl (H) units in milled wood lignin (MWL) and *in situ* lignins from softwoods, hardwoods, softwood compression woods and softwood pulp fibres. Also, for MWL samples the method proved useful for determining the amounts of uncondensed G, condensed G, S and H units present

as free phenolic and etherified moieties. A further benefit of performing the method was that it allowed the levels of individual condensed units, such as β-5, 5-5 and 4-O-5, in MWL and *in situ* lignin to be determined.

Initial investigations with model compounds found that quantitative ^{31}P NMR spectra were collected even when thioacidolysis was performed prior to ^{31}P NMR spectroscopy. This was significant, as prior to this work we had been concerned that thioethyl incorporation into sterically crowded 5-5 and β-5 structures may have hindered quantitative analysis.

Dibenzodioxocin structures have recently been reported as important units in lignin polymer crosslinking, therefore the thioacidolysis of a dibenzodioxocin model compound was studied. The dibenzodioxocin reacted primarily *via* an acid catalysed ring rearrangement to yield a dibenzooxepine. The incomplete cleavage of dibenzodioxocin ring during thioacidolysis suggested that the method might be under reporting the levels 5-5 units.

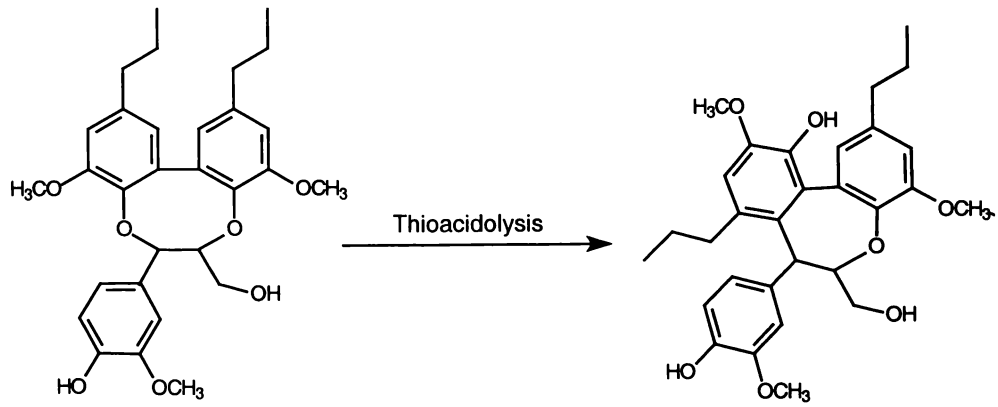

Dibenzodioxocin Dibenzooxepine

Thioacidolysis/^{31}P NMR spectroscopy was initially applied to MWL and *in situ* lignin from radiata pine wood. In both samples around 35% of the phenylpropane units were condensed. As MWL originates primarily from the secondary wall (SW), this finding suggests that the SW and middle lamella (ML) lignin in radiata pine are more similar than previously believed. Thioacidolysis/^{31}P NMR spectroscopy was also applied to lignin *in situ* in wood from slabwood, corewood, earlywood and latewood regions of a mature radiata pine. In all samples around 35% of the phenylpropane units in the total lignin were condensed. While the concentration of lignin in these

different regions of the tree has been shown to vary markedly, these results suggest that the proportion of condensed units remains the same.

Thioacidolysis/^{31}P NMR spectroscopy was next applied to MWL and *in situ* lignin samples from a hardwood and a softwood compression wood. For eucalypt MWL, 37% of the free phenolic groups were S units but 73% of the phenolic groups released by thioacidolysis were S units. On the other hand for compression wood around 90% of the H units were found to be present as free phenolic groups, with few H units released during thioacidolysis. These results can be seen as further confirmation of the preference of S units to be present as etherified moieties and H units as free phenolic moieties in lignin.

The method was next applied to lignins in *in situ* thermomechanical and chemithermomechanical pulp fibres. The lignin in both thermomechanical pulping (TMP) and medium density fibreboard (MDF) fibres contained around 35% condensed units. This indicated that mechanical refining at elevated temperatures did not significantly change the proportions of condensed units in the lignin. However, for thermomechanical refining in the presence of added sulphite, results showed that around 38% of the C9 units in lignin were condensed moieties. This increased proportion of condensed units relative to radiata slabwood, was due to a decrease in the amount of uncondensed units, rather than an increase in the amount of condensed units. This lower yield of uncondensed units was attributed to α-sulphonation of the lignin during the pulping process, which may block the degradation of lignin by thioacidolysis. This effect was highlighted in the heavily sulphonated Ontario Paper Co. (OPCO) pulp, where a very low overall yield was observed.

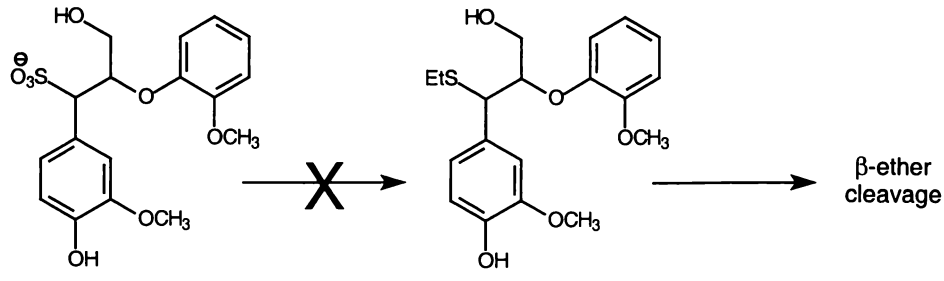

Finally thioacidolysis/^{31}P NMR spectroscopy was applied to a number of different kraft spent liquor lignins (KSLLs). KSLLs were found to contain up to 45% condensed G units. This increased proportion of condensed structures, relative to *in situ* pine lignin was consistent with numerous literature reports. However, thioacidolysis/^{31}P NMR spectroscopy was found to be less applicable to these heavily modified lignins, as they were much less comprehensively degraded on thioacidolysis than wood lignins.

Acknowledgements

First and foremost I wish to thank my two supervisors, Dr Rick Ede (formerly at Forest Research, now at FPP, CSIRO) and Dr Ian Suckling (Forest Research), for their guidance and support throughout this work. They were initially responsible for the creation of this topic and showed great enthusiasm when the going got tough. Thanks must also go to my University of Waikato supervisor Dr Michéle Prinsep for her assistance in liasing with the University and for helpful comments during the writing up.

I gratefully acknowledge the financial assistance provided by the University of Waikato in the form of a Ph.D. scholarship. Also I must acknowledge the financial support provided by Forest Research in the provision of lab space, equipment, and chemicals. Without these I would not have been able to undertake this research. Thanks must also go to DuPont Chemical Co. and Appita for the 1996 Bleaching Award, which allowed me to attend the 1997 International Symposium on Wood and Pulping Chemistry in Montreal.

I give special thanks to Roger Meder for all his help in running the NMR spectrometers at Forest Research. Secondly to Dr Ralph Thomson for his help in running the NMR spectrometer at the University of Waikato and for making all that weekend time available when the Forest Research spectrometer was out of action. Also Hank Kroese (Forest Research) for helping me run the mass spectrometer.

Thanks must go to Professor Göesta Brunow (University of Helsinki) for supplying the dibenzodioxocin model compound. Also to Jacinta Dalgety (University of Waikato) for supplying the KSLL samples from different phases of delignification.

On a personal level I would like to thank my family, Bert, Jeanet, John, *Claudia*, Oscar, Kellie and Jorinde. For all their support, encouragement and love during the past twenty-eight years.

I would also like to thank all my friends who have made my stay in Rotorua that much more enjoyable, in particular Dave, Garth, Eben, Jason, Kirk, Kelpy, Ed and Brett.

A special mention must be made of all the wonderful people at the Rotorua Aikido Club, with whom it was an absolute pleasure to train, grow and socialise. In particular I would like to thank Sensei Dianne, Sensei Paul, Sensei Barry and my friends and training partners Adam, Blair, Carl, Darren and Nick. Especially to Dene for persevering with my Nikyo's and Sankyo's during those Sunday morning kyu-grade training sessions.

And finally to Melissa, thank you for all your love, advice, support, friendship and understanding. Also thank you for proof reading this thesis. I promise to use shorter sentences in the future.

Table of Contents

List of Figures

List of Tables

List of Abbreviations

acac	acetylacetonate
AR	analytical reagent
Å	angstroms
b	broad
B_o	magnetic field strength
°C	degrees Celsius
ca	circa
CAD	cinnamyl alcohol dehydrogenase
cm	centimetre
CML	compound middle lamella
COSY	correlation spectroscopy
CTMP	chemithermomechanical pulping
d	doublet
δ	chemical shift
DEPT	distortionless enhancement by polarisation transfer
DFRC	derivatisation followed by reductive cleavage
DHP	dehydrogenation polymerisation
DWS	dilution water sulphonation
EAS	electrophilic aromatic substitution
EW	earlywood
g	grams
G	guaiacyl
GC	gas chromatography
H	*p*-hydroxyphenyl
HMBC	heteronuclear multiple bond correlation
HMQC	heteronuclear multiple quantum coherence
HOHAHA	homonuclear Hartman-Hahn
HPLC	high performance liquid chromatography
Hz	hertz
IGD	inverse gated decoupling
ISTD	internal standard
J	coupling constant
kPa	kilopascal
KSLL	kraft spent liquor lignin
LW	latewood

m	multiplet
m-	meta
MDF	medium density fibreboard
MHz	mega hertz
ML	middle lamella
mm	millimetre
µm	micrometre
mmol	millimole
µmol	micromole
MS	mass spectrometry
MW	molecular weight
MWL	milled wood lignin
N°	number
NOE	nuclear Overhauser effect
NMR	nuclear magnetic resonance
o-	ortho
OPCO	Ontario Paper Company
P	primary wall
p-	para
PEG	polyethylene glycol
plc	preparative layer chromatography
ppm	parts per million
q	quartet
s	singlet
S	syringyl
sec	seconds
SEM	scanning electron microscopy
spp.	species
SW	secondary wall
S1	outer layer of the secondary wall
S2	middle layer of the secondary wall
S3	inner layer of the secondary wall
S_N1	substitution, nucleophilic, unimolecular
t	triplet
T_1	spin lattice relaxation time
tlc	thin layer chromatography
TMP	thermomechanical pulping
TMS	trimethylsilyl
UV	ultraviolet
1°	primary
2°	secondary
2D	two dimensional
3D	three dimensional

If I have seen further,
it is by standing on the shoulders of giants.

Sir Isaac Newton

Chapter 1

Introduction

The purpose of the studies carried out in this thesis was to develop a new analytical technique for lignin analysis. This Chapter provides a review of wood, lignin and analytical literature relevant to the work performed in this thesis.

1.1 The Macroscopic Structure of Wood

Trees (Spermatophytae) are subdivided into two classes, namely gymnosperms (Gymnospermae) and angiosperms (Angiospermae) [1, 2, 3, 4]. Coniferous woods or softwoods belong to the first group, while deciduous woods or hardwoods belong to the second group [1, 2, 3, 4].

1.1.1 Macroscopic structure of softwoods

Radiata pine (*Pinus radiata*) is a softwood and has features typical of softwood trees such as being non-deciduous, having needles and forming seeds in cones [4, 5]. Like other gymnosperms, the anatomical structure of radiata pine is relatively simple. Figure 1.1 shows the macroscopic structure of a typical softwood.

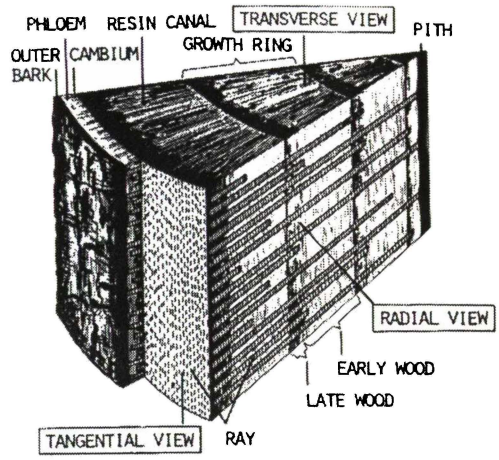

Figure 1.1: The macroscopic structure of softwood [1].

The pith, at the very centre of the tree, represents tissues formed during the tree's first growth year [1, 4]. The subsequent xylem, or wood, is organised in concentric growth rings (annual increments) of earlywood (springwood) and denser latewood (summerwood) [1, 5, 6]. Depending on the age of the tree, the growth rings can be divided into a darker inner region, the heartwood and a lighter outer region, the sapwood [1, 4]. Compared with sapwood, heartwood has been shown to be drier, to contain more extractives and is essentially the dead skeletal material left by the living tree, which does not transport water [7]. The cambial zone is a thin layer of living cells between the xylem and the inner bark, or phloem. It is in this cambial zone where the cell division and the radial growth of the tree takes place [1, 4]. Ray cells, which extend radially from the bark to the pith or to an annual ring, typically make up 5-10% of the wood volume in softwoods [1, 5, 6]. Resin canals are vertical or radial cavities within the tissue of most softwoods. They are involved in the storage and transport of extractives [1, 5, 6].

Typically, 90-95% of softwood material is comprised of tracheid cells, which are long (ca 2-4 mm), slender (ca 40 μm) and oriented in the longitudinal direction of the stem [1, 4, 5, 6, 8]. These tracheids have been shown to be hollow and have a square to rectangular cross section with tapered ends that overlap [1, 4, 6, 8]. Interconnection between the different tracheid cells occurs through pairs of bordered pits that allow fluid transport [4, 5, 8]. Figure 1.2 shows the major softwood cell types.

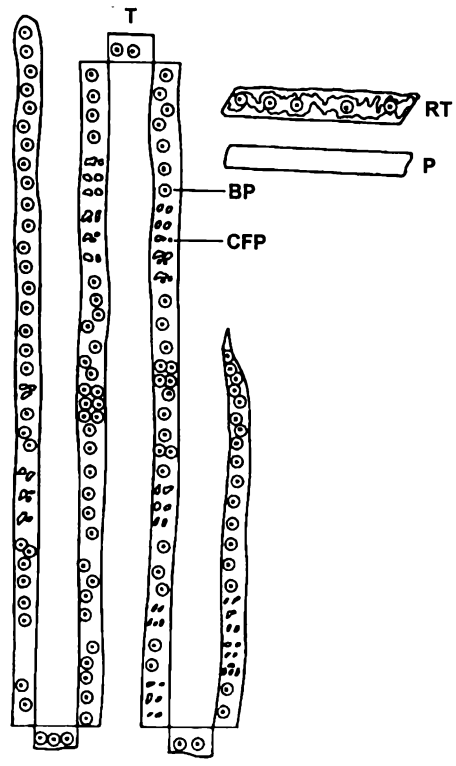

Figure 1.2: Softwood cell types [5].
T = tracheid, BP = bordered pits, CFP = pits to ray parenchyma (cross-field pits), RT = ray tracheids, P = parenchyma cells.

In solid wood, the axially oriented tracheids are arranged in radial rows. They show a gradual increase in cell wall thickness, from the first formed part of the annual growth layer (earlywood, springwood), to the last formed cells (latewood, summerwood). In addition to being thick-walled, these latewood cells are also radially compressed (Figure 1.3) [5, 6, 8]. The contrast between the latewood of one year and the earlywood of the succeeding year causes the annual rings in a log cross section. The thick-walled latewood tracheids provide strength, while the thin-walled earlywood tracheids, with the large lumen, predominantly conduct water and minerals within the tree [5, 6, 8].

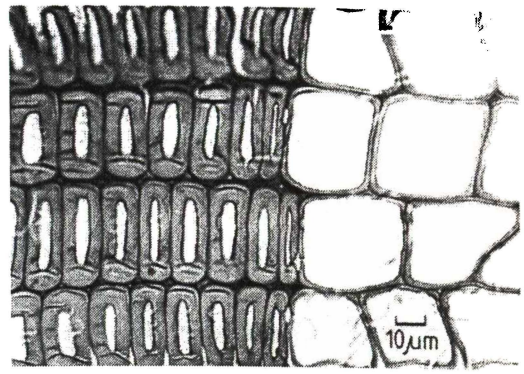

Figure 1.3: Cross section of the annual ring border in a softwood (*Picea abies*) [6].

1.1.2 Macroscopic structure of softwood compression woods

Trees react to strain forces acting on stems (e.g. high wind or geotropic erection) by producing reaction wood in regions of compression or tension [5, 6, 9, 10]. In softwoods, the formation of compression wood on the lower side of the branch or stem is promoted to enable their righting [5, 6, 9, 10]. Compression wood is heavier and denser than normal wood, with a lower modulus of elasticity [5, 10]. This allows compression wood to absorb considerable compressive force without tracheid damage. Compression wood tracheids are significantly shorter (ca 1.5-2.5 mm) than normal softwood ones (ca 2-4 mm) [11-14]. The tracheids in compression wood have a rounded outline, rather than a rectangular cross section, much thicker cell walls and a lumen that is much smaller than normal wood tracheids (Figure 1.4) [5, 11, 15].

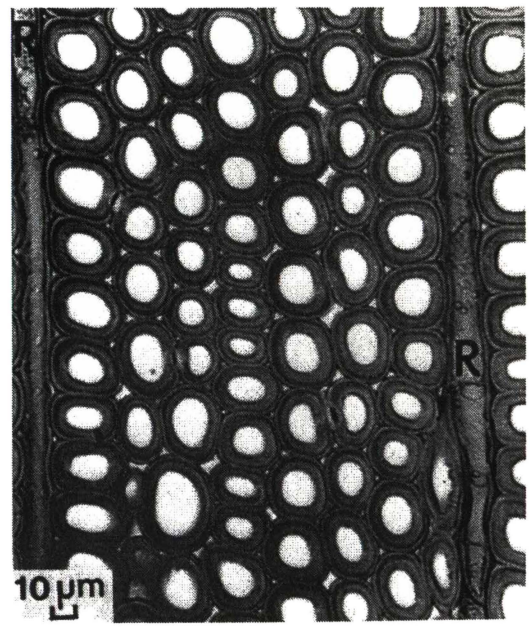

Figure 1.4: Compression wood of *Picea abies* in the middle of a growth ring with rounded tracheids and two ray cells (R) [11].

1.1.3 Macroscopic structure of hardwoods

Hardwoods contain mainly libriform cells as the supporting tissue, typically 65-70% of the stem volume [1, 4, 6, 8]. Compared with the softwood tracheids, these hardwood libriform fibres are shorter, about 0.8-1.6 mm in length and have a diameter of 14-40 μm [1, 4, 8]. Running through the strength-providing fibres are conducting vessels which are short (0.3-0.6 mm) and often contain large lumen. These vessels are stacked on top of each other to form long pipes ranging from a few centimetres up to some metres in length and are single elements, with open perforated ends [4]. Figure 1.5 compares hardwood vessel elements (A) with hardwood libriform cells (B) and a softwood tracheid (C) [1, 8].

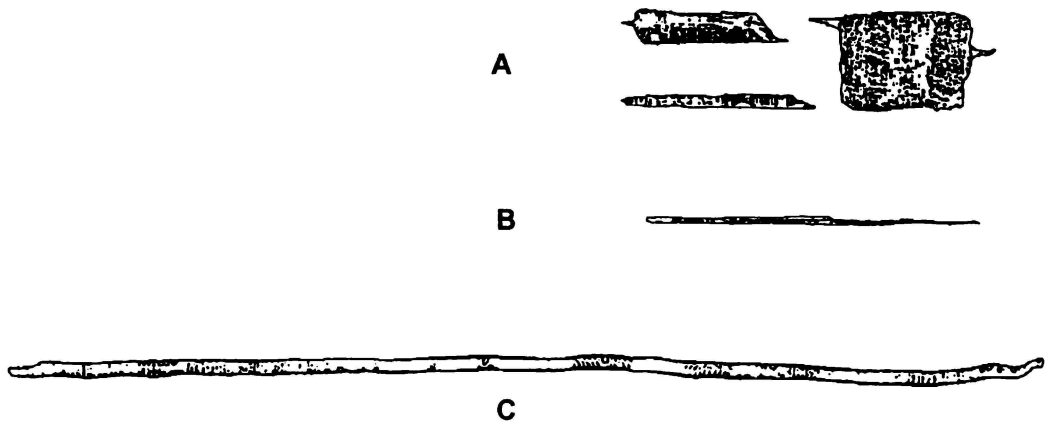

Figure 1.5: Comparing hardwood and softwood cells [1].

Several ways of packing these hardwood cells together in the xylem have been observed, the most common are diffuse-porous and ring-porous structures [4, 6]. Diffuse-porous woods (e.g. maples (*Acer* spp.), birches (*Betula* spp.) and poplars (*Populus* spp.) are characterised by a homogeneous distribution of vessels, both in terms of size and number, throughout the whole growth ring [4, 6]. Ring-porous woods (e.g. oaks (*Quercus* spp.), elms (*Ulmus* spp.) and ashes (*Fraxinus* spp.), contain spacious vessels in the earlywood and narrow vessels in the latewood [4, 6]. Figure 1.6 shows the structural differences between diffuse-porous and ring-porous hardwoods.

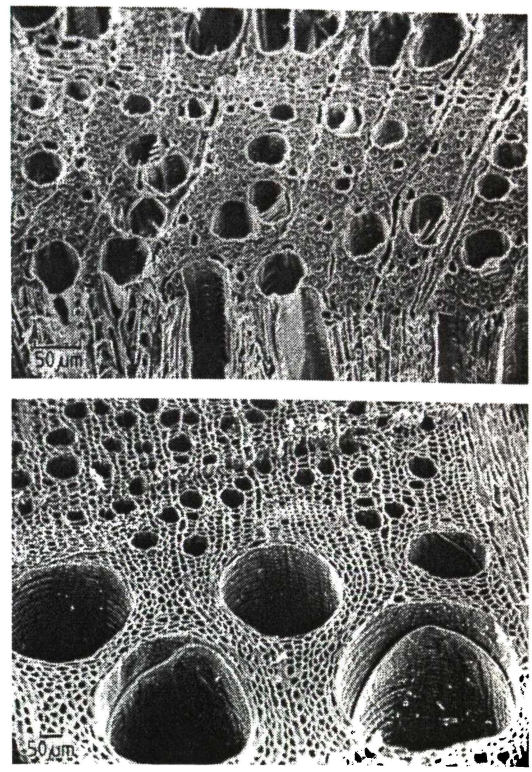

Figure 1.6: Transverse plane scanning electron microscopy (SEM) micrograph of (top) diffuse-porous hardwood (*Betula verrucosa*) and (bottom) ring-porous hardwood (*Quercus robur*) [6].

1.2 The Microscopic Structure of Wood

1.2.1 Microscopic structure of softwoods

The cell wall of each tracheid is composed of cellulose, hemicellulose and lignin (Section 1.3) [1, 4, 5, 6, 8, 16]. Cellulose exists in the form of minute strands called microfibrils and provides the tensile strength in wood, while lignin acts as an encrusting material in the cell wall, which binds the polysaccharide framework [1, 4, 5, 6, 8, 16].

The cell wall has been shown to consist of several layers (Figure 1.7), which differ from one another with respect to their structure, as well as their chemical composition [1, 4, 5, 6, 8, 16]. The middle lamella (ML) is located between cells and acts as a glue to bind the cells together. During the early stages of cell growth, the ML is essentially comprised of a pectic substance, but eventually becomes highly lignified [1]. The primary wall (P) is the first layer laid down during cell formation

and features crossed layers of cellulose microfibrils (Section 1.3.1). The next layer formed is the outer layer of the secondary wall (S1), where the cellulose microfibrils are laid down with a shallow angle relative to the horizontal [1, 4, 5, 6, 8, 16]. The thickest (2-10 μm) layer in the cell wall is the middle layer of the secondary wall (S2), which forms the main body of the fibre and has a steep microfibrilar angle, which is close to vertical [1, 4, 5, 6, 8, 16]. The inner layer of the secondary wall (S3), again, has a shallow microfibrilar angle relative to the horizontal. This pattern results in a layered cell wall, which exhibits great strength for its size [1, 4, 5, 6, 8, 16].

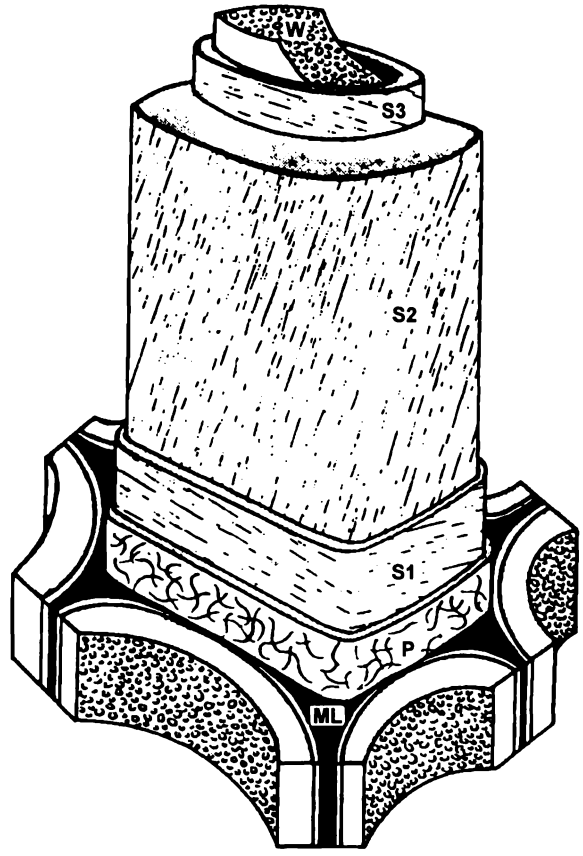

Figure 1.7: Model of tracheid cell wall structure [8].

1.2.2 Microscopic structure of softwood compression woods

Two main differences in the ultrastructure of softwood tracheids arise due to the formation of compression wood. Due to the presence of rounded tracheids, there is a high incidence of intercellular spaces (IS), not only between tracheids, but also between tracheids and ray cells (Figure 1.4) [6, 11, 15]. Also, the S2 layer of compression wood is not homogeneous like the S2 layer in normal softwood. Instead, compression wood tracheids feature a highly lignified outer portion and less

lignified helical ribs or ridges which protrude into the lumen (Figure 1.8) [5, 6, 11, 15, 17, 18]. The role of these helical cavities (small arrows) is thought to be to act like a long spring when under load [15].

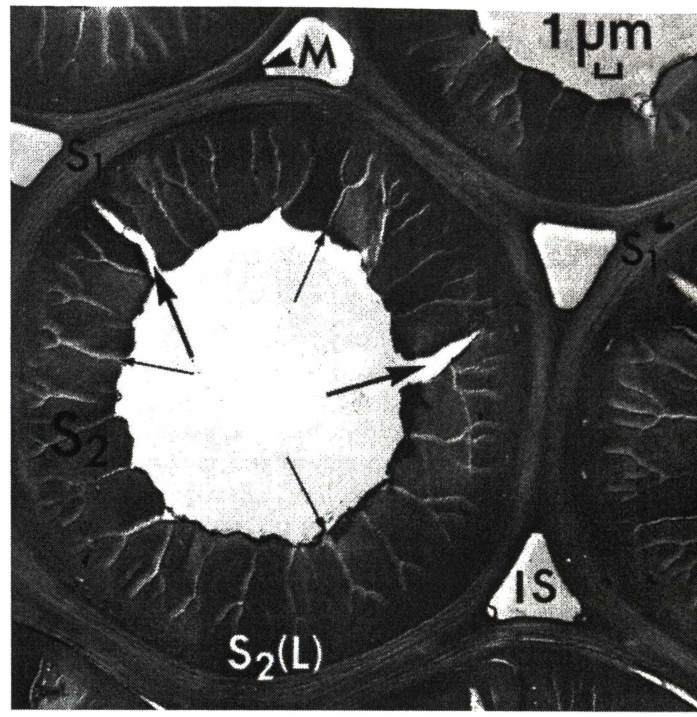

Figure 1.8: Transverse section of compression wood tracheids in tamarack (*Larix laricina*), showing intercellular spaces [11]. (large arrows indicate checks introduced during drying)

1.3 The Chemical Composition of Wood

Wood consists of four major chemical components; cellulose (Section 1.3.1), hemicellulose (Section 1.3.2), extractives (Section 1.3.3) and lignin (Section 1.3.4.) [1, 16, 19, 20]. Table 1.1 shows the approximate amounts of each component present in a typical softwood, softwood compression wood or hardwood sample. Characteristically, softwoods contain around 26-30% lignin and 40-44% cellulose [19, 20]. In pronounced compression wood, the most noticeable chemical feature is a high lignin content (35-40%) and a decrease in the cellulose content (around 30%) [9, 15]. Hardwood samples generally contain less lignin (around 20-22%) and more cellulose (around 45%) than softwoods [19].

Table 1.1: The average composition of softwood, compression wood and hardwood

Component	% Composition		
	Softwood [19]	Compression Wood [9]	Hardwood [19]
Cellulose	42 ± 2	30 ± 2	45 ± 2
Hemicelluloses	27 ± 2	29 ± 3	30 ± 5
Lignin	28 ± 3	37 ±2	20 ± 4
Extractives	3 ± 2	4 ± 2	5 ± 3

1.3.1 Cellulose

Cellulose is composed entirely of β-D-glucose monomers **1** , which are linked through a β-(1→4) glycosidic bond (Figure 1.9) [16, 20, 21, 22]. Typically, a single cellulose chain is composed of about 8000-12000 anhydroglucose monomers and is 4-6 μm in length [23, 24].

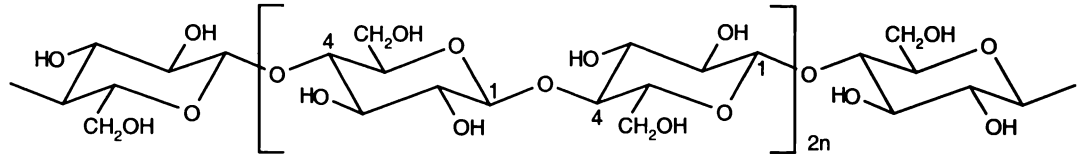

Figure 1.9: The structure of cellulose [21].

Intra and inter molecular hydrogen bonding plays an important part in the structure and physical behaviour of cellulose [16, 20, 21, 22]. This is due to each anhydroglucose monomer **1** containing three un-substituted OH groups [16, 20, 21, 22]. Hydrogen bonding causes cellulose molecules to aggregate in microfibrils, either in a highly ordered (crystalline) or less ordered (amorphous) manner.

Due to this fibrous structure and the strong hydrogen bonding, cellulose exhibits a high tensile strength and is insoluble in most solvents. However, glycosidic structures will undergo hydrolysis under acidic conditions [25, 26, 27]. These hydrolysis reactions lower the degree of polymerisation and affect the fibre strength [27, 28]. It is for this reason that alkaline conditions are generally favoured over acidic ones for the pulping of wood.

1.3.2 Hemicelluloses

Hemicelluloses are a group of heterogeneous polysaccharides, which typically contain 100-200 monomers [21, 29]. The principal constituent sugars in softwood hemicellulose are the pentose sugars, arabinose 2 and xylose 3, and the hexose sugars, glucose 1, mannose 4 and galactose 5 [21, 29]. The exact amount of hemicellulose, its structure and chemical composition, is species dependent.

In radiata pine, the main hemicellulose has been shown to be galactoglucomannan, which comprises around 15% of the dry wood weight [21, 20, 30]. Galactoglucomannan consists of a glucomannan backbone with a mannose to glucose ratio of approximately 3.7 to 1 [21, 29, 31]. Galactose and acetyl residues are attached to this backbone [21, 31]. Hence, it is more accurately called O-acetyl-galactoglucomannan. Radiata pine also contains xylan (arabino-4-O-methylglucuronoxylan) comprising around 7% of dry wood weight [20, 21, 30, 32]. Softwood xylan, is constructed from arabinose 2, xylose 3 and 4-O-mehylglucuronic acid 6 (in the ratio 1.0:5.8:1.1) [20, 21, 33, 34]. These softwood xylans consist of a β-D-xylopyranose 3 backbone, with arabinose 2 and 4-O-methylglucuronic acid 6 groups branching off. In Figure 1.10, part of a typical galactoglucomannan structure is shown, in both structural and written shorthand form.

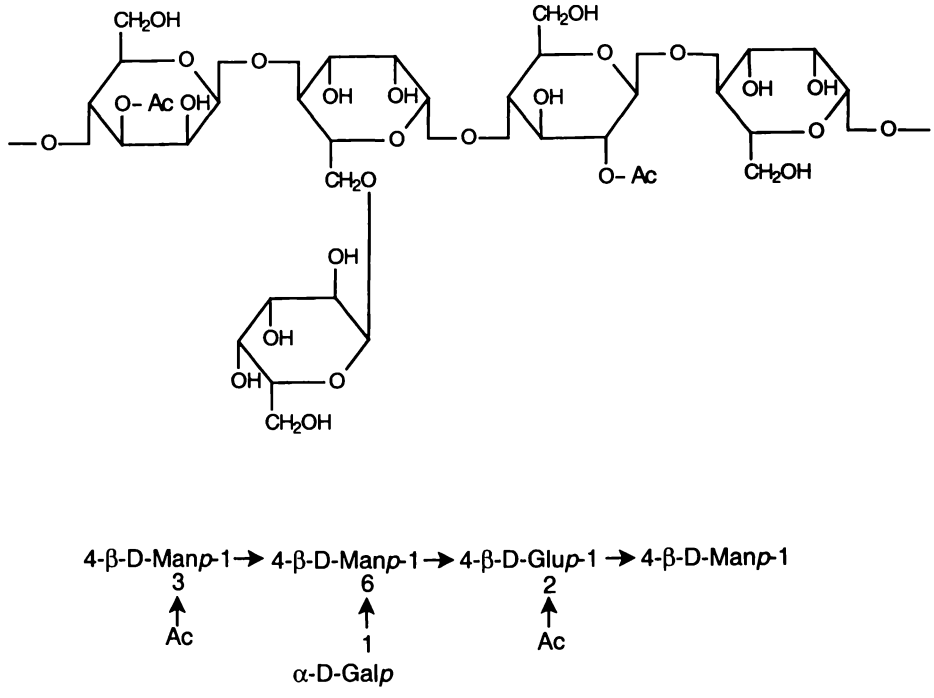

Figure 1.10: The structure of a softwood galactoglucomannan [21].

Although the hemicelluloses in various hardwood species differ from each other both quantitatively and qualitatively, the major component is glucuronoxylan (O-acetyl-4-O-methylglucurono-β-D-xylan) [21, 29, 35]. Depending on the hardwood species, the glucuronoxylan content may vary between 15-30% of the dry wood [21, 29]. The backbone of the glucuronoxylan consists of β-D-xylopyranose **3** units. Acetyl groups are found at C2 or C3 of most xylose units (about seven per ten xylose units). The 4-O-methylglucuronic acid **6** groups branch off this backbone [35]. Figure 1.11 contains the abbreviated formula of a hardwood glucuronoxylan.

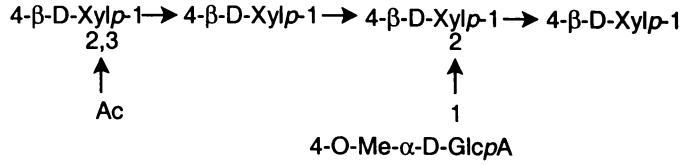

Figure 1.11: Shorthand formula of a hardwood glucuronoxylan [29].

Hardwoods may also contain 2-5% glucomannan, with the glucose:mannose ratio varying between 1:2 and 1:1 depending on wood species [21, 33, 36].

Like cellulose, hemicelluloses act as a support material in the cell walls. Compared with cellulose, however, the water solubility of hemicelluloses is much higher and they are much more easily hydrolysed, especially the bond between the galactose and the main hemicellulose chain.

1.3.3 Extractives

Extractives are low molecular weight compounds, which can be extracted from the wood by water or neutral organic solvents such as methanol, acetone or dichloromethane [37, 38]. The content and composition of extractives varies among wood species and with geographical location within species. Softwoods typically contain extractives of between 1 and 5% of their dry wood weight [37, 39, 40]. Hardwoods on the other hand typically contain a higher extractive content, up to 30% [38, 41, 42].

Within softwoods there are two main regions of extractive formation and/or storage. Firstly, epithelial cells, which surround the resin canals, secrete extractives mainly in the form of monoterpenes (**7**, **8**) or resin acids (**9**, **10**) [38, 39, 43]. These extractives act to protect the tree against biological damage. Alternatively, significant amounts

of extractives may also be found in the ray parenchyma cells [38, 43]. Extractives in these cells act as a supply of reserve food and are predominantly fatty acids (11, 12), triglycerides (13), sterols (14) and waxes. A number of different extractives are shown in Figure 1.12, reflecting the major types of softwood extractives.

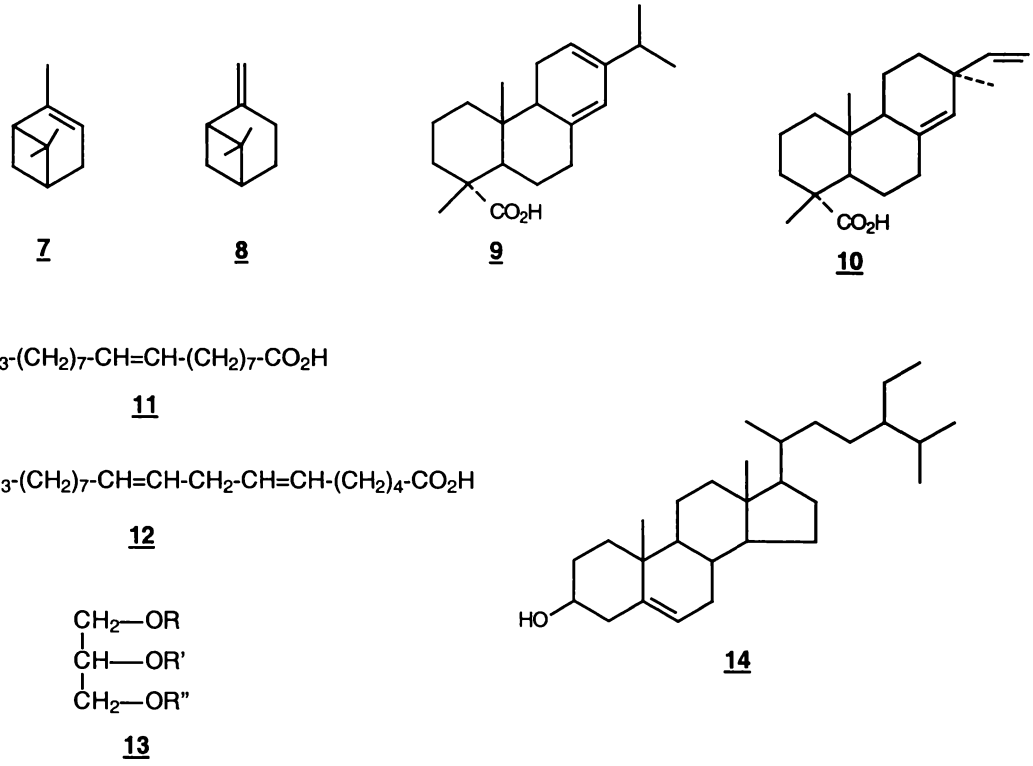

7 8 9 10

CH_3-$(CH_2)_7$-CH=CH-$(CH_2)_7$-CO_2H

11

CH_3-$(CH_2)_7$-CH=CH-CH_2-CH=CH-$(CH_2)_4$-CO_2H

12

CH_2—OR
CH—OR'
CH_2—OR"

13

14

Figure 1.12: Some softwood extractives. (7) α-pinene, (8) β-pinene, (9) levopimaric acid, (10) pimaric acid, (11) oleic acid, (12) linoleic acid, (13) fats (R,R' and R" may be fatty acid residue or hydrogen (mono-, di- or triglycerides)), (14) β-sitosterol.

The extractive content of different trees and its composition has been shown to vary considerably, depending on factors such as place of growth, age and species [38, 44, 45, 46]. Within the same tree, the distribution of extractives is also heterogeneous [38, 39, 47]. For pines, the amount of resin in the heartwood is considerably higher than in sapwood, rising from around 2-4% to 8-12% of dry wood weight [39, 47]. Table 1.2 summarises a typical extractive distribution in relation to radial position (age) in a radiata pine stem.

Table 1.2: Distribution of resin acids, fatty acid esters and neutral components in a tree [39].

Components	Extractives (% of oven-dry wood)		
	Inner heartwood	Outer heartwood	Sapwood
Resin acids	6.8	2.8	0.8
Fatty acid esters	0.8	0.8	0.5
Neutral components	0.4	0.3	0.3
Total	8.0	3.9	1.6

Synthesis of specific fungicides and phenolic compounds is thought to significantly increase during heartwood formation. For example, radiata pine contains pinosylvin 15, pinocembrin 16 and pinobanksin 17 in the heartwood (Figure 1.13) [38, 48, 49].

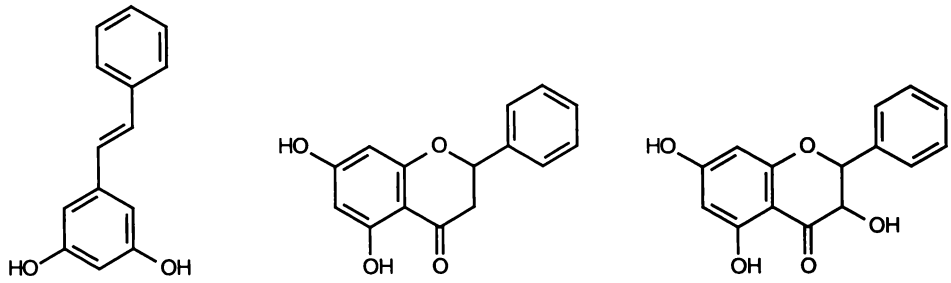

15 16 17

Figure 1.13: Stilbenes and polyphenols in radiata pine heartwood [20].

Hardwoods contain some monoterpenes, one example being camphor from *Cinnamonum camphora*. They also contain fatty acids and alcohols similar to those in softwoods, the fatty acids being present as triglycerides [44]. Typically few resin acids are present in hardwoods (<1% of acetone extract) [37, 38, 44]. However, hardwoods do frequently contain triterpenoid (C30) compounds, either as alcohols or acids. One example of such compounds is the steroid β-sitosterol 14, which is present in most hardwoods [37, 38, 44].

Hardwoods also contain a wide variety of phenolic (polar) materials and related constituents [37, 38, 41, 50]. This group of extractives includes hydrolysable tannins, flavonoids, lignans and stilbenes (Figure 1.14). Hydrolysable tannins are a group of extractives that yield gallic acid 18, ellagic acid 19 and glucose 1 upon acid hydrolysis [38, 41]. These tannins are not very common in woods and are

predominantly found in eucalypt species originating from southeastern Australia (e.g. *Eucalyptus regnans* and *E. nitens*) [41]. More commonly hardwood species (e.g. *Acacia, Quercus* and western *Eucalyptus* (e.g. *E. grandis*) contain condensed, rather than hydrolysable tannins [37, 38, 41, 50]. These condensed tannins consist of polymers formed from flavonoid monomers, such as dihydroquercetin **20** and catechin **21**.

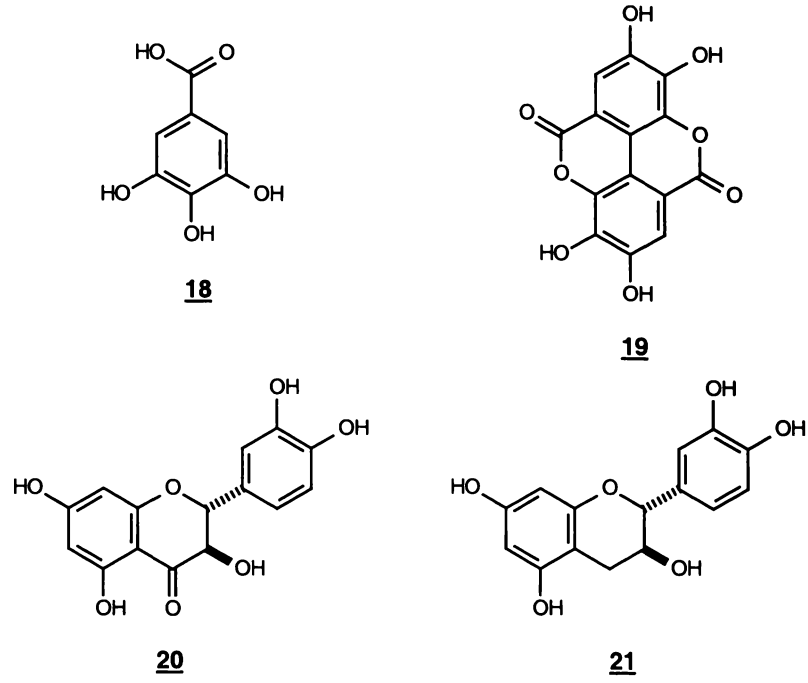

Figure 1.14: Examples of hydrolysable tannins and flavonoids [37].

1.3.4 Lignin

1.3.4.1 Introduction

Lignin is the "encrusting material" in which the cellulose fibres of a plant are imbedded [5, 8, 51, 52, 53]. It is the second most abundant terrestrial organic material, behind cellulose, making up typically 15-40% of the woody tissue mass in vascular plants [4, 8, 51, 52, 53, 54]. Incorporation of lignin into the cell wall structure of plants provides them with increased mechanical strength properties, better transport of water, nutrients and metabolites and protection from attack by micro-organisms [4, 8, 52, 54]. In softwoods, the secondary wall (SW) contains most of the lignin (~ 70%) found in the plant tissues [4, 53, 55, 56]. While the middle lamella contains a high concentration of lignin (60-80%), it only represents 15-20% of the total lignin [53, 55, 56].

Much of the information on lignin structure has been obtained from degradative techniques (such as nitrobenzene oxidation) applied to isolated lignin preparations. Two major approaches have been used to obtain these non-native lignins:

- Björkman [57] devised a method for extracting lignin from ball milled wood, the so-called milled wood lignin (MWL). This lignin is thought to be only slightly modified relative to the *in situ* lignin. However, even in this preparation, a lower molecular weight and a higher proportion of free phenolic groups are observed compared with native lignin [58, 59, 60]. Also, some carbohydrates have been shown to be present in the MWL [57, 61, 62].
- Dehydrogenation polymerisate (DHP) lignins have been synthesised by enzyme (peroxidase/H_2O_2) initiated polymerisation of coniferyl alcohol [51, 63, 64]. These have been shown to contain structural similarities to spruce Björkman lignin, but are recognised as being significantly different from natural lignins [65, 66, 67]. Much literature data highlights the structural variation in DHP's according to the experimental factors of their synthesis, such as:
    - type of phenolic precursor [68]
    - mode of precursor addition [64, 69]
    - reaction medium conditions [70, 71]
    - the presence of different carbohydrates [72, 73]

1.3.4.2 Lignin composition

Lignin is a structurally complex, heterogeneous, three-dimensional polymer, constructed from three main precursors, *p*-coumaryl alcohol **22** (*p*-hydroxyphenyl), coniferyl alcohol **23** (guaiacyl) and sinapyl alcohol **24** (syringyl), (Figure 1.15) [52, 53, 54, 63, 74, 75]. Due to this structural complexity, lignin has proven difficult to fully describe. However, modern techniques such as genetic engineering and characterisation by two dimensional (2D) nuclear magnetic resonance (NMR) spectroscopy are providing a better understanding of lignin structure and biosynthesis.

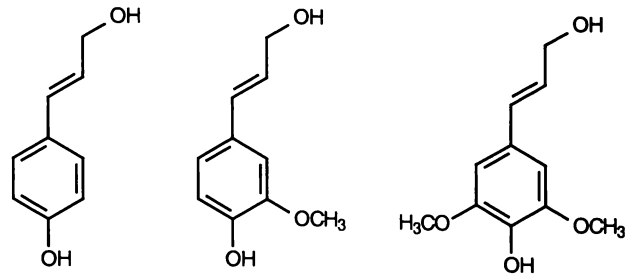

22 23 24

Figure 1.15: Lignin precursors [53].

The lignins in softwood, softwood compression wood and hardwood all contain varying concentrations of the three main monomers, guaiacyl (G), syringyl (S) and *p*-hydroxyphenyl (H) units [54, 74, 76, 77]. Softwood lignins have been shown to predominantly contain guaiacyl type monomers, with small amounts of *p*-hydroxyphenyl units also present and typically contain only trace levels of syringyl type monomers. Such softwood lignins are generally quite uniform between species and values of around 90% guaiacyl and 10% *p*-hydroxyphenyl can be considered typical [78, 79, 80].

Softwood compression wood lignin has been found to contain a significantly higher proportion of *p*-hydroxyphenyl units than sapwood softwood lignin [9, 15, 76, 77, 81]. According to Latif [82], compression wood lignin from Douglas fir (*Pseudotsuga menziesii*) consisted of 70% guaiacyl and 30% *p*-hydroxyphenyl units, compared with 88% and 12% for normal wood. However, the proportion of *p*-hydroxyphenyl units in compression wood lignin can vary markedly, depending on the extent of compressive force exerted. For this reason, a general G:H ratio can not be given for compression wood.

Hardwood lignins by contrast, are predominantly formed from guaiacyl and syringyl phenylpropane units [54, 74, 76, 77]. The ratio of guaiacyl to syringyl phenylpropane units in hardwood lignins varies depending on species and morphological origin of the lignin. Syringyl contents of different hardwood lignins may vary between 20 and 60% [54, 83]. Only small quantities of *p*-hydroxyphenyl units are detected in hardwood lignins, with their frequency typically lower than in softwood lignins.

In order to aid the further discussion of lignin chemistry a labeled structure of coniferyl alcohol is provided in Figure 1.16.

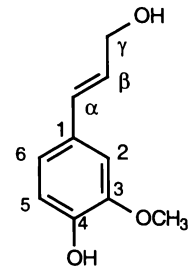

23

Figure 1.16: Lignin labelling convention used in this thesis.

1.3.4.3 Lignin precursor biosynthesis

Biosynthesis of the lignin precursors **22**, **23**, and **24**, is thought to start with glucose **1** formed during photosynthesis (Figure 1.17) [51, 53, 54, 64, 74, 75]. The glucose **1** is converted *via* shikimic acid **25** to the two aromatic amino acids, phenylalanine **26** and tyrosine **27**. These two products are subsequently converted to *p*-coumaric acid **28** *via* the cinnamic acid pathway. The *p*-coumaric acid **28** can be converted to *p*-coumaryl alcohol **22** through the action of reductase and dehydrogenase enzymes. Alternatively, the *p*-coumaric acid **28** may be methoxylated in the 3- and/or 5-position of the aromatic ring, by consecutive actions of phenolase and 4-O-methyltransferase enzymes, to give ferulic **29** or sinapic acid **30**. These products can then be converted, through a similar enzyme action as used for *p*-coumaryl alcohol **22**, to coniferyl alcohol **23** and sinapyl alcohol **24**.

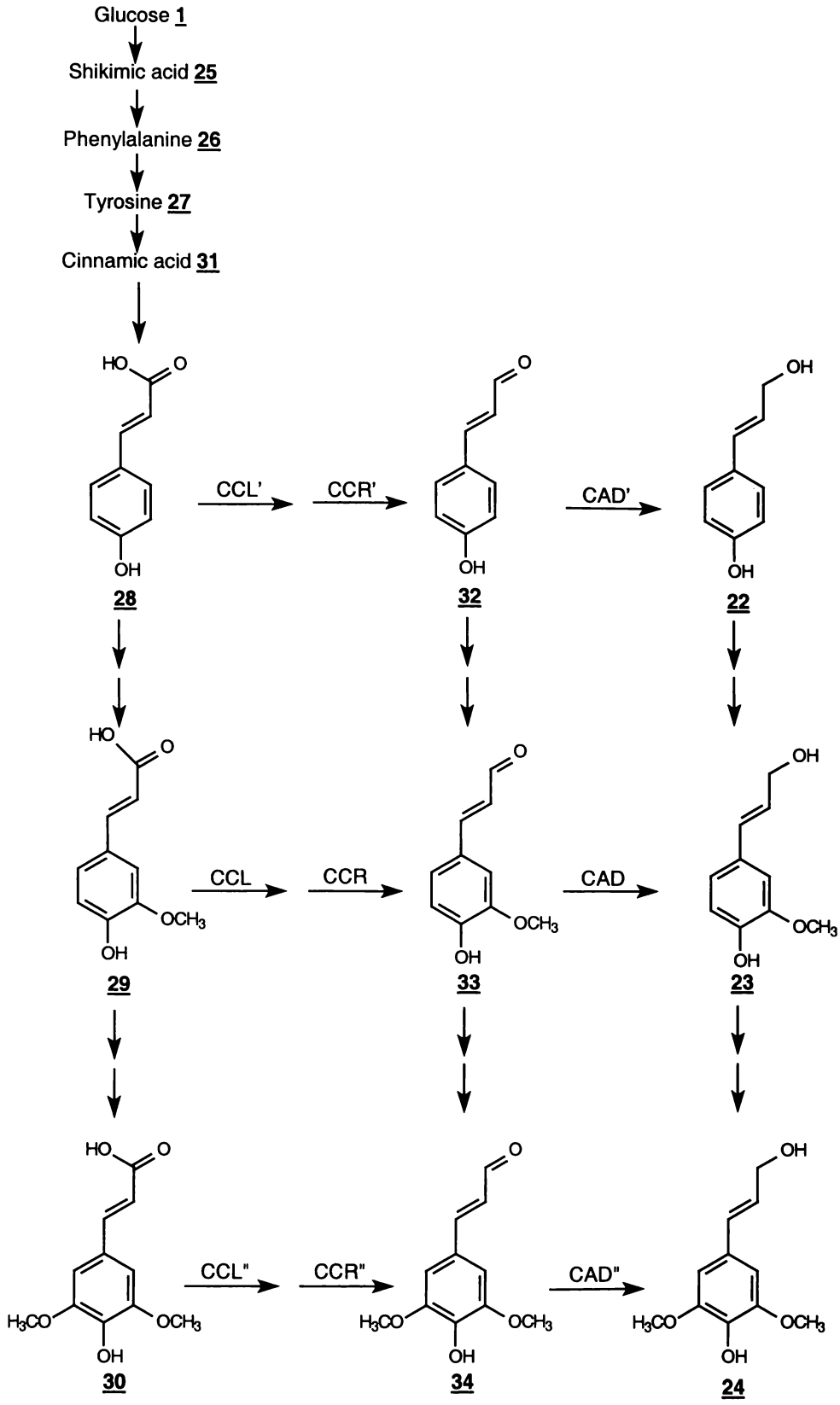

Figure 1.17: Metabolic pathway to the formation of lignin precursors [84]. CCL = hydroxycinnamate:CoA ligase, CCR = hydroxycinnamoylCoA:NADPH oxidoreductase, CAD = cinnamyl aldehyde dehydrogenase.

As well as these three hydroxy cinnamyl alcohol monomers, 22, 23 and 24, other minor components are recognised to be present. Until recently, these minor components have been thought of as aberrations. However, recent studies with a natural pine mutant indicate that lignin is quite flexible in regard to the monomers it can incorporate [84, 85, 86].

A naturally occurring loblolly pine (*Pinus taeda*) with a low cinnamyl alcohol dehydrogenase (CAD) activity (~1% activity *cf.* normal pine) has recently been reported [87-89]. This CAD deficiency heavily impeded conversion of coniferaldehyde 33 to coniferyl alcohol 23, the main monolignol precursor in softwood lignin. In response, the mutant pine incorporated non-traditional monomers into its lignin, including coniferaldehyde 33, dihydroconiferyl alcohol 35 and vanillin 36 (Figure 1.18) [84, 85, 86]. The incorporation of these monomers led to extensive structural changes in the lignin which were not predicted by the current view of the lignin biosynthetic pathway. This work therefore, suggested that the traditional proportions of lignin monomer composition might be too restrictive.

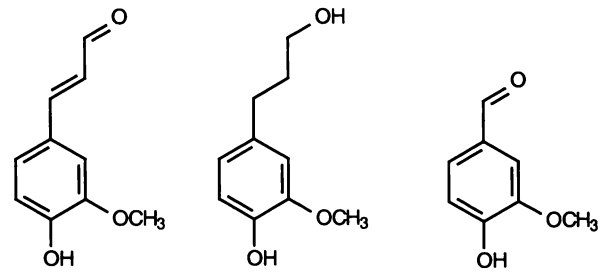

33 35 36

Figure 1.18: Products that build up when the CAD enzyme is suppressed [85].

1.3.4.4 Lignin polymerisation

The first step in the biochemical pathway for building lignin macromolecules is thought to involve electron transfer-initiated enzyme dehydrogenation of the monolignols [53, 54, 63, 64, 74, 75]. This yields a phenoxy radical, which is resonance stabilised through the ring and side chain. The mesomeric forms of the resonance-stabilised phenoxy radical from *E*-coniferyl alcohol are shown in Figure 1.19. Only phenoxy radicals I-IV are actually involved in lignin biosynthesis, V does not couple due to steric considerations.

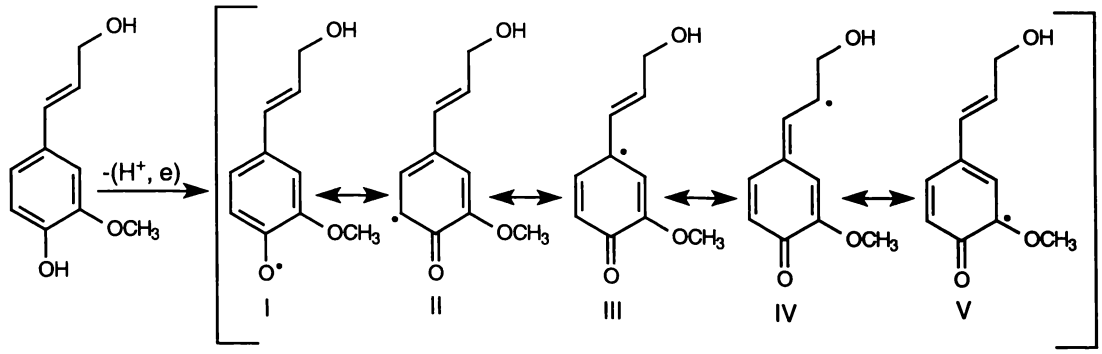

Figure 1.19: Mesomeric forms of the phenoxy radical formed through dehydrogenation of coniferyl alcohol [63].

These resonance structures make possible a variety of different radical couplings, producing dimers and oligomers containing different inter-unit linkages. The relative electron density of the different phenoxy radicals determines, in part, the frequency of the different sites involved in coupling reactions [54]. The resultant product of such radical coupling is proposed to be a quinonemethide intermediate [53, 54, 63, 64, 90]. This quinonemethide can then undergo stabilisation through nucleophilic addition reactions, by addition of water or intramolecular attack.

Figure 1.20 shows β-O-4 radical coupling of two coniferyl alcohol radicals, followed by reaction of the β-O-4 quinonemethide with water, to yield an arylglycerol-β-aryl ether structure. Figure 1.21 shows β-5 radical coupling followed by intramolecular addition, resulting in the phenylcoumaran structure.

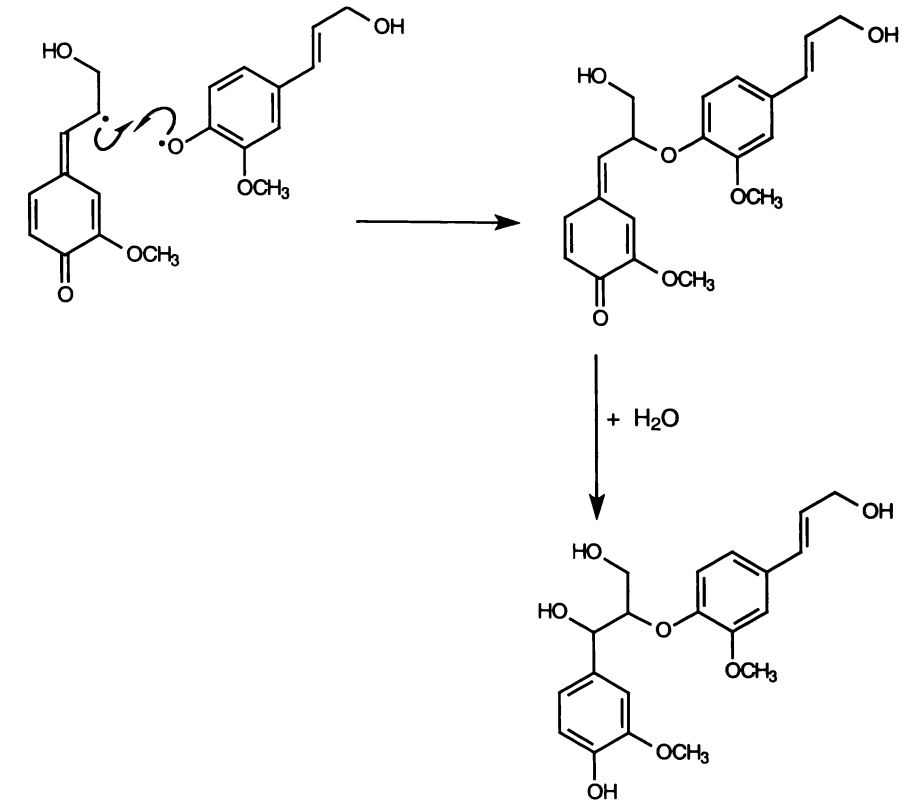

Figure 1.20: Formation of an arylglycerol-β-aryl ether linkage [63].

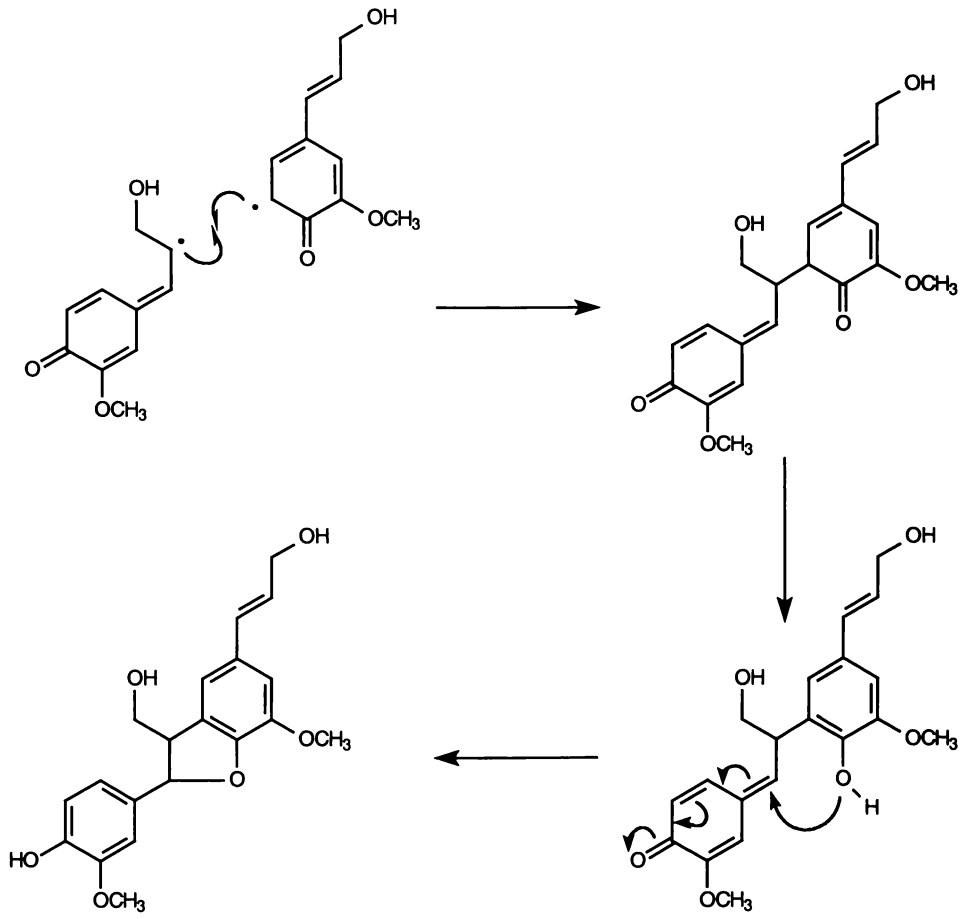

Figure 1.21: Formation of a phenylcoumaran linkage [63].

Sarkanen [64] showed that the structure of DHP depended on the mode of monomer addition. When all the monomer was added at the start ("Zulaufverfahren"), the dominant reaction was the formation of dimers, as outlined above, followed by further polymerisation to tetrameric and higher molecular weight aggregates [51, 74]. On the other hand, "Zutropfverfahren" polymerisation involves gradual addition of monomer and catalyst to the dehydrogenation system. After initial formation of the dimers, the low concentration of monomers led to coupling of the monomeric radicals with polymeric radicals, "endwise polymerisation", rather than monomer-monomer couplings. In other words, endwise polymerisation involves monomers adding onto the ends of the growing polymer.

This end-wise polymerisation leads to two major coupling patterns, namely β-O-4 and β-5 type inter-unit linkages [64]. However, polymer branching does occur, taking place through radical coupling to form biphenyl (5-5) and diaryl ether (4-O-5) structures [53, 63, 64]. The latter two are primarily formed through reaction of two end group radicals (quenching), although initial formation as dimers also occurs. It has been proposed that since the concentration of monomers in the "reaction zone" of the lignifying cell wall is low, polymerisation in plants should proceed essentially as endwise polymerisation after initial formation of dimers [63].

There is currently much debate about whether the radical coupling process is random or proceeds under enzymatic control [85, 86, 90b, 90c 91]. Much of the early literature discussed the coupling as a random process [51, 63, 64]. However, problems existed with accurately reproducing lignin biosynthesis *in vitro*. This has led some investigators to propose that the process is "exquisitely orchestrated" by the intervention of templates [91, 92]. This concept implies that lignin coupling is stereochemically controlled. Some recent work [91, 91b] which highlighted the ability of one specific dirigent protein to stereoselectively produce (+)-Pinoresinol supports the notion of "exquisite control". However, little further evidence has been forthcoming, indeed lignin is one of the few biopolymers that exhibits little optical activity or stereochemical order [90c]

The recent work with a naturally occurring CAD deficient mutant pine, also contradicts the use of a template in lignin construction [84, 85, 86]. The lignin isolated from this mutant pine contained large proportions of aldehyde structures (such as 33 and 36) and large proportions of dihydroconiferyl alcohol 35 (~30% *cf.* ~3% in non-mutant pine). This indicated that the lignification process was "metabolically plastic", or that plants could synthesise lignins from certain available phenolics, when their ability to produce "normal" lignin was impeded [84]. However, the issue of stereochemical control remains an active area of debate.

1.3.4.5 Inter-unit linkages

Figure 1.22 shows the principal inter-unit linkages proposed to be present in "natural lignin", with their approximate proportions as determined by Adler [63] summarised in Table 1.3 below. An asterisk next to several values in Table 1.3 indicates that new information has become available since the Adler publication. Explanations in regard to the new information are provided below Table 1.3.

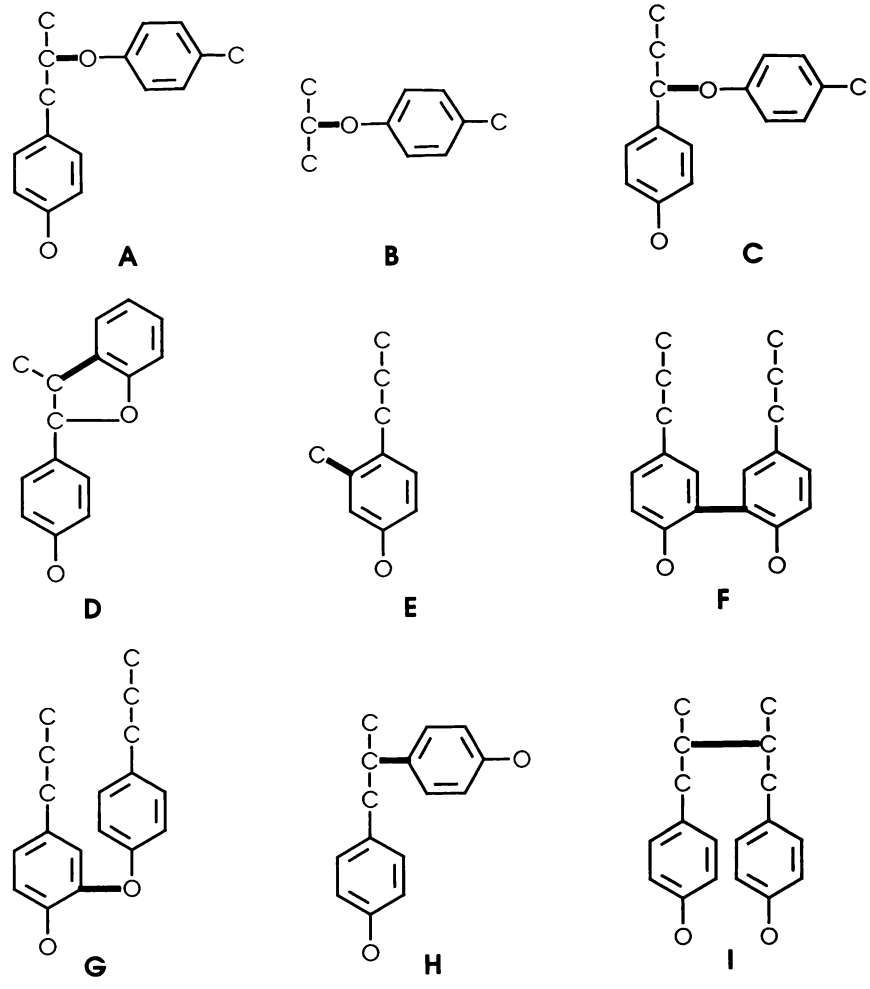

Figure 1.22: Principal inter-unit linkages in softwood lignin [63].

Table 1.3: Percentages of different bond types in softwood (Spruce) and hardwood (Birch) lignin, according to Adler [63].

		Percentage	
	Bond Type	Spruce	Birch
A	Arylglycerol-β-aryl ether	48	60
B	Glyceraldehyde-2-aryl ether	2	2
C	Noncyclic benzyl aryl ether	6-8*	6-8*
D	Phenylcoumaran	9-12	6
E	Structures condensed in 2 or 6 positions	2.5-3	1.5-2.5
F	Biphenyl	9.5-11*	4.5*
G	Diarylether	3.5-4	6.5
H	1,2-Diarylpropane	7*	7*
I	β,β-linked structures	2	3
* see discussion			

C The determination of noncyclic benzyl aryl ether (α-O-4) has received much attention in recent years. The proportions of such structures in lignin are considered important to both the chemistry of lignification and delignification, due to these structures potentially providing a reactive cross linkage in the lignin polymer [93]. Their commonly quoted level [63] is around 6-8% of inter-unit linkages in lignin, although values from <3 [94, 95]-13% [95] have been quoted. However, it has since been shown by 2D homonuclear Hartman-Hahn (HOHAHA) [96] and heteronuclear multiple quantum coherence (HMQC) [97, 98] NMR experiments that α-O-4 structures are either not present in softwood MWL, or present in concentrations below the detection limits of these NMR techniques [99]. The observed concentrations as reported previously have since been attributed to the acidolytic determination used, which relied on hydrolysis of the α-O-4 being completely selective. Cleavage of other ether linked phenolic structures may have led to an overestimation of α-O-4 units.

F Recent advances in 2D NMR spectroscopy have drawn attention to a number of correlation peaks, which cannot be assigned to any traditional linkage in lignin. In particular, Karhunen *et al.* [105] found prominent correlation peaks in a HMQC spectrum of a softwood MWL and these were shown by a HOHAHA experiment to be of adjacent carbon atoms. The correlations were attributed to a novel dibenzodioxocin structure containing an 8-membered ring. Formation of these structures was proposed to occur through oxidative cross coupling of a lignin biphenyl structure with coniferyl alcohol (Figure 1.23) [106].

F Adler [63] reported that the proportions of biphenyl structures in softwood were around 9-11% of the C9 units in lignin. However, according to current estimates, 20-26% of the phenyl propane units are involved in such inter-unit bonds [107]. Therefore the presence of the 8-membered dibenzodioxocin structures, involving a biphenyl group, may have important consequences for lignin reactivity.

H The relative abundance of diarylpropane (β-1) inter-unit linkages in lignin has also been under some investigation recently [100, 101, 102, 103]. Estimates of the relative abundance of β-1 structures in lignin have varied from <3% [94] to ~10% [75] of the inter-unit linkages, depending on the analytical technique used and the method used for lignin isolation. Recent work by Lapierre *et al.* [104] and Ede *et al.* [100] has shown that β-1 distribution throughout the cell wall is rather heterogeneous, with β-1 concentrations highest in carbohydrate rich regions of the cell wall. The value of 7 inter-unit linkages per 100 C9 indicated for softwood lignin in Table 1.2 should therefore be considered as a rough, although high indicator. Due to the varying concentrations in the different fractions of the cell wall, no fixed value can be given.

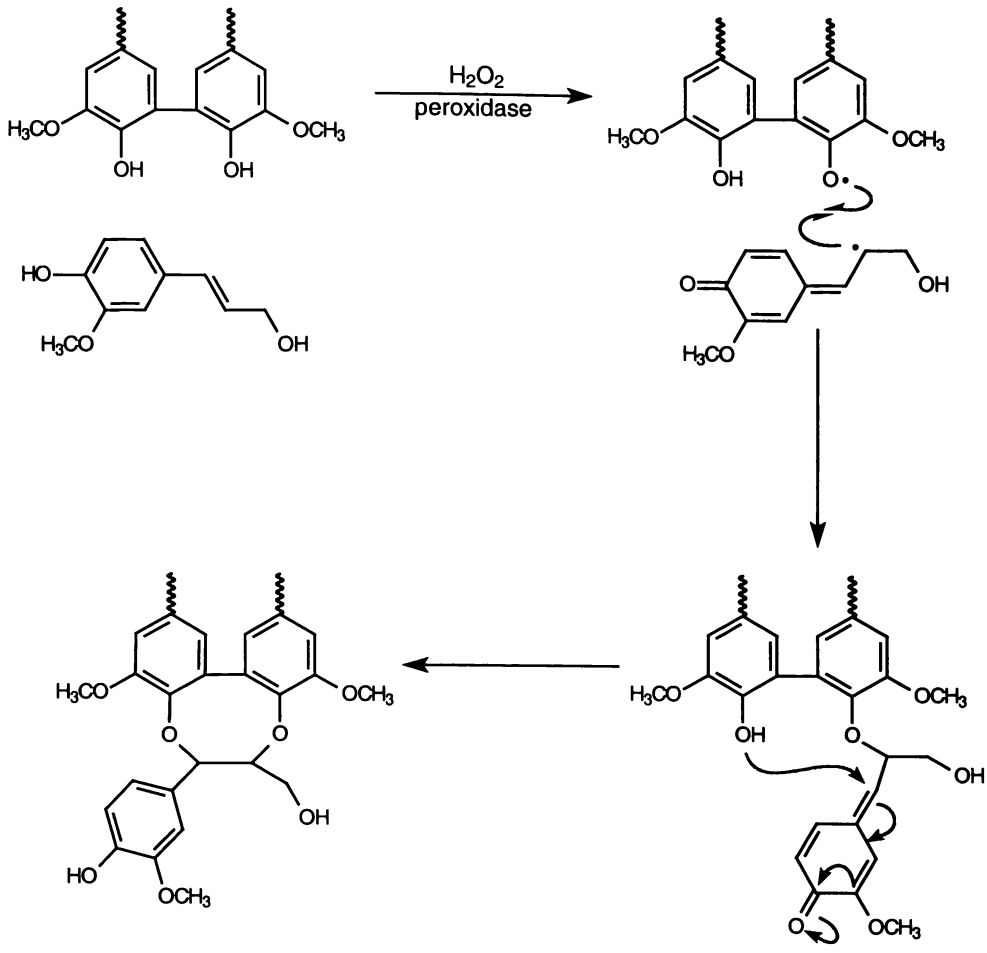

Figure 1.23: The formation of a dibenzodioxocin linkage by oxidative coupling [106].

In this thesis, two particular definitions have been used in regard to lignin chemistry:

- *Condensed* units are defined as those moieties which contain a covalent inter-unit linkage between its C5 and a carbon or oxygen in a second phenylpropane monomer. Examples of inter-unit linkages containing such moieties include phenylcoumaran, biphenyl and diarylether inter-unit linkages in Figure 1.22 and Table 1.3. *Uncondensed* units on the other hand are phenylpropane monomers, where a hydrogen atom is bonded to the C5 position.
- *Free phenolic* units are defined as those moieties containing a phenolic oxygen bonded to a labile proton. On the other hand *etherified* units are those moieties where the phenolic oxygen is covalently bonded to another phenyl propane unit, for example arylglycerol-β-aryl ether.

These definitions are important because the analytical technique used throughout this thesis focuses on quantification of the condensed and uncondensed units, present as both free phenolic and etherified moieties.

Significant structural differences occur between the lignin in softwoods and hardwoods [54, 63, 76]. As mentioned earlier, while softwood lignins predominantly contain guaiacyl monomers, hardwoods contain both guaiacyl and syringyl type monomers. The presence of a methoxyl at C5 of the aromatic ring in syringyl monomers prevents these monomers being involved in condensed inter-unit linkages (Figure 1.24). Indeed, hardwood lignin has been shown to generally contain fewer condensed inter-unit linkages than softwood lignin [63]. Conversely, hardwood lignins typically contain a larger proportion of β-O-4 structures than softwoods. This difference in proportions of condensed structures is in part responsible for the ease of hardwood kraft pulping (lower temperatures, shorter time and lower sulphidity), when compared with softwood kraft pulping [108, 109].

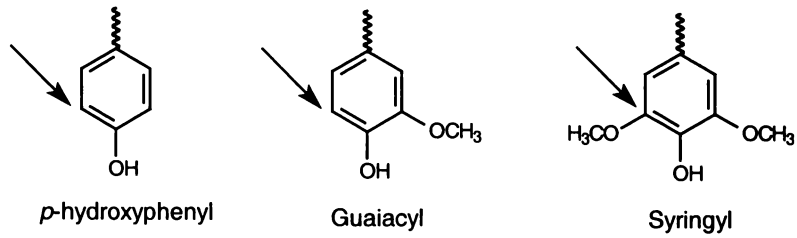

Figure 1.24: C5 position in *p*-hydroxyphenyl, guaiacyl and syringyl monomers.

Compression wood has been reported to have a higher proportion of condensed structures than normal softwood [9, 82, 110, 111]. For example, studies by Yasuda and Sakakibara [111, 112, 113] and Sakakibara [110] on *Larix leptolepis* showed that the compression wood lignin contained 65% more condensed structures than normal wood. A detailed structural analysis of compression wood lignin from *Pseudotsuga menziesii* by Latif [82] showed that, compared with normal softwood lignin, the former contained more biphenyl and phenylcoumaran inter-unit linkages, but less arylglycerol-β-aryl ether and 1,2-diguaiacylpropane linkages. This higher proportion of condensed structures has been predominantly attributed to the higher monolignol concentration in compression wood, leading to more bulk type polymerisation [51, 64, 74], and the higher proportions of *p*-coumaryl alcohol moieties in compression wood lignin (*cf.* normal softwood) [9, 114, 115]. The *p*-

hydroxyphenyl moiety has the ability to form condensed type structures through both the C3 and the C5 position on the aromatic ring (Figure 1.24), compared with the C5 position alone for the guaiacyl monomer.

1.3.4.6 Functional groups in lignin

The predominant functional groups, which influence the reactivity of lignin, are phenolic hydroxyl, benzylic hydroxyl and carbonyl groups. Table 1.4 summarises typical values for these functional groups in softwood and hardwood lignins. The concentration of these groups may vary significantly depending on wood species and morphological location.

Table 1.4: Functional groups in lignin per 100 C_6C_3 units [63].

Group	Spruce Lignin	Birch Lignin
Methoxyl	92-96	139-158
Phenolic hydroxyl (free)	15-30	9-13
Benzyl alcohol	15-20	
Noncyclic benzyl ether	7-9	
Carbonyl	20	

1.3.4.7 Structural scheme of softwood lignin

The culmination of all this type of information gathering is the ability to construct a model or a statistically average lignin molecule [63, 78, 116]. One simple, and dated, model that summarises the structures in softwood lignin is shown in Figure 1.25.

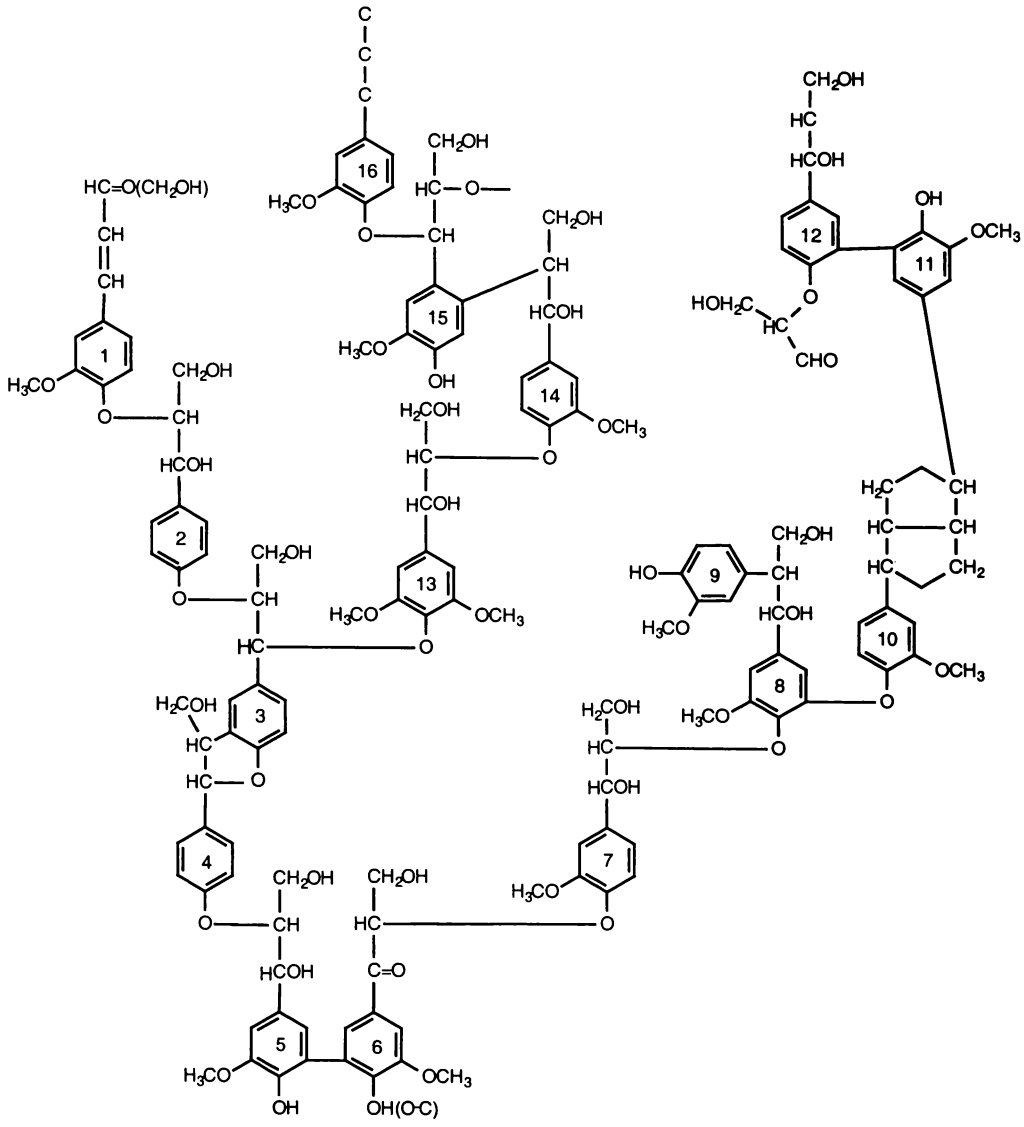

Figure 1.25: A structural scheme of softwood lignin, according to Adler [63].

1.3.5 Origin of MWL

One of the most important methods for obtaining a relatively unchanged lignin from wood is Björkman's procedure for producing milled wood lignin (MWL) [57, 117]. This procedure involves vibratory ball milling of a wood meal to destroy the cell wall structure of the wood, followed by extraction of a portion of the lignin with a dioxane-water mixture. While the resulting lignin is usually considered to be little changed relative to native wood lignin, it is acknowledged that some changes, such as creation of free phenolic groups, are introduced by the ball milling and subsequent dissolution [58, 62].

One problem with MWL is that only a small portion of the lignin in the wood is extracted [57, 58, 117], usually < 10%. However, native lignin is known to vary with respect to morphological location in the cell wall [56, 118, 119], and with respect to the growing sage of the lignin during differentiation of the cell wall [120, 121, 122]. Therefore, it is important to know to what extent the information obtained from MWL can be applied to lignin in the cell wall. Two main theories about the morphological origin of MWL exist:

- MWL originates mainly from compound middle lamella (CML) lignin.
- MWL originates mainly from secondary wall (SW) lignin.

Many of the early investigations indicated that MWL originated primarily from the CML [58, 123, 124]. However, Whiting and Goring [125] have shown that a spruce tissue fraction, consisting of predominantly SW tissue, produced a higher yield of MWL on grinding than the CML fraction. Also Maurer and Fengel [126] observed the dissolution behaviour of lignin from the spruce cell wall during milling and dioxane extraction. Results indicated that the middle lamella region was more resistant to ball milling and that SW lignin was released more easily than the middle lamella lignin. Terashima *et al.* [127] showed by radiolabelling of the SW and ML, with different radiotracers, that SW lignin was degraded more easily by ball milling than CML lignin, to yield MWL. Due to these studies, it is now generally accepted that MWL originates primarily from lignin residing in the SW of the tracheid.

1.4 Pulping

Pulping is the term used to describe the various processes whereby cellulose fibres suitable for paper making, are produced from the wood chip feedstock. This process can be achieved through chemical means (Section 1.5.1), mechanical means (Section 1.5.2) or through a combination of the two (Section 1.5.3). While there are many different commercial pulping processes in operation, for the purpose of this thesis, only a selection of processes are discussed in this introduction.

1.4.1 Kraft pulping

In kraft pulping, chemicals are used to degrade and solubilise the lignin, thereby freeing the cellulose fibres for subsequent processing. Although the aim of kraft pulping is to selectively remove the lignin from the cellulose fibre, significant amounts of carbohydrates, particularly hemicelluloses, are also dissolved in the pulping liquor and degraded to some extent.

Kraft pulping involves the heating of wood chips in an aqueous solution of sodium hydroxide and sodium sulphide (white liquor), from a temperature of 90°C to 160-180°C, followed by cooking for 1-3 hours at this temperature [108, 109, 128, 129]. Kraft pulping can be divided into three distinct phases (Figure 1.26); initial, bulk and residual [108, 128]. Each phase has a quite different selectivity towards lignin and carbohydrate dissolution.

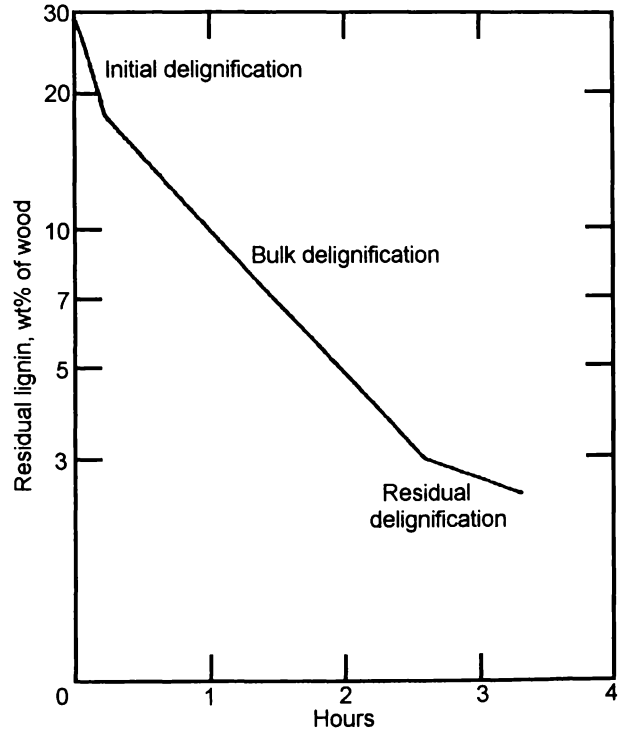

Figure 1.26: The three phases of kraft pulping.

The fast initial phase is largely diffusion controlled and takes place at temperatures below 140°C [128]. Lignin depolymerisation in this phase has been tentatively ascribed to cleavage of β-O-4-aryl ether bonds in lignin units containing free phenolic groups [130, 131]. Due to the limited amount of free phenolic groups in lignin, this rapid initial phase delignification is, therefore, restricted to about 20% delignification. During initial phase delignification, a considerable amount of carbohydrate is also solubilised, almost exclusively hemicelluloses [108, 109, 128, 129]. Figure 1.27 shows the proposed mechanism for the degradation of a phenolic β-O-4-aryl ether structure [132, 133, 134, 135]. It involves initial formation of a quinone methide formed from the phenolate anion generated by the elimination of an OH^- from the α-carbon. This quinone methide, in the presence of hydrosulphide ions, undergoes rapid cleavage of the β-aryl ether bonds, through formation of a thiirane intermediate.

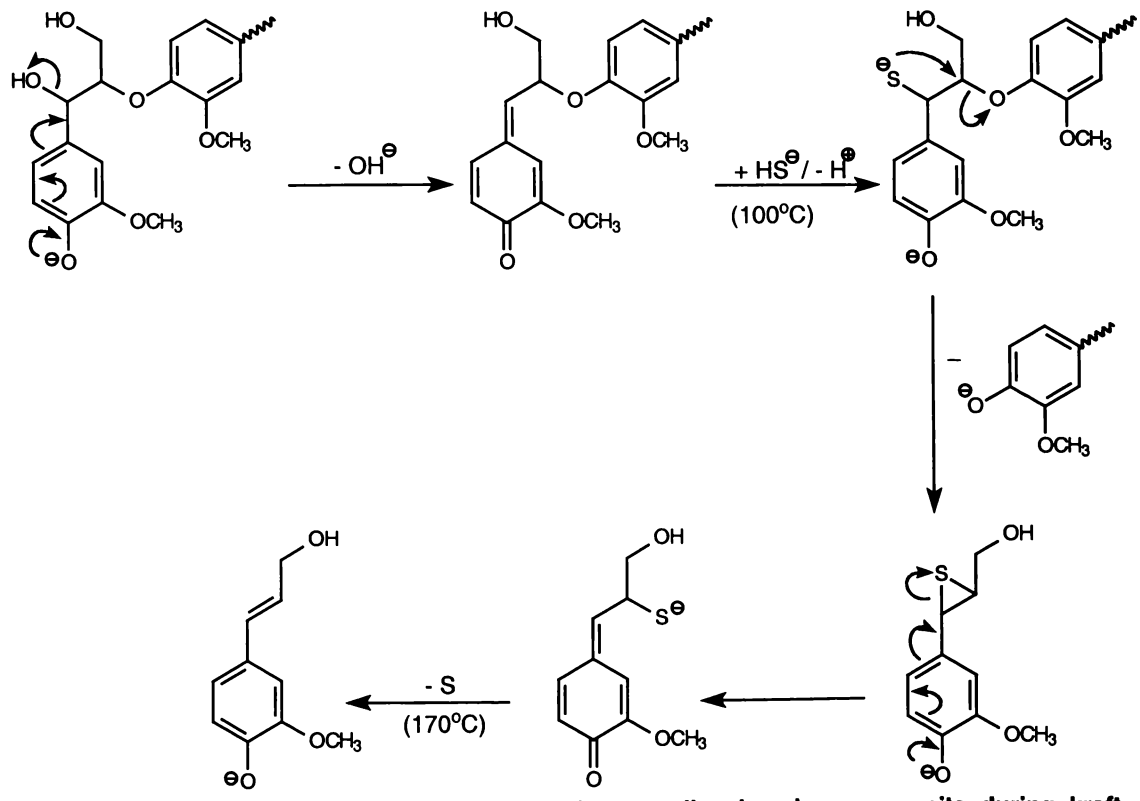

Figure 1.27: Cleavage of β-aryl ether bonds in phenolic phenylpropane units during kraft pulping [132].

Above 140°C, bulk phase delignification begins. The rate determining reaction, in this phase, is considered to be the cleavage of non-phenolic β-aryl ethers [108, 109, 129]. The rate of lignin dissolution remains high during the bulk phase, until about

90% of the lignin has been removed [128]. Bulk phase delignification is also characterised by a low rate of carbohydrate dissolution relative to delignification, compared with the other two phases. In etherified phenylpropane structures, the β-aryl ether linkage is proposed to cleave *via* an oxirane intermediate, through the mechanism shown in Figure 1.28 [109, 133-135].

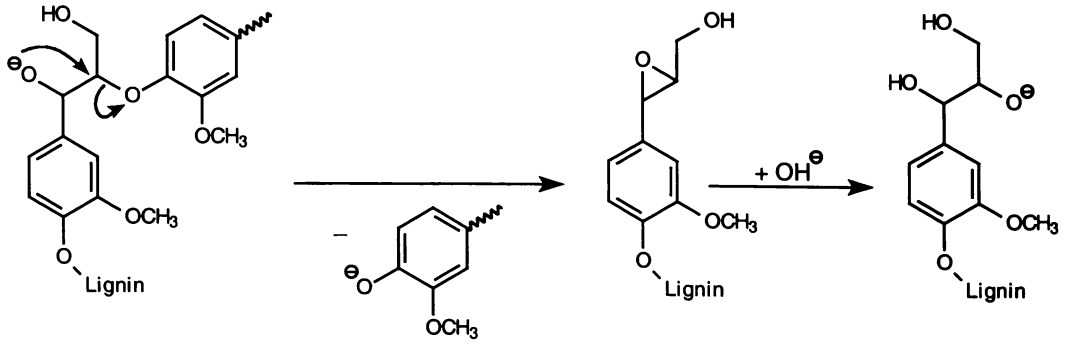

Figure 1.28: Cleavage of a β-aryl ether linkage in structures containing an etherified phenolic group [132].

During these first two phases of kraft pulping, the α-ether bonds in structures, such as phenolic phenylcoumaran, are also readily cleaved by the action of hydroxide ions [133]. This is usually followed by the release of formaldehyde (Figure 1.29). By contrast, α-ether bonds are stable in all etherified structures, as the required quinone methide cannot be formed.

Once most of the β-ether linkages have been cleaved, the reaction slows down into the residual phase [108, 109, 136]. Delignification in this phase is attributed to the cleavage of carbon to carbon bonds. However, due to the high cooking temperatures needed to effect inter-unit cleavage, significant amounts of carbohydrates (e.g. cellulose) are dissolved in this phase, affecting pulp yield [137-139].

Due to this cellulose dissolution, in a typical commercial softwood kraft pulp, the cook is often stopped just after the end of the bulk phase, leaving about 10% of the original lignin still present in the pulp [108, 109, 128, 140]. Typically 80-90% of the lignin, 50% of the hemicelluloses, 90% of the extractives and up to 10% of the cellulose is dissolved in a kraft cook. Overall softwood kraft pulps typically have a brown stock yield of around 45%.

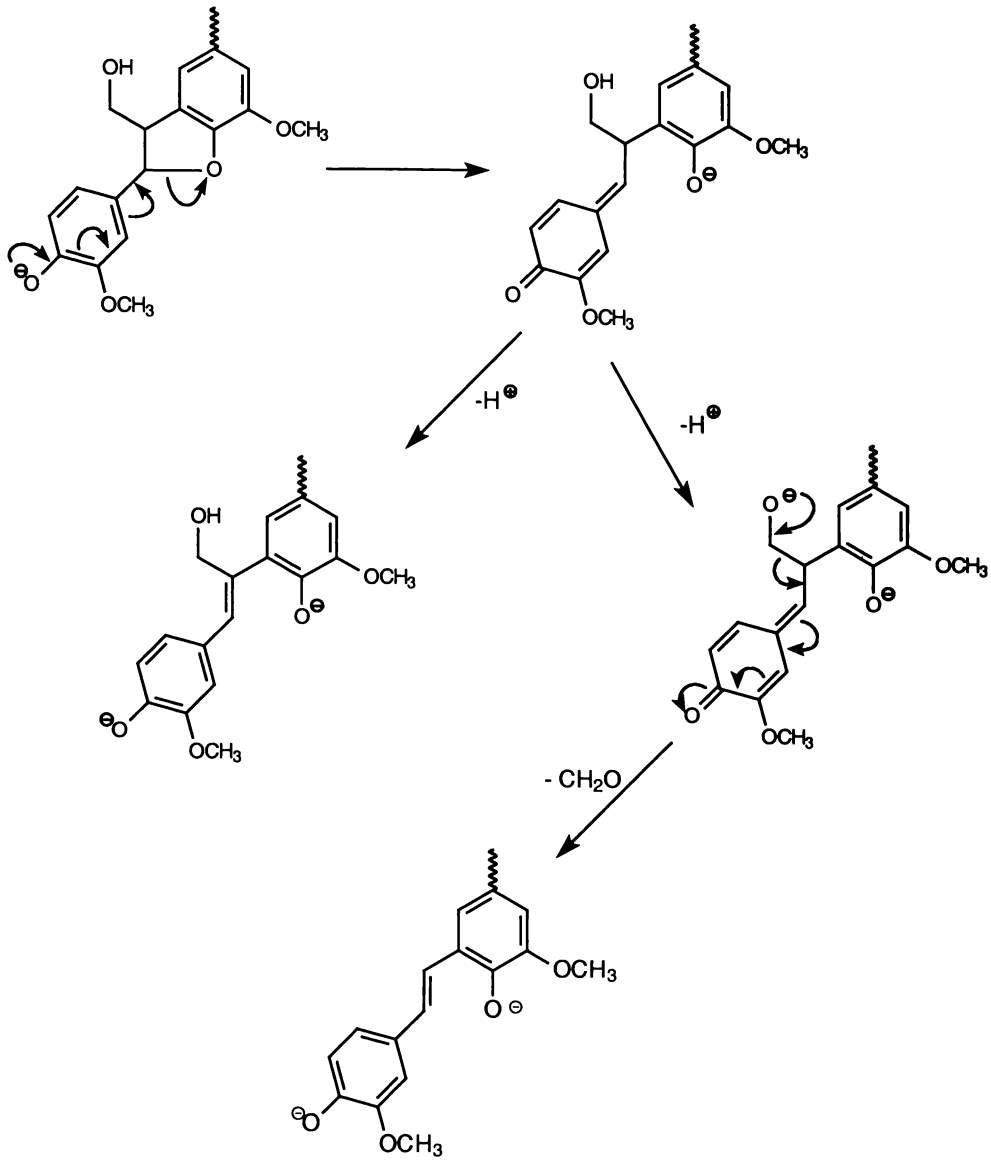

Figure 1.29: Base catalysed cleavage of α-aryl ether bonds in phenylcoumaran structures, *via* an intermediate quinone methide, also showing elimination of formaldehyde [133].

Many commercial uses of kraft pulps require a "white" pulp. The colour of pulp is mainly associated with its lignin component [141, 142, 143]. For this reason, residual lignin is either:

- Removed from the pulp (also called delignifying bleaching). Typically this is performed by the use of oxygen, chlorine dioxide or ozone amongst others [108, 140, 142, 143].
- Freed from its chromophores (strongly light-absorbing groups), also called lignin preserving bleaching or final brightening. Typically this is performed with chlorine dioxide or hydrogen peroxide [108, 140, 142, 143].

During kraft pulping a variety of condensation reactions are known to occur [108, 109, 132-135]. It has been shown that a major part of these condensation reactions occur at the C5 position of free phenolic guaiacyl units (Figure 1.30) [109, 133-135]. The formation of these condensed structures presents a problem for the bleaching of kraft pulps. This is because condensed structures have been shown to be less reactive with bleaching reagents than uncondensed ones.

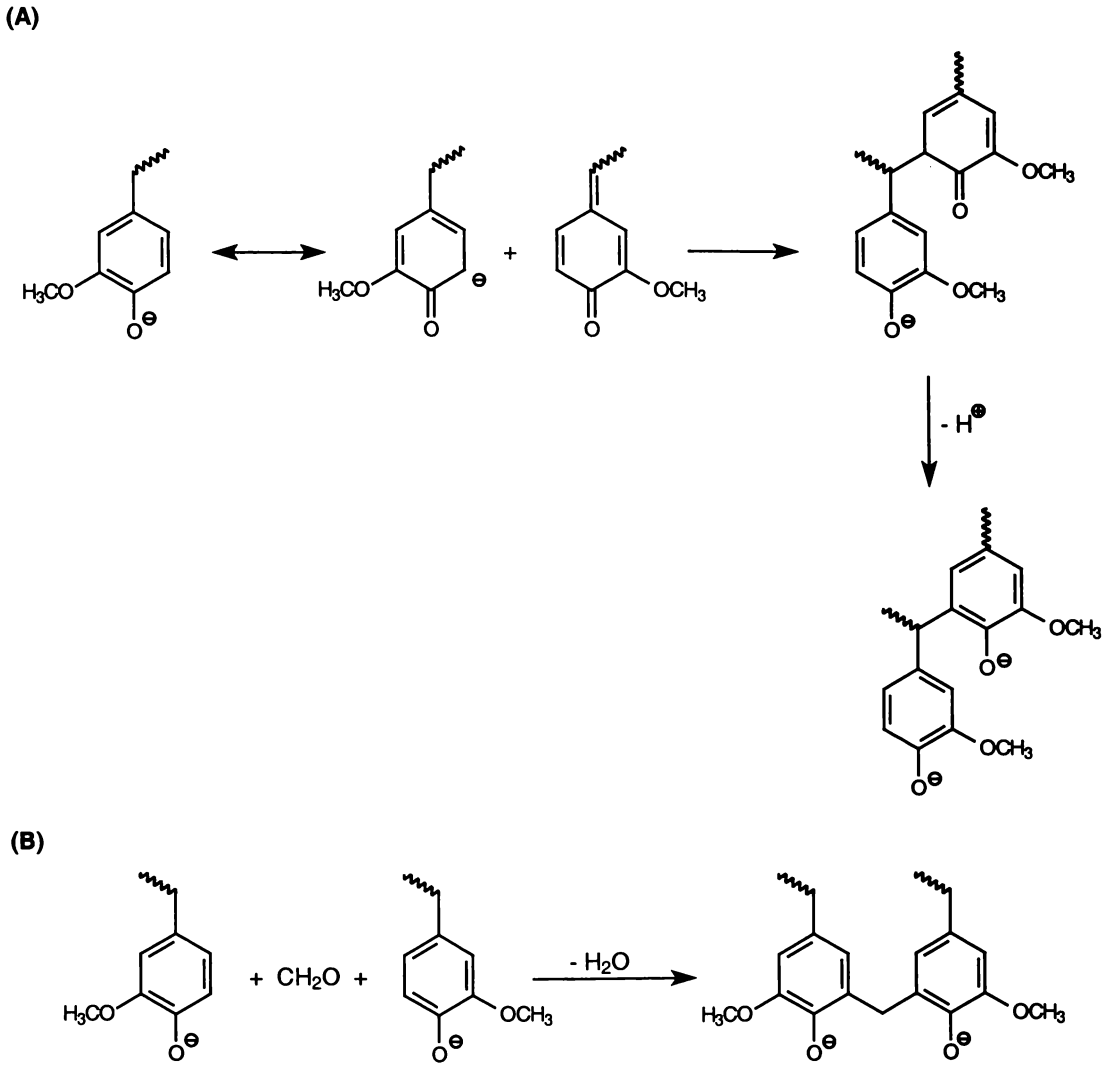

Figure 1.30: Examples of condensation reactions during kraft pulping. (A) formation of an α-5 structure. (B) formation of diarylmethane structure [133].

One major drawback of the kraft process is the production of highly volatile and malodorous products [108, 109, 132]. Methyl mercaptan and dimethyl sulphide cause an air pollution problem that is difficult to control. These malodorous products are formed through reaction of the hydrosulphide ion with the methoxyl groups in lignin, forming methyl mercaptan (Figure 1.31) [133]. This mercaptan may then react with another methoxyl group to form dimethyl sulphide or in the presence of oxygen, it may be oxidised further to dimethyl disulphide.

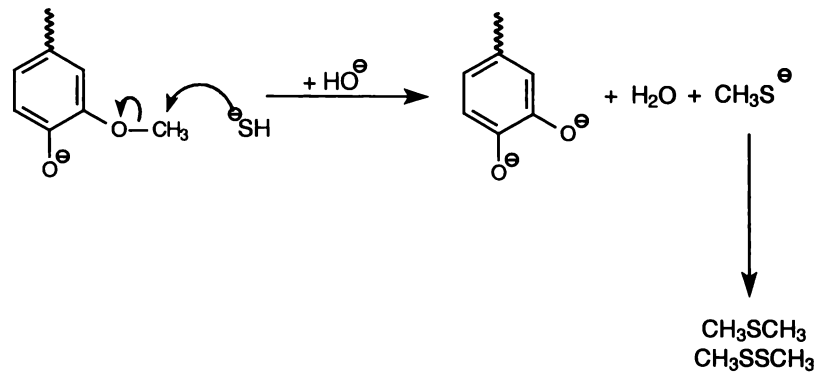

Figure 1.31: Cleavage of methyl aryl ether bonds, with formation of methyl mercaptan (CH_3SH), dimethyl sulphide (CH_3SCH_3) and dimethyl disulphide (CH_3SSCH_3), during kraft pulping [133].

Despite these drawbacks, the kraft pulping process remains one of the most economical means of removing lignin from wood. However, the amount of lignin that can be removed by the process is limited. Typically, pulping beyond a 4% residual lignin content is not performed, due to the marked reduction in fibre strength observed. A number of modified kraft pulping systems have been developed with the aim of extending kraft delignification [144-146]. These systems include modified continuous cooking (MCC™) by Ahlstrom/Kvaerner, rapid displacement heating (RDH™) by Beloit and the Superbatch™ process by Sunds.

These systems rely on four main principles to achieve the improved delignification [147, 148].

- Even alkali concentration throughout pulping.
- High sulphide concentration prior to maximum temperature.
- Low dissolved lignin concentrations.
- Low maximum temperature.

By using some or all of these principles, it has been possible to achieve pulps with a lower lignin content, without sacrificing fibre strength. This reduces the need for bleaching chemicals, providing environmental advantages and costs savings.

1.4.2 Mechanical pulping

As the name implies, mechanical pulping relies on applied mechanical force to break the wood up into fibres [140, 149, 150]. However, in some processes (discussed later), chemicals are applied during mechanical refining. The main mechanical pulping processes used in New Zealand are based on pulps generated through refining. The original refiner mechanical pulping (RMP), which was a low temperature, atmospheric disc refining process, has largely been replaced by thermomechanical pulping (TMP), which involves pressurised presteaming followed by refining [140, 150].

Typically, in thermomechanical pulping (Figure 1.32) the chips are softened by pre-steaming at 120-140°C for about 4 minutes, before being defibred in a pressurised disc refiner operating at 100-360 kPa, with an applied energy of 1000-1200 kWh/odt [150, 151]. Two metal discs, with at least one of them rotating, perform the mechanical work [151]. The wood fibres are separated by the action of the grooves and bars on the surfaces of these discs. This first stage refining may operate alone, or be followed by a second stage of refining, which may also be under pressure.

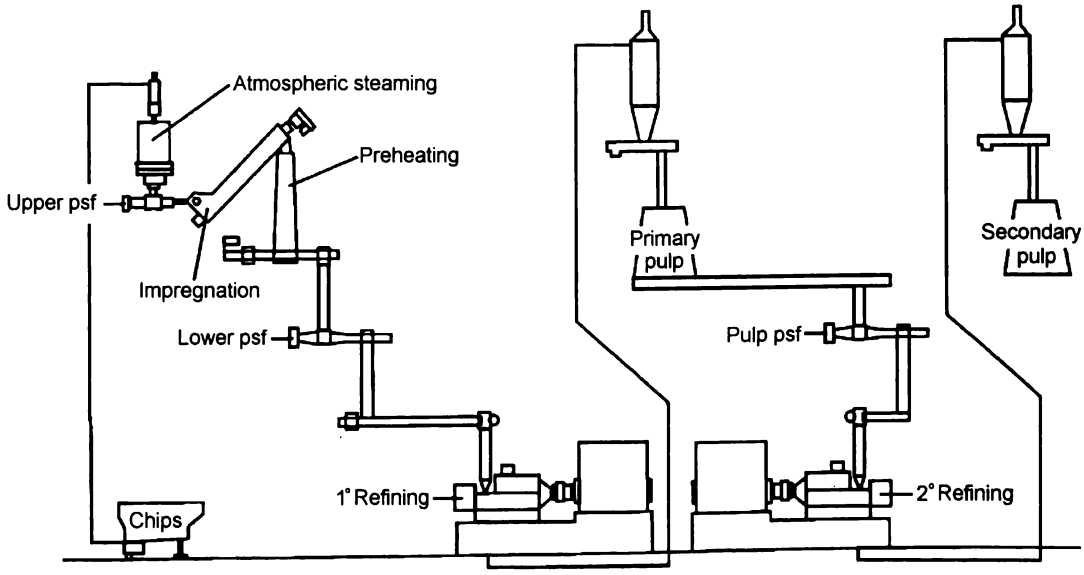

Figure 1.32: Scheme of typical TMP pulping operation.

The main benefit of mechanical pulping is that essentially, all of the constituents of the wood are retained in the pulp, which contributes to their relatively low overall cost [149, 150]. Due to the mixed nature of the pulp and because the lignin has not been removed, mechanical pulps have properties that make them suitable for certain grades of paper. These properties are a small average particle length and a relatively stiff fibre (preventing packing), giving a paper with high bulk, good opacity and good printability. Disadvantages of mechanical pulps, include a relatively low strength, a harsh feel and a lack of permanence [140, 150, 149].

1.4.3 Chemimechanical pulping

By using sodium sulphite (Na_2SO_3) at elevated temperatures, the properties of the mechanical pulps can be modified. Reaction with sodium sulphite makes the hydrophobic lignin much more hydrophilic, and after mechanical treatment the fibres exhibit improved fibre flexibility [140]. Typically, chemithermomechanical pulping (CTMP) involves impregnation of the wood chips with aqueous sodium sulphite (at 60°C for 5 minutes) prior to steaming at a temperature near 125°C and mechanical defibration [150]. For softwoods, a sodium sulphite application level of 1-6% is required to introduce improved flexibility characteristics. Mechanical defibration is essentially the same as described for the TMP.

For radiata pine, addition of sodium sulphite into the refiner during pressurised refining, has been shown to substantially reduce the energy required to give a pulp of similar qualities to CTMP [152]. This dilution water sulphonation (DWS) process uses similar levels of sulphite addition and, apart from the sulphite addition point, the process conditions are similar to those of CTMP.

For CTMP, the sulphite enters the centre of the fibre through the lumen and then diffuses out through the fibre wall into the middle lamella [153, 154]. In contrast, for the DWS process, the sulphite is added as the chips enter the refining zone, meaning there is insufficient time for the sulphite diffusion to occur before the refining occurs. Essentially, the sulphite is added to the surface of the fibres of a TMP pulp as they are separated in the refiner [153, 154].

Sulphonation levels in the CTMP and DWS fibres are similar. More extensively sulphonated chemithermomechanical pulps are also produced, one example of this is the Ontario Paper Company (OPCO) process [150, 155]. The benefit of such pulps is that, while they are produced in a high yield, the extensive sulphonation also enables the pulps to be used instead of chemical fibres in newsprint furnish. The OPCO process involves sodium sulphite treatment of thermomechanical fibres, most commonly between the two refining stages, but in some cases after secondary refining [150]. Sodium sulphite application is usually 7-10% at a temperature between 130-180°C for 15-120 minutes at a consistency of over 10% (also some NaOH added). Compared with the other chemimechanical pulps discussed above, the OPCO is a far more severe treatment, with a higher Na_2SO_3 content in the pulp lignin. This severe sulphonation leads to increased lignin and carbohydrate loss.

1.4.4 MDF refining

Medium density fibreboard (MDF) is a dry formed panel product made from lignocellulosic fibres, combined with a synthetic resin and compressed to a density of between 600 and 800 kg/m^3 [156, 157]. MDF fibres are produced using a disc refining procedure similar to that for thermomechanical pulp (TMP) fibres. The main difference is that the chips for MDF production are heated to much higher temperatures prior to disintegration, than thermomechanical pulping defibration.

For amorphous polymers such as lignin, the softening point, where the material passes from a glassy to a rubber-elastic state, is called the glass transition point [158, 159]. In the production of MDF fibres, the pulping is performed above the glass transition temperature of lignin. This significantly reduces the refining energy demand, relative to that of the TMP pulping process [156, 157]. The glass transition temperature of native lignin has been shown to be dependent on its moisture content and to vary between 115°C and 205°C [159]. In a MDF refining process, a glass transition temperature of around 150°C may be considered typical. By operating above the glass transition point, the lignin is softened/plasticised and is more easily sheared. During MDF refining, the fibres have been shown to separate in the middle lamella [156]. The lignin-rich (hydrophobic) fibre surfaces in the resultant pulp, are unable to hydrogen bond together and are unsuitable for papermaking, unless chemically modified.

Compared with the conditions discussed for TMP, MDF chips are typically preheated to 170-180°C for a residence time of 2-5 minutes. Although still considerable, the demand for electrical energy at 200-250 kWh/odt is much lower than that required for TMP pulping. While it is common to use a single stage of refining for the production of MDF fibres, certain commercial operations in New Zealand, for example Canterbury Wood Products in Rangiora and Fletcher Wood Panels in Taupo, do use two stages of refining.

1.5 Lignin Analysis

Isolated lignin samples are highly complex in nature, containing different ratios of monomeric building blocks, different types and levels of inter-unit linkages and different concentrations of functional groups (Section 1.3.4). Extensive literature is available detailing methods for the analysis of different structural features and functional groups in lignins. For the purpose of this thesis, a range of pertinent analytical techniques has been detailed below.

- Section 1.5.1 Quantification of phenolic hydroxyl groups.
- Section 1.5.2 Degradative methods for lignin analysis.
- Section 1.5.3 Methods for measuring condensed:uncondensed units.

1.5.1 Phenolic hydroxyl determination

Phenolic hydroxyl groups are one of the most important functional groups in lignin, significantly affecting its chemical and physical properties [63]. For example, phenolic hydroxyl groups play a key role in pulping and bleaching processes. They can affect the chemical reactivity of lignin during chemical modification and contribute to the poor brightness stability of high-yield pulps [160-162]. Quantitative determination of phenolic hydroxyl groups therefore provides important information on the structure and reactivity of lignin.

A range of different physical and chemical methods, or a combination of both methods, are available for determining the amounts of phenolic hydroxyl groups in lignin. Some of the more commonly used techniques are described briefly below. Techniques such as potentiometric [163] and conductometric titrations [164], diazomethane methylation [165] and acetylation [166] are now largely of historical significance and seldom used as stand alone techniques for the determination of phenolic hydroxyl groups.

1.5.1.1 Ultraviolet ionisation spectroscopy

Ultraviolet (UV) ionisation spectroscopy has been successfully used to determine the phenolic hydroxyl content of lignin samples [165, 167, 168, 169]. This method is based on the ionisation of phenolic hydroxyl groups in lignin (Figure 1.33), which results in displacement of the UV absorption maxima to a longer wavelength and an increase in absorption intensity [168, 169, 170]. A difference spectrum ($\Delta\varepsilon_i$) is generated by subtracting $Absorption_{neutral}$ from $Absorption_{alkali}$. The height of the peaks in the difference spectrum can be used to calculate the levels of free phenolic groups in the lignin. As the etherified structures are not ionised in alkaline solution, they are not measured by this method.

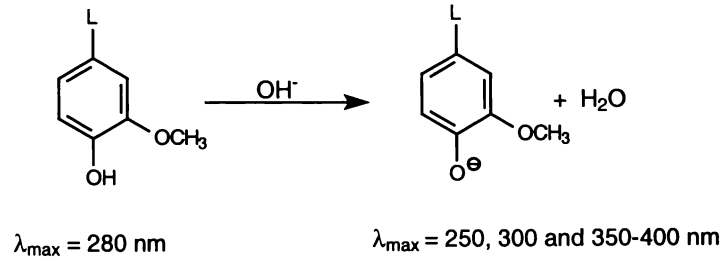

Figure 1.33: Ionisation of a guaiacyl unit for UV analysis [169].

The original method by Aulin-Erdtman [168] was straightforward and simple, but was recognised to have some reliability problems [171]. Several of these problems may be overcome by modifying the method to take into account the effects of α-conjugated aromatic structures on the UV ionisation spectrum. However, even with these modifications, there are still problems with quantifying biphenyl structures [170].

1.5.1.2 Periodate oxidation

Periodate oxidation is a technique based on the oxidation of guaiacyl phenolic compounds with aqueous sodium periodate solution to *ortho*-quinone structures [172, 173, 174]. This results in a concomitant release of an almost equimolar amount of methanol (Figure 1.34). By measuring the methanol yield, the level of free phenolic guaiacyl groups in a lignin can be determined. One significant advantage is that the periodate method can be applied to *in situ* wood lignins, as well as isolated lignins [175, 176, 177]. However, no information about the proportions of condensed and uncondensed free phenolic groups in the lignin are imparted.

A specific drawback of the method is that it only measures phenols with an *ortho* methoxyl substituent, meaning that catechol and *p*-hydroxyphenyl structures are not measured.

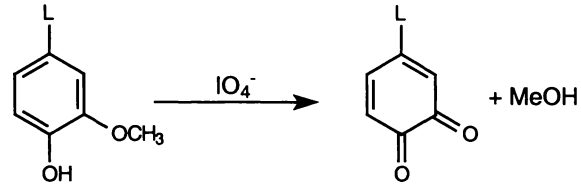

Figure 1.34: Oxidation of guaiacyl structures by periodate [174].

1.5.1.3 Aminolysis

In the presence of pyrrolidine, phenolic acetates in acetylated lignins are deacetylated much more rapidly than aliphatic acetates (Figure 1.35) [178, 179, 180].

Deacetylation of phenolic acetates

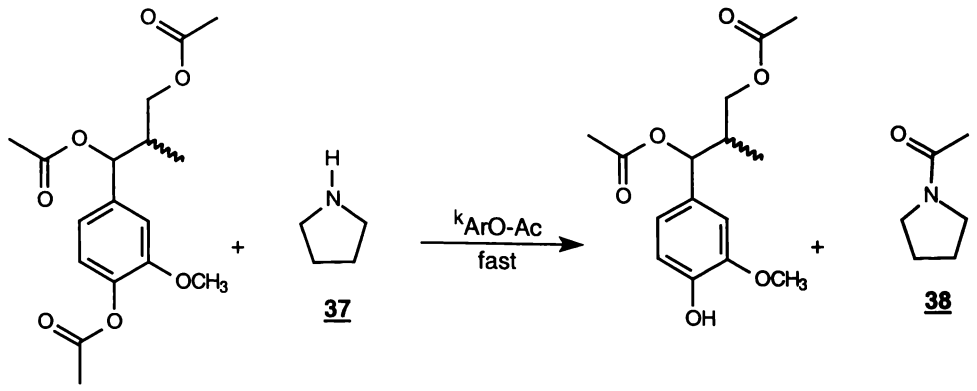

Deacetylation of aliphatic acetates

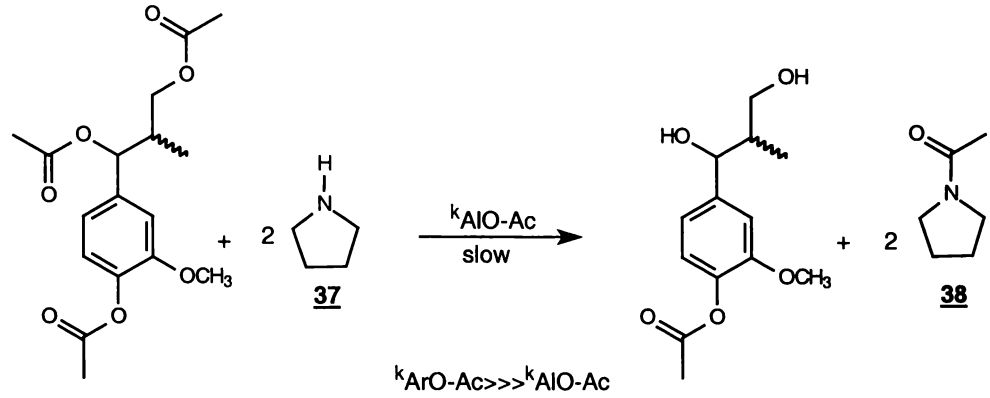

Figure 1.35: Aminolysis reaction of phenolic and aliphatic acetates.

The main product of the reaction, N-acetyl pyrrolidine 38, is determined by gas chromatography (GC) as a function of time [174, 178, 180]. By plotting the yield of N-acetyl pyrrolidine 38 as a function of time, and extrapolating the linear (later) part of the curve back to zero time, the level of rapidly deacetylated phenolic acetates can be determined.

Whilst aminolysis provides information about the total amount of phenolic hydroxyl groups present in the lignin, it does not impart any information about the nature of the phenolic groups. Another drawback of aminolysis is that it is a time consuming and tedious method to perform.

1.5.1.4 Quantitative carbon-13 NMR spectroscopy

Acetylation of lignin, followed by acquisition of a quantitative ^{13}C NMR spectrum, can be used to determine hydroxyl concentrations for isolated lignin samples [66, 181, 182]. When the hydroxyl groups are acetylated, the carbons of the methyl and carboxyl groups give signals at 20.8 and about 170 ppm respectively. In these regions of the spectrum there is little or no overlapping with original lignin signals.

Due to their homogeneity and concentration, the intensity of these acetyl signals is high compared with other signals in the spectrum (Figure 1.36) [66]. This makes analysis of hydroxyl content by quantitative ^{13}C NMR spectroscopy particularly useful.

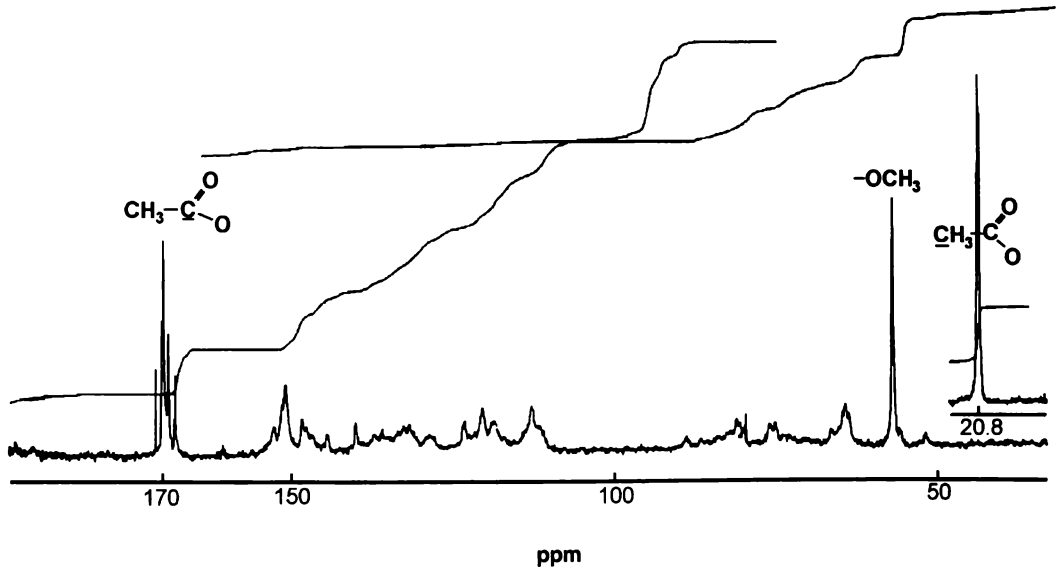

Figure 1.36: ^{13}C NMR spectra of acetylated spruce MWL [66].

For ^{13}C NMR spectra of acetylated lignins acquired at high field, that is above 50 MHz for the carbon, the resolution of the signals of the acetyl carboxyl carbons is sufficient to allow separate estimation of primary aliphatic, secondary aliphatic and phenolic acetyl groups (170.8, 170 and 168.9 ppm respectively, Figure 1.37) [66, 181]. However, there is no differentiation between the uncondensed and condensed guaiacyl units.

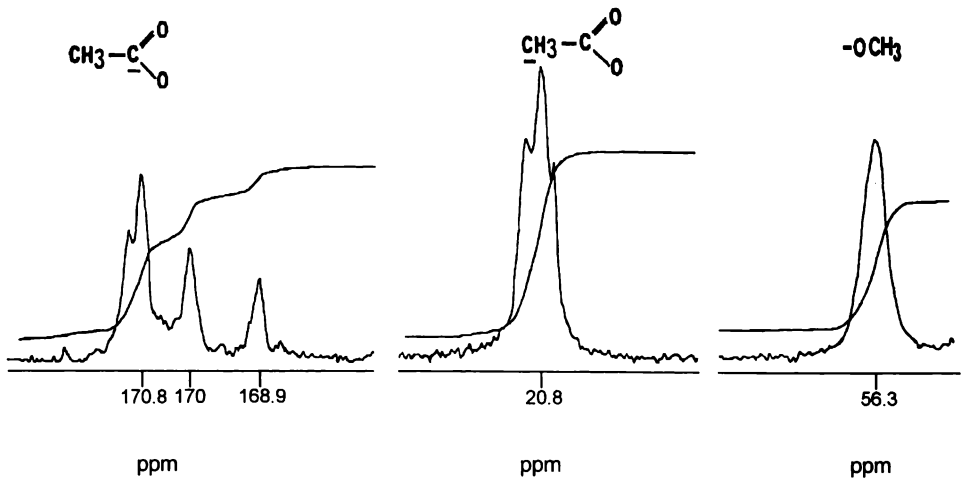

Figure 1.37: Expanded regions of carboxyl, methyl and methoxyl signals from Figure 1.36 [66].

1.5.1.5 Phosphorus-31 NMR spectroscopy

In recent years, a number of different magnetic resonance techniques like ^{13}C (see above), ^{1}H [183] and ^{19}F [184] NMR spectroscopy have been used for the determination of free phenolic groups in lignin. Of particular interest is the development of solution state ^{31}P NMR spectroscopy, to elucidate structural details of phosphorus derivatised lignocellulosic materials [185, 186, 187, 188, 189].

Phosphorus-31 is a particularly useful nucleus for NMR spectroscopy, due to its 100% natural abundance and a sensitivity only about 15 times lower than that of a proton NMR experiment. Also, whilst the range of ^{31}P chemical shifts is quite large, more than 1000 ppm, organophosphorus compounds give signals within narrow ranges, depending on the oxidation state of the phosphorus [190].

Early work in this field was performed by Verkade's group [191, 192] in the mid-eighties. They determined concentrations of alcohols, phenols and carboxylic acids in coal samples by derivation with various phospholane chlorides, followed by ^{31}P NMR spectroscopy. Their work and literature review suggested that the ^{31}P nucleus is most sensitive to the nature of the adjacent substituents, when present in a 5-membered ring.

More recent work by Argyropoulos *et al.* [185, 188] focussed on using 2-chloro-1,3,2-dioxaphospholane **39** as a derivatising reagent for lignin samples. Their technique involved derivatisation of hydroxyl groups in the lignin with 2-chloro-1,3,2-dioxaphospholane **39** (Figure 1.38), followed by ^{31}P NMR spectroscopy [185, 193]. Of particular note is that the phosphorus atom in the resultant phosphite ester is surrounded by 3 oxygen atoms. This ensures that the ^{31}P NMR spectroscopy signals from such derivatives appear as singlets, with no coupling information. Also, by employing gated decoupling of the protons in collection of these ^{31}P NMR spectra, the intensity distortions, due to the Nuclear Overhauser Effect (NOE), can be minimised.

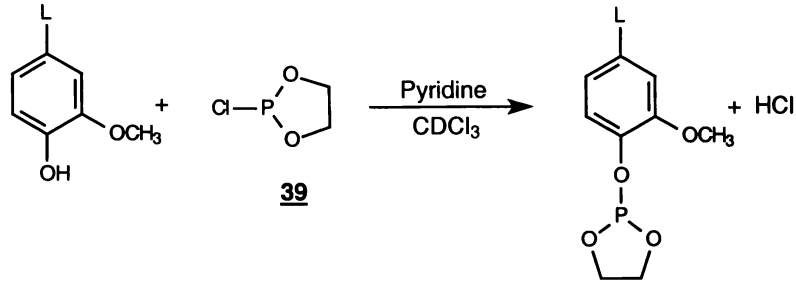

Figure 1.38: Derivation of a free phenolic hydroxyl group with 2-chloro-1,3,2-dioxaphospholane (39).

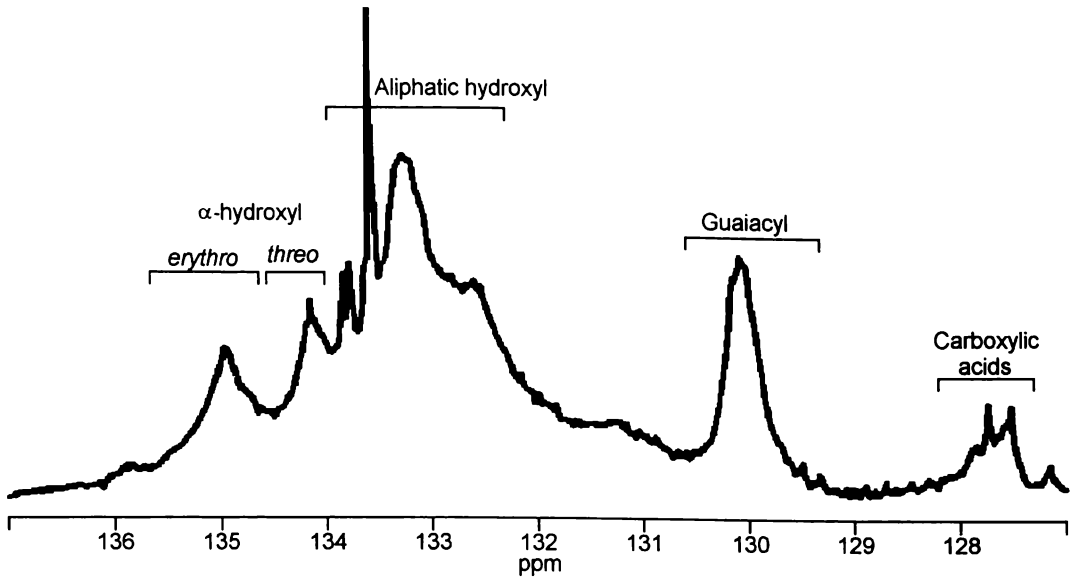

Figure 1.39: Spectrum of phosphitylated (2-chloro-1,3,2-dioxaphospholane) spruce MWL [187].

Figure 1.39 shows a typical spectrum of a spruce MWL derivatised with 2-chloro-1,3,2-dioxaphospholane **39**. A clear distinction can be made between the aliphatic and phenolic hydroxyl groups in the lignin. Quantification was performed by calculating the integral of the regions of signal associated with the different hydroxyl groups, relative to the added internal standard, dimethyl-L-tartrate.

In this thesis, a sterically hindered version of 2-chloro-1,3,2-dioxaphospholane **39** was used, namely 2-chloro-4,4,5,5-tetramethyl-1,3,2-dioxaphospholane **41** (Figure 1.40). The benefit of using the tetramethyl-dioxaphospholane **41** was a significant improvement in the resolution of the phenolic region of the ^{31}P NMR spectra, 7.5 *vs.* 3 ppm [189]. This improved resolution in the phenolic region comes at the expense of fine detail about the aliphatic hydroxyl groups. However, because the aim in this work was to focus on quantification of phenolic structures, 2-chloro-4,4,5,5-tetramethyl-1,3,2-dioxaphospholane **41** was most suitable.

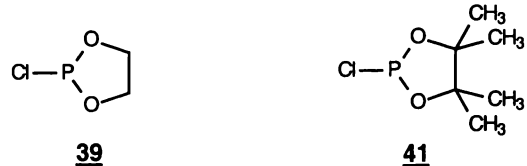

39 **41**

Figure 1.40: A comparison of 2-chloro-1,3,2-dioxaphospholane (39) and 2-chloro-4,4,5,5-tetramethyl-1,3,2-dioxaphospholane (41).

Several factors significantly affect the ^{31}P NMR chemical shift of the post derivatisation phosphite ester [190, 191, 194]. One factor is the effect of hybridisation of the carbon atom adjacent to the derivatised oxygen. Phenols and carboxylic acids, where the adjacent carbon is sp^2 hybridised, generally exhibit a chemical shift in the range of 134-144.5 ppm [194]. On the other hand, where the carbon atom adjacent to the derivatised oxygen is sp^3 hybridised, as for aliphatic hydroxyls, the signal comes at a lower field, in the range 144.5-150 ppm [194].

For phosphitylated phenolic moieties, the difference in the ^{31}P chemical shift, is predominantly due to the nature of the groups attached *ortho* to the phenolic group [194]. *Para* and *meta* substituents have little effect on the chemical shift observed after phosphitylation [194]. It is this chemical shift difference, arising from the effect of the substituents in the *ortho* position, that allows the levels of condensed and uncondensed guaiacyl units to be determined (Figure 1.41).

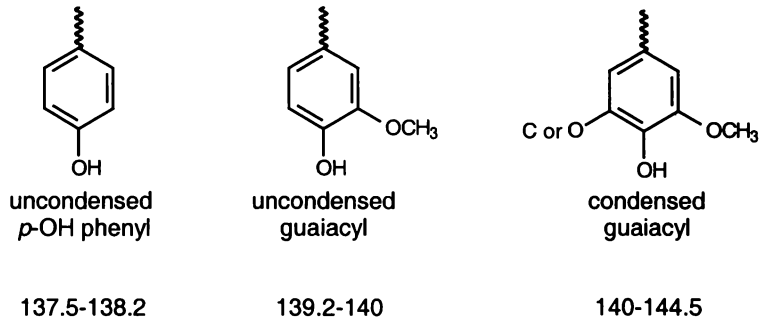

	uncondensed *p*-OH phenyl	uncondensed guaiacyl	condensed guaiacyl
$\delta^{31}P$	137.5-138.2	139.2-140	140-144.5

Figure 1.41: Chemical shift ranges of common lignin structures [194].

This dependence on *ortho* substitution, means that structural determination by ^{31}P NMR spectroscopy, does not reveal information about the levels of β-β and β-1 type condensed structures in the lignin. The ^{31}P signals from these phosphitylated structures are indistinguishable from those of guaiacyl-type signals.

Figure 1.42 shows a typical spectrum of milled wood lignin phosphitylated with 2-chloro-4,4,5,5-tetramethyl-1,3,2-dioxaphospholane **41**, with cholesterol **40** as an internal standard. Signals associated with aliphatic hydroxyl and phenolic hydroxyl groups remain well separated. Also, for the phenolic groups, clear regions of signal associated with *p*-hydroxyphenyl, uncondensed guaiacyl and condensed guaiacyl may be seen. The ^{31}P NMR spectroscopy technique, as described above, may be used

to determine the proportions of condensed and uncondensed structures present as free phenolic groups in the lignin [189, 194].

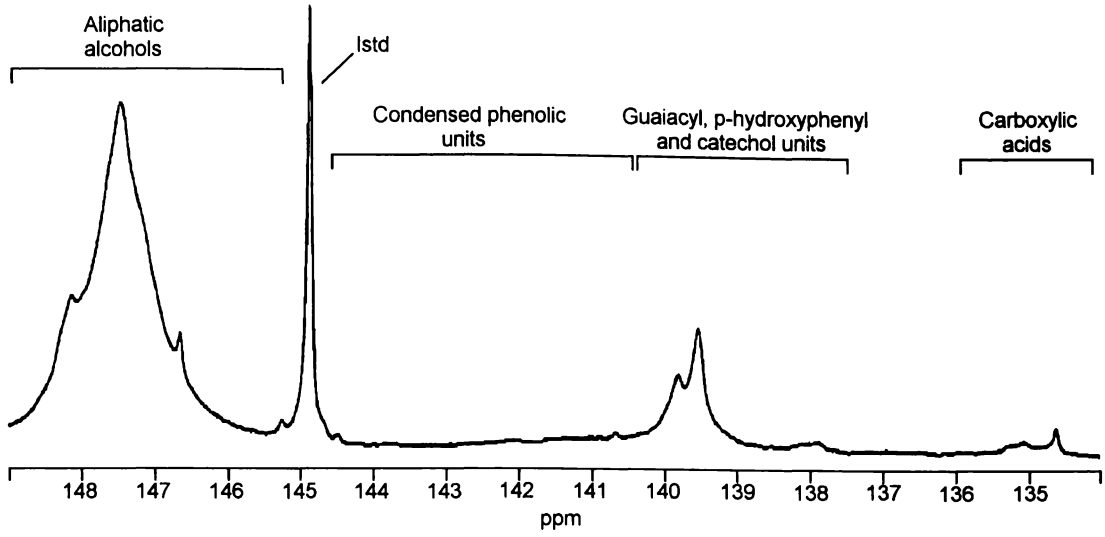

Figure 1.42: Spectra of phosphitylated (2-chloro-4,4,5,5-tetramethyl-1,3,2-dioxaphopholane) *Pinus radiata* MWL [189].

1.5.2 Degradation studies

Many analytical techniques focus on depolymerisation of lignin in a defined way, to yield low molecular weight degradation products. The resultant low molecular weight mixture is then analysed and used to yield structural details about the original lignin. Several analytical techniques have not been included in this review, these include:

- Ozonolysis [195], which involves degradation of the aromatic ring, to yield information about the phenyl propane side chain. It is therefore not used for determining the nature of phenolic groups.
- Hydrogenolysis [196], which is historically significant, as it was the first technique where products contained the complete C_6C_3 structure. Also, many of the condensed inter-unit linkages were left intact. However, hydrogenolysis is rarely used these days, due to the complex product mixture produced.

A summary of some of the more important current techniques in lignin chemistry is provided below.

1.5.2.1 *Oxidative degradation*

Oxidative degradation involves selective degradation of the aliphatic side chains attached to aromatic moieties, by reaction with a sodium periodate/permanganate mixture, followed by hydrogen peroxide (Figure 1.43) [51, 63, 197, 198]. Due to the severity of these oxidations, methylation of the free phenolic hydroxyl groups is required prior to oxidation, to prevent oxidation of the aromatic rings. This means, that although this method gives detailed quantitative information about the free phenolic units in lignin, it gives no information about etherified phenolic structures [197].

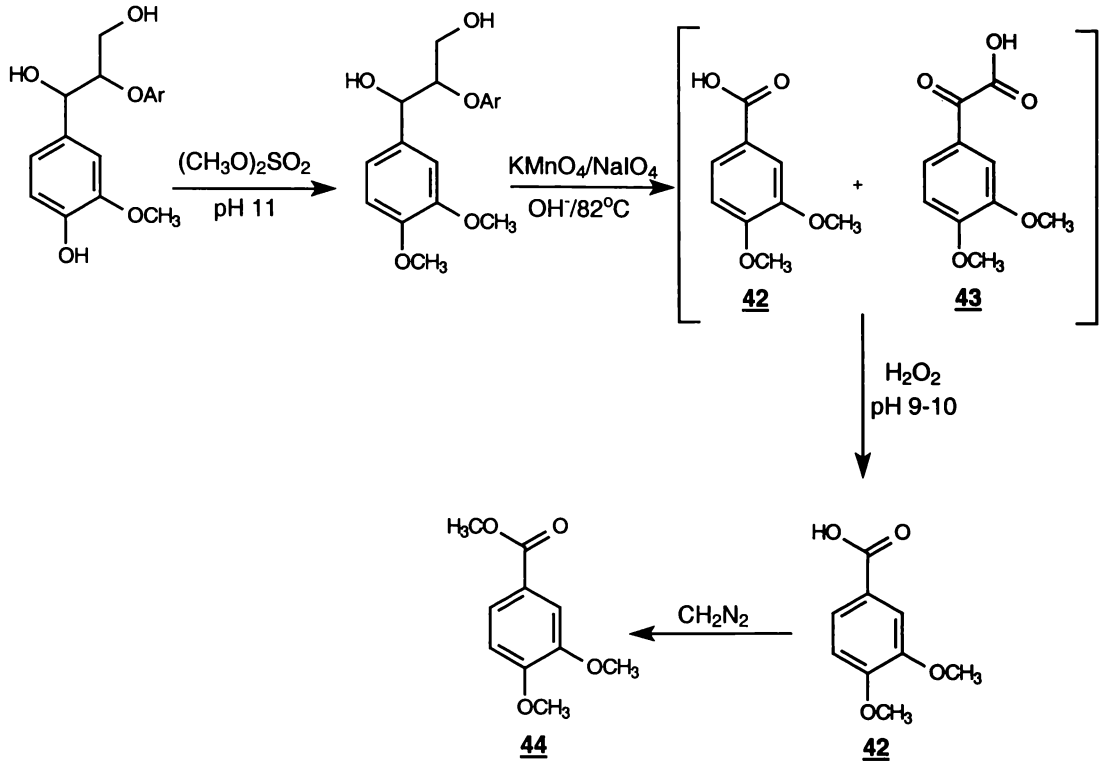

Figure 1.43: Chemistry of oxidative degradation of a guaiacyl free phenolic unit [63].

Oxidative degradation yields a simple mixture of aromatic carboxylic acids, including uncondensed *p*-hydroxyphenyl, uncondensed guaiacyl, 5-5 condensed guaiacyl and 4-O-5 condensed guaiacyl acids (Figure 1.44) [63, 197].

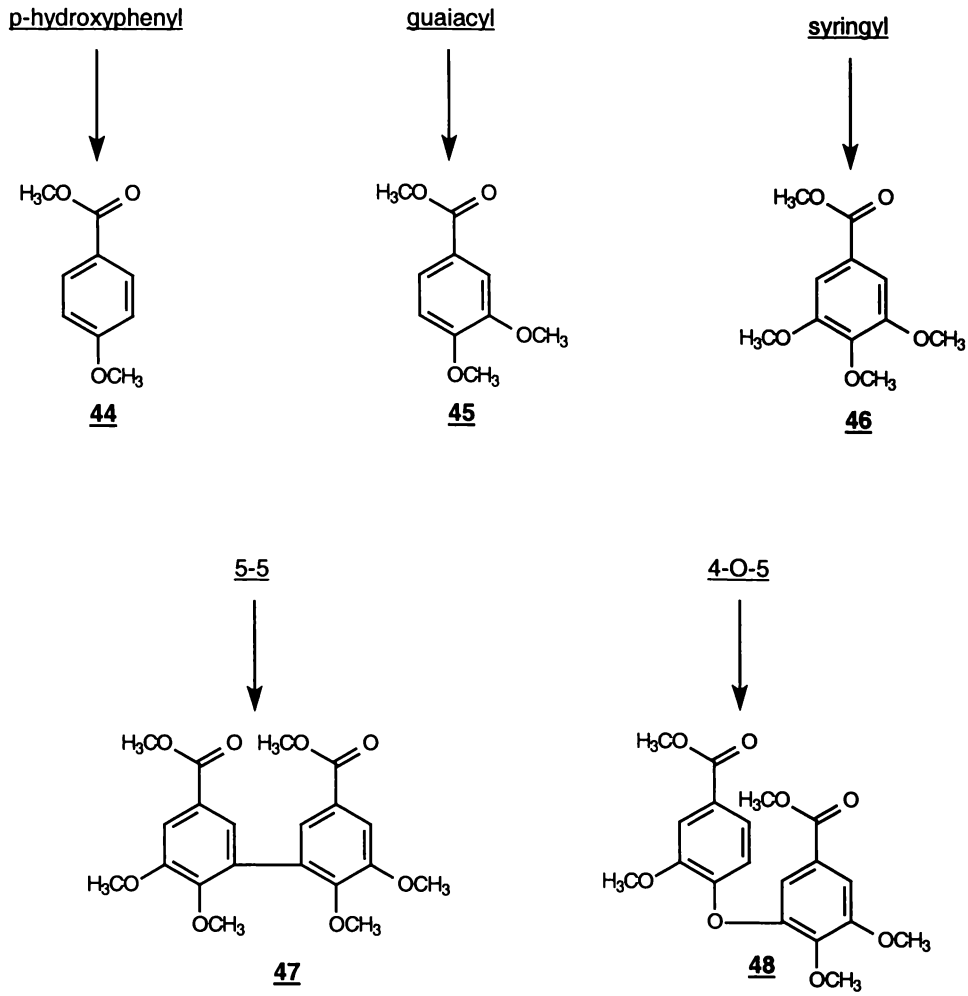

Figure 1.44: Major carboxylic acid methyl esters recovered from softwood lignin oxidation with potassium permanganate [197].

The methoxyl substituted aromatic carboxylic acids (e.g. 42) are methylated and analysed by GC (Figure 1.43). The major degradation products obtained by permanganate oxidation, reflect the distribution of the various types of uncondensed phenylpropane and condensed phenylpropane units in a lignin sample. However, due to the degradation of side chains during oxidative degradation, all phenylcoumaran structures are destroyed.

1.5.2.2 Nitrobenzene oxidation

Similar, but less detailed information to that of oxidative degradation, may be gained from the degradation of lignin with nitrobenzene in hot aqueous alkali [63, 198, 199, 200]. Nitrobenzene oxidations yield a mixture of monomeric aldehydes and acids (Figure 1.45). Softwood lignins predominantly give rise to vanillin 36 and vanillic acid 49 upon nitrobenzene oxidation. In addition, small amounts of *p*-hydroxybenzaldehyde 50 and *p*-hydroxybenzoic acid 51 are recovered. Typically,

around 24-28% vanillin 36 yield, based on Klason lignin content, has been reported for softwoods [199]. For hardwood lignins, on the other hand, the syringyl monomers syringaldehyde 52 and syringic acid 53 are found in the nitrobenzene oxidation products.

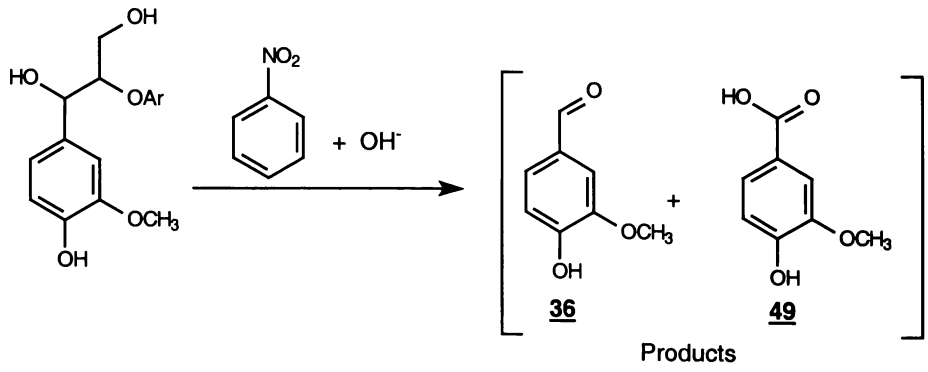

Figure 1.45: Reaction of lignin during nitrobenzene oxidation.

With such results, nitrobenzene oxidations are useful for determining the amounts and relative proportions of uncondensed *p*-hydroxyphenyl, uncondensed guaiacyl and syringyl units in lignin. In particular the G/S ratio of a lignin sample is easily determined using the equation below.

$$\frac{\text{vanillin + vanillic acid}}{\text{syringaldehyde + syringic acid}} \longrightarrow \frac{G}{S} \text{ ratio}$$

Monomer determination is commonly performed by GC or GC/MS on the trimethylsilyl (TMS) derivatives of the nitrobenzene oxidation products.

Like permanganate oxidations, much information about the lignin structure is lost due to the severity of oxidation and side chain degradation. However, 5-5 coupled structures, such as dehydrodivanillin 54 and dehydrodiveratric acid 55, have been reported [199]. This allows some information about the condensed structures in lignin to be obtained.

1.5.2.3 Nucleus exchange

Nucleus exchange is an analytical technique that has been used to determine uncondensed structures in lignin [201, 202, 203]. As applied to softwood lignin, the nucleus exchange reaction quantitatively converts the non-condensed phenyl nuclei to guaiacol **56** and catechol **57**. The TMS derivatives of these products are separated and determined by GC, allowing the amount of uncondensed phenyl nuclei in the original lignin to be determined.

The nucleus exchange reaction includes alkylation and dealkylation in the presence of boron trifluoride and excess phenol (Figure 1.46). The reaction consists of three steps: first, formation of diphenylmethane-type structures by phenolation of the side chain; second, the exchange of a lignin phenyl nucleus for phenol and finally demethylation of guaiacol **56**.

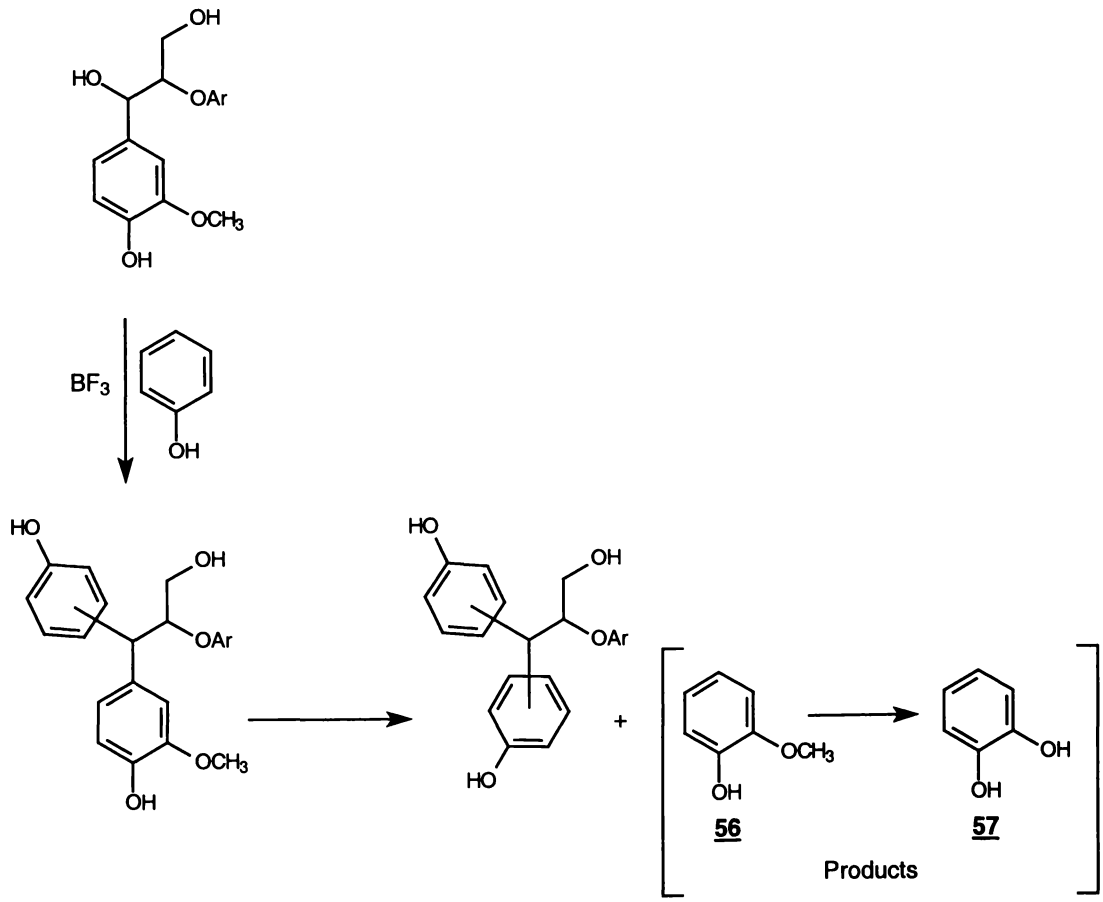

Figure 1.46: Formation of guaiacol (56) and catechol (57) during nucleus exchange [201].

1.5.2.4 Acidolysis

In acidolysis, lignin is heated to 90-95°C with 0.2 M hydrochloric acid in dioxane-water (9/1, v/v) [204, 205, 206, 207]. This causes the selective cleavage of arylglycerol-β-aryl ethers and other labile ether linkages. The resulting low molecular weight degradation products may then be characterised, by the GC analysis, as TMS derivatives. The amounts and types of monomers recovered impart information about the original lignin sample.

In comparison to degradative methods such as nitrobenzene oxidation, in which the C_6C_3 phenylpropanoid skeleton is broken down to C_6C_1 compounds, acidolysis leads to products that retain much of their C_6C_3 nature [63, 205, 208]. Due to this, acidolysis studies have offered evidence for the occurrence of structural elements in the lignins of the β-O-4, β-5, β-β, β-1 and cinnamyl aldehyde types, amongst others [209, 210]. While the identification of dimeric acidolysis products is possible, routine analytical procedures have been developed only for monomeric acidolysis products. Figure 1.47 shows most of the acidolysis monomers, which have been detected in either hardwoods or softwoods [205].

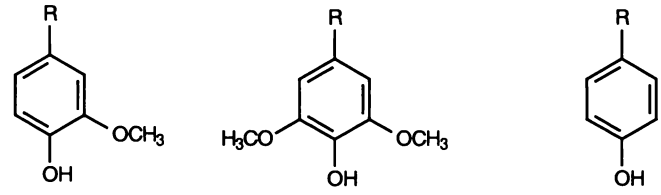

			R
✓	✓	✓	$-CH_2COCH_2OH$
✓	✓	✓	$-CH(OH)COCH_3$
✓	✓	✓	$-COCH(OH)CH_3$
✓	✓	✗	$-CH_2COCH_3$
✓	✓	✓	$-COCOCH_3$
✓	✓	✓	$-CH_2CHO$
✓	✓	✓	-CHO
✓	✓	✓	-COOH
✓	✓	✓	-CH=CHCHO
✓	✗	✓	-CH=CHCOOH

Figure 1.47: Monomeric products from acidolysis [205].

Acidolysis proceeds *via* an S_N1 type mechanism, with the formation of a carbocation intermediate before ether bond cleavage occurs [206, 207, 211]. An unfavourable consequence of this, is that in an acidic medium and at high temperatures, this intermediate benzylic carbocation can undergo condensation reactions. A second unfavourable feature of the acidolysis procedure is that, due to the acidic conditions used, product side chain rearrangement can occur. These unfavourable side reactions lead to a decreased yield and increased complexity of monomers being recovered from the arylglycerol ether splitting.

1.5.2.5 Thioacetolysis

Like acidolysis, depolymerisation of lignin in thioacetolysis proceeds through the cleavage of arylglycerol-β-aryl ether linkages [63, 212, 213]. The thioacetolysis procedure was developed to try to avoid the condensation reactions observed during acidolysis [206, 212]. Treatment of the lignocellulosic material with thioacetic acid and boron trifluoride, converts the arylglycerol-β-aryl ether unit *via* the benzylic carbocation into a S-benzyl thioacetate (Figure 1.48), limiting unfavourable condensation reactions [63, 213]. This is followed by a saponofication reaction, with NaOH, to create a benzyl thiolate ion. From this structure, the β-aryloxy group is lost through nucleophilic attack of the neighbouring thiolate ion to give an episulphide. In the final step, treatment with Raney Nickel removes the sulphur groups to yield the final product. These products are then analysed by GC and allow determination of the levels of β-aryl ethers in the lignin.

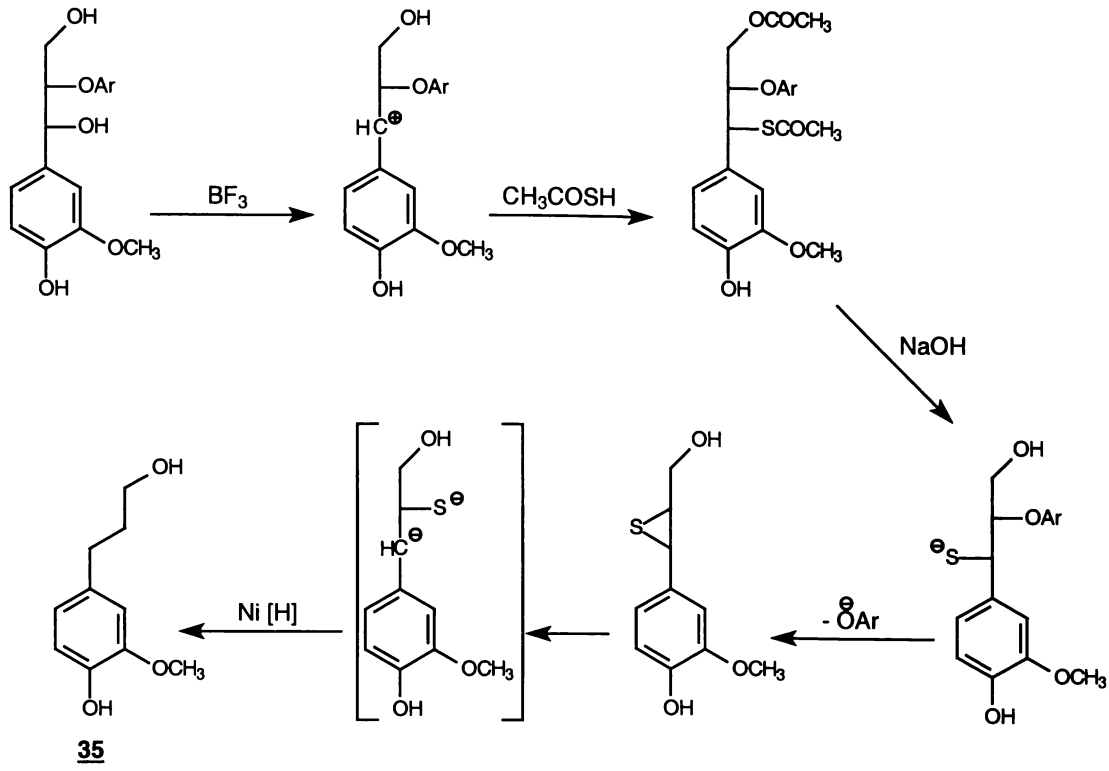

35

Figure 1.48: Degradation of a lignin structure by thioacetolysis [213].

1.5.2.6 Thioacidolysis

As a further extension of thioacetolysis, Lapierre *et al.* [207, 214, 215, 216, 217] developed the thioacidolysis procedure. Thioacidolysis combines a hard Lewis acid, boron trifluoride, and a soft nucleophile, ethane thiol, under anhydrous conditions to depolymerise lignin [218, 219]. Like acidolysis and thioacetolysis, depolymerisation of lignin in thioacidolysis proceeds mainly through the cleavage of arylglycerol-β-aryl ether linkages. It leads to formation of thiolated monomers, dimers and oligomers, almost all of which are free phenolic [207, 214, 215, 216].

The main benefit of thioacidolysis is that the mixture of monomeric products is far less complex than the products generated by acidolysis [207, 214]. The second benefit is that, due to the avoidance of unfavourable side reactions, monomeric yields are significantly higher for thioacidolysis than for acidolysis [207, 214]. This allows for a much better estimation of the arylglycerol-β-aryl ether bonds in lignin.

The resultant monomeric product for uncondensed guaiacyl structures is predominantly 1-(4-hydroxy-3-methoxyphenyl)-1,2,3-(tris thioethyl) propane 58 (Figure 1.49) [215]. For syringyl and *p*-hydroxy structures, the products are 1-(4-

hydroxy-3,5-dimethoxy phenyl)-1,2,3-(tris thioethyl) propane 59 and 1-(4-hydroxyphenyl)-1,2,3-(tris thioethyl) propane respectively 60 [215]. Determinations of these monomeric products by GC or GC/MS, as the trimethylsilyl (TMS) derivatives, allows the amounts of uncondensed *p*-hydroxyphenyl, uncondensed guaiacyl and syringyl β-ethers in the total lignin to be determined.

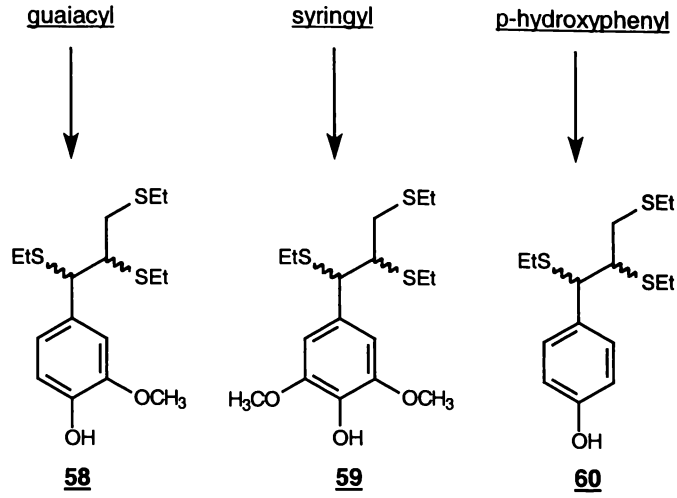

Figure 1.49: Trithioether monomeric thioacidolysis products [215].

The GC chromatogram of the trimethylsilylated derived monomers from thioacidolysis of poplar MWL is shown in Figure 1.50. The monomers derived from the thioacidolysis are, in this case, predominantly located in the pairs of G and S peaks of the chromatogram (11 and 13, Figure 1.50), corresponding to the guaiacyl and syringyl derivatives respectively.

One significant advantage of thioacidolysis is that β-ethers can be determined in both MWL and *in situ* lignin samples.

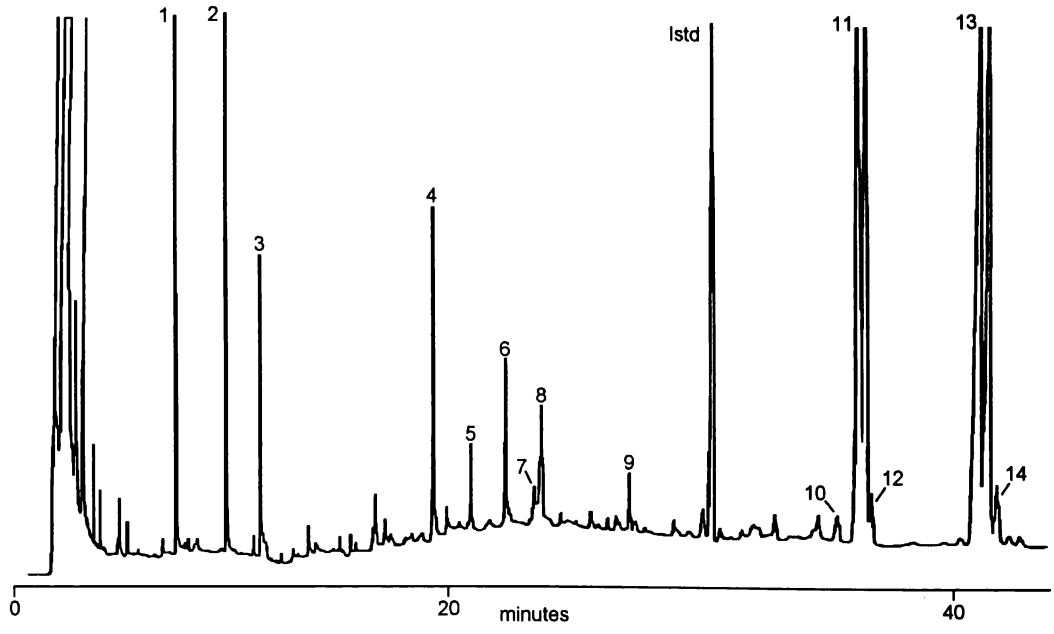

Figure 1.50: GC chromatogram of poplar MWL thioacidolysis product, derivatised with TMS [214].

Cleavage of the arylglycerol-β-aryl ether structures proceeds *via* the mechanism described in Figure 1.51 [207, 214, 216]. Initial reaction occurs through coordination between the vacant orbital on the Lewis acid (BF_3) and the benzylic oxygen (α-OH) to form an oxonium ion. This is followed by nucleophilic attack of EtSH at the activated benzyl carbon, to complete the substitution at Cα through elimination of an OH or ether group. Substitution of Cβ, with ether bond cleavage, takes place through intramolecular attack by the introduced thioethyl group at Cα. The EtSH attacks the cyclic sulphonium intermediate, yielding a pair of *erythro* and *threo* isomers independent of the stereochemistry of the starting material. This *erythro/threo* isomerism leads to the pairs of chromatogram peaks observed in Figure 1.50. Substitution at Cγ then follows by a similar mechanism.

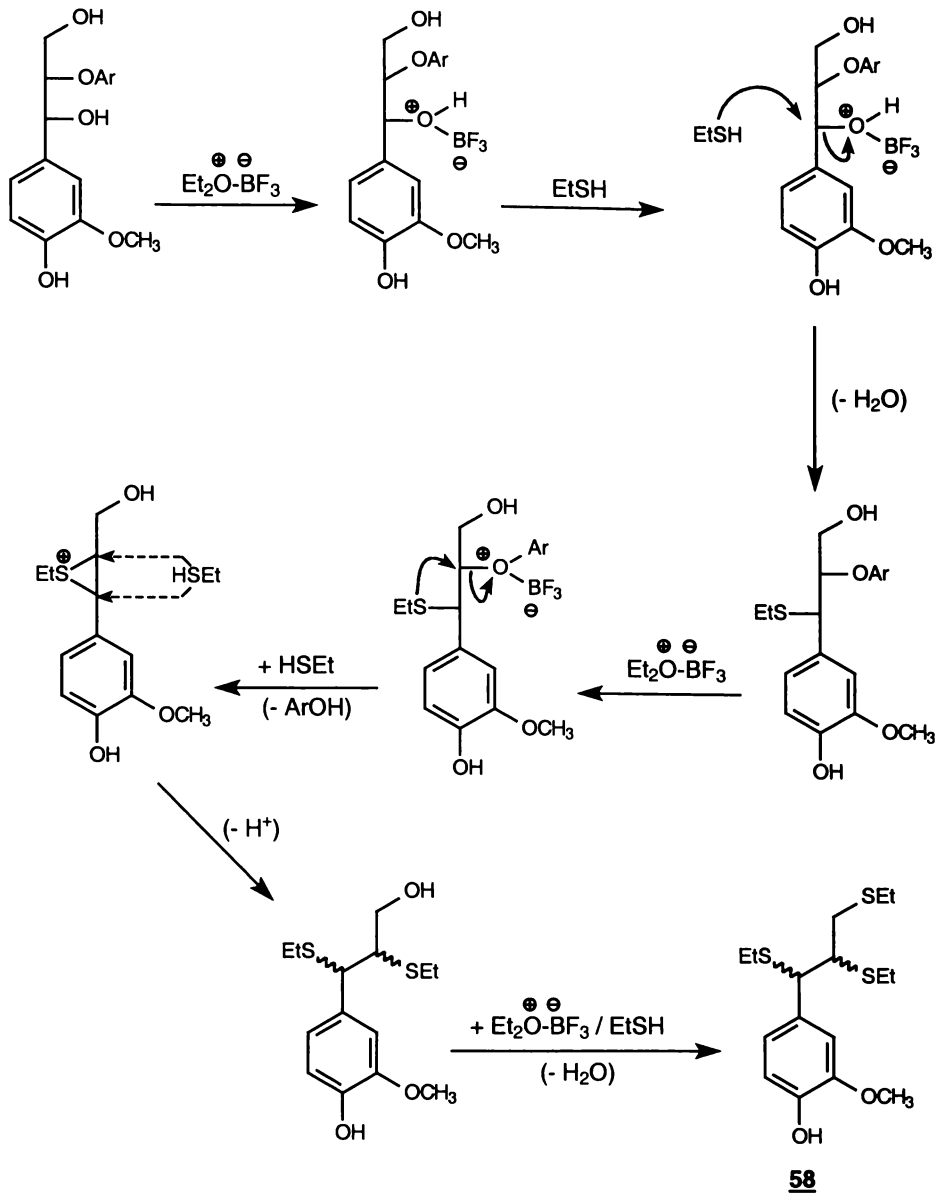

Figure 1.51: Lignin depolymerisation through thioacidolysis [214].

Thioacidolysis can be effectively used to determine the levels of enol ethers in kraft lignins [214, 220, 221, 222]. Thioacidolysis of these structures leads to a C_6C_2 dithioacetal (Figure 1.52). These dithioacetal compounds are also formed in small amounts during the thioacidolysis of arylglycerol-β-aryl ether structures. For this reason, a correction must be applied when using the levels of the dithioacetal, to determine the level of enol ethers in lignin samples [220, 221, 222].

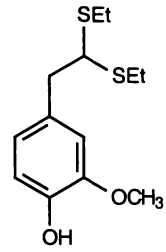

Figure 1.52: Enol ether thioacidolysis product.

Apart from the major monomers recovered, various C_6C_3 and C_6C_2 monomeric products in the thioacidolysis mixture impart much information about the structure of the original lignin sample. Table 1.5 shows some of the structural features in lignin and their thioacidolysis product(s).

Table 1.5: Various phenolic structures and their main thioacidolysis products [214].

Initial Structure	Main Product
C_6C_3 arylglycerol-β-aryl ether	R-CHSEt-CHSEt-CH_2SEt
C_6C_3 β-aryl ether, with α-CO	R-CSEt=CSEt (Z and E)
Cinnamylaldehyde end groups	R-CHSEt-CH_2-CH$(SEt)_2$
Cinnamyl alcohol end groups	R-CHSEt-CH_2-CH_2SEt
C_6C_2 enol ether	R-CH_2-CH$(SEt)_2$

R = *p*-hydroxyphenyl, guaiacyl or syringyl rings.

1.5.2.7 Derivatisation followed by reductive cleavage

Derivatisation followed by reductive cleavage (DFRC) has recently been used to cleave arylglycerol-β-aryl ether linkages in lignin [223, 224, 225, 226]. The analysis of the monomeric products provides similar information about the levels of uncondensed β-ether linkages to thioacidolysis. Results have shown the product mixture from this method to be cleaner than the mixture yielded from thioacidolysis [223, 224]. The observed monomeric yield in the DFRC product mixture, measured by GC, has been shown to be higher than those previously reported for thioacidolysis [223, 224, 225]. The main benefit of the DFRC method is that it does not use the highly malodorous ethanethiol (EtSH) as a reagent.

The initial step in this method involves derivatisation of lignin samples using acetyl bromide, to yield a β-bromo ether (Figure 1.53). This product is then reacted with zinc dust under acidic conditions to reductively cleave the inter-unit ether linkage. After acetylation, the resultant product primarily consists of 4-acetoxycinnamyl acetate, coniferyl diacetate and sinapyl diacetate monomers, from *p*-hydroxyphenyl, guaiacyl and syringyl units respectively.

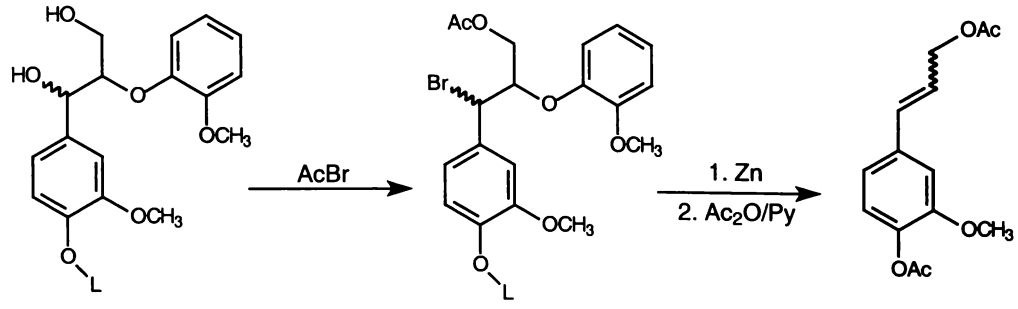

Figure 1.53: Ether cleavage of softwood lignin by the DFRC method [223].

Recently modifications to this technique have been published to allow identification of naturally occurring acetates in lignin [227]. In particular, these modifications involve performing the reactions in the absence of acetates. Bromination is performed by propionyl bromide in propionic acid, with reductive cleavage using zinc in propionic acid and a final derivatisation using propionic anhydride.

1.5.3 Measuring condensed:uncondensed units in lignin

Historically, techniques such as the Fremy salt oxidation [228] and the Mannich reaction [229] have been used to determine the proportions of condensed phenolic C9 units in lignin samples. More recently, techniques such as ^{31}P NMR spectroscopy (Section 1.5.1.6) and oxidative degradation (Section 1.5.2.1) have been used to determine the proportions of condensed and uncondensed free phenolic units in lignin. Fewer techniques are available to determine the proportions of condensed and uncondensed structures in the total lignin. These are discussed below.

1.5.3.1 Thioacidolysis

Although arylglycerol-β-ether linkages are the most abundant inter-unit bonds in lignin and they are quantitatively cleaved by thioacidolysis, there are some bonds that are not broken by thioacidolysis [207, 214, 217, 230]. Examples of inter-unit linkages not cleaved by thioacidolysis are presented in Figure 1.54.

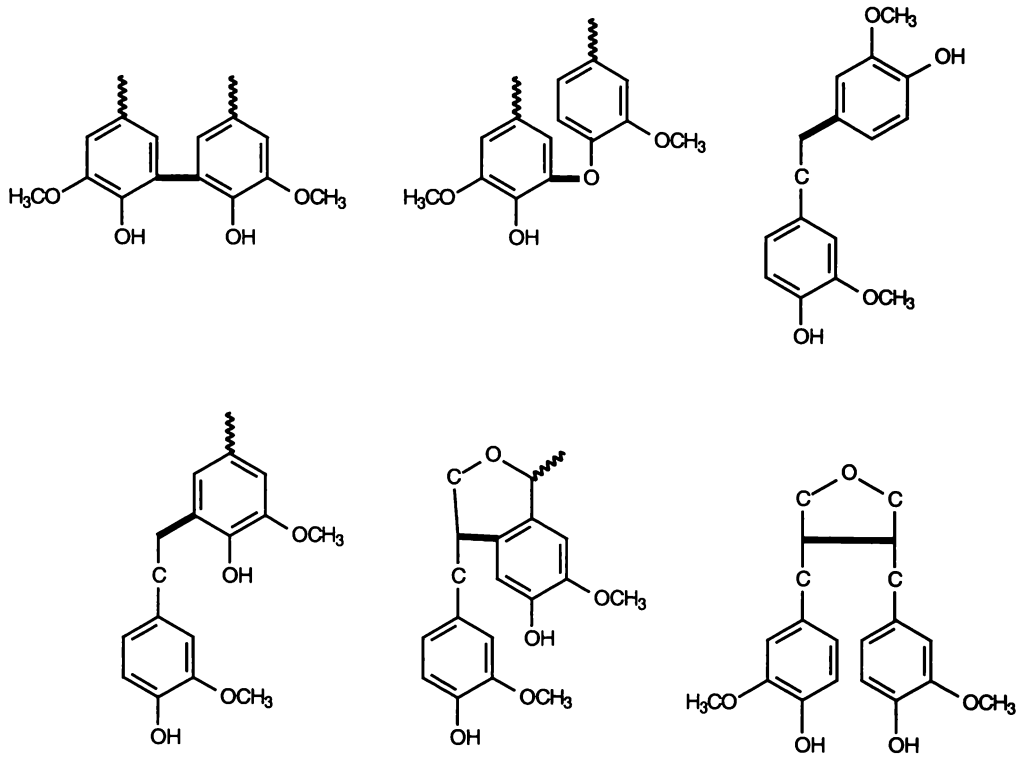

Figure 1.54: Linkages not cleaved by thioacidolysis.

Most of these dimeric products with uncleaved carbon-carbon inter-unit linkages also contain a number of thioethyl groups (e.g. Figure 1.55). Due to their high molecular weight and large number of isomers, these highly thiolated dimers are difficult to analyse by gas chromatography. However, the thioethyl side chains can be cleaved using Raney Nickel desulphurisation. This reduces both the molecular weight and the isomeric forms of the thioacidolysis products [217, 230, 231, 232].

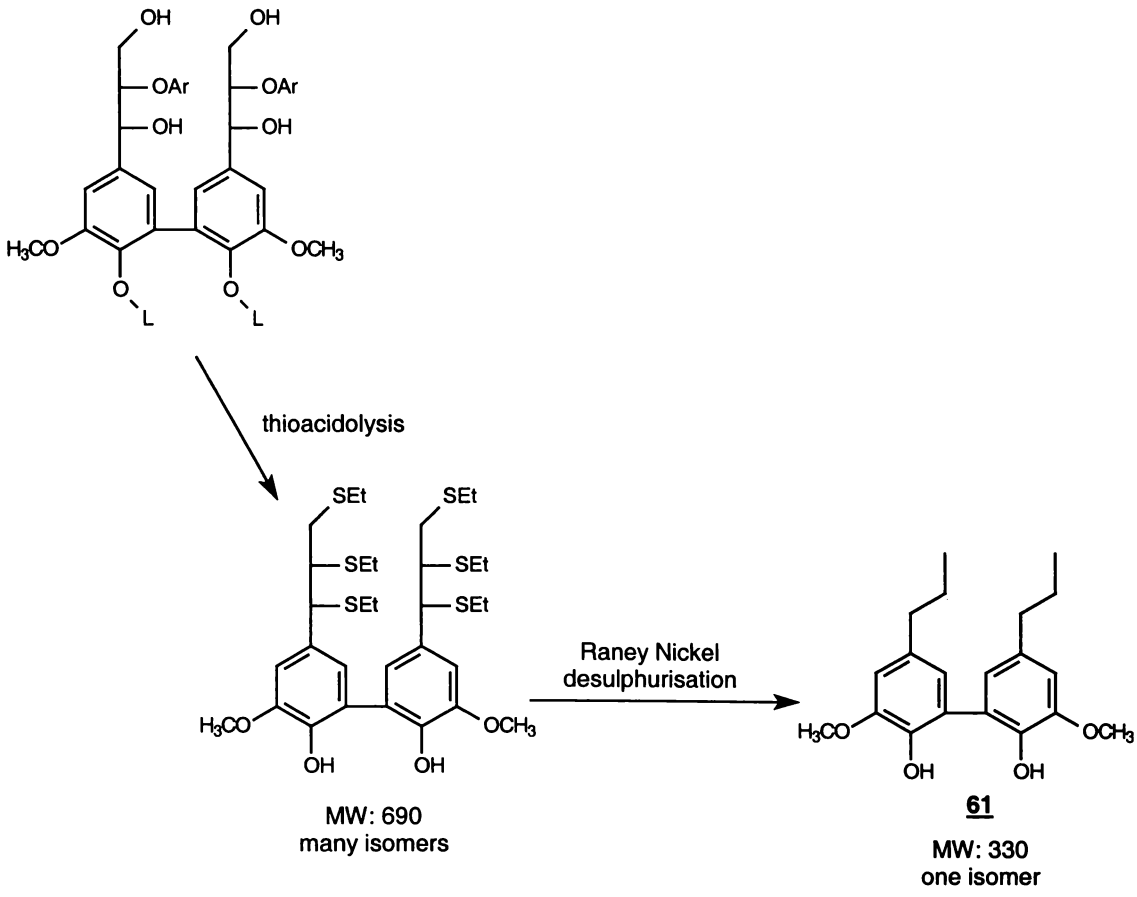

Figure 1.55: Comparison of a biphenyl structure, with and without desulphurisation through Raney Nickel [230].

Analysis of the dimeric products is usually performed after Raney Nickel desulphurisation and silylation by GC or GC/MS [230, 232]. Due to the low number of undesirable condensation reactions occurring during thioacidolysis, the types and levels of dimeric products detected, represent the presence of the corresponding condensed linkages in the original lignin sample. Figure 1.56 shows the GC chromatogram of trimethylsilylated degradation products of spruce MWL. Peaks 1 and 2 represent monomeric thioacidolysis products, whilst peaks 3-13 are peaks of identified dimeric thioacidolysis products, such as the structure shown in Figure 1.55. Clearly the peak splitting due to isomerism is gone, making the resultant chromatogram significantly simpler.

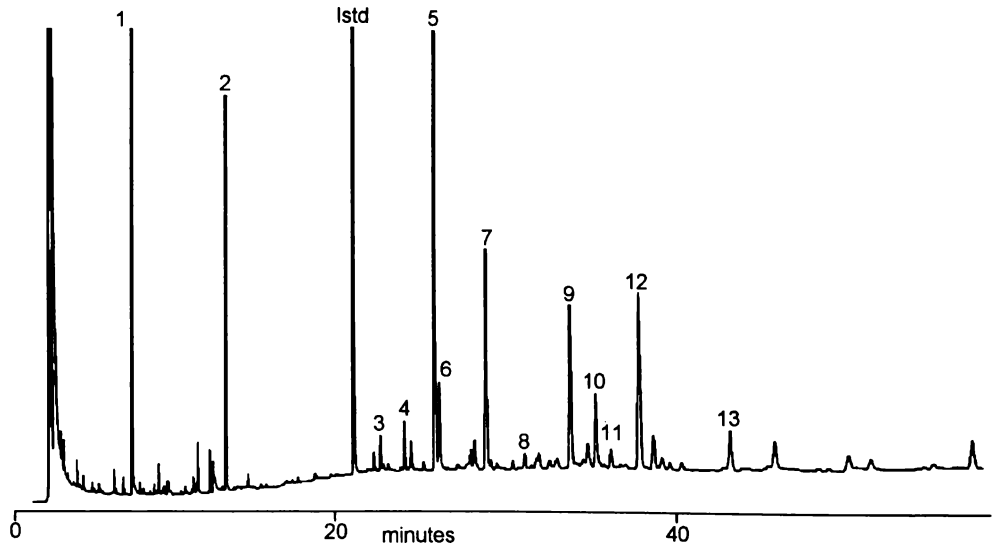

Figure 1.56: GC analysis of spruce MWL after thioacidolysis/Raney nickel desulphurisation, as TMS ethers [232].

The main problem with this analytical method is the low (<10%) yield of dimeric lignin fractions from the hydrogenolysis step. Also, trimeric and tetrameric products are not analysed. Both these issues affect the ability of the thioacidolysis/Raney Nickel procedure to be used to provide quantitative information.

1.5.3.2 DFRC

Peng *et al.* [233] have identified a large number of structures containing carbon-carbon inter-unit linkages in the DFRC product mixture. The dimeric and trimeric reaction products may therefore be analysed by GC to provide similar information to the thioacidolysis/Raney Nickel analysis of lignin inter-unit linkages. However, due to the recent development of the DFRC method, the analysis of dimers by DFRC is currently less developed than that for thioacidolysis.

During the DFRC depolymerisation, all the carbohydrates are dissolved, compared with only a small amount due to the action of thioacidolysis [233]. This presents somewhat of a problem, as a Bio bead separation was required to remove the carbohydrates, prior to analysis of the degraded lignin. Peng *et al.* [233] showed that DFRC degraded products of pinewood (*Pinus taeda*) may be readily analysed by GC/MS for condensed structures once the overwhelming carbohydrates and monomers were removed. The resultant GC chromatogram of condensed structures has been shown to be clean, with good separation of the dimers possible.

Like thioacidolysis, the DFRC method does not analyse the trimeric and tetrameric degradation products, thus affecting the determined yield.

For both thioacidolysis and the DFRC method, a large number of dimeric products are produced. This creates a significant problem, as, for quantitative analysis, a response factor (RF) needs to be determined for each degradation product.

1.5.3.3 Nucleus exchange and nitrobenzene oxidation

A combination of nucleus exchange and nitrobenzene oxidation has been used to determine the proportions of uncondensed guaiacyl, condensed guaiacyl and diphenylmethane structures in kraft lignins [234, 235]. This technique is based on the premise that diphenylmethane structures give nucleus exchange products, but do not give nitrobenzene oxidation products. The difference in product yields from the two techniques reflects the diphenylmethane content of the pulp lignin (diphenylmethane structures negligible in native softwood). Chan *et al.* [236] have shown that some diphenylmethane structures do give nitrobenzene oxidation products, raising questions about the use of nucleus exchange and nitrobenzene oxidation combined.

1.5.3.4 Extended oxidative degradation

By itself, oxidative degradation can only analyse free phenolic condensed and uncondensed structures. However, several modifications have been made to allow such determinations to be made. In particular Tamminen *et al.* [237] and Bose *et al.* [238] have recently extended the "standard" oxidative degradation method, to allow both free phenolic and etherified C9 units to be determined.

Under the normal permanganate degradation (Section 1.5.2.1), free phenolic groups are methylated prior to oxidation to prevent degradation of the aromatic ring. The etherified C9 units are degraded during oxidative degradation. However, by preceding the methylation with an alkaline hydrolysis (e.g. CuO), most of the inter-unit linkages may be cleaved prior to permanganate oxidation. This converts most etherified structures to free phenolic ones. A typical oxidative degradation process (Figure 1.57) involves ethylation of the free phenolic groups, followed by CuO alkaline hydrolysis to cleave most of the inter-unit linkages. The released free

phenolic groups are then methylated and reacted with potassium permanganate to yield the respective acids. The acid products are then methylated and analysed by GC.

By comparing the amounts of condensed and uncondensed ethyl-phenyl and methyl-phenyl ethers, the proportions of structures present as free and etherified phenolic units can be determined.

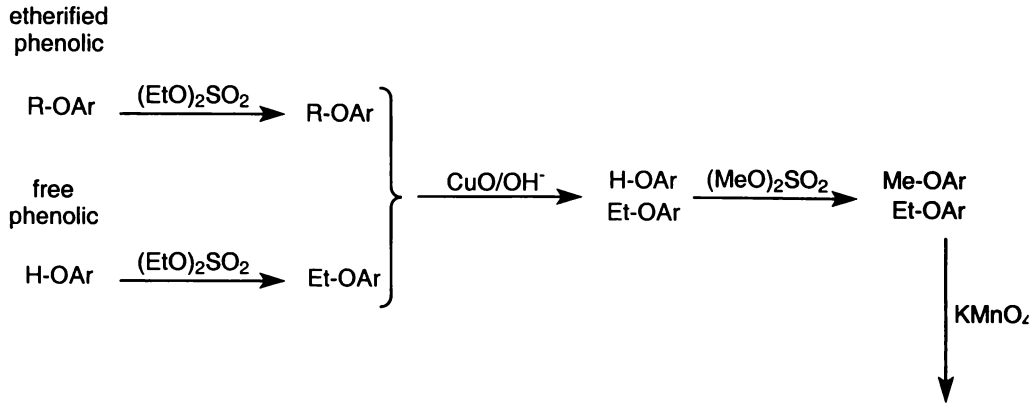

Figure 1.57: Extended oxidative degradation of lignin.

1.5.3.5 Quantitative carbon-13 NMR spectroscopy

Quantitative ^{13}C NMR spectroscopy may also be used to determine the proportion of C5 condensed units in lignin [181, 239, 240, 241]. A combination of Distortionless Enhancement by Polarisation Transfer (DEPT) [242] and Inverse Gated Decoupling (IGD) experiments allows the number of quaternary aromatic carbons to be determined.

The technique involves obtaining a quantitative ^{13}C NMR spectrum using an inverse gated decoupling sequence. Subsequently, quantitative DEPT spectra are collected for CH, CH_2 and CH_3 resonances. After employing small correction factors for the integral intensities, the quantitative DEPT spectra are subtracted from the IGD quantitative ^{13}C NMR spectrum [181, 241]. This yields a resultant spectrum containing signals due to quaternary carbons only. The number of quaternary carbon atoms present, which are neither C1, C4 or methoxylated C3/C5 are considered to be C5 units containing condensed carbon-carbon bonds.

The method suffers, particularly, from the long acquisition times required for the four separate quantitative ^{13}C NMR spectra of a single lignin sample. However, compared to many of the degradative analysis techniques, one of the benefits of this NMR technique is the non-destructive analysis of the lignin sample. Another benefit of this technique is that the collected NMR spectra provide a lot of other information about the lignin.

1.6 The Aim of this Project

As discussed previously (Section 1.4.4), softwood lignin contains both uncondensed (protonated at C5) and condensed (bonded through C5 to other phenyl propane units) guaiacyl moieties. The proportion of these condensed and uncondensed units present in lignin determines, in part, how the lignin will behave during mechanical and chemical processing. In general, the condensed units have a much lower reactivity to pulping and bleaching chemicals than uncondensed units.

There are currently few analytical techniques available that can simultaneously determine the proportions of condensed and uncondensed units in wood and pulp fibre. The aim of this thesis, was to develop a new method, which allows simultaneous quantification of condensed and uncondensed units in *in situ* lignin.

Phosphorus-31 NMR spectroscopy is currently used to determine the proportions of condensed and uncondensed units in lignin. However, the ^{31}P NMR technique is only applicable to isolated lignins and only measures the free phenolic groups. Thus it does not necessarily reflect the proportions of condensed and uncondensed units in the whole sample. This new analytical technique involves lignin depolymerisation and solvation through thioacidolysis, prior to ^{31}P NMR spectroscopy. The thioacidolysis involves depolymerisation of the lignin polymer (Section 1.6.7) by cleaving arylglycerol-β-aryl ether inter-unit linkages, leading to the formation of thiolated monomers, dimers and oligomers, almost all of which are free phenolic. These free phenolic monomers, dimers and oligomers can then be derivatised by 2-chloro-4,4,5,5-tetrametyl-1,3,2-dioxaphospholane **41** and measured by quantitative ^{31}P NMR spectroscopy.

In this thesis, the initial work to check yields and chemical shifts was performed with a range of lignin model compounds. Results from this work are discussed in Chapter 2. Following this model compound work, it was important to establish the applicability of thioacidolysis/^{31}P NMR spectroscopy. In Chapter 4 method development work and validity of the technique are discussed. In particular, the effects of carbohydrates, extractives, technique reproducibility and cooktime optimisation were examined. In Chapter 5, this newly developed technique was applied to a range of isolated and *in situ* lignins.

If we knew what we were doing,
it wouldn't be called research,
would it?

Albert Einstein

Chapter 2
Thioacidolysis and ^{31}P NMR Spectroscopy of Model Compounds

2.1 Introduction

In this chapter, lignin model compounds were used to mimic the behaviour of macromolecular lignin during thioacidolysis and subsequent quantitative ^{31}P NMR spectroscopy. A range of model compounds was prepared according to previously published methods. Details of preparation and identification are contained in Section 6.3. These model compounds, and some compounds obtained commercially, were then subjected to thioacidolysis and their products purified and characterised. Subsequently, the effect of thioethyl incorporation on quantitative ^{31}P NMR spectroscopy of lignin was modeled. This was achieved by comparing the quantitative ^{31}P NMR spectroscopy results, of both the original model compounds and their thioacidolysis products, when derivatised with 2-chloro-4,4,5,5-tetramethyl-1,3,2-dioxaphospholane **41**.

2.1.1 Model compounds

The low molecular weight model compounds are valuable to the lignin chemist because they are easier to manipulate and characterise than native lignin. However, due to the structural diversity of lignin, no single compound can serve as a universal model for lignin, hence a range of model compounds is often used.

In this study, a number of lignin model compounds containing guaiacyl (G), β-5 and 5-5 structural features were prepared. Both phenylethane and phenylpropane model compounds were used. Phenylethane model compounds are less representative of

native lignin than phenylpropane ones, however, they contain no diastereomeric forms and are easier to synthesise. Whilst it would have been desirable to include the use of 4-O-5 model compounds, they were not prepared, due to the time consuming multi-step synthesis required to produce them [243].

Owing to the ^{31}P chemical shift being predominantly influenced by the nature of the substituent group(s) in the position *ortho* to the phenolic hydroxyl [193, 194], it is not possible to quantify inter-unit linkages, which do not involve the C5 position (e.g. β-β, β-1). The ^{31}P NMR chemical shifts of phenolic hydroxyl groups in such β-1 and β-β condensed units are essentially identical to G units [193, 194]. For this reason, β-1 and β-β coupled model compounds were not studied.

2.1.2 Internal standard

An internal standard (ISTD) is a compound incorporated in a fixed concentration into each sample. For ^{31}P NMR spectroscopy the relative signal intensity between the ISTD and the signals of interest allows a concentration determination to be made. Two important features of internal standards used for NMR spectroscopic based work are:

- That they are not present in the original sample.
- That their chemical shift does not interfere with the units being measured.

In this work, cholesterol **62** was used as the ISTD. This offered a number of potential advantages over the cyclohexanol **40**, which was used in earlier work by Granata and Argyropoulos [189] and Jiang *et al.* [194]. Firstly, cholesterol **62** is much less volatile than cyclohexanol **40**. This was important due to the potential loss of material during the thioacidolysis work-up. Secondly, the T_1 of cholesterol **62** derivatised with 2-chloro-4,4,5,5-tetramethyl-1,3,2-dioxaphospholane **41** was shorter than the T_1 observed for phosphitylated cyclohexanol **40**. This allowed a shorter relaxation time to be used. Due to the similar hydroxyl group environment in **40** and **62**, the ^{31}P NMR spectroscopy chemical shifts observed for the two ISTD's were similar. However, the chemical shift of **62** is slightly better resolved from the derivatised aliphatic alcohols, occurring at 144.9 ppm (*cf.* 145.2 ppm for **40**). Finally, cholesterol has the added advantage of being crystalline, hence easier to manipulate. These attributes of cyclohexanol and cholesterol are summarised in Table 2.1 below.

Table 2.1: Comparing key characteristics of cyclohexanol and cholesterol.

	cyclohexanol **40**	cholesterol **62**
molecular weight	100.2	386.6
boiling point	161°C [244]	360°C [245]
δ ^{31}P NMR	145.2	144.9
T_1	2.8	1.3

2.1.3 Polyethylene glycol

Polyethylene glycol (PEG) from the oil bath was frequently found as a contaminant in the model compound thioacidolysis products. It was identified by the presence of a singlet at 3.64 ppm in the ^{1}H NMR spectra of the thioacidolysis products. Also, a ^{31}P NMR signal in the same products, derivatised with the phosphitylating reagent **41**, was observed at 147.2 ppm. These ^{1}H and ^{31}P NMR spectroscopy result are identical to those observed for straight PEG. The contamination meant that crude gravimetric yield determinations often gave results ranging from 120 to 150%. Ways of reducing this contamination were not investigated as PEG did not interfere with the subsequent phosphitylation and ^{31}P NMR spectroscopy of phenolic compounds.

For initial thioacidolysis product identification and accurate gravimetric yield determination, the thioacidolysis products were purified using preparative layer chromatography (plc). In the final, rapid and simple laboratory technique, it was undesirable to purify all samples after thioacidolysis, as the overall goal was to keep the number and complexity of steps to a minimum. Therefore ^{31}P NMR spectroscopy of the thioacidolysis products was performed without chromatographic purification. In some cases, yields determined by ^{31}P NMR spectroscopy and gravimetric techniques differed slightly.

Performing ^{31}P NMR spectroscopy without prior chromatographic purification requires that PEG does not interfere with the ^{31}P NMR spectra of condensed or uncondensed phenolic groups or the ISTD. The ^{31}P NMR signal for **41** derivatised polyethylene glycol at 147.2 ppm overlapped only with the signals due to the aliphatic hydroxyl groups. However, phenolic hydroxyl signals, which fall in the range 137-144.5 ppm, were not affected. With the objective of this study being the quantitative assessment of phenolic groups by ^{31}P NMR spectroscopy, it was therefore not necessary to remove the polyethylene glycol from the thioacidolysis products.

2.2 Thioacidolysis of Model Compounds

Thioacidolysis of the model compounds was performed according to the standard method outlined in Section 6.7.1. For brevity, these reaction conditions are not presented with each individual reaction scheme. This model compound work was particularly important in order to understand how the different functional groups and inter-unit linkages behave during thioacidolysis. The model compounds used were either the product of syntheses discussed in Section 6.3 or were sourced commercially. Details about the structural identification of the different thioacidolysis products are contained in Section 6.7.2.

The yields reported in this Section are gravimetric yields, performed on thioacidolysis products, purified using preparative layer chromatography (plc). The exceptions to this were the β-5 thioacidolysis products (Section 2.2.5), which rapidly underwent acid catalysed phenylcoumaran reformation, preventing plc purification. For these compounds, the yield reported was obtained by quantitative ^{31}P NMR spectroscopy.

2.2.1 Thioacidolysis of α-β unsaturated model compounds

Thioacidolysis of isoeugenol 63 led to HSEt addition across the ring-conjugated double bond (Figure 2.1). Addition of the SEt group occurred solely at the Cα position of the propyl side chain to give a yield of 90%. Lapierre *et al.* [216] observed this same addition for thioacidolysis of coniferaldehyde 33 and coniferyl alcohol 23.

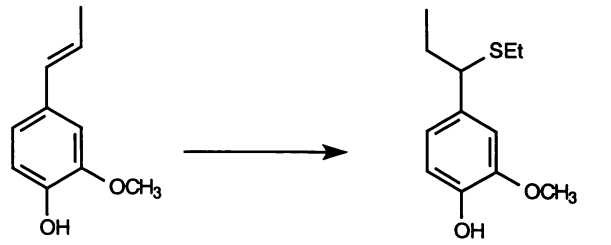

63 64 90%

Figure 2.1: Thioacidolysis of isoeugenol (63).

2.2.2 Thioacidolysis of α-OH model compounds

Compared with the addition of HSEt across an α-β unsaturated bond, model compounds containing an α-hydroxyl group (65 and 66) underwent substitution of the α-hydroxyl with a thioethyl group. This α-substitution with SEt was consistent with that previously reported by Lapierre *et al.* [216] for other model compounds. The thioacidolysis substitution reaction was complete as both 67 and 68, were recovered in excellent yield.

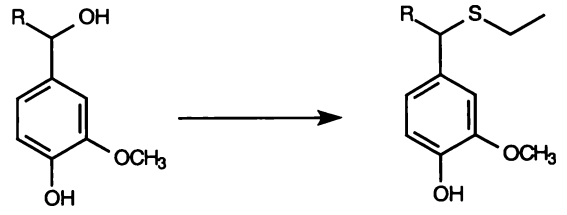

R=H 65 67 89%

R=CH3 66 68 92%

Figure 2.2: Thioacidolysis of α-OH model compounds.

2.2.3 Thioacidolysis of α-carbonyl model compounds

During thioacidolysis, model compounds containing α-ketones, 36 and 69, were found to form dithioacetal substituted products, 70 and 71. Rolando *et al.* [246] have previously reported such dithioacetal formation for benzaldehyde side chains. The 93% yield observed for vanillin was similar to that observed for the three models discussed previously. On the other hand, for acetovanillone, the thioacidolysis procedure was incomplete, with 37% of the starting material remaining unreacted.

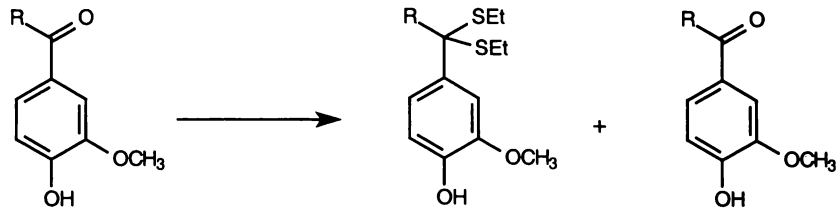

R=H	36	70 93%	-
R=CH_3	69	71 63%	69 37%

Figure 2.3: Thioacidolysis of α-carbonyl model compounds.

2.2.4 Thioacidolysis of 5-5 (biphenyl) model compounds

In all cases, the 5-5 inter-unit linkage remained intact during thioacidolysis. This was consistent with the results observed by Lapierre *et al.* [230, 231, 232]. For the three 5-5 model compounds 72, 73 and 54, the side chain substitution patterns, after thioacidolysis, were identical to those observed for the comparable monomeric products, that is 65, 66 and 36. Excellent recovery yields of between 90 and 95% were observed.

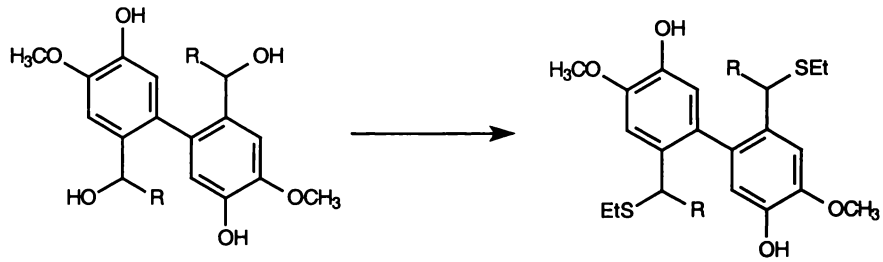

R=H	72	74	93%
R=CH_3	73	75	95%

Figure 2.4: Thioacidolysis of α-OH biphenyl model compounds.

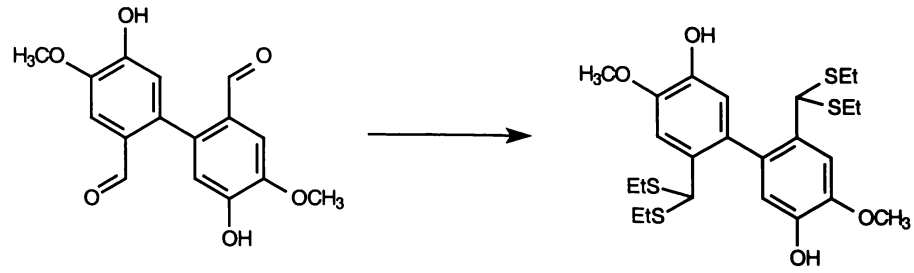

54 76 90%

Figure 2.5: Thioacidolysis of dehydrodivanillin (13).

2.2.5 Thioacidolysis of phenylcoumaran model compounds

Cyclised β-5 structures, such as dehydrodiisoeugenol 77 and dehydrodihydrodiisoeugenol 78, contain two chiral centres, at the A-ring Cα and Cβ. This would imply the presence of four (2^2) diastereoisomers, namely a pair of *erythro* and a pair of *threo* isomers. However, crystallographic work by Ede [247] has shown that only the *erythro* stereochemistry exists in phenylcoumaran structures such as 77. This was consistent with our ^{1}H and ^{13}C NMR spectra, which indicated that 77 and 78 were diastereomerically pure.

Upon thioacidolysis of model compounds 77 and 78, epimerisation at Cα occurred through the addition of a thioethyl group at the α-carbon, with cleavage of the α-O ether linkage in the 5-membered phenylcoumaran ring. However, thioacidolysis did not cleave the β-5 inter-unit linkage in either phenylcoumaran model compound 77 or 78. This resilience of the inter-unit linkage to thioacidolysis was consistent with the results published by Lapierre *et al.* [231, 230, 232].

Thioacidolysis of 78 led to product 79, which contained two chiral carbons, at Cα and Cβ on the A-ring side chain. This led to the formation of four (2^2) isomers, or two diastereomeric pairs (Figure 2.6). However, for the thioacidolysis of dehydrodiisoeugenol 77, as well as epimerisation at the A-ring Cα, thioethyl addition occurred at the Cα in the B-ring side-chain. This introduction of two thioethyl groups led to the presence of three asymmetric centres in product 80, with eight (2^3) isomers or four diastereomeric pairs.

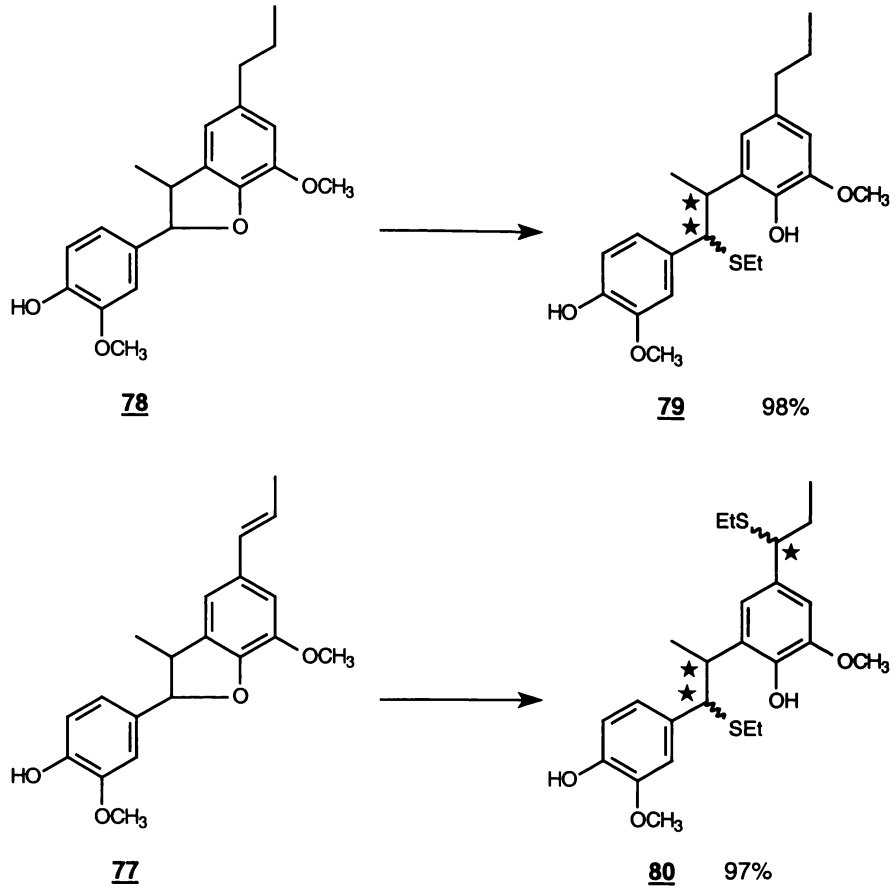

Figure 2.6: Thioacidolysis of phenylcoumaran model compounds (top) dehydrodihydrodiisoeugenol and (bottom) dehydrodiisoeugenol.

For thioacidolysis products 79 and 80, separation of the diastereomeric pairs was not possible, due to their rapid decomposition. This low stability was primarily due to the ability of 79 and 80 to undergo acid catalysed elimination of the thioethyl group on the α-carbon of the A-ring, with reformation of the α-O bond, yielding 81 (Figure 2.7). Presumably this reaction occurred because the thioethyl unit is a good leaving group under acidic conditions [248]. The decomposition proceeded so easily, that trace concentrations of HCl in deuterochloroform had to be removed using aluminium oxide prior to NMR spectroscopic analysis.

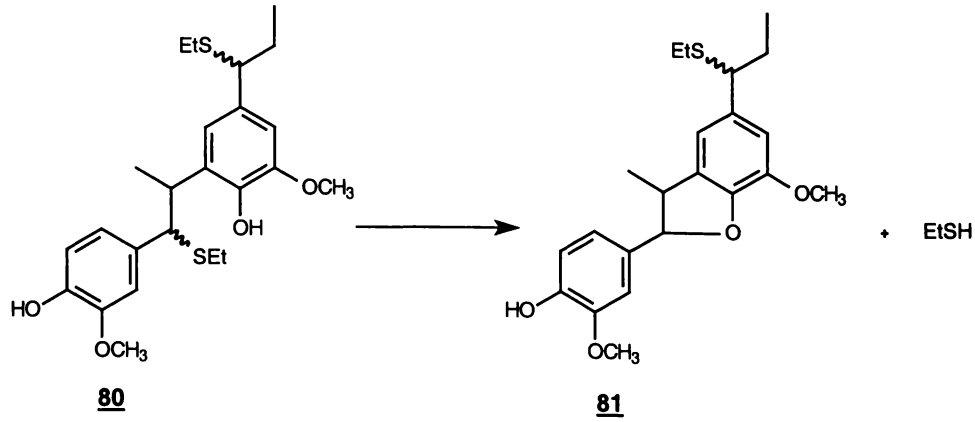

Figure 2.7: Reformation of the phenylcoumaran structure.

Initially the reformation of the β-5 ring in 79 and 80 was characterised through the appearance, over time, of a signal in the ^{1}H NMR spectrum at approximately 5.08 ppm and a signal in the ^{13}C NMR spectrum at 93.7 ppm. These chemical shifts correlated exactly to those observed for Hα and Cα in the model compounds 77 and 78 during the synthetic work. The stable decomposition product of 80 was purified using preparative layer chromatography (20% EtOAc/CH_2Cl_2) and characterised using NMR spectroscopic and mass spectrometric techniques, producing data consistent with the assigned structure, 81. Like 77 and 78, no diastereomeric pairs were observed for 81. This result was consistent with the acid catalysed dehydrogenation performed by Ede [247] during synthesis of phenylcoumaran structures, where only *erythro* phenylcoumaran structures were formed.

For 79 and 80, characterisation was performed on a mixture of diastereomeric isomers using NMR techniques. This characterisation was possible due to the slight differences in signal chemical shift between the different diastereomeric pairs. Connectivity of the protons and carbons was established through 2D NMR spectroscopic techniques, namely COSY90 [249], short-range proton to carbon (HMQC) [97, 98] and long range proton to carbon (HMBC) [250].

For product 79, which has only two superimposed spectra to separate, this exercise was relatively straightforward. However, for product 80, the presence of an extra thioethyl group and four different diastereomeric pairs made assignment quite difficult. Tentative assignments for most protons and carbons in the isomers were possible. However, a number of unresolvable ambiguities arose with signal

assignment, particularly for the thioethyl side chains and methoxyl groups (Section 6.7.2.12).

2.2.6 Thioacidolysis of β-ether model compounds

For all three model compounds, the β-aryl ether linkage was quantitatively cleaved (Figure 2.8). Introduction of thioethyl groups was observed, along with the elimination of OH and OR groups from the starting material. The products identified were consistent with those previously identified by Lapierre *et al.* [207, 215, 216] for thioacidolysis of β-aryl-ether structures. The NMR spectroscopic assignments associated with the trithioether products **58** and **60**, were complicated by the presence of *erythro* and *threo* isomers in the product. In previous work by Lapierre *et al.* [215], the isomers of **58** have been separated using preparative high performance liquid chromatography (HPLC) and characterised by NMR spectroscopy. In order to avoid duplication of this work, the products were characterised as a mixture of isomers.

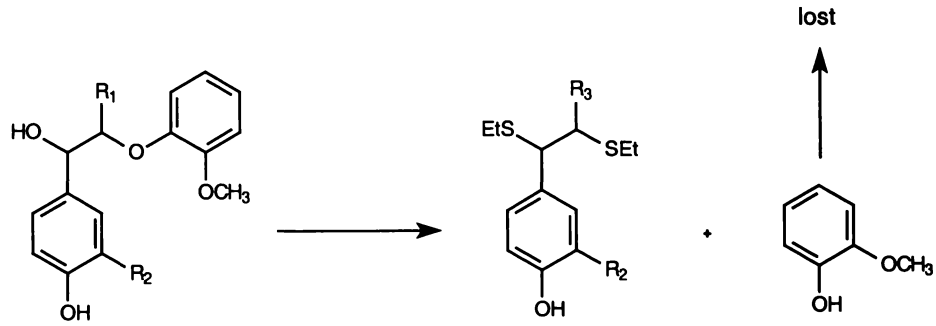

R_1=H, R_2=OCH_3	**82**	R_3=H	**85**	93%	**56**
R_1=CH_2OH, R_2=OCH_3	**83**	R_3=CH_2SEt	**58**	90%	**56**
R_1=CH_2OH, R_2=H	**84**	R_3=CH_2SEt	**60**	97%	**56**

Figure 2.8: Thioacidolysis of β-ether model compounds.

2.2.7 Thioacidolysis of non-phenolic model compounds

A small proportion of the phenolic oxygen groups in the lignin polymer are present as non-phenolic propyl ether structures (~ 2% [63, 251, 252]). Although they only constitute a small portion of the overall phenyl propane units, it is important to establish the ability of thioacidolysis/^{31}P NMR spectroscopy to measure these units. To that end, model compound **86** was prepared (Sections 6.3.14). Figure 2.9

compares the non-phenolic model compounds used in this investigation with the propyl ether structures in lignin.

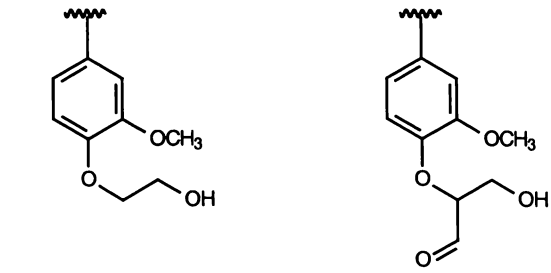

2-hydroxy ethyl ether "model" | propyl ether "lignin"

Figure 2.9: Comparison of lignin and model compound ether structures.

No degradation or reaction between the thioacidolysis reagent and the 2-hydroxy ethoxy chain in 86 was observed. For 86, reaction with the thioacidolysis reagent occurred solely through the side chain, with the α-hydroxyl group undergoing substitution as observed for apocynol 66. This result suggests that propyl ether groups in lignin may not convert to free phenolic ones, and therefore would not be measured by any subsequent ^{31}P NMR spectroscopy.

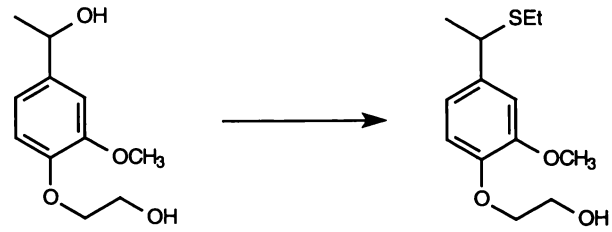

86 87 93%

Figure 2.10: Thioacidolysis of 4-(2-hydroxyethoxy)-apocynol (86).

2.2.8 Models unreactive to thioacidolysis

A number of model compounds, 56, 61, 88 and 89, were found to be unreactive to the action of thioacidolysis (Figure 2.11). Typically, these model compounds had side chains, which did not contain centres of high electron density. In particular, they did not contain any lone electron pairs or double bonds. This absence of electron density means that the vacant orbital on the BF_3 can not co-ordinate to the model compound, effectively blocking the first step in the thioacidolysis reaction. As the ^{1}H and ^{13}C NMR spectral and probe mass spectrometric data for the starting materials and products were identical, the results are not presented.

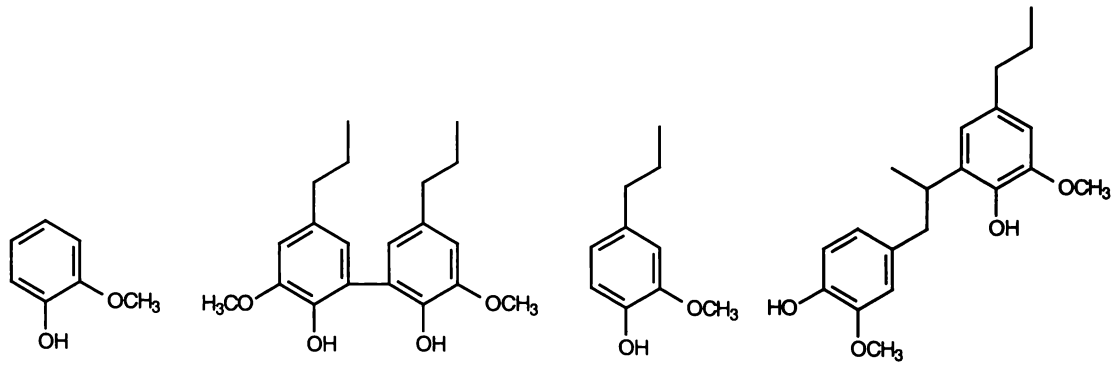

56 61 88 89

Figure 2.11: Four model compounds not reactive to thioacidolysis.

2.3 *Phosphorus NMR Spectroscopy of Model Compounds*

It was important to determine whether thioacidolysis, prior to ^{31}P NMR spectroscopy, adversely affected either the chemical shift or the observed ^{31}P NMR spectroscopic quantification. To this end, Tables 2.2-2.5 compare the ^{31}P NMR spectroscopic results for a range of lignin model compounds prior to and after thioacidolysis. The yields reported in Tables 2.2-2.5 were determined by quantitative ^{31}P NMR spectroscopy on the crude thioacidolysis product. Signal intensity of the model compound was measured relative to added internal standard (ISTD), cholesterol 62. These results therefore, differ slightly from the gravimetric results presented earlier.

This thesis focuses on the quantification of lignin phenolic groups. For this reason, only the chemical shifts of phenolic groups are reported here and information about signals associated with the aliphatic hydroxyl groups was omitted.

2.3.1 ^{31}P NMR spectroscopy of guaiacyl model compounds

After thioacidolysis, all the guaiacyl model compounds were measured in an essentially quantitative yield, with results ranging from 94-100% (Table 2.2). This compares favourably with the same model compounds as measured prior to thioacidolysis. In that case, a slightly narrower range of ^{31}P NMR spectroscopic yields, 96-100%, was determined (Table 2.2).

Due to the incomplete thioacidolysis of acetovanillone 69, both the dithioacetal product 71 and the starting material 69 were present in the thioacidolysis product. During the ^{31}P NMR spectroscopy of the crude thioacidolysis product, two signals were observed at 138.97 and 139.32 ppm respectively. The yield of 95% quoted in Table 2.2 for 67, represents a summation of the total area of these two signals.

Table 2.2: ^{31}P NMR spectroscopic results for guaiacyl monomers.

Models Before Thioacidolysis				Models After Thioacidolysis		
Structure	N°	δ	^{31}P yield (%)	N°	δ	^{31}P yield (%)
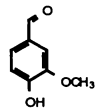	36	138.92	97	70	139.33	100
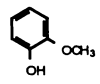	56	139.67	99			
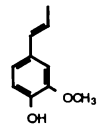	63	139.53	99	64	139.45	95
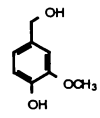	65	139.53	97	67	139.49	94
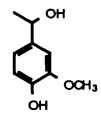	66	139.51	100	68	139.46	97
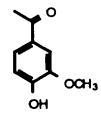	69	138.97	96	71	138.97 139.32	95*
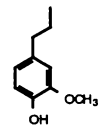	88	139.62	97			

* 35% recovered 69 also present

These results suggested that there was little to no loss of G monomers during the thioacidolysis work-up. The results also suggested that inclusion of SEt in the model compound side chain did not interfere with the phosphitylation procedure or subsequent ^{31}P NMR spectroscopic quantification.

A range of chemical shifts from 138.92 ppm to 139.67 ppm, was observed for the guaiacyl model compounds prior to thioacidolysis (Table 2.2). Within this grouping, the α-carbonyl containing model compounds, **36** and **69**, exhibited a ^{31}P NMR chemical shift approximately 0.6 ppm upfield from the chemical shifts of the other model compounds. These observed chemical shifts were entirely consistent with those previously published by Jiang *et al.* [194].

For model compounds containing hydroxyl or olefinic groups in their side chain, small upfield changes in their ^{31}P NMR chemical shift of between 0.04 and 0.2 ppm were observed after thioacidolysis. However, the substitution of an α-carbonyl group with two thioethyl groups, caused a downfield movement of 0.3-0.4 ppm for the observed ^{31}P NMR signals. This suggests that the inclusion of thioethyl groups into the side chain does not adversely affect the chemical shift exhibited by a phosphitylated phenol.

2.3.2 ^{31}P NMR spectroscopy of 5-5 linked model compounds

In Table 2.3, the results observed reflect a similar trend to that observed for the guaiacyl monomers shown in Table 2.2. Prior to thioacidolysis, the 5-5 linked model compounds exhibited chemical shifts ranging from 140.92 to 141.53 ppm. These chemical shifts are similar to those reported by Jiang *et al.* [194]. After thioacidolysis, the chemical shift of the phosphitylated 5-5 model compounds was little changed, with values between 140.96 and 141.13 ppm being observed.

Table 2.3: ^{31}P NMR spectroscopic results for 5-5 linked dimers.

Models Before Thioacidolysis				Models After Thioacidolysis		
Structure	N°	δ	^{31}P yield (%)	N°	δ	^{31}P yield (%)
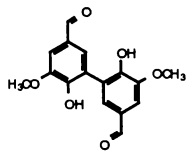	54	140.92	99	76	141.13	95
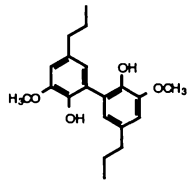	61	141.53	100			
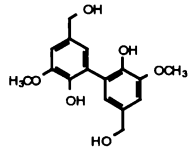	72	141.35	98	74	141.08	100
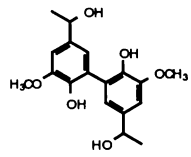	73	141.33	100	75	140.96	102

Of particular note with the 5-5 model compounds, were the quantitative yields (95-102%) measured for the model compounds after thioacidolysis. This suggests that there is no steric hindrance to complete phosphitylation of the phenolic groups. Prior to these results, we had been concerned that the presence of the 5-5 inter-unit linkage, combined with introduction of one or two thioethyl groups during thioacidolysis, may sterically interfere with complete phosphitylation. This was pertinent, given the bulky 5-membered ring in 2-chloro-4,4,5,5-tetramethyl-1,3,2-dioxaphospholane 41. Clearly, there is no such impediment in the model compounds studied here.

2.3.3 ^{31}P NMR spectroscopy of β-5 linked model compounds

Table 2.4: ^{31}P NMR spectroscopic results for β-5 linked dimers.

Models Before Thioacidolysis				Models After Thioacidolysis		
Structure	N°	δ	^{31}P yield (%)	N°	δ	^{31}P yield (%)
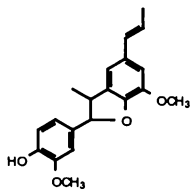	77	139.79	97	80	139.37, 139.66, 143.46, 143.54, 143.65	104* 97*
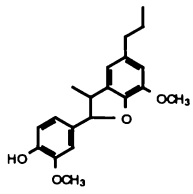	78	139.79	99	79	139.26, 139.58, 143.69, 143.95	98* 101*
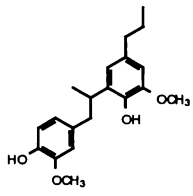	89	139.77, 143.89	100, 98			
* yields quoted are summation of multiple signals						

The chemical shifts and yields observed for the A-ring of β-5 model compounds prior to thioacidolysis were very similar to the results reported in Table 2.2, for guaiacyl monomers.

For 79, 80 and 89, a chemical shift of between 143.46 and 143.95 ppm was observed for the signal(s) associated with the B-ring phenolic group (Table 2.4). The chemical shift for the B-ring phenoxy group in β-5 structures was not reported in previous model compound work by Jiang *et al.* [194]. However, they did report the chemical shift of two diaryl methane model compounds, 90 and 91 (Figure 2.12), which contain a phenolic environment structurally similar to the B-ring of β-5 structures. They reported ^{31}P NMR chemical shifts for 90 and 91, 143.71 and 143.95 ppm

respectively [194], were similar to the chemical shift of the β-5 phenolic structures reported here.

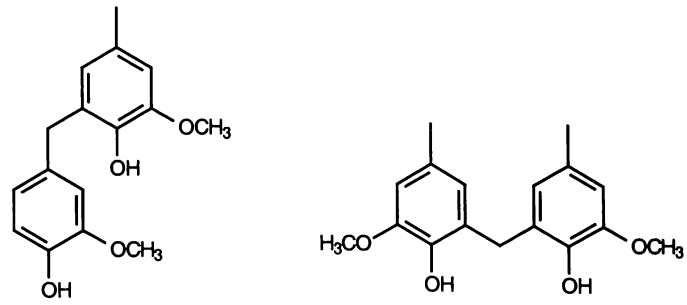

90 91

Figure 2.12: Diarylmethane model compounds used by Jiang *et al.* [194].

As discussed in Section 2.2.5, compounds 79 and 80 contain chiral centres, leading to the presence of two and four diastereoisomeric pairs respectively. As some of the diastereoisomers exhibit a slightly different ^{31}P NMR chemical shift, multiple signals arise. Figure 2.13 shows the ^{31}P NMR spectra of the three different β-5 linked structures (79, 80 and 89). With no diastereomers, 89 exhibited a single signal for both the G and β-5 phenolic hydroxyl groups. The signals due to the two isomers in 79, remain well separated in both regions of interest. However, for 80, there was clearly some signal overlap for the four different diastereoisomeric pairs.

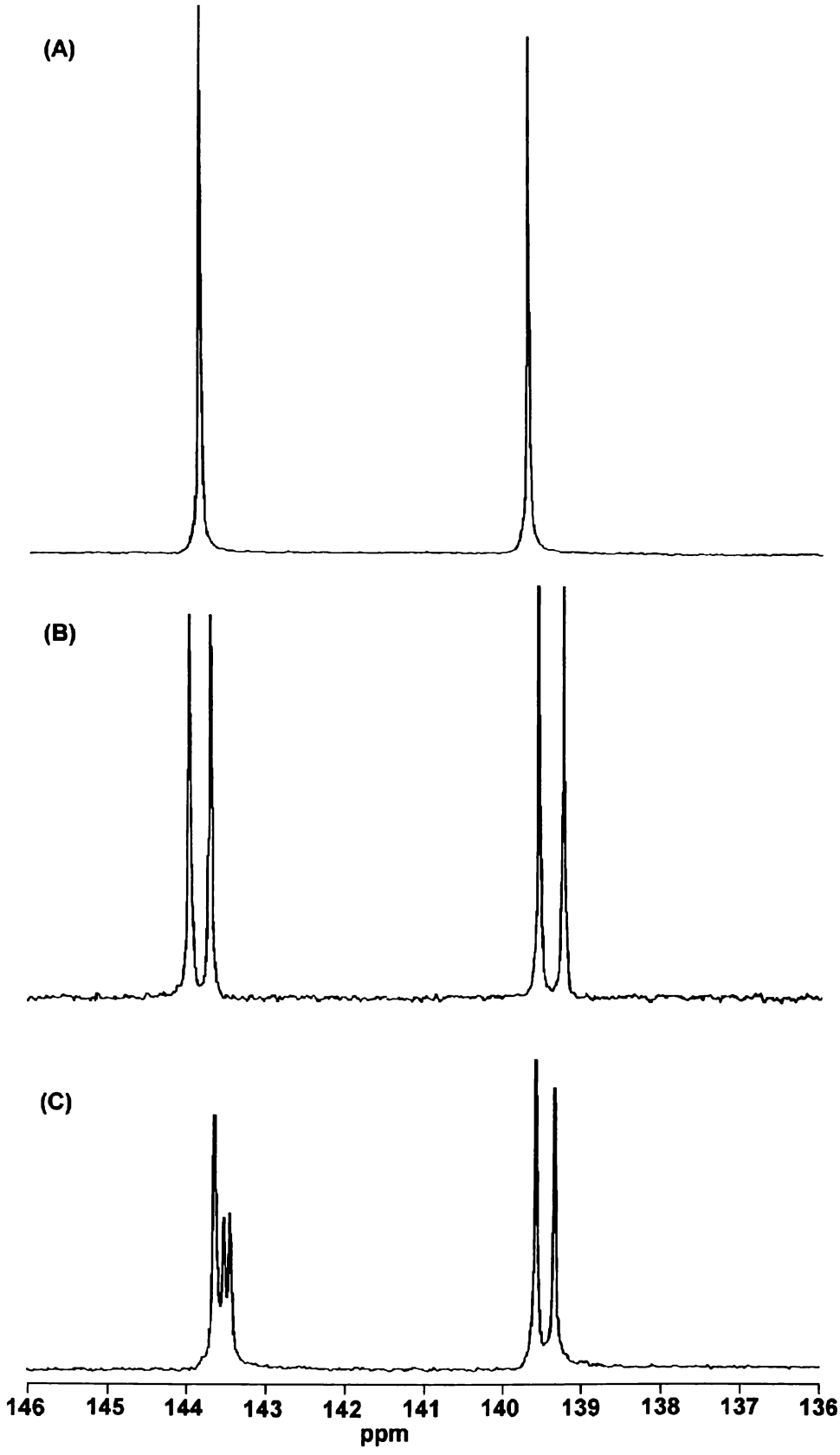

Figure 2.13: ^{31}P NMR spectra for β-5 thioacidolysis products (A)=(89), (B)=(79) and (C)=(80).

Independent of the signal complexity, the phenylcoumaran thioacidolysis products were recovered in quantitative yields, ranging from 97 to 104%. This indicated that inclusion of thioethyl groups did not promote steric hindrance, to phosphitylation with 2-chloro-4,4,5,5-tetramethyl-1,3,2-dioxaphospholane **41**, for β-5 linked structures. This result is similar to observations for 5-5 coupled model compounds.

2.3.4 ^{31}P NMR spectroscopy of β-arylether model compounds

The β-aryl ether linkage constitutes around 48% of the inter-unit linkages in softwood lignin [53, 58, 63, 116]. The predominant monomeric product in a softwood thioacidolysate, therefore, is the trithioether G structure **58** [207, 214, 215, 216]. Both this structure and the *p*-hydroxy equivalent, **60**, exist as *erythro* and *threo* isomers. Table 2.5 and Figure 2.14 show the phosphitylated phenolic groups in the *erythro* and *threo* isomers. Like the β-5 structures discussed previously, the two different diastereoisomers of **58** and **60** exhibit a slightly different chemical shift. This leads to the acquisition of two signals for each of the phenolic hydroxyl environments in **58** and **60**. For example, the two trithioether-G **58** diastereoisomers produced ^{31}P NMR spectroscopic signals at 139.43 and 139.47 ppm.

Table 2.5: ^{31}P NMR spectroscopic results for β-aryl ether model compounds.

Models Before Thioacidolysis			Models After Thioacidolysis			
N°	δ	^{31}P yield (%)	Structure	N°	δ	^{31}P yield (%)
82	139.48	98	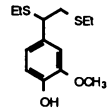	**85**	139.45	93
83	139.51, 139.55	96	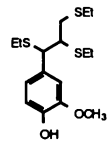	**58**	139.43, 139.47	98*
84	137.87, 137.91	99	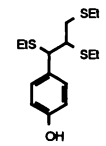	**60**	137.74, 137.78	99*

* yields quoted are summation of multiple signals

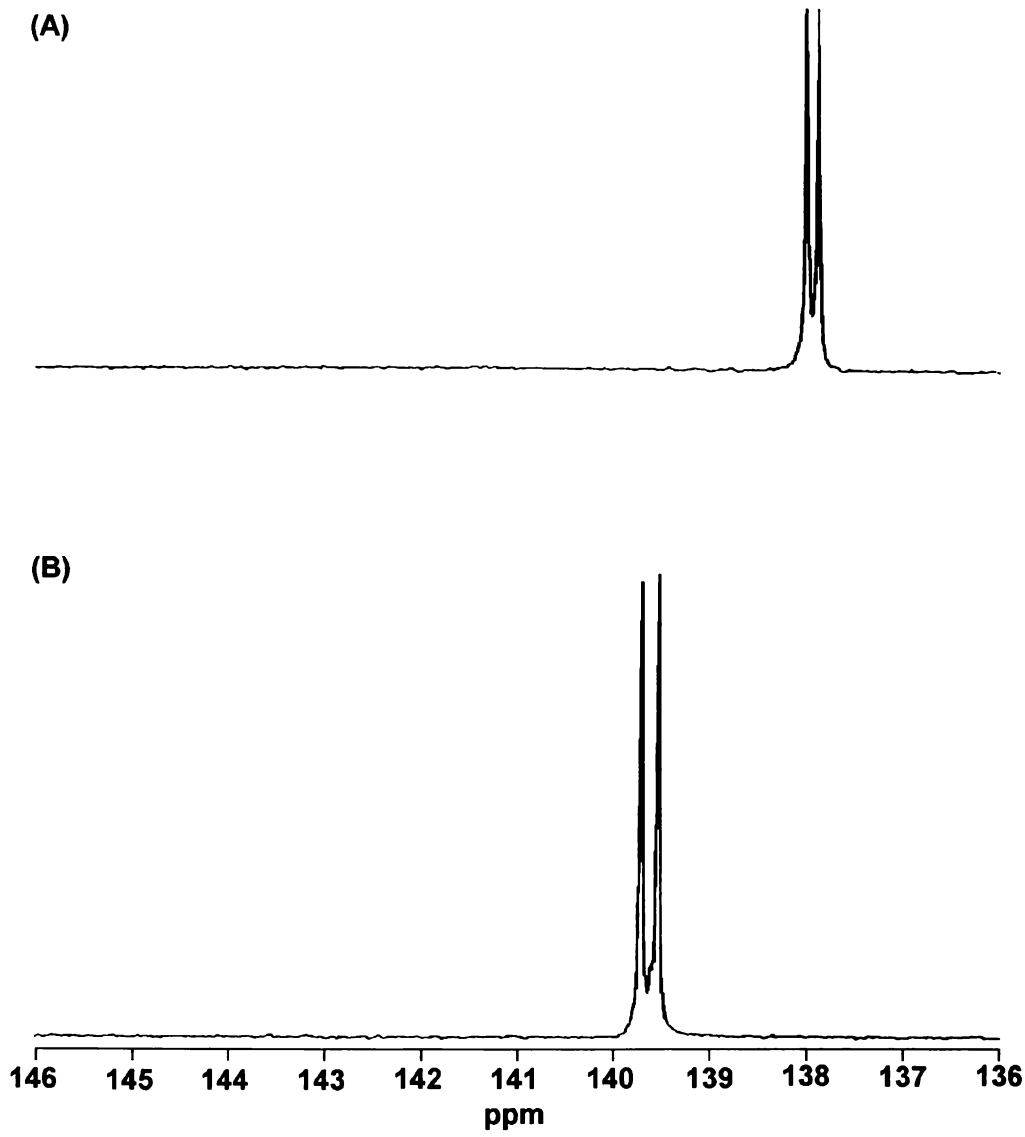

Figure 2.14: ^{31}P NMR spectra for two trithioether thioacidolysis products, (A)=(58) and (B)=(60).

These multiple signals for the trithioether and β-5 model compounds, could potentially be removed by using Raney Nickel desulphurisation [230, 231, 232]. The removal of the thioethyl groups from Cα and Cβ would also remove the chirality of these centres. This should result in sharper and better-resolved NMR spectra when applied to lignin samples. However, desulphurisation was not used in this study. Although signal resolution would be improved, actual quantification of lignin thioacidolysis products would be affected. This is due to the poor yield of lignols from the Raney Nickel desulphurisation.

2.3.5 ^{31}P NMR spectroscopy of non-guaiacyl model compounds

Table 2.6 shows the chemical shifts of some non-guaiacyl model compounds derivatised with 2-chloro-4,4,5,5-tetramethyl-1,3,2-dioxaphospholane **41**. The chemical shifts observed for the different model compounds closely reflect previous values reported by Jiang *et al.* [194] for similar structures. One example, is the range of chemical shifts reported here for syringyl models (142.22-142.48 ppm), which correlates well with the 142.82 reported previously for a S stilbene structure [194].

Table 2.6: ^{31}P NMR spectroscopic results for non-guaiacyl model compounds, without thioacidolysis.

Model Compound			δ ^{31}P NMR	
Name	Structure	N°	Phenolic OH	Non-phenolic OH
p-hydroxy acetophenone	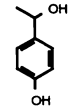	**92**	137.71	
p-hydroxy β-O-4 model	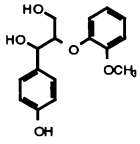	**84***	137.87, 137.91	147.45, 147.77,148.20
Catechol		**57**	138.97	
4-methyl catechol		**93**	139.19 (d, J=7.8 Hz) 138.90 (d, J=7.8 Hz)	
Ferulic Acid	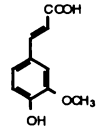	**29**	139.41	135.16
Syringic acid	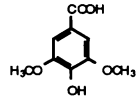	**53**	142.22	135.14
Syringyl aldehyde	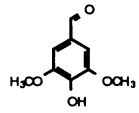	**52**	142.34	
Syringyl alcohol	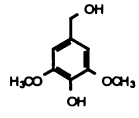	**94**	142.48	146.78

* Present as *erythro* and *threo* isomers

Of particular interest in Table 2.6 was the signal multiplicity observed for 4-methyl catechol 93. The signals centred at 139.19 and 138.90 ppm (Table 2.7) were actually doublets (J = 7.8 Hz) and were attributed to ^{31}P-^{31}P coupling between phosphorus atoms on the *ortho* catechol phenolic groups. No other lignin model compounds previously published had shown any through-bond or through-space coupling [194].

A ^{31}P-^{31}P COSY 90 experiment (Figure 2.15), performed on 93 derivatised with phosphitylating reagent 41, confirmed that this coupling was real and not due to any dihedral angle effects.

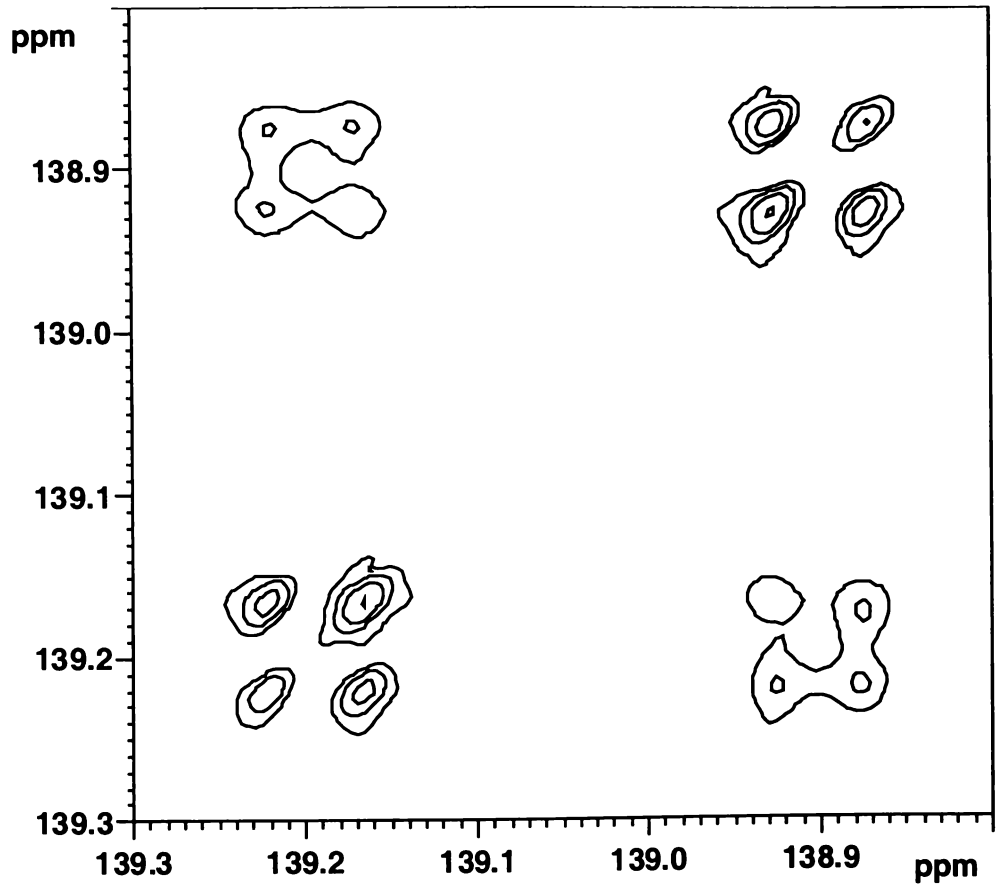

Figure 2.15: ^{31}P-^{31}P COSY 90 of (41)-derivatised 4-methyl catechol (93)

The observed coupling in 93 was attributed to ^{5}J ^{31}P-^{31}P through-space coupling rather than through-bond coupling. To date, no ^{5}J ^{31}P-^{31}P through-bond coupling has been reported. For ^{2}J P-X-P type systems a coupling constant of 70-90 Hz is typical [253]. It was therefore unlikely, that a coupling constant as large as 8.0 Hz would be observed for a ^{5}J P-O-C-C-O-P system. However, through-space coupling for

sterically congested phosphorus atoms has previously been reported by Pastor *et al.* [254] in the two bis(aryloxy)oxazaphospholidines 95 and 96 (Figure 2.16).

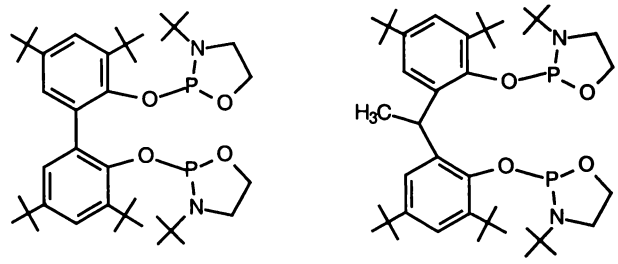

95 96

Figure 2.16: Structure of bis(aryloxy)oxazaphospholidines (95) and (96) [254].

In the solution ^{31}P NMR spectrum of 95, seven-bond ^{31}P-^{31}P J-coupling of 30.3 Hz was observed, while eight-bond ^{31}P-^{31}P J-coupling of 30.6 Hz was observed for 96 [254]. The separation of the aromatic π systems by a sp^3 hybridised carbon in 96, together with an intramolecular P-P distance of 3.70 Å in 95 and 4.50 Å in 96, suggested a through-space coupling mechanism in these compounds [254].

To determine the ^{31}P-^{31}P distance through space, molecular modelling of 93 derivatised with 41 was performed using the SPARTAN Version 5.0 program from Wavefunction. A semi-empirical AM1 [255] model was used (Section 6.10). This semi-empirical model is essentially, a simplified *ab initio* [256] calculation, reducing computational time and costs [257].

For 93, the calculated ^{31}P-^{31}P intramolecular distance was 4.20 Å. This distance was slightly greater than the sum of the van der Waals' radii of phosphorus (3.80 Å) [258]. However, the collisional and vibrational energy of the derivatised model compounds in solution, may lead to the population of states with shortened intermolecular P-P distances, allowing through space coupling. Such an argument has previously been used to explain a large ^6J ^{31}P-^{31}P observed by Szalontai *et al.*[259], and the ^7J ^{31}P-^{31}P and ^8J ^{31}P-^{31}P coupling observed by Pastor *et al.* [254] in 95 and 96 respectively.

2.3.6 ^{31}P NMR spectroscopy of a mixture of model compounds

To demonstrate that the method could be used for analysis of more complex systems, thioacidolysis/^{31}P NMR spectroscopy was applied to two mixtures of model compounds. Each mixture contained a known amount of three different model compounds, representing uncondensed guaiacyl, 5-5 biphenyl and β-5 phenylcoumaran structures. For mixture 1 (Table 2.7, Figure 2.17), the model compounds used were isoeugenol 63, diapocynol 73 and dehydrodiisoeugenol 77. Mixture 2 (Table 2.8) on the other hand consisted of apocynol 66, divanillyl alcohol 72 and dehydrodihydrodiisoeugenol 78.

In Tables 2.7 and 2.8, the terms μmoles added and μmoles detected refer to the number of μmoles of phenolic groups added/measured, not to the μmoles of model compound added/measured. The difference is, that 1 mole of 5-5 model compound contains 2 moles of phenolic hydroxyl. Also, in these tables the results are presented in terms of the aromatic substitution pattern, rather than by model compound. This is primarily due to the signal overlap between the guaiacyl model compounds and the A-ring of the β-5 structures.

Table 2.7: ^{31}P NMR spectroscopic results for quantification of mixture 1.

Structure Type	From Model(s)	μmoles added	μmoles detected	Yield (%)
5-5	73	20.1	19.0	95
β-5	77	29.9	28.0	94
uncondensed G	73 + 77	53.3	51.9	97
Total		**103.3**	**98.9**	**96**

Table 2.8: ^{31}P NMR spectroscopic results for quantification of mixture 2.

Structure Type	From Model(s)	μmoles added	μmoles detected	Yield (%)
5-5	72	27.2	26.1	96
β-5	78	34.1	32.7	96
uncondensed G	66 + 78	41.9	40.6	97
Total		**103.2**	**99.4**	**96**

As can be seen from Table 2.7 and 2.8, the observed yields for individual structural types in the two mixtures ranged between 94% and 97%, with the total phenolic yield of the two mixtures being 96%.

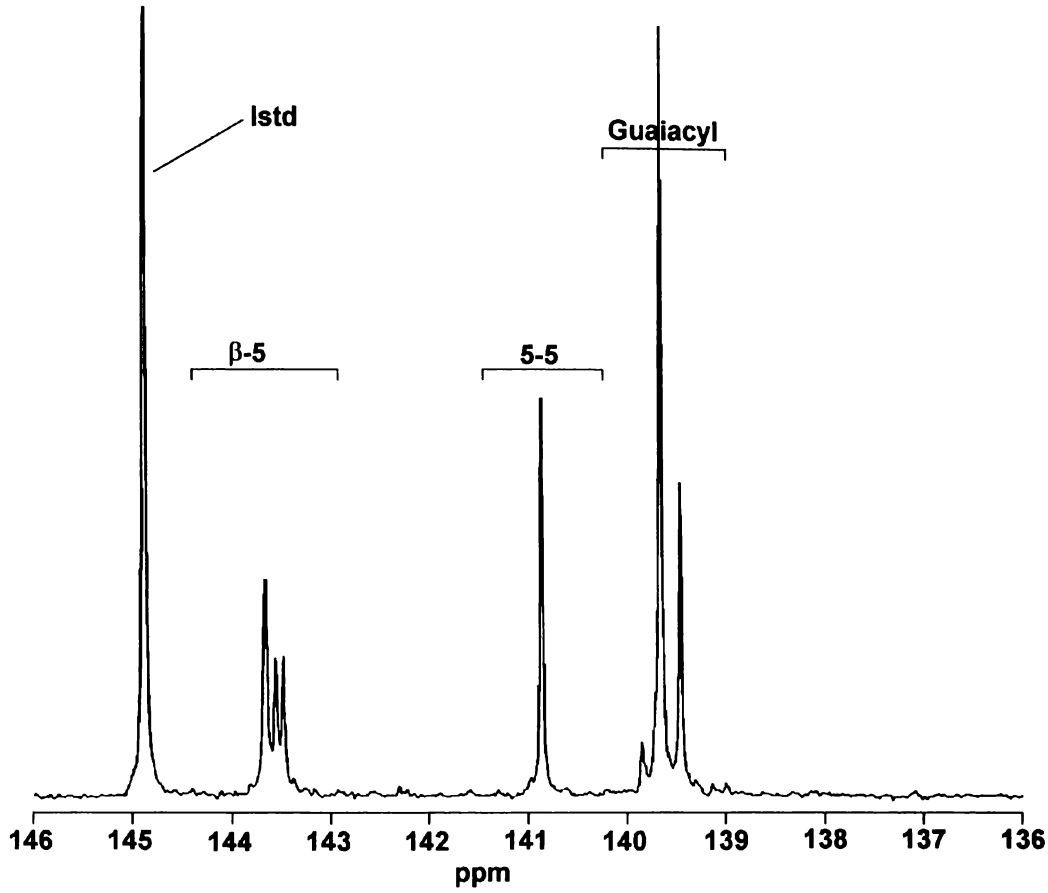

Figure 2.17: ^{31}P NMR spectrum for mixture 1 post thioacidolysis.

In Figure 2.17, the ^{31}P NMR spectroscopy signals of the different functional groups remain well separated, allowing accurate quantification. Given the errors inherent in quantification of moieties using quantitative NMR spectroscopy, these results are regarded as satisfactory. The results suggested that quantification of more complex systems after thioacidolysis is indeed possible.

2.4 *Conclusions*

- Thioacidolysis of lignin model compounds led to side chain thioethyl incorporation consistent with previous literature.

- Thioethyl incorporation in the side chain led to only small changes in the observed ^{31}P NMR chemical shift of the model compounds tested. These small changes indicated that thioacidolysis prior to ^{31}P NMR spectroscopy would not lead to signal overlap and/or signal complications.

- Thioethyl incorporation in lignin model compounds did not negatively affect their quantification by ^{31}P NMR spectroscopy. Prior to these results we had been concerned that thioethyl incorporation in sterically crowded 5-5 and β-5 structures may hinder quantitative analysis.

- Novel ^{5}J ^{31}P-^{31}P coupling was observed for doubly **41** derivatised 4-methyl catechol **93**. This was attributed to through-space rather than to through-bond coupling.

Problems cannot be solved,
at the same level of awareness that created them.

Albert Einstein

Chapter 3
Thioacidolysis of a Dibenzodioxocin Model Compound

3.1 Introduction

One important feature of softwood lignin is the presence of 5-5 coupled biphenyl structures [53, 54, 58, 63, 116]. Current estimates suggest that the proportion of phenylpropane units in lignin involved in biphenyl coupling, may be as high as 20-26% [107]. In recent work, Karhunen *et al.* [105, 106] have shown that a large portion of these biphenyl structures are connected by ether bonds to other phenylpropane units, forming 8-membered dibenzodioxocin structures (Section 1.3.4.5). Currently, no information about the reactivity of these dibenzodioxocin structures during thioacidolysis is available. However, the behaviour of dibenzodioxocin structures during thioacidolysis, may have significant implications in the subsequent quantification of lignin by ^{31}P NMR spectroscopy. To evaluate this issue, a dibenzodioxocin model compound, kindly supplied by Professor G. Brunow, was subjected to thioacidolysis followed by NMR spectroscopic analysis.

3.2 Thioacidolysis of Dibenzodioxocin

3.2.1 Thioacidolysis results

Thioacidolysis of *trans*-6,7-dihydro-7-(4-hydroxy-3-methoxyphenyl)-4,9-dimethoxy-2,11-dipropyl-dibenzo[*e,g*][1,4]dioxocin-6-ylmethanol 97 led to the formation of three different reaction products. As shown in Figure 3.1, around 20% of the dibenzodioxocin 97 reacted *via* pathway **(A)**, leading to formation of 6,6'-dihydroxy-

5,5'-dimethoxy-3,3'-dipropylbiphenyl 61 and 1-(4-hydroxy-3-methoxyphenyl)-1,2,3-(tris-thioethyl)propane 58. Most of the remainder, approximately 70%, reacted *via* pathway **(B)**, leading to *trans*-11-hydroxy-7-(4-hydroxy-3-methoxyphenyl)-6-hydoxymethyl-4,10-dimethoxy-2,8-dipropyl-6,7-dihydrodibenzo[*b*,*d*]oxepine 98. Products were isolated by flash column chromatography [260] and yields reported are on purified products.

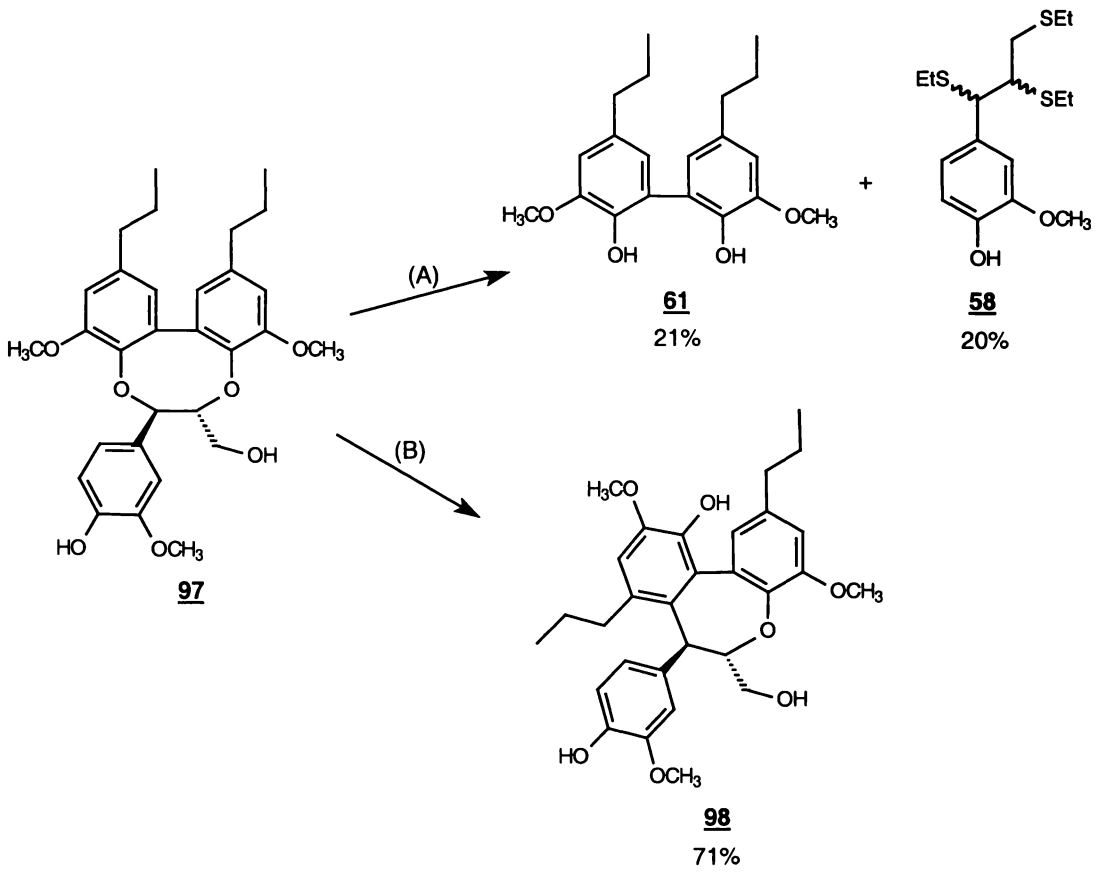

Figure 3.1: Thioacidolysis of dibenzodioxocin model compound (97). (A) and (B): EtSH, BF_3OEt_2, dioxane, 110°C, 4 hrs.

3.2.2 NMR spectroscopy labelling

In order to facilitate the subsequent discussion, Figure 3.2 shows the labelling convention used for product 98. This labelling similarly applies for the original dibenzodioxocin model 97.

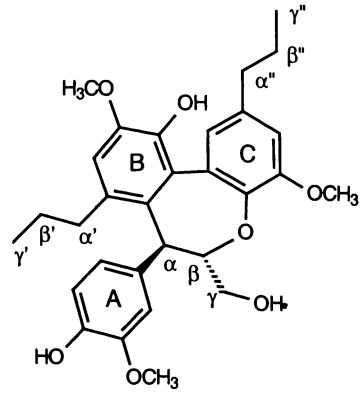

98

Figure 3.2: Labelling convention for dibenzooxepine structures.

3.2.3 Discussion of reaction pathway (A)

The ^{1}H and ^{13}C NMR spectroscopic and probe mass spectrometric data collected for products 58 and 61, was consistent with the proposed structures and spectral data previously reported in the literature [107, 215].

Formation of products 61 and 58 was proposed to occur *via* cleavage of the oxo bonds in the dibenzodioxocin 97, as shown in Figure 3.3. This mechanism was essentially identical to that previously reported by Lapierre *et al.* [216], for the cleavage of β-aryl ether linkages during thioacidolysis. Initial reaction occurred through coordination between the vacant *p*-orbital on the Lewis acid (BF_3) and the A-ring α-oxo oxygen, to form an intermediate oxonium ion. Subsequently, nucleophilic attack by the HSEt occurred at the activated benzyl carbon with the elimination of a phenolic group (B ring). Lapierre *et al.* [216] have however, reported that it is unclear whether this step proceeds with or without an intermediate carbonium ion. It was proposed, that after formation of an oxonium ion at the A-ring Cβ, further reaction occurred through intramolecular attack by the thioethyl group at Cα. This resulted in formation of a sulphonium intermediate and complete cleavage of the 8-membered ring. Further thioacidolysis of the released monomer may then occur, *via* the normal thioacidolysis mechanism [214, 216].

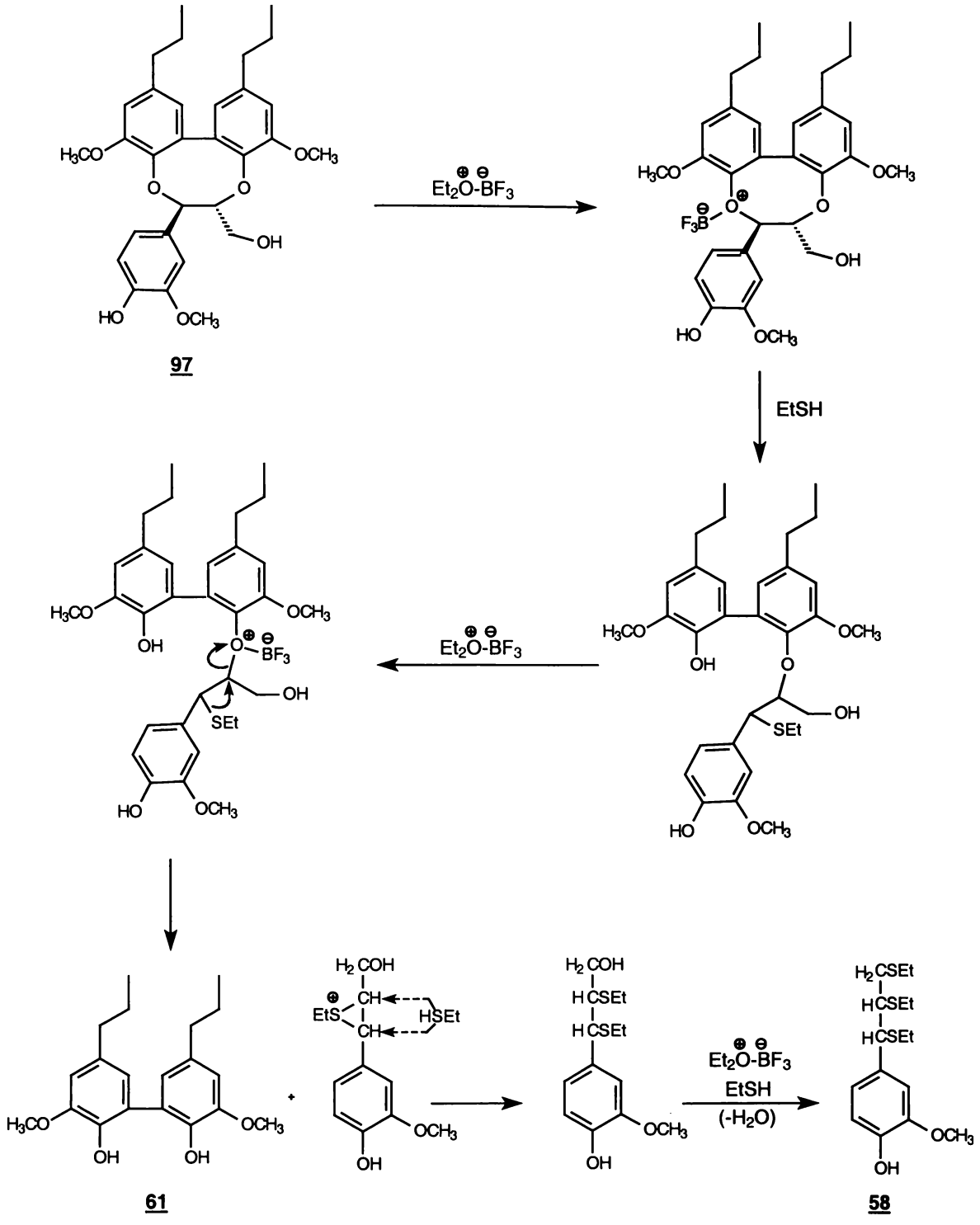

Figure 3.3: Proposed reaction of dibenzodioxocin (97) to yield products (61) and (58).

3.2.4 Discussion of reaction pathway (B)

The dibenzooxepine **98** was characterised both underivatised and as the corresponding acetate **99**. The resultant 1D NMR (^{1}H, ^{13}C, DEPT 90 [242] and DEPT 135 [242]) spectra and probe mass spectrometric data were consistent with the structures proposed and the data previously reported for these structures [261]. In order to fully solve and unambiguously assign the NMR spectra, COSY 90 [249], HMQC [97, 98] and HMBC [250] spectra were acquired. The correlations observed in these 2D spectra were consistent with the dibenzooxepine **98**.

The only isomer of **98** present in the thioacidolysis product mixture, was the *trans* Hα-Hβ dibenzooxepine. This isomer was characterised by the A-ring α-CH proton signal, a singlet ($J_{\alpha\beta}$ = 0 Hz) at 4.36 ppm [261]. The same proton, in the *cis* isomer, has previously been reported to resonate as a doublet ($J_{\alpha\beta}$ = 7.4 Hz) at 4.65 ppm [261].

The Karplus-equation [262] relates the vicinal coupling constants, to the torsion angle between the coupling protons. The magnitude of the coupling constant observed is a function of cosϕ, where ϕ is the angle between the two protons in a Newman projection [262, 263, 264, 265]. This implies a maximum coupling constant at 0° and 180°, with a minimum coupling constant at 90° and 270°. The 0 Hz Hα-Hβ coupling constant in the dibenzooxepine **98**, therefore suggests a dihedral angle close to 90° between the Hα and Hβ.

Currently there is no X-ray crystallographic data available to confirm this dihedral angle. However, conformational analysis by molecular modelling (Section 6.10) showed, that the most thermodynamically stable ring conformer of **98** contained an Hα-Hβ dihedral angle of 94°. This fits closely with the dihedral angle predicted on the basis of the observed coupling constant. Figure 3.4 contains two snapshots of the most stable *trans* conformer.

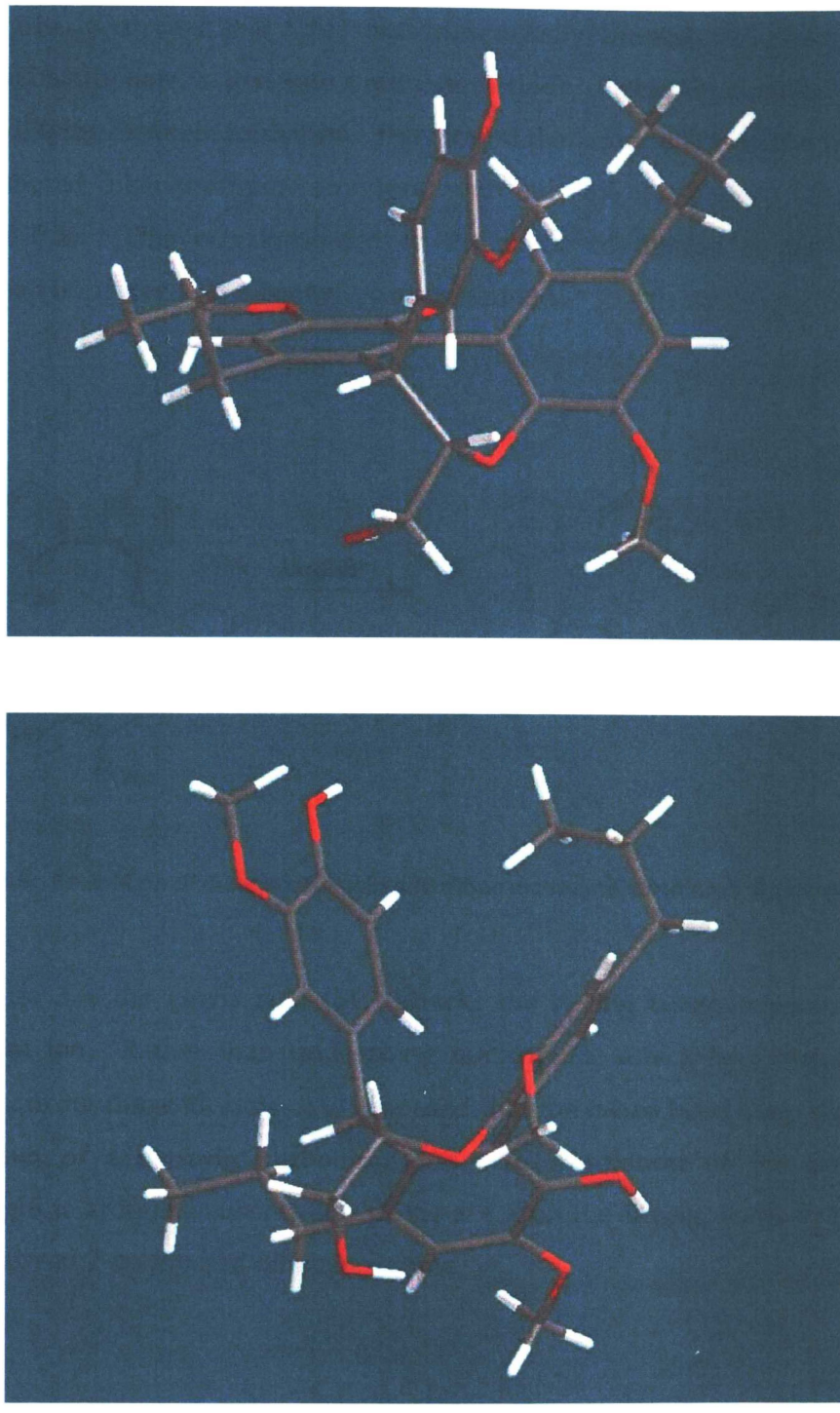

Figure 3.4: Two snapshots of the most stable *trans* conformer of (98).

While no mechanistic studies were undertaken, formation of the 7-membered dibenzooxepine 98 was proposed to occur *via* acid catalysed rearrangement of the dibenzodioxocin, as shown in Figure 3.6. Two pieces of information support this mechanism. Firstly, when the dibenzodioxocin 97 was cooked under thioacidolysis conditions in the absence of EtSH, the dibenzooxepine 98 was the sole reaction product. This indicated that BF_3 alone, was responsible for the rearrangement of 97

to 98. Also, Karhunen *et al.* [261] used trimethylsilyl bromide (Me_3SiBr), followed by sodium bicarbonate, to generate a quinonemethide, during the final ring closure step of the dibenzodioxocin formation. They found that around 82% of the product was a 7-membered dibenzooxepine structure, with only 8% the desired dibenzodioxocin (Figure 3.5). This was attributed to the acidic conditions of the Me_3SiBr and proposed to proceed *via* a benzylic carbonium ion.

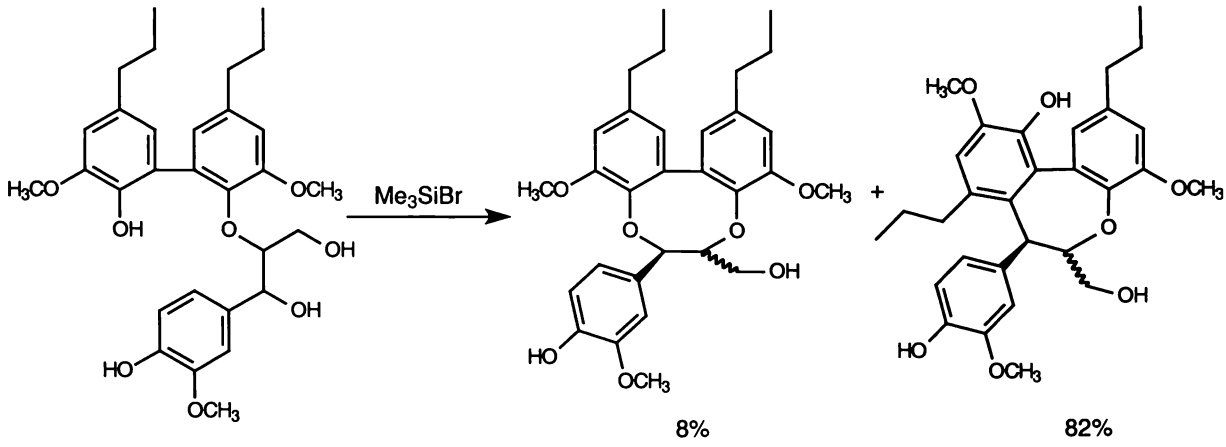

Figure 3.5: Formation of dibenzodioxocin and dibenzooxepine structures during ring closure [261].

In Figure 3.6, the Lewis acid (BF_3) attacks the A-ring α-oxo oxygen, to form an oxonium ion. Rather than undergoing nucleophilic attack by HSEt, as normally occurs during thioacidolysis, it is proposed that the α-oxo bond may break with the formation of a benzylic carbonium ion. After rotation of the aromatic ring, electrophilic aromatic substitution (EAS) at C2 on the B-ring, leads to formation of the observed 7-membered dibenzooxepine.

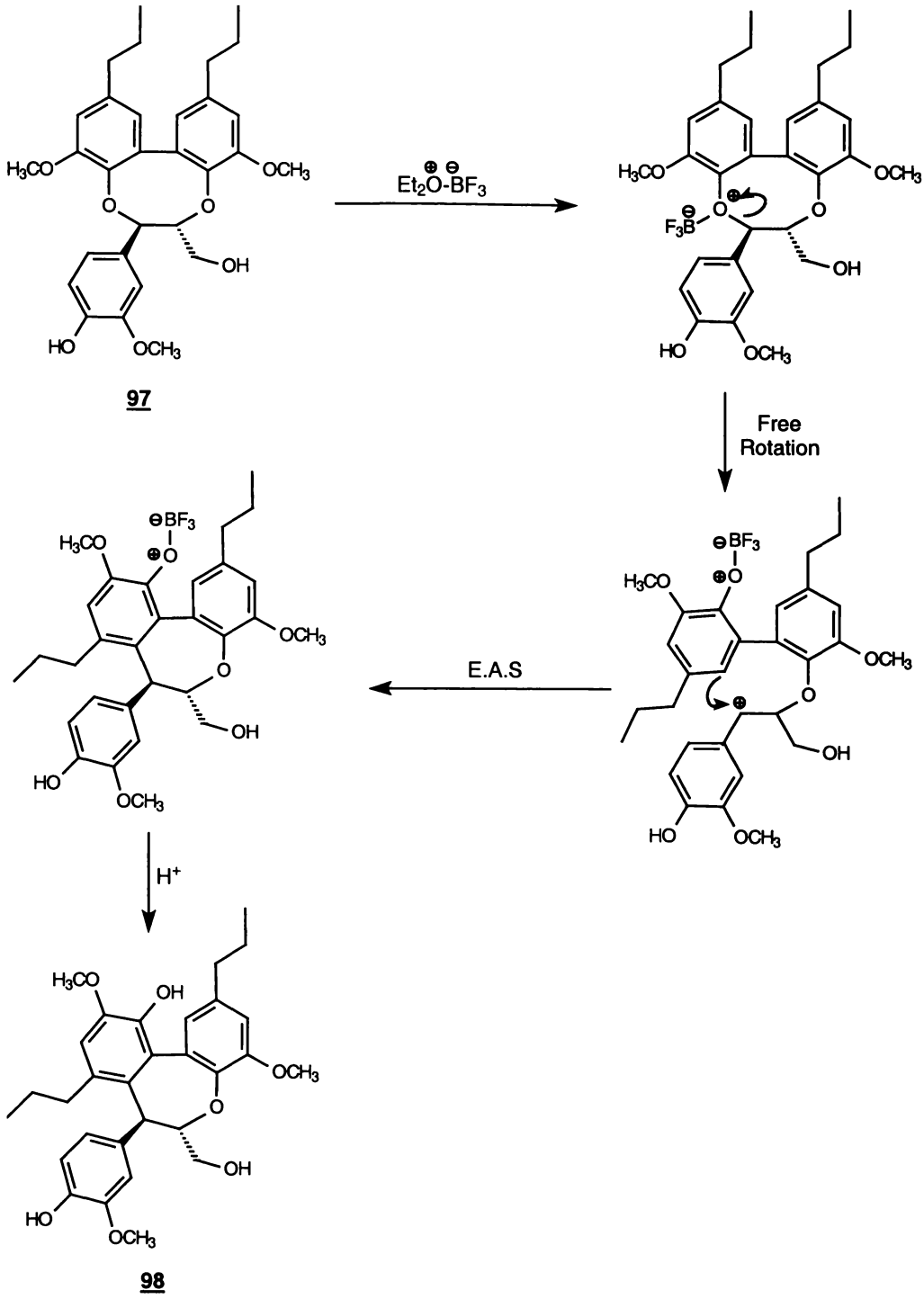

Figure 3.6: Acid catalysed formation of a dibenzooxepine (98) during thioacidolysis of dibenzodioxocin (97).

Interestingly, during the Me_3SiBr catalysed formation of the dibenzooxepine, Karhunen *et al.* [261] found both *cis* (~20%) and *trans* (~80%) isomers of the dibenzooxepine structure present. However, during the BF_3 catalysed ring rearrangement of dibenzodioxocin 97 to dibenzooxepine 98, only the *trans* isomer was observed.

The formation of only the *trans* isomer may either be due to thermodynamic or kinetic considerations. Some possible explanations for the formation of solely the *trans* isomer during thioacidolysis, are offered below.

The *trans* isomer of 98 may be preferentially present in the thioacidolysis product, because it is the more stable of the *cis* and *trans* isomers, as has been shown by molecular modeling (Section 6.10). Under the severe thioacidolysis conditions, BF_3 may be a strong enough Lewis acid (*cf.* Me_3SiBr) to facilitate a reversible formation of the Wheland intermediate during EAS. This could allow epimerisation to occur at Cα, and lead to formation of the more stable *trans* isomer only, during thioacidolysis.

Alternatively, the preferential formation of *trans* 98 may be attributable to the transition state geometry required for the dibenzooxepine formation. For the electrophilic aromatic substitution (EAS) to occur, overlap between the π electron cloud of the aromatic ring and the empty *p*-orbital lobes, above and below the plane of the sp^2 hybridised carbonium ion, must exist [266]. Figure 3.7 shows the two possible orientations for such a transition state, with EAS occurring *via* either lobe of the empty carbonium ion *p*-orbital.

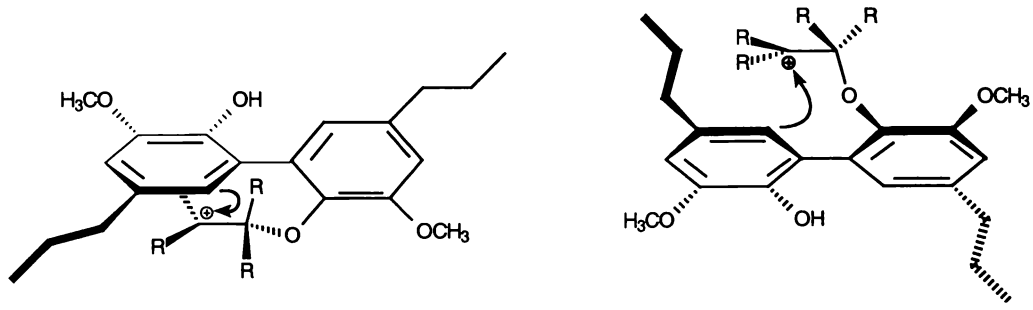

Figure 3.7: Required orientation for dibenzooxepine formation.

Replacing R in Figure 3.7, with the actual substituents in 97, it is possible to generate four different transition states (Figure 3.8), which would allow the EAS step to proceed.

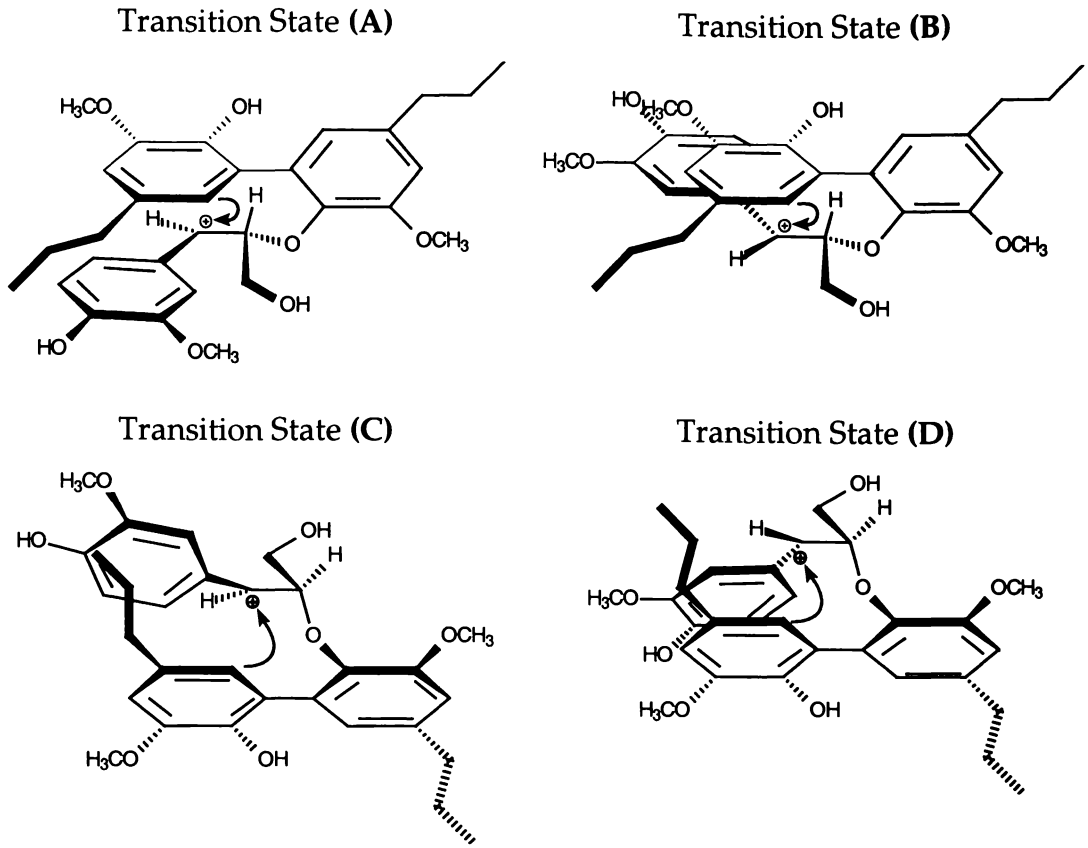

Figure 3.8: Possible transition states during dibenzooxepine formation.

From these four transition states, transition states **(A)** and **(D)** lead to the formation of a *trans* isomer, while transition states **(B)** and **(C)** lead to the formation of a *cis* isomer. It is possible to argue that in transition states **(A)** and **(C)** there would be significant interaction between the A-ring and the B-ring phenyl propane group, making these transition states unfavoured. Also, there may potentially be interaction between the A-ring β-proton and the 5-5 coupled aromatic rings, in the **(B)** transition state. Such interactions could suggest, that transition state **(D)** is the most favoured of the four drawn above. This transition state leads to the formation of the *trans* isomer shown in Figure 3.4.

This transition state argument is identical for the product formation in the work by Karhunen *et al.* [261] and the work presented here. It therefore can not solely account for the 100% *trans* isomer recovered here, *cf.* 80/20 *cis/trans* distribution reported earlier. However, in the presence of excess BF_3, many of the oxygen lone pairs of electrons may form adducts with BF_3. It is possible, that the 100% *trans*

dibenzooxepine recovered in this work, may be attributed to the steric hindrance introduced by the formation of these BF_3 adducts.

While not investigated in this work, the formation of dibenzooxepine structures during thioacidolysis of dibenzodioxocin structures, may prove to be a useful probe for dibenzodioxocin structures in *in situ* lignin. In particular, the novel Hβ/Cβ HMQC correlation at 5.17/88.0 for thioacidolysis product **98**, may provide further supporting evidence for the presence of dibenzodioxocin structures in wood lignin. Currently, HMQC [250] Hα/Cα and Hβ/Cβ correlations present in isolated lignin samples, are used to identify the presence of dibenzodioxocin structures [105]. However, these HMQC spectra are collected on isolated not *in situ* lignin samples. Therefore, it is unclear how many, if any, of the dibenzodioxocin structures are created or destroyed during the lignin isolation process. The benefit of dibenzooxepine structure identification in the lignin thioacidolysate, is the potential to use *in situ* lignin samples, rather than isolated lignin.

There is however, one potential hindrance to the detection of the dibenzooxepine Hβ/Cβ HMQC correlation in *in situ* lignin thioacidolysates. This it that the structural constraints in the *in situ* lignin polymer may not allow the free rotation about the 5-5 interunit bond, which is needed for the dibenzooxepine formation.

Such investigations may form the basis of some potentially exciting future work.

3.3 Phosphorus NMR Spectroscopy for Dibenzodioxocin

Analysis of the dibenzodioxocin thioacidolysis products, by ^{31}P NMR spectroscopy, was performed to evaluate, the impact of dibenzooxepine formation on subsequent ^{31}P NMR spectroscopic quantification. Figure 3.9 shows the ^{31}P NMR spectra of the dibenzodioxocin **97** and its thioacidolysis product mixture, as well as the dibenzooxepine **98**. In Table 3.1, the chemical shifts of the different compounds are shown. The chemical shifts of **61** and **58** have however, been previously presented in Chapter 2.

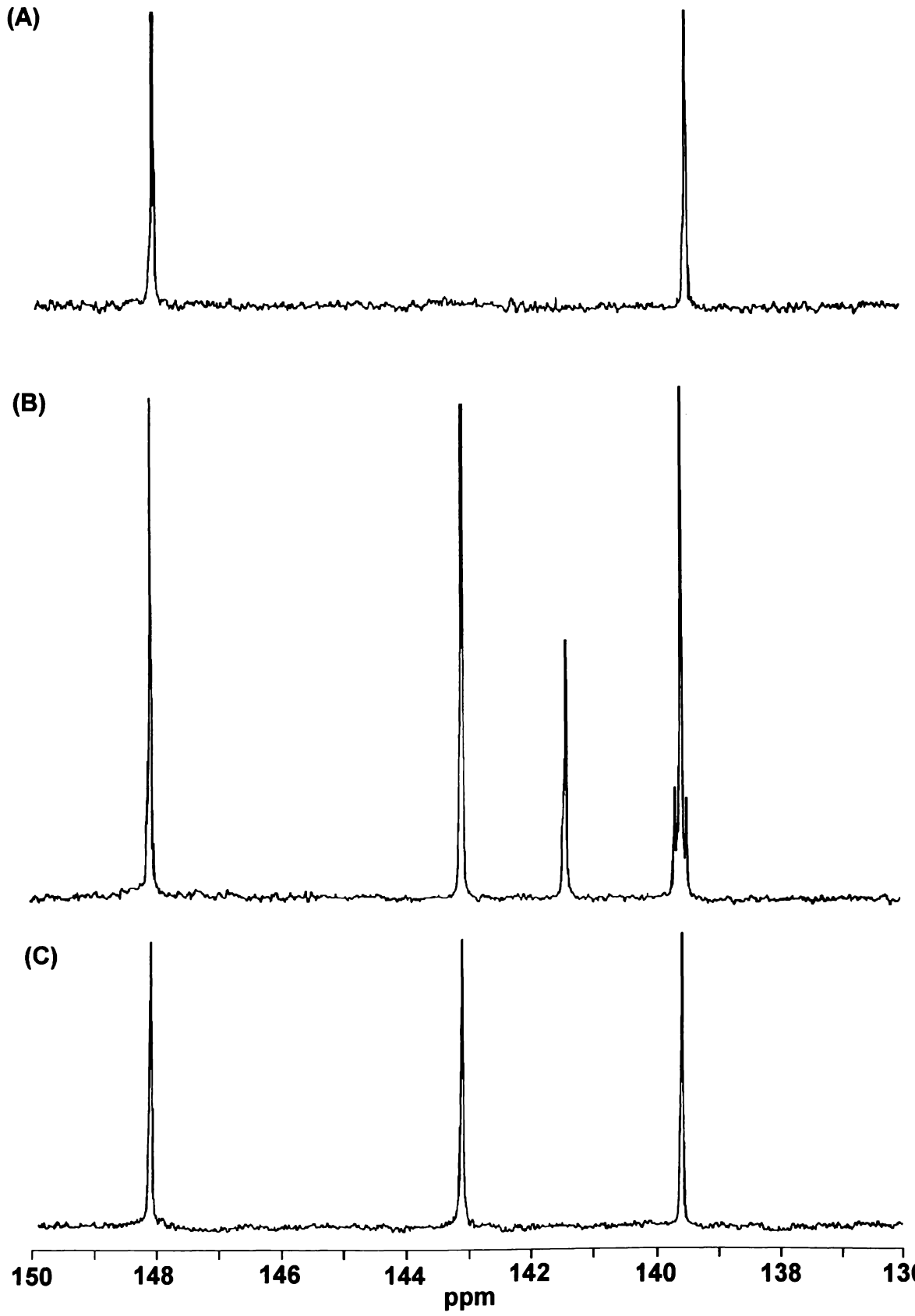

Figure 3.9: ^{31}P NMR spectra of (A) dibenzodioxocin (97), (B) the dibenzodioxocin thioacidolysis mixture and (C) dibenzooxepine (98).

Table 3.1: ^{31}P NMR spectroscopic data for dibenzodioxocin thioacidolysis.

Compound	N°	δ ^{31}P
Dibenzodioxocin	97	139.71 148.31
Dipropylguaiacol	61	141.51
Guaiacyl trithioether	58	139.61 139.72
Dibenzooxepine	98	139.68 143.15 148.13

Dibenzodioxocin 97 gave two signals in the ^{31}P NMR spectrum, one at 148.31 ppm (aliphatic hydroxyl) and the other at 139.71 ppm (G phenolic). These chemical shifts were consistent with those observed previously. This indicated, that the presence of the 8-membered ring in the dibenzodioxocin 97, did not significantly affect chemical shift.

As discussed earlier, the mixture of compounds in the dibenzodioxocin 97 thioacidolysis product, contained 58, 61 and 98. In Figure 3.9 (B), the ^{31}P NMR spectrum of this mixture is shown. Assignment of the individual signals was relatively straightforward. On the basis of earlier work with model compounds (Chapter 2), the signal at 141.51 ppm was attributed to the 5-5 coupled dipropylguaiacol 61, and the two signals centred at 139.70 ppm, to the G trithioether 58.

Of significantly more interest was the assignment of signals due to the 7-membered dibenzooxepine 98. The ^{31}P NMR spectrum of 98 alone is shown in Figure 3.9 (C). Signals at 148.13 and 139.70 ppm were assigned to the aliphatic hydroxyl and the G phenolic groups, respectively. The remaining signal at 143.15 ppm was attributed to the biphenyl phenolic group, generated during acid catalysed rearrangement.

Typically, the B-ring of β-5 compounds (for example **89**) exhibit a chemical shift around 143 ppm and not 5-5 coupled G units. Biphenyl structures typically exhibit a chemical shift around 141 ppm. Two factors could contribute to the difference between the chemical shift of "normal" biphenyl units and that observed for the dibenzooxepine **98**. Firstly, as part of the 7-membered ring, the dibenzooxepine phenolic was substituted in the *meta* position. However, results by Jiang *et al.* [194] indicate that *meta* substitution with CH_2Ph, actually lowers the observed phenolic chemical shift by 0.11 ppm. The more probable explanation for the observed increase in chemical shift, is that steric and electronic effects associated with the 7-membered ring, including the *ortho* 5-5 bond, are the primary cause of the downfield shift for the 5-5 substituted phenolic group.

These results suggest that reactions of dibenzodioxocin structures, during thioacidolysis, may significantly affect quantification of lignins during ^{31}P NMR spectroscopic analysis. In particular, the formation of dibenzooxepine structures during thioacidolysis, may lead to a significant underestimation of the quantities of biphenyl units and an overestimation of the quantities of β-5 units.

How, and to what extent the presence of dibenzodioxocin structures will affect quantification by ^{31}P NMR spectroscopy, will also depend on a number of contributing issues. Firstly, although some estimates place biphenyl concentration in softwood lignin as high as 20-26% [107] there is no hard evidence about the proportion of these units involving dibenzodioxocin type structures. Secondly, the behaviour of dibenzodioxocin structures in "whole" lignin may differ from that of the pure model compound, during thioacidolysis. For example, structural constraints in the lignin polymer may not allow free rotation about the 5-5 inter-unit bond, which is needed for dibenzooxepine formation.

3.4 Conclusions

- During thioacidolysis of the dibenzodioxocin model compound **97**, approximately 70% reacted *via* an acid catalysed rearrangement, to yield dibenzooxepine **98** as the primary product. A further 20% reacted *via* "normal" thioacidolysis to yield dipropylguaiacol **61** and the guaiacyl trithioether **58** as products.

- The ^{31}P NMR spectroscopy results for the dibenzooxepine **98** suggested that the incomplete cleavage of dibenzodioxocin structures during thioacidolysis, was a potential source for under reporting of 5-5 units and an over reporting of β-5 units in lignin samples.

- Potentially exciting future work may come from the novel Hβ/Cβ HMQC correlation at 5.17/88.0 ppm for dibenzooxepine structure **98**. This correlation may allow further supporting evidence for the presence dibenzodioxocin structures in lignin to be collected. In particular the determination of this Hβ/Cβ correlation in an *in situ* lignin thioacidolysate circumvents the need for lignin isolation that is currently required for dibenzodioxocin determination.

There are no such things as applied sciences,
only applications of science.

Louis Pasteur

Chapter 4
Results for Radiata Pine and Method Development

4.1 Introduction

This chapter demonstrates the applicability of the thioacidolysis/^{31}P NMR spectroscopy technique to real lignin samples. Initially, thioacidolysis/^{31}P NMR spectroscopy was applied to radiata pine (*Pinus radiata*) milled wood lignin (MWL) (Section 4.2). This was then extended to *in situ* radiata pine wood lignin (Section 4.3). Radiata pine was selected for this work, because it is a typical softwood and is the most important commercial wood species in New Zealand [267].

The thioacidolysis/^{31}P NMR spectroscopy performed in Sections 4.2 and 4.3 were performed under optimised conditions. A number of method development issues related to technique optimisation, are discussed in Sections 4.4 to 4.8. In particular, reaction cook time (Section 4.4); quantitative ^{31}P NMR spectroscopic relaxation delay (Section 4.5); method reproducibility (Section 4.6); interference of carbohydrates (Section 4.7) and interference of extractives (Section 4.8) were investigated. The importance of these method development issues is best understood once an understanding of the overall method has been established.

4.2 *Thioacidolysis/Phosphorus NMR Spectroscopy of Pine MWL*

4.2.1 Phosphorus NMR spectra

Figure 4.1 compares the ^{31}P NMR spectra of radiata pine MWL and the pine MWL thioacidolysis product. In the two spectra, distinct regions of signal associated with aliphatic hydroxyl (145-148 ppm); internal standard (~144.9 ppm); condensed guaiacyl (G) (140.5-144.5 ppm); uncondensed G (139.5-140.5 ppm) and *p*-hydroxyphenyl (H) (~139 ppm) moieties can be observed.

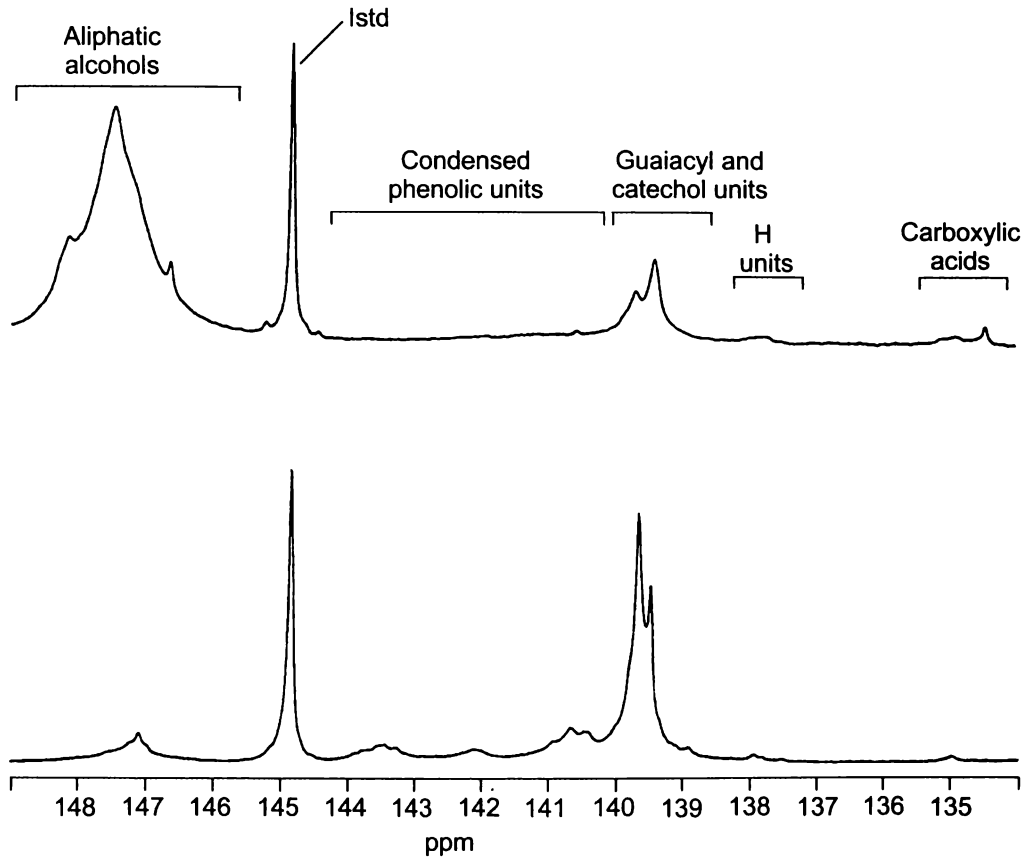

Figure 4.1: ^{31}P NMR spectra of phosphitylated (A) *Pinus radiata* MWL and (B) *P. radiata* MWL thioacidolysis product.

From the comparison of these spectra, a number of points may be seen:

- Only minor changes in the ^{31}P NMR chemical shifts of G, H and acidic groups were observed as a result of thioacidolysis. This observation fits closely with the small upfield shift observed, during thioacidolysis of various model compounds (Section 2.3).

- Thioacidolysis greatly reduced, but did not fully remove, the peaks at 146-148 ppm in the ^{31}P NMR spectrum associated with the aliphatic hydroxyl groups. This suggested, that while thioacidolysis led as expected [207, 214, 216], to replacement of most aliphatic hydroxyls in the lignin side chain, low levels of hydroxyls still remain in the lignin thioacidolysis product [232]. Polyethylene glycol ($\delta^{31}P$ = 147.2 ppm), introduced from the oil bath during thioacidolysis, may also contribute to the signal between 146-148 ppm.

- When ^{31}P NMR spectroscopy alone was performed on MWL, the uncondensed guaiacyl region (138.5-139.5 ppm) was a single broad signal, whereas for the thioacidolysis product, two partially resolved signals at 139.5 and 139.7 ppm were seen. This double signal was attributed to the diastereoisomerism present in the G trithioether product **58**, formed through thioacidolysis of β-ethers in lignin (as discussed in Section 2.3).

4.2.2. Quantification of phosphorus NMR spectra

Numerical data from integration of the spectra in Figure 4.1 is presented in Table 4.1. Before discussing these results, some definitions are required. The moieties identified as "Condensed", refer to condensed G units (Section 1.4.4). These are calculated by integration of the region 140.5-144.5 ppm. On the other hand, the "Guaiacyl" moieties, refer to uncondensed G (Section 1.4.4) units. These are calculated by integration of the 138.5-140.5 ppm region. The term "Free Phenolic", refers to phenolic moieties measured by ^{31}P NMR spectroscopy alone (Figure 4.1A), whereas "Total Lignin", refers to the phenolic moieties measured after thioacidolysis (Figure 4.1B). The values labelled "Etherified C9" in Table 4.1, refer to those units released by the thioacidolysis cleavage of β-aryl ether linkages in the MWL. These were determined by difference between the total lignin and the free phenolic groups.

Table 4.1: ^{31}P NMR spectroscopic results for *Pinus radiata* MWL.

	C9 units, mmol/g of lignin		
	Free Phenolic	Etherified C9	Total Lignin
Aliphatic hydroxyl	3.61	-	0.55
Condensed	0.36	1.01	1.37
Guaiacyl	0.61	1.87	2.48
p-hydroxyphenyl	0.08	0.01	0.09
Acidic	0.11	-	0.07
Measured phenolic	1.05	2.89	3.94
% Condensed	34	35	35

As expected, depolymerisation of lignin by thioacidolysis, led to a significant increase in the concentration of phenolic groups measured by ^{31}P NMR spectroscopy. For example, prior to thioacidolysis, 1.05 mmol of phenols/g of lignin was observed for radiata pine MWL. This equates to about 0.2 phenols per C9 unit, assuming a C9 molecular weight (MW) of 187 [51, 78, 123]. This value correlates closely to the 0.19-0.26 free phenolic units/C9 reported previously by various investigators for softwood MWL's [62, 66, 268, 269]. After thioacidolysis, around 0.75 phenols per C9 unit (3.94 mmol/g lignin) were measured. In other words, after thioacidolysis, the degree of condensation of around three-quarters of the C9 units in lignin could be determined.

The ^{31}P NMR spectroscopic quantification results were indirectly verified by combining two analytical techniques. Firstly, the proportions of methoxyl groups per C9 unit (OCH_3/C9) were determined by micro-analytical elemental analysis and methoxyl group determination [119, 270]. Subsequently, the ratio of phenolic hydroxyl groups to methoxyl groups (OH/OCH_3) was determined by performing quantitative ^{13}C NMR spectroscopy [66, 181, 271] on a sample of the lignin, which had been acetylated. By combining these two results, it was possible to calculate the proportions of free phenolic groups present in a given sample independently of the ^{31}P NMR spectroscopic result. The results are presented below in Table 4.2, and are compared with the appropriate ^{31}P NMR spectroscopy results.

Table 4.2: Yield analysis data for *Pinus radiata*.

Sample	Molecular formula	^{13}C NMR OH/OCH$_3$	calculated OH/C9	^{31}P NMR OH/C9
MWL	$C_9H_{9.0}O_{2.8}(OCH_3)_{0.89}$	0.25	0.22	0.20
MWL thioacidolysate	$C_9H_{10.4}O_{1.22}(OCH_3)_{0.88}SEt_{1.56}$	0.92	0.81	0.75

For MWL, the 0.22 phenolic moieties per C9 unit calculated in Table 4.2, correspond closely to the 0.2 phenolic moieties per C9 unit determined by ^{31}P NMR spectroscopy. Also, for the MWL thioacidolysis product, there was a reasonable agreement between the methoxyl/quantitative ^{13}C NMR spectroscopy results and the ^{31}P NMR spectroscopy results.

It is important to note that the molecular formula used in the above discussion only determines the average number of G units per C9 and that H units per C9 are not determined. This is not perceived to be a significant issue for radiata slabwood, where low concentrations of H units are present. However, analysis of lignins using the molecular formula and quantitative ^{13}C NMR spectroscopy may be less useful in compression woods where H units may account for up to 15% of all the C9 units.

While performing thioacidolysis significantly improved the amount of phenylpropane units measured, around 25% of the C9 units in lignin were still not measured, by either ^{31}P or ^{13}C NMR spectroscopy. This indicated that not all the phenyl propane units in the lignin were converted to phenolic moieties during thioacidolysis. One reason for this low yield may be incomplete thioacidolysis. Ralph and Grabber [272] have previously shown, that the thioacidolysis yield is less than 100%, with some β-aryl ether units remaining uncleaved. Another contributing factor may be the presence of 4-O-5 and dibenzodioxocin structures in lignin (Figure 4.2).

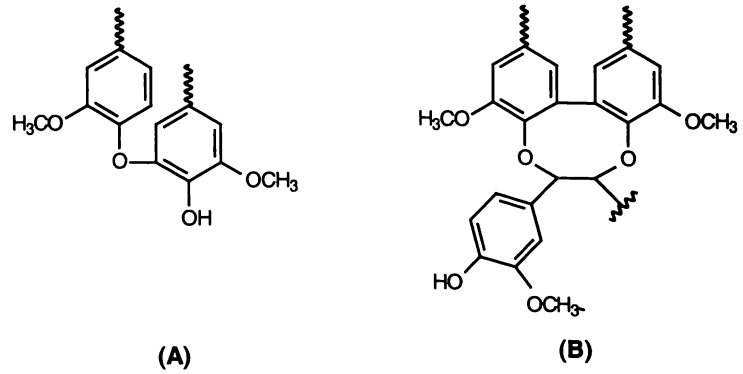

(A) (B)

Figure 4.2: Structures containing etherified structures not fully cleaved by thioacidolysis (A) 4-O-5, (B) oxepine.

Lapierre *et al.* [230, 231, 232] have shown that 4-O-5 inter-unit linkages are not cleaved by thioacidolysis. Thus, for every measured 4-O-5 phenolic moiety, a non-phenolic phenylpropane unit is also present in the thioacidolysate. Typically, these 4-O-5 type bonds comprise around 4% of the inter-unit linkages in softwood MWL [63, 78, 80].

Recent work has shown that many 5-5 units in native lignin may in fact be present as dibenzodioxocin structures [105, 106]. Currently, it is unclear exactly how many of the 5-5 inter-unit linkages are involved in dibenzodioxocin structures. Model compound work in Chapter 3 showed that dibenzodioxocin structures such as 97, undergo acid catalysed rearrangement during thioacidolysis. This rearrangement of 97, led to formation of a dibenzooxepine structure 98 (75% yield), which contained a 7-membered heterocyclic ring (Figure 4.3). In this dibenzooxepine product, one of the "5-5" phenolic oxygen groups remained etherified within the oxepine ring. The etherified phenolic oxygens in these dibenzooxepine structures may also contribute to the C9 units unaccounted for.

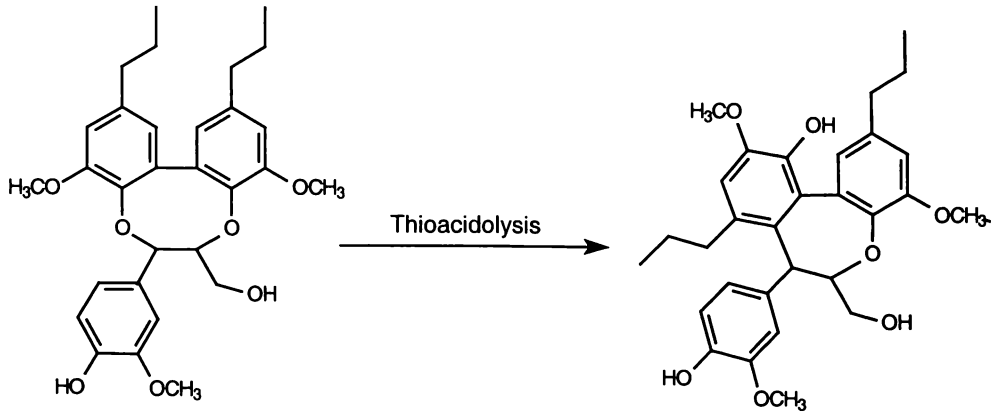

97 98

Figure 4.3: Thioacidolysis of dibenzodioxocin model compound (97) to yield an oxepine product (98).

4.2.3. Comparison between MWL and MWL thioacidolysate

For radiata pine MWL, the proportion of condensed to uncondensed units in the free phenolic and total lignin samples was very similar, 34% *vs.* 35% (Table 4.1). This indicated that for this sample, the composition of the free phenolic groups in MWL, at least in terms of condensed:uncondensed unit ratio, did reflect the nature of the majority of the lignin.

The main difference in lignin composition between the free phenolic portion and the total lignin, was the proportions of H units present. For radiata pine MWL, the H units measured in the lignin after thioacidolysis (0.09 mmol/g), were only slightly higher than those found as free phenolic units (0.08 mmol/g). This indicated that around 90% of the H units in the radiata pine MWL were present as free phenolic moieties. This result closely matches previous findings by Lapierre and Rolando [273], who reported that 90-93% of the H units in various poplar lignin preparations were present as free phenolic units.

4.2.4. Analysis of condensed structures

A further benefit of performing thioacidolysis prior to ^{31}P NMR spectroscopy, is the significant increase in resolution of peaks in the condensed region of the spectrum (140.5-144.5 ppm). Prior to thioacidolysis, the entire region was a single broad hump. However, after thioacidolysis, three distinct regions of signal were resolved. This improved resolution was attributed to the depolymerisation of the macromolecular lignin and subsequent decrease in the NMR spectroscopic linewidths.

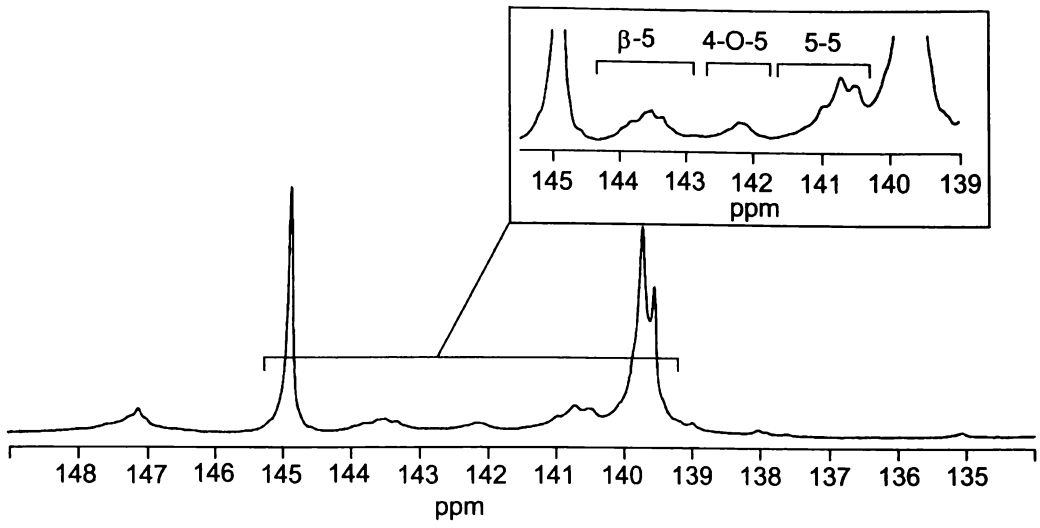

Figure 4.4: Close up of the condensed region in a ^{31}P NMR spectrum of a MWL thioacidolysis product.

Figure 4.4 shows a close up of the condensed region in the ^{31}P NMR spectrum of the MWL thioacidolysis product, with signal assignment indicated. The peaks centred at 143.6 and 141.2 ppm were attributed to β-5 and 5-5 type units respectively, based on the model compound results in Section 2.3 and the literature [194]. The third major peak, centred at 142.5 ppm, was attributed to 4-O-5 type units. There were two main reasons for this assignment. Firstly, 4-O-5 type units are the next most abundant condensed units in softwood lignins, after β-5 and 5-5 units [63, 78, 80]. Secondly, 4-O-5 type units have oxygen in the C5 position *ortho* to the phenolic OH group. The chemical shift of these units should be quite similar to that of syringyl (S) moieties, which are also bonded to oxygen at C5. Syringyl type model compounds show a chemical shift of 142.5 ppm [194]. However, in radiata pine, the level of S units is considered to be negligible [51, 54, 63, 76]. Ideally the chemical shift of 4-O-5 inter-unit links should be confirmed by model compound work. Due to the fact that the identification of this signal does not affect the validity of the overall technique and the time consuming nature of the complex multi step synthesis, no 4-O-5 models were prepared.

With individual regions of condensed units well resolved, it was possible to tentatively quantify the individual units in the condensed region, (Table 4.3).

Table 4.3: Comparison of levels of condensed units in MWL and wood.

	% of C9 units	
	MWL	Ref. [63]
β-5	8	9-12
4-O-5	5	~4
5-5	13	20-26*
* Drumond *et al.* [107] reported 20-26%.		

The results show that ^{31}P NMR spectroscopic quantification of the three condensed units (5-5, β-5, 4-O-5) gave results, which were reasonably consistent with those reported previously. The most significant difference was, that by thioacidolysis/^{31}P NMR spectroscopy, 13% of the C9 units in lignin were 5-5 type units, compared with 20-26% in the literature.

This difference in proportions of 5-5 units determined may be due to the presence of dibenzodioxocin structures in softwood lignins. As outlined previously, there is much evidence to suggest, that many 5-5 units in native lignin may in fact, be present as dibenzodioxocin structures [105, 106]. The acid catalysed rearrangement observed, during thioacidolysis of **97** (Figure 3.4), may explain why the observed 5-5 yield was lower than that previously reported. In the dibenzooxepine product **98**, one of the "5-5" phenolic oxygen groups remained etherified in a 7-membered heterocycle, whilst the free phenolic "5-5" exhibited a chemical shift around 143 ppm. Clearly, neither exhibit a chemical shift traditionally associated with 5-5 units derivatised with 2-cholro-4,4,5,5-tetramethyl-1,3,2-dioxaphospholane **41**. Acid catalyzed rearrangement of dibenzodioxocin structures in lignin during thioacidolysis may, significantly contribute to the underreporting of 5-5 type units.

Thioacidolysis followed by quantitative ^{31}P NMR spectroscopic analysis of the phosphitylated thioacidolysis product, was a viable method for determining the proportions of condensed and uncondensed units in isolated MWL samples. The

method also enables the levels of β-5, 5-5, 4-O-5 and G units in three-quarters of the C9 units in isolated lignin to be determined.

4.3 *Thioacidolysis/Phosphorus NMR Spectroscopy of in situ Pine Lignin*

Previous work by Lapierre *et al.* [216, 274, 275] has shown that thioacidolysis can readily be used to measure the levels of uncondensed β-ether units in *in situ* lignin samples, with carbohydrates not interfering with the analysis. Therefore, we looked at applying the thioacidolysis/^{31}P NMR spectroscopy technique to whole wood, to measure condensed and uncondensed units in *in situ* lignin. Figure 4.5 compares the ^{31}P NMR spectrum of the thioacidolysis products from radiata pine MWL and from radiata pine *in situ* lignin. The numerical data from integration of these spectra is presented in Table 4.4.

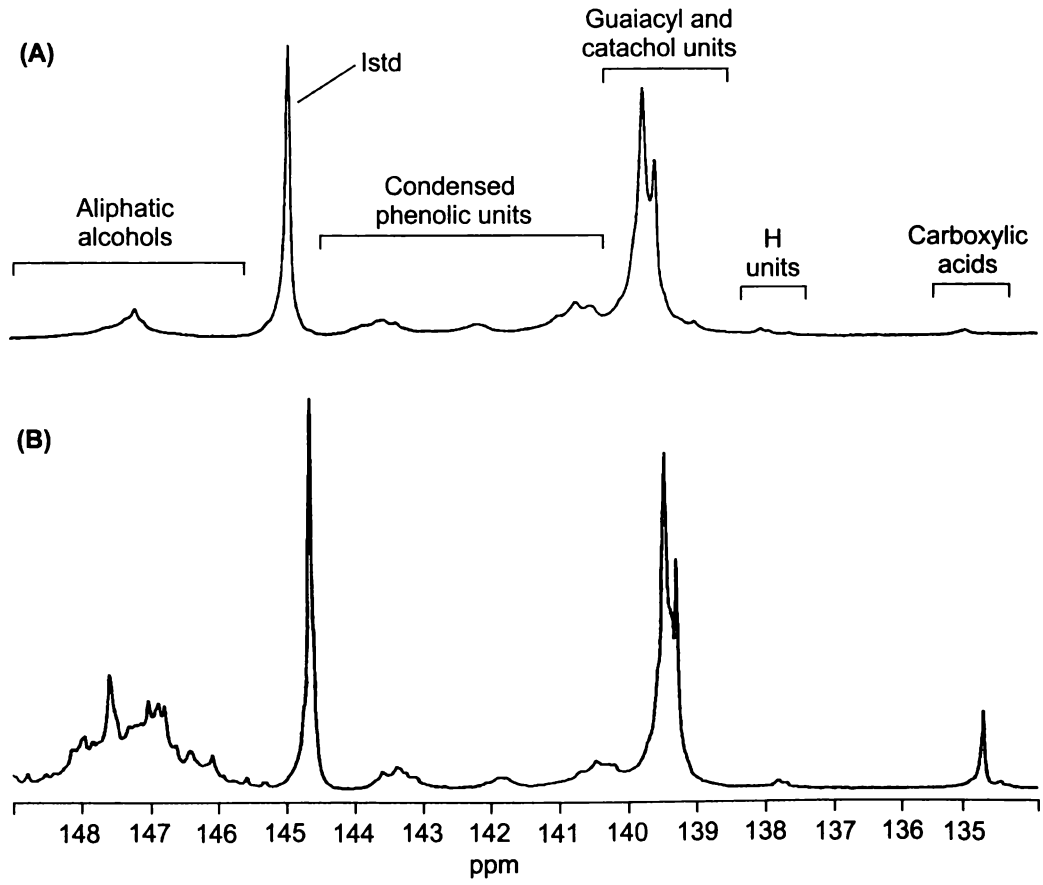

Figure 4.5: ^{31}P NMR spectrum of the thioacidolysis products from (A) radiata pine MWL and (B) radiata pine *in situ* lignin.

The concentration of aliphatic hydroxyl groups is the most obvious difference between the ^{31}P NMR spectrum of the MWL thioacidolysis product (Figure 4.5A) and that of the *in situ* wood lignin thioacidolysis product (Figure 4.5B). For the MWL sample, there was a small single peak, which was attributed largely to polyethylene glycol contamination. Some γ-hydroxyl groups have been shown to remain in the lignin after thioacidolysis [232] and may also contribute to this signal. On the other hand, for *in situ* wood lignin, a region of signal was observed from 145-148 ppm. Results from the carbohydrate model compound work (Section 4.7) suggest, that this region of signal with its multiple peaks, was predominantly due to the presence of carbohydrate material. These aliphatic hydroxyl/carbohydrate signals do not interfere with the quantification of phenolic units. Apart from this difference, the ^{31}P NMR spectrum of *in situ* and isolated *Pinus radiata* lignin were very similar.

For radiata pine *in situ* lignin, the total phenolic concentration in the thioacidolysate was determined at around 4.0 mmol/g of lignin (Table 4.4). This corresponds to around 0.77 phenolic moieties per C9 unit, which was essentially identical to the value determined for isolated MWL. However, attempted verification of the results from quantitative ^{31}P NMR spectroscopy by methoxyl content/quantitative ^{13}C NMR spectroscopy, as outlined for MWL (Section 4.2), was unsuccessful. Incorporation of soluble carbohydrates meant, that only around 0.50 methoxyl units per "C9" unit were measured by elemental analysis of the *in situ* lignin thioacidolysate.

Table 4.4: ^{31}P NMR spectroscopic results for *P. radiata* MWL and *in situ* lignin thioacidolysis products.

	C9 units, mmol/g of lignin	
	MWL	Wood
Aliphatic hydroxyl	0.55	3.61
Condensed	1.39	1.43
β-5	0.38	0.48
4-O-5	0.32	0.28
5-5	0.69	0.67
Guaiacyl	2.51	2.61
p-hydroxyphenyl	0.09	0.09
Total phenolic	3.99	4.04
% Condensed	35	35

The measured concentrations of condensed G (1.43 mmol/g), uncondensed G (2.61 mmol/g) and H (0.09 mmol/g) units, for *in situ* radiata pine lignin were comparable to those observed for MWL. The results indicate, that for both isolated MWL and *in situ* wood lignin, around 35% of the total phenolic moieties measured were condensed type units.

This result is interesting, because it may suggest, that there may be little difference in the proportions of condensed and uncondensed units in middle lamella (ML) and secondary wall (SW) lignin. Based on several considerations:

- There is much evidence to suggest that MWL actually comes predominantly from lignin residing in the SW, rather than being representative of the lignin in the total wood [125, 126, 127].
- A high proportion (77 %) of the total lignin was analysed for *in situ* radiata pine lignin, indicating that lignin from the total cell wall was being analysed.
- The similar proportions of condensed units in the MWL and the *in situ* lignin (Table 4.4) may therefore indicate that the ML lignin present in the *in situ* lignin sample contained similar proportions of condensed units to the SW lignin.

Recent work by Adams [276] indirectly supports the conclusion that ML and SW lignin may be quite similar in terms of amounts of condensed units present. Adams [276] compared lignin chemistry of fibres and fines separated from an MDF fibre preparation. It was found that the fines, which contained a high proportion of ML lignin, yielded similar amounts of uncondensed β-ethers by thioacidolysis as the fibres enriched in SW lignin. Indirectly this suggested that the amounts of condensed units in ML and SW lignin were more similar than previously reported.

However, both these conclusions contradict much literature, which suggests that ML lignin contains a higher proportion of condensed units than SW lignin.

- Early work by Matsukura and Sakakibara [277] showed from the analysis of oxidation and ethanolysis products of Ezomatsu (*Picea jezoensis*), that lignin from wood residue contained higher proportions of condensed units, than MWL or lignin in lignin-carbohydrate complex (LCC).

- Sarkanen [64] has shown that during DHP preparation, two polymerisation mechanisms can exist, namely bulk polymerisation and end-wise polymerisation. It has been argued that the higher concentration of lignin in the ML (*cf.* SW lignin) should lead to more bulk polymerisation, with the production of a more condensed lignin.
- More direct analysis by Terashima *et al.* [122] and Tomimura *et al.* [278, 279] used addition of [ring-U-^{14}C-5-^{3}H] labeled ferulic acid to the differentiating xylem of a pine, to monitor formation of condensed units. The tritium to ^{14}C ratios in ML lignin were shown to be lower (loss of C5 tritium) than in the SW lignin. This indicated a higher proportion of condensed inter-unit linkages in the ML lignin.
- Using the above radiotracer method, Terashima and Seguchi [72] have shown, that the proportions of condensed units in DHP lignin, was affected by the presence of carbohydrates. In particular, they reported that DHP formed in the presence of pectin contained more condensed units than the DHP formed in the presence of mannan. With the high concentrations of pectin present in the ML, and mannan in the SW, these results also suggested a higher proportion of condensed units in the ML *cf.* the SW.

One possible explanation for our results may lie in the assumptions made during the study. To reach our conclusion about the proportions of condensed units in ML and SW lignin, it was assumed that MWL was representative of SW lignin, where as *in situ* wood lignin represented both SW and ML lignin. Whilst it has been shown, that MWL originates primarily from lignin in the SW [125, 126, 127], some ML lignin may also be present in the MWL. It could therefore be argued that these isolated and *in situ* lignin samples were not significantly different, with one, the *in situ* lignin, being only slightly more enhanced in ML lignin. The differences between the ML and SW lignin may therefore be masked, due to the volume of SW lignin (75% of lignin in the softwood tracheid) combined with mixing of cell wall fractions in both samples.

Another possible explanation for our results may be, that thioacidolysis/^{31}P NMR spectroscopy is the first method which can simultaneously and directly quantify the proportions of condensed and uncondensed G units in the total *in situ* lignin. For example, in the radio tracer work by Terashima *et al.* [122] and Tomimura *et al.* [278, 279], the total activity of the aldehydes was only 8-19% of the labeled wood meal.

The information obtained was, therefore, restricted to only a part of the lignin macromolecule. It could be argued that thioacidolysis/^{31}P NMR spectroscopy is the first technique that can fully and accurately determine the proportions of condensed and uncondensed units.

The thioacidolysis/^{31}P NMR spectroscopy discussed in Sections 4.2 and 4.3 were performed under optimised conditions. Sections 4.4-4.8 discuss the method optimisation experiments performed.

4.4 Effect of Cook Time

Lapierre *et al.* [207] performed thioacidolysis at 100°C for 4 hours, to maximise the trithioether yields when using glass tube reaction vessels. However, work by Pasco and Suckling [220] showed, that in stainless steel reaction vessels, trithioether yield was maximised by performing thioacidolysis at 110°C for 2 hours. In the work presented here, teflon-lined steel reaction vessels were used, but rather than maximising trithioether yield, it was important to maximise total phenolic yield.

In order to optimise the reaction conditions for the thioacidolysis of isolated and *in situ* lignin, cooks were performed at 110°C and stopped at a range of times, (Figures 4.6 and 4.7).

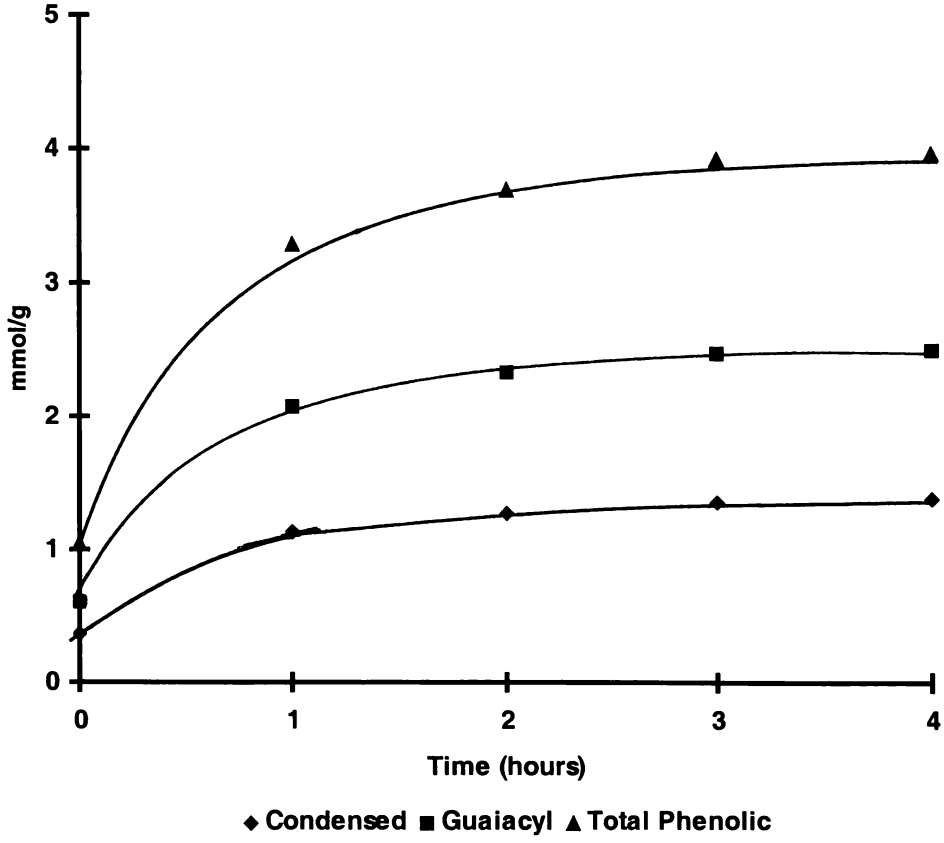

Figure 4.6: MWL yield (mmol of phenolic groups) as a function of thioacidolysis cook time.

For isolated MWL, ^{31}P NMR spectroscopy without thioacidolysis measured 1.05 mmol/g of phenolics (Figure 4.6). Due to cleavage of the β-O-4 linkages in lignin [207, 214, 216], the measured concentration of phenolic groups increased as the thioacidolysis time increased. The concentration of phenolic groups reached a maximum of around 4 mmol/g after 3 hours, with little increase in phenolic yield observed after this time.

The yield of phenolic units as a function of cook time (Figure 4.7), increased more slowly for *in situ* lignin than for MWL. For example, after 1 hour around 2.5 mmol/g of phenolic units were measured for *in situ* lignin, compared with 3.3 mmol/g for MWL. This lower rate of reaction is hardly surprising given the complexity of *in situ* lignin compared with isolated MWL. Diffusion effects, associated with transporting reaction chemicals into the fibres and solubilising lignin fractions out, add a dampening effect on the yield of phenolic groups as a function of time. Like MWL, a maximum yield of around 4 mmol/g of phenolic units was

observed. However, for *in situ* lignin, there was a difference of around 0.1 mmol/g between 3 hours and 4 hours, showing that the maximum yield was achieved sometime after 3 hours of cooking.

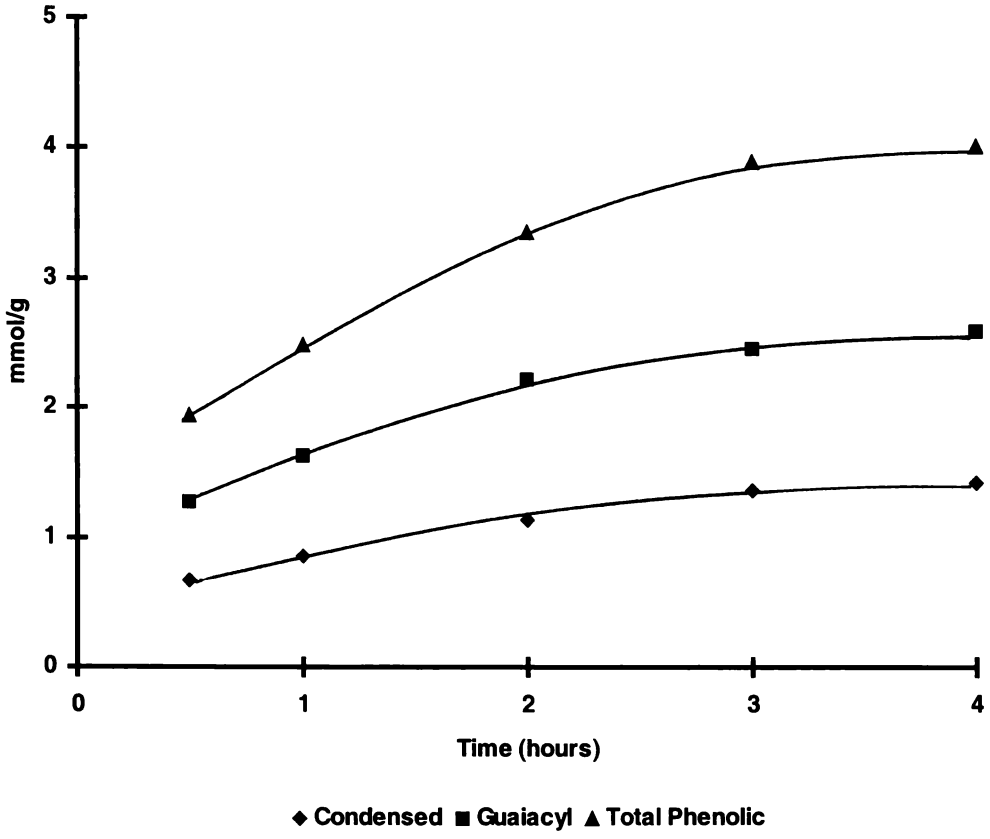

Figure 4.7: in *situ* wood lignin yield as a function of thioacidolysis cook time.

Of particular interest is the relative yield of condensed and uncondensed units as a function of thioacidolysis cook time. For both MWL and *in situ* lignin, the composition of the lignin at all stages of depolymerisation, was essentially identical. Around 35% of all the phenolic groups measured were condensed units at all reaction times.

On the basis of the above results, a constant cook time of 4 hours was used for all samples analysed in this thesis.

4.5 *Effect of Relaxation Delay*

4.5.1 Introduction

In order to obtain accurate signal areas during quantitative NMR spectroscopic experiments, sufficient delay time between pulses should be used. During a NMR spectroscopic experiment, one important way for the excited nuclei to dissipate energy is through spin lattice relaxation (T_1) [280, 281]. This spin lattice relaxation occurs by energy exchange between the high-energy nuclei and either the solvent molecules or neighbouring atoms. If the relaxation delay between pulses is too short, not all the excited nuclei have time to reach the equilibrium spin distribution. This can significantly affect the relative signal intensities measured.

In previous work, Argyropoulos *et al.* [282] have determined the ^{31}P spin lattice relaxation times for a variety of lignin model compounds. In the presence of paramagnetic chromium ($Cr(acac)_3$), the ^{31}P spin lattice relaxation times observed for lignin model compounds derivatised with the phosphitylating reagent 2-chloro-1,3,2-dioxaphospholane **39** were 2-5 seconds. Allowing 5 T_1 between pulses implies that a delay of 25-30 seconds should be used for quantitative determinations [283]. Argyropoulos *et al.* [282] have also published experimental details about quantitative ^{31}P NMR spectroscopy of MWL samples derivatised with 2-chloro-4,4,5,5-tetramethyl-1,3,2-dioxaphospholane **41**, using a delay time between pulses of 25 seconds.

There are a number of procedural differences that occur between the work reported in this thesis and that previously reported by Granata and Argyropoulos [189]. In this work, thioacidolysis was performed prior to ^{31}P NMR spectroscopy to depolymerise the lignin and cholesterol **62** was used as an internal standard (*cf.* cyclohexanol **40**). To see how these changes affect the required delay time, T_1 of a range of model compounds was measured. Subsequently, the effect of varying the delay time on the quantitative ^{31}P NMR spectroscopic results for a MWL thioacidolysis product was also assessed.

4.5.2 Calculating T_1 of model compounds

When calculating T_1, approximately 30 mg/mL of each model compound was used. This concentration was the same as the 30 mg/mL of MWL used during the quantitative ^{31}P NMR spectroscopy experiments. These similar concentrations of phenolic material were used, because it is well known that T_1 measurements are concentration dependent [284]. Also, paramagnetic $Cr(acac)_3$ was present as a relaxation agent, in both the model compound T_1 calculations and the quantitative ^{31}P NMR spectroscopy on actual lignin samples. The presence of $Cr(acac)_3$ meant no degassing of samples, prior to the T_1 determination, was performed.

Table 4.5 shows the T_1 values of various phosphitylated lignin model compounds, obtained under intermittent pulsing (delay time = 20 sec) using inversion recovery. Most T_1 values were collected on a Bruker Avance 200 spectrometer, operating at 81 MHz.

Excluding cyclohexanol **40**, the model compounds presented in Table 4.5, derivatised with **41**, exhibited ^{31}P NMR spin lattice relaxation times at 81 MHz, of between 1.5 and 2.3 sec. These T_1 values are typically shorter than the range of 2-5 sec reported by Argyropoulos *et al.* [282] for model compounds derivatised with **39**. The comparison of the two different internal standards was of particular significance. The spin lattice relaxation time measured for the more bulky cholesterol **62** (1.7 sec) was considerably lower than the T_1 measured for **40** (3.1 sec).

Table 4.5: ^{31}P NMR spectroscopic T_1 measurements for selected model compounds.

				161 MHz	81 MHz
Compound	N°	MW	$\delta\ ^{31}P$ (ppm)	T_1 (sec)	T_1 (sec)
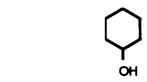	40	100		2.8	3.1
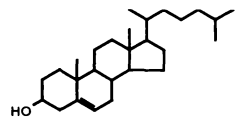	62	386		1.3	1.7
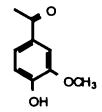	69	162	138.9	2.0	2.3
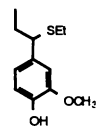	64	226	139.5		2.1
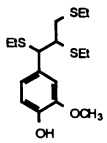	58	346	139.4 139.5		1.9
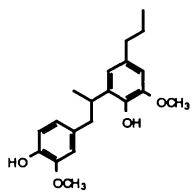	89	330	139.7 143.8		2.0 1.5
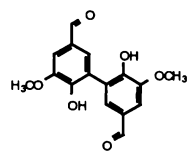	72	302	140.9		1.6
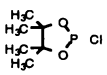	41	182.5	144.9		2.1
Reaction product of 41 with water		310	132.2		2.0

For the G monomers (58, 64 and 69), spin lattice relaxation time values ranged between 1.9 and 2.3 seconds. The introduction of thioethyl groups, such as in model compounds 64 and 58, did not significantly affect the T_1. Rather, as the molecular weight of the phenolic compounds increased, T_1 decreased.

The introduction of bulky substituents near the derivatised functional group (72 and 89) also reduced T_1. For example the phosphitylated biphenyl compound 72 exhibited a T_1 of 1.6 sec and the phosphitylated B-ring of 89 exhibited a T_1 of 1.5 sec. This compares with a T_1 of 2.1 sec for phosphitylated 64. This result is as expected given that the proximity of bulky groups aids in the dissipation of energy from the excited phosphorus atom. The shortening of T_1 due to the proximity of bulky groups was similarly observed by Argyropoulos *et al.* [282]. They reported a T_1 of 5.1 sec for dipropylguaiacol 61, compared with 7.2 sec for the phenolic group in cinnamic acid 29.

To determine the effect of B_0 on the measured T_1 values, some T_1 values were also collected at 161 MHz on a Bruker Avance 400 spectrometer. For the 3 compounds (40, 62 and 69) investigated at 161 and 81 MHz, the T_1 values measured at 161 MHz were typically 0.3-0.4 seconds shorter, than the T_1 values at 81 MHz (Table 4.5). This indicates that for the ^{31}P NMR spectroscopy of these compounds, B_0 only had a small, but measurable, effect on the measured T_1.

4.5.3 Effect of delay time on MWL quantification

Allowing 5 T_1 between successive pulses in a quantitative NMR spectroscopy experiment would imply that quantitative ^{31}P NMR spectroscopy could be collected by using a delay time around 12-15 seconds. In order to confirm this, a phosphitylated MWL thioacidolysis product was analysed using a range of delay times (Figure 4.8).

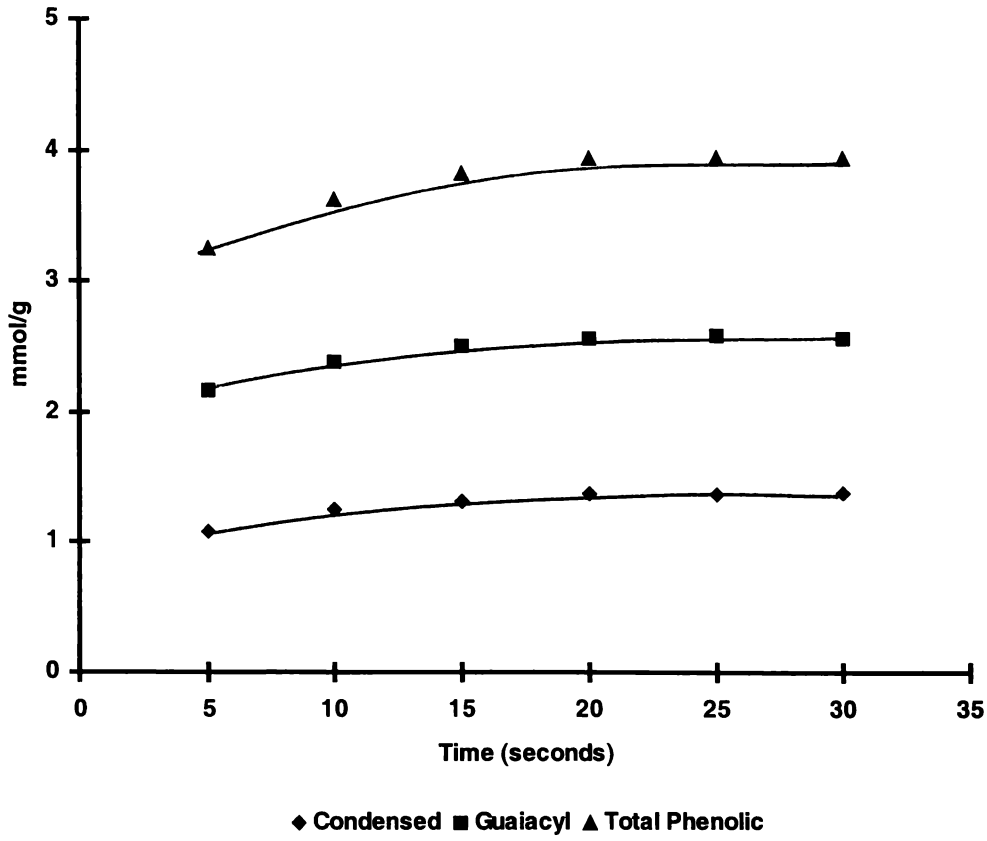

Figure 4.8: Yield of ^{31}P NMR spectroscopy as a function of delay time between pulses.

The measured lignin phenolic content at a 15 sec delay time was about 0.1 mmol/g lignin lower than the values measured using 20, 25 and 30 sec delay times. This indicated that the maximum quantification was not reached at 15 seconds as predicted by the T_1 work above, and that a 20-sec delay time would give a better result. It is unclear why there is this discrepancy between the delay calculated from T_1 and those observed for the real MWL sample.

In summation, the conditions used in this thesis allowed a relaxation delay of 20 seconds to be used for quantitative ^{31}P NMR spectroscopy.

4.6 *Reproducibility*

4.6.1 Introduction

Reproducibility results in this section are divided into two distinct parts. Firstly, errors present in the ^{31}P NMR spectroscopic analysis were examined. This was to determine the effect of the changed conditions, relative to previous work [185, 188, 193] on the estimated errors. To do this, twelve sub-samples of a thioacidolysate, prepared using 360 mg of radiata pine MWL, were derivatised and analysed by ^{31}P NMR spectroscopy and spectral reprocessing. The results are shown in Table 4.6 and the complete data is presented in Appendix B.2.

It was also necessary to estimate the reproducibility of the whole analysis procedure including thioacidolysis. For this, twelve identical MWL samples were subjected to thioacidolysis, ^{31}P derivatisation, NMR spectroscopy and FID processing. By comparing these results with the reproducibility data generated for ^{31}P NMR spectroscopy alone, an estimate about the influence of thioacidolysis can be made. The results for these experiments are presented in Table 4.7, with the complete data also in Appendix B.2.

Confidence intervals were constructed using the Student t distribution. This was possible because of the small population size and the assumption that the measured values were random with an approximate normal distribution. The general equation for the construction of a (1-α) 100% confidence interval, where n<30, is presented below.

$$\bar{x} - t_{\alpha/2}\frac{s}{\sqrt{n}} < \mu < \bar{x} + t_{\alpha/2}\frac{s}{\sqrt{n}}$$

Where $t_{\alpha/2}$ is the t value with n-1 degrees of freedom, above which the area under the normal curve equals $\alpha/2$. The percent error in Tables 4.7 and 4.8 refers to the error associated with the 99% confidence interval.

4.6.2 Errors in ^{31}P NMR spectroscopy

Table 4.6: Error calculations for ^{31}P NMR spectroscopy.

Lignin functional group	Mean Value (mmol/g)	Standard deviation	99% confidence limit	% error
β-5	0.38	0.015	0.013	3.5
4-O-5	0.31	0.012	0.011	3.4
5-5	0.68	0.026	0.023	3.5
Condensed	1.38	0.036	0.032	2.3
Guaiacyl	2.48	0.056	0.050	2.0
p-hydroxyphenyl	0.10	0.007	0.006	6.6
Total phenolic	3.96	0.082	0.073	1.9

Reproducible results were obtained for the derivatisation/^{31}P NMR spectroscopy of the homogeneous radiata pine MWL thioacidolysate. The main regions, such as condensed, guaiacyl or total phenolic, exhibited an error of around ±2%. However, for regions of signal where the phenolic concentration was lower, the observed error increased slightly, for example for individual condensed units around ±3% error was observed. These errors are considerably smaller than those observed previously by Argyropoulos [185], where the 99% confidence interval for the different regions of signal was between ±6% and ±9%.

There are a number of reasons why smaller errors were observed in this study than in previous work [185]. Firstly, around three-quarters of the phenolic units in lignin were determined, compared to around 40% in the earlier study. The increased yield reduces the percentage error of consistent errors. Another reason for the improved reproducibility in this work compared with Argyropoulos *et al.* [185], was the collection of twelve spectra for the error determination rather than the four determinations used previously. Typically, using a larger sample population will reduce the standard deviation and therefore decrease the observed confidence intervals [285].

The improvement in quantitative errors may also be due to the significant improvement in spectral resolution.

- The use of 2-chloro-4,4,5,5-tetramethyl-1,3,2-dioxaphospholane **41**, as a derivatising reagent, led to much better separation between signals associated with aliphatic hydroxyl and phenolic groups, than when using phosphitylating reagent **39**.
- Thioacidolysis prior to ^{31}P NMR spectroscopic analysis lead to significant peak sharpening and markedly improved delineation between areas of signal (Section 4.2).

4.6.3 Errors in thioacidolysis/^{31}P NMR spectroscopy

Table 4.7: Error calculations for thioacidolysis and ^{31}P NMR spectroscopy.

Lignin functional group	Mean Value (mmol/g)	Standard deviation	99% confidence limit	% error
β-5	0.38	0.025	0.022	5.9
4-O-5	0.31	0.022	0.019	6.2
5-5	0.68	0.044	0.040	5.8
Condensed	1.38	0.062	0.056	4.0
Guaiacyl	2.49	0.092	0.083	3.3
p-hydroxyphenyl	0.11	0.013	0.012	10.8
Total phenolic	3.98	0.148	0.133	3.4

Table 4.7 shows the errors associated with quantitative determinations combining thioacidolysis and ^{31}P NMR spectroscopy. The introduction of errors associated with the thioacidolysis step, approximately doubled the confidence intervals for the different phenolic units. Compared with the ±2% (Table 4.6), the errors for guaiacyl, condensed and the total phenolic region were ±3-4%, when the complete thioacidolysis/^{31}P NMR spectroscopy was investigated. Also, for the smaller individual condensed regions, the error terms have increased from around ±3% to typically ±6%. The worst results were observed for the small signal associated with the H units, where the error was approximately ±10%.

These confidence intervals for the determination of the mean values are clearly quite good. However, for time and cost considerations, it is highly impractical to analyse each lignin sample twelve times. For that reason, only duplicate determinations were performed in this thesis, with the average value of the duplicates reported.

4.7 Phosphorus NMR Spectroscopy of Derivatised Carbohydrates

For thioacidolysis/^{31}P NMR spectroscopy applied to an isolated MWL sample, there was little possibility of carbohydrate interference on the quantification of phenolic units. However, it is important for the application of thioacidolysis/^{31}P NMR spectroscopic methods to *in situ* lignins, that carbohydrates exhibit both a limited reactivity to thioacidolysis [207, 216] and little interference with the quantification of phenolic compounds or the ISTD by ^{31}P NMR spectroscopy.

Table 4.8 summarizes the results from the ^{31}P NMR spectroscopy of various phosphorus derivatised carbohydrate model compounds. Both D-xylose **3** and D-arabinose **2**, which both have four hydroxyl groups, gave four sharp and well separated signals between 145.8 and 147.6 ppm. For D-glucose **1**, D-galactose **5** and D-mannose **4**, which all have five hydroxyl groups, five well-resolved signals of approximately equal intensity were observed between 145.6 and 148.3 ppm. However, for D-galactose **5** and D-mannose **4**, as well as the five major signals, five much smaller peaks (~10% intensity) were also observed (*the chemical shift of these smaller peaks is not reported in Table 4.8). This suggests, that in these two samples, both the α and β anomers were present, one in a much lower quantity than the other.

For the uronic acids **100** and **101**, four signals were observed between 146.4 and 147.8 ppm, consistent with the four-hydroxyl groups present in each model. Also, as expected, the carboxylic acid groups on **100** and **101** fell further upfield at 135 and 135.4 ppm respectively.

In earlier work, Archipov *et al.* [286] have determined the chemical shifts of carbohydrate model compounds derivatised with 2-chloro-1,3,2-dioxaphopholane 39. By using various substituted sugars (e.g. 3-O-Methyl-α-D-glucose or 4,6-O-Ethylidene-α-D-glucopyranose), they were able to assign each of the hydroxyl groups in the original sugars. In this study, this type of detail was not required. However, what is of importance, is whether the carbohydrate groups interfere with the phenolic and ISTD regions of the ^{31}P NMR spectrum and whether the thioacidolysis degradation products of carbohydrates interfere with the analysis.

Table 4.8: ^{31}P NMR spectroscopic results for carbohydrates.

		δ ^{31}P (ppm)	
Carbohydrate	N°	Before thioacidolysis	After thioacidolysis
D-Glucose	1	146.7, 146.8, 147.3, 147.9, 148.1	146.6-148.6
D-Arabinose	2	146.5, 146.7, 146.9, 147.1	146.2-147.6
D-Xylose	3	145.8, 146.3, 147.1, 147.6	145.7-147.3
D-Mannose	4	145.6, 146.4, 146.5, 147.6, 148.3*	145.8-147.9
D-Galactose	5	146.6, 146.9, 147.3, 147.4, 147.8*	145.9-148.3
D-Galacturonic acid	100	135.0, 146.7, 147.1, 147.3, 147.4	
D-Glucuronic acid	101	135.4, 146.4, 147.6, 147.7, 147.8	
* see discussion above			

The use of 2-chloro-4,4,5,5-tetramethyl-1,3,2-dioxaphospholane 41 as a derivatising reagent for carbohydrate model compounds, led to an approximately 3 ppm spread for hydroxyl groups, from 145.6-148.3 ppm. Given the range of chemical shifts observed above, carbohydrates should not interfere with the determination of phenolic hydroxyl groups (137-144 ppm) or the internal standard (144.9 ppm).

After thioacidolysis, the carbohydrates, 1, 2, 3, 4 and 5, did not exhibit signals in the phenolic hydroxyl (137-144.5 ppm) or cholesterol 62 (144.9 ppm) regions, during ^{31}P NMR spectroscopy (Table 4.8). The carbohydrate thioacidolysis product contained a number of partially thiolated products. In these cases, the ^{31}P NMR spectroscopy was performed on the mixture of products, with no attempt made to separate the

different thioacidolysis products in the product mixtures. These thioacidolysis mixtures gave a broad region of signal (145.8-148.6 ppm), for example Figure 4.9.

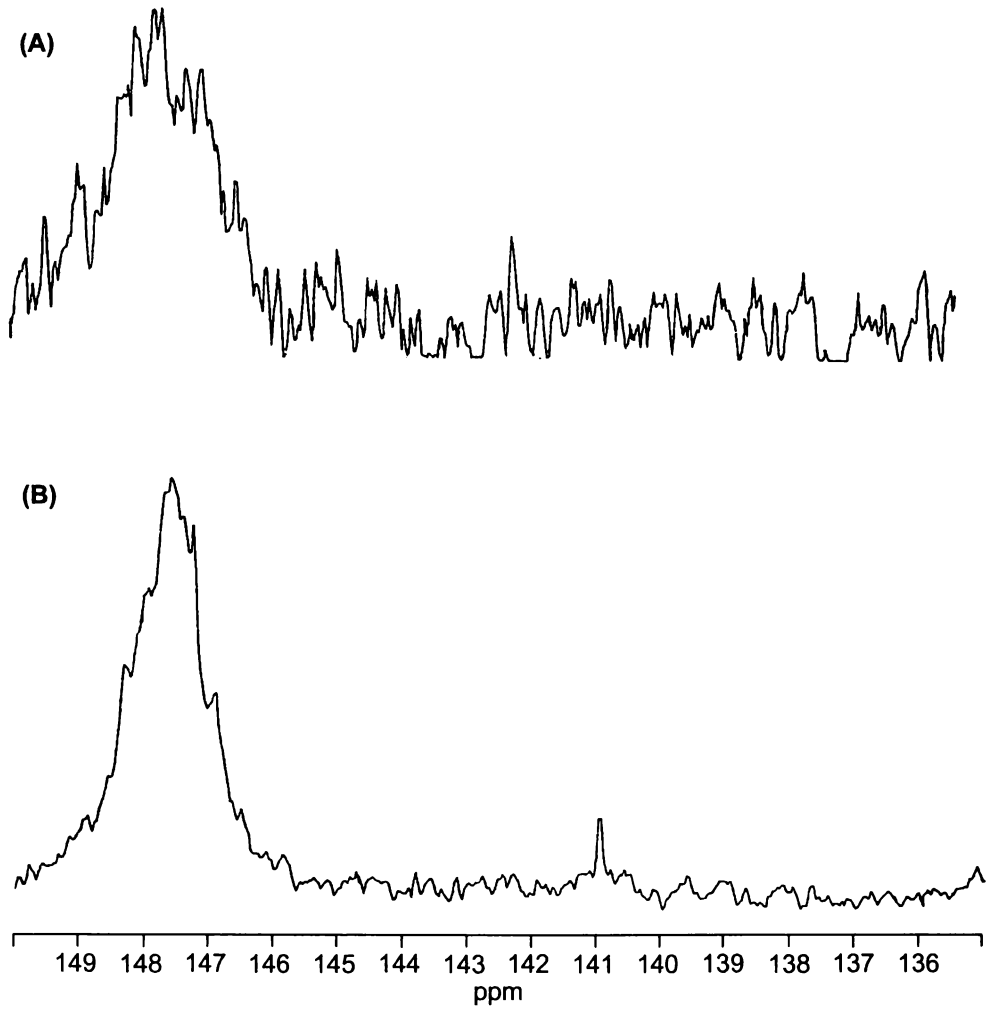

Figure 4.9: ^{31}P NMR spectra of carbohydrate model compounds after thioacidolysis, (A) Glucose (1) and (B) Xylose (2).

As well as model compounds, the ^{31}P NMR spectra of a *Pinus radiata* wood holocellulose [287] thioacidolysis product was inspected (Figure 4.10). No signals were observed in the phenolic region, with minor signals around 135 and 147 ppm, which can be attributed to carboxylic and aliphatic groups, respectively. Combined with the results for the carbohydrate model compounds, this suggests that there is no interference from carbohydrate units on the ^{31}P NMR spectroscopic quantification of phenolic groups in *in situ* lignin.

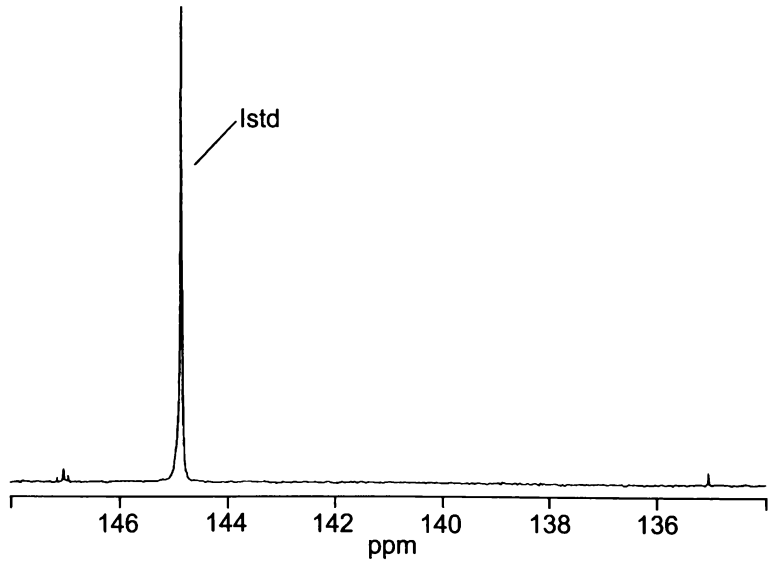

Figure 4.10: ^{31}P NMR spectrum of holocellulose thioacidolysis product.

4.8 Effect of Extractives

4.8.1 Introduction

Besides the main cell wall components, wood contains numerous low molecular weight extractive compounds (Section 1.3.3). Due to the potential of some of these compounds to interfere with the quantitative ^{31}P NMR spectroscopy of lignin structures, it was important to investigate these extractives.

As outlined in Section 1.3.3, extractives include a wide range of compounds including steroids, fatty acids, resin acids, terpenes and polyphenols. The extractive model compounds selected reflect the major types of extractives in both softwoods and hardwoods.

- Terpenes such as α-pinene 7 and β-pinene 8, constitute a large proportion of the monoterpenes present in softwoods like *Pinus radiata* [20, 38, 44, 288, 289]. However, all the wood samples used in this study were oven dried prior to use. For this reason, volatile monoterpenes [20, 37, 244] were not expected to be present in the wood samples subjected to thioacidolysis/^{31}P NMR spectroscopy. The extractive work presented here focused on the effects of non-volatile extractives only.

- Mono, di and triglycerides constitute a large proportion of the extractives in both *Pinus radiata* and eucalypt species [20, 37]. However, these compounds are not expected to interfere with the analysis of phenolic compounds. Firstly, triglycerides lack free hydroxyl groups, therefore lacking the ability to undergo phosphitylation. On the other hand, the less abundant mono and diglycerides only contain aliphatic hydroxyl groups and, therefore, also do not interfere with the quantification of phenolic units by ^{31}P NMR spectroscopy.
- Although resin acids were not expected to interfere with the quantification of the phenolic region in ^{31}P NMR spectra, three resin acid model compounds levopimaric **9**, pimaric acid **10** and dehydroabietic **102** were investigated.
- To determine the effect of sterols on the ^{31}P NMR spectroscopy of wood samples, β-sitosterol **14** was used as a model compound.
- The main interference of extractives with the ^{31}P NMR spectroscopy of wood samples, was expected to come from phenolic and polyphenolic extractives. This is due to the presence of numerous phenolic groups on each compound. Model compounds were selected to cover the three main categories of polyphenolic extractives present in hardwoods and softwoods; flavonols, dihydroflavonols and hydrolysable tannins [38, 41, 49, 50]. To this end, the model compounds morin **103**, dihydroquercetin **104**, pyrogallol **105**, gallic acid **18** and ellagic acid **19** were used.

4.8.2 Resin acids

Three resin acid model compounds were chosen to model the behaviour of these extractives during ^{31}P NMR spectroscopy. The ^{31}P NMR chemical shifts observed for these model compounds are shown in Table 4.9.

Table 4.9: ^{31}P NMR spectroscopic results for wood extractives.

Compound	N°	δ ^{31}P (ppm)
Levopimaric acid	**9**	134.9
Pimaric acid	**10**	134.8
Dehydroabietic acid	**102**	135.7

The resin acids used in this model compound work, 9, 10 and 102, exhibited ^{31}P NMR spectroscopic signals at approximately 135 ppm, essentially identical to that previously observed for other carboxylic acids [194]. Resin acids therefore, only interfere with the quantification of carboxylic acid groups in the lignin. However, this study is focussing solely on the quantification of phenolic compounds. For this reason, the resin acids do not need to be removed from wood samples prior to thioacidolysis/^{31}P NMR spectroscopy.

4.8.3 Sterols

Not unexpectedly, the observed chemical shift of 144.92 ppm for β-sitosterol 14 was essentially identical to the 144.95 ppm observed for cholesterol 62. Figure 4.11 shows the structures of 14 and 62. The only difference between the two is the inclusion of an extra ethyl group on the side chain of 14. The similarity of the ^{31}P NMR chemical shift between 14 and 62 indicated that the presence of β-sitosterol in a wood sample would lead to an over estimation of the cholesterol peak and a subsequent underestimation of the lignin/phenolic content. Although the sterol concentration in the genus *Pinus* is typically around 1-2% of total extractives [20, 37, 290, 291], it is still important to completely remove sterols, like 14, from a wood sample prior to thioacidolysis/^{31}P NMR spectroscopy. This sterol removal becomes even more important for hardwood samples, where the sterols can comprise around 4-5% of extractives [292, 293].

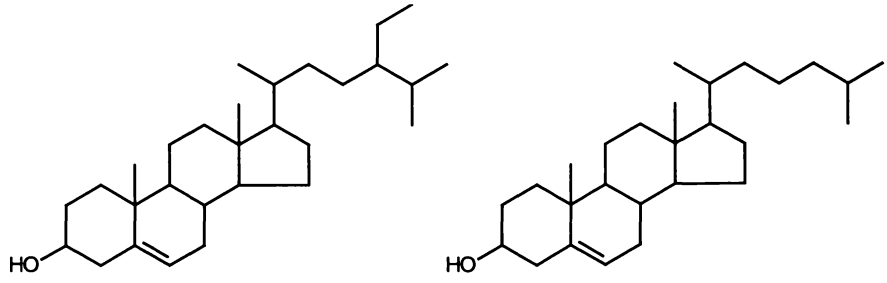

β-sitosterol 14 cholesterol 62

Figure 4.11: Comparison of β-sitosterol and cholesterol.

4.8.4 Polyphenolic extractives

Model compounds reflecting the three main categories of polyphenolic extractives (Section 1.3.3) were used to determine any interference with the quantitative ^{31}P NMR spectroscopy of lignin. To aid discussion, the carbon skeletons and numbering systems of flavonols, dihydroflavonols, gallic acid and ellagic acid are shown in Figure 4.12.

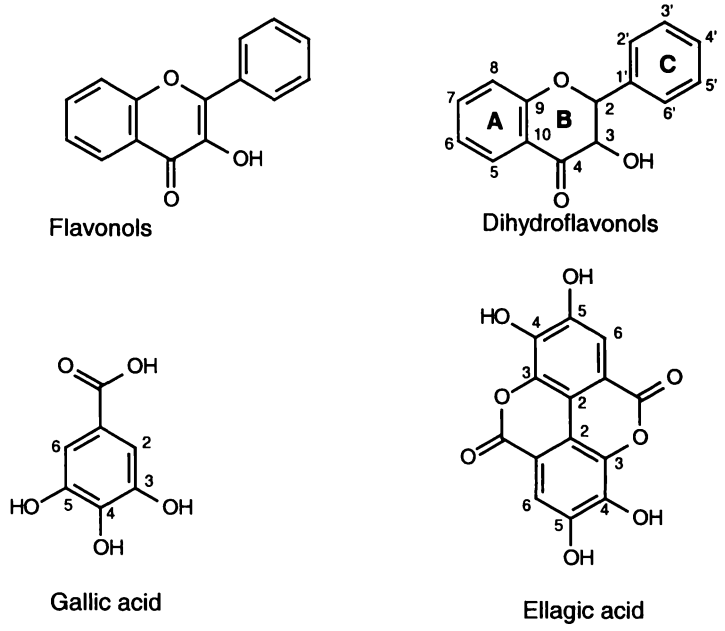

Figure 4.12: Numbering system of flavonols, dihydroflavonols, gallic acid and ellagic acid.

Table 4.10 contains a summation of the data collected by performing ^{31}P NMR spectroscopy on various polyphenolic model compounds derivatised with 2-chloro-4,4,5,5-tetramethyl-1,3,2-dioxaphospholane 61.

Table 4.10: ^{31}P NMR spectroscopic results for polyphenolic extractive model compounds.

Extractive Model	N°	δ ^{31}P NMR (ppm)*	Tentative Assignment
Morin	**103**	136.74 (s, 1P); 137.49 (s, 1P); 138.15 (s, 1P); 139.18 (s, 1P).	C5-OH, C7-OH, C3'-OH, C4'-OH
		140.67 (s, 1P).	C3-OH
Dihydroquercetin	**104**	136.42 (s, 1P); 136.98 (s, 1P).	C5-OH, C7-OH
		138.94 (d, J = 7.8 Hz, 1P); 139.17 (d, J = 7.8 Hz, 1P).	C4'-OH, C3'-OH
		146.93 (s, 1P).	C3-OH
Pyrogallol	**105**	138.32 (d, J = 8.0 Hz, 2P).	C3-OH,C5-OH
		142.39 (t, J = 8.0 Hz, 1P).	C4-OH
Gallic Acid	**18**	134.36 (s, 1P).	COOH
		138.63 (d, J = 7.8 Hz, 2P).	C3-OH, C5-OH
		141.58 (t, J = 7.8 Hz, 1P).	C4-OH
Ellagic Acid	**19**	139.17 (d, J = 8.1 Hz, 2P).	C5-OH
		141.64 (d, J = 8.1 Hz, 2P).	C4-OH

* chemical shift, multiplicity, intensity.

For the flavonol and dihydroflavonol model compounds, morin **103** and dihydroquercetin **104**, the substituent effects published by Jiang *et al.* [194] only allowed tentative assignments of hydroxyl groups to be made. For example, for dihydroquercetin **104**, it was possible to assign the singlets at 136.42 and 136.98 ppm to the A-ring phenolic groups. The doublets, centred at 138.94 and 139.17 ppm, could be assigned to the B-ring catechol phenolic groups. Assignment of signals to individual phenolic groups was however, not possible due to the substituent groups at C9, C10 and C1'. Compared with the linear two and three carbon substituents reported by Jiang *et al.* [194], these substituents were part of the 6-membered heterocycle.

In order to fully assign the ^{31}P NMR spectra of flavonols and dihydroflavonols, model compound work would be required to:

- Fill in some of the gaps in regard to the effects of *ortho* and *meta* substitution.
- Determine the substituent effects of different substituents, such as the 6-membered heterocycle.

This type of work clearly falls outside the scope of this thesis.

Assignment of the phenolic groups for the hydrolysable tannin model compounds was rather more straightforward. Symmetry present in 18, 19 and 107, combined with the substitution effects published by Jiang *et al.* [194], allowed straightforward differentiation between phenolic groups with one *para* substituent and those with two.

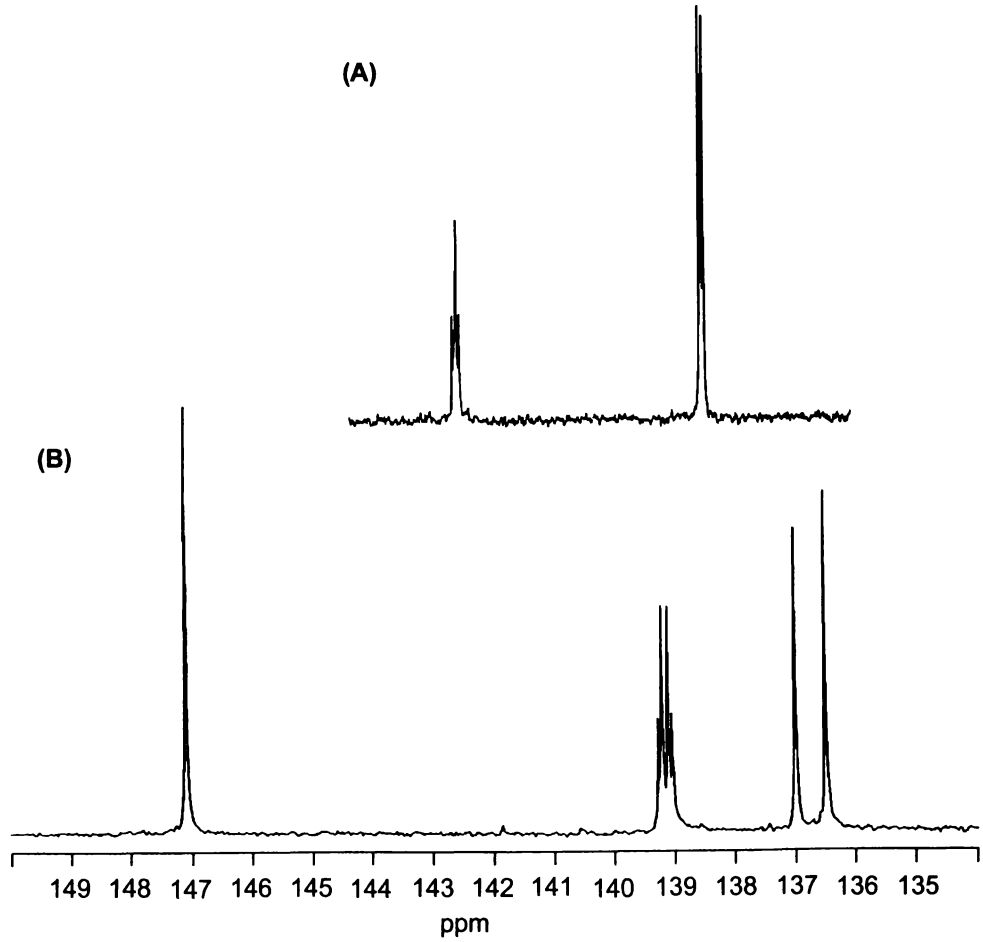

Figure 4.13: ^{31}P NMR spectra of (A) pyrogallol (105) and (B) dihydroquercetin (104).

Of particular interest in Table 4.12 is the observed multiplicity in 18, 19, 104 and 105. Figure 4.13 shows two examples of such coupling, for pyrogallol 105 and dihydroquercetin 104. This observed multiplicity was attributed to ^{5}J ^{31}P-^{31}P through

space coupling [254], similar to that previously discussed for 4-methyl catechol **93** (Section 2.3).

Coupling in the polyphenolic extractives was confirmed by ^{31}P-^{31}P COSY 90 experiments. Also, the calculated (Section 6.10) ^{31}P-^{31}P distances through space, for **105** (Table 4.11), was around 4.10 Å, shorter than that calculated for 4-methyl catechol **93**. This distance is still slightly longer than the sum of the van der Waals' radii of phosphorus (3.80 Å) [258]. However, the collisional and vibrational energy of the derivatised model compounds in solution, may lead to the population of states with shortened intermolecular ^{31}P-^{31}P distances, allowing through space coupling [254, 259].

Table 4.11: Calculated ^{31}P-^{31}P intramolecular distances.

Extractive Model	N°	Calculated intramolecular ^{31}P-^{31}P distance
4-methyl catechol	**93**	4.20
Pyrogallol	**105**	4.08, 4.13

For all five model compounds in Table 4.10, the phenolic groups exhibited chemical shifts in the range 136.42-142.39 ppm. Given this range of chemical shifts, polyphenolic extractives could interfere with the quantification of the various lignin phenolic units. Due to this potential interference, it is important that polyphenolic extractives are completely removed from wood samples prior to thioacidolysis/^{31}P NMR spectroscopy. While dihydroflavonols only constitute a small proportion of the extractives in softwoods, accuracy of quantification is aided by their removal.

4.8.5 Extractives in wood samples

As extractives interfere with ^{31}P NMR spectroscopy of phenolic compounds, they need to be completely removed from lignin samples with a suitable solvent. This following section describes a number of extraction methods, as applied to real wood samples of both radiata pine and Eucalypt. The work was based around the premise that a single stage extraction procedure was more desirable in terms of routine application than the more comprehensive extraction procedure involving dichloromethane, water and ethanol (C/H/E). The C/H/E extraction was chosen as a benchmark, due to its ability to thoroughly remove extractives from wood samples

[127, 294]. Also, the extraction procedure was targeted at polar extractives such as polyphenolic materials, which have been shown to interfere with the ^{31}P NMR spectroscopy of other phenolic material (Section 4.8.3). To this end, non-polar extraction solvents such as ether or dichloromethane, were not evaluated.

Initially, the methanol extractives from both radiata pine sapwood and eucalypt were evaluated for quantity and ^{31}P NMR spectroscopic interference. Subsequently, the quantitative ^{31}P NMR spectra of these same two wood samples were compared, using either a single step methanol or three step C/H/E extraction.

Figure 4.14 shows the qualitative ^{31}P NMR spectra of the radiata pine toplog and commercial eucalypt chip methanol extracts, derivatised with 2-chloro-4,4,5,5-tetramethyl-1,3,2-dioxaphospholane **41**. The 1.4% methanol extractives content for *Pinus radiata* slabwood and 3.6% methanol extractives content for eucalypt, determined gravimetrically, correlated favourably with extraction quantities published previously [19, 20, 30, 39, 41, 44, 50].

In both methanol extracts, steroid material (for example β-sitosterol **14**) was present, as evidenced by the signal at approximately 145 ppm. This was particularly noticeable for the eucalypt methanol extract. The almost complete lack of any ^{31}P NMR spectroscopic signals between 137 and 144.5 ppm in Figure 4.14(A), indicated that essentially no phenolic material was removed from the *P. radiata* wood by methanol extraction. This was consistent with the previously reported low concentrations of polyphenolic compounds in *P. radiata* sapwood [39, 40, 48, 295]. As expected, the radiata pine extract did contain significant amounts of resin acids, ~135 ppm, compared with the extract from the commercial eucalypt. For the eucalypt sample (Figure 4.14(B)), uncondensed phenolic extractives were removed from the wood by methanol extraction, as evidenced by the signals around 139 ppm. However, the lack of signal around 142 ppm (*cf.* ellagic acid) indicates a lack of hydrolysable tannin material in the methanol extract.

The ^{31}P NMR spectroscopic observations in Figure 4.14 reflect the distribution of extractive compounds in *P. radiata* and eucalypt as reported previously [20, 37, 39, 40, 41, 48, 295].

The area of signal between 146 and 148 ppm indicated that methanol extraction also removed some carbohydrate material from both radiata pine and Eucalypt.

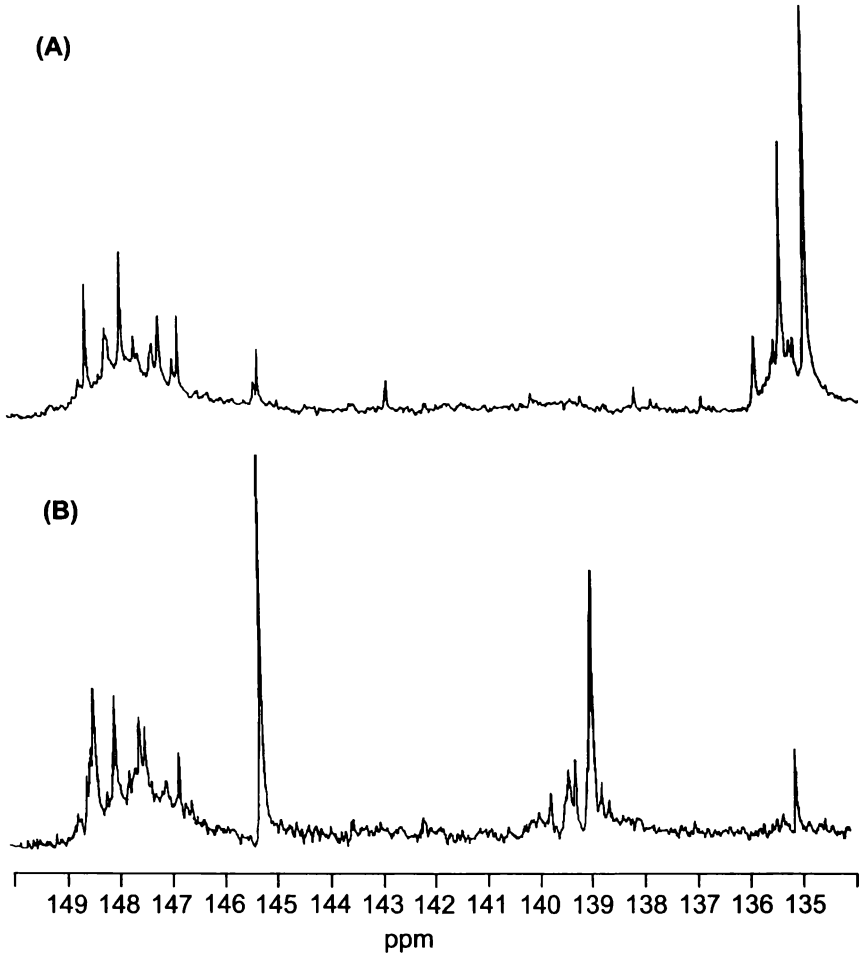

Figure 4.14: ^{31}P NMR spectra of methanol extractives from (A) *Pinus radiata* and (B) eucalypt.

Table 4.12 compares the quantification of lignin units, in *in situ* radiata pine lignin by thioacidolysis/^{31}P NMR spectroscopy, after different extraction procedures have been applied. Without performing methanol extraction prior to thioacidolysis/^{31}P NMR spectroscopy, the quantitative ^{31}P NMR spectroscopy underestimated the quantities of all the measured phenolic units. This was attributed to the inclusion of some sterols, like β-sitosterol, in the spectrum, leading to a larger signal at 144.95 ppm. The overall yield of phenolic units was around 6% lower when determined without prior extraction. Methanol extraction gave results essentially identical to those observed for the three step extraction involving CH_2Cl_2, H_2O and EtOH (C/H/E).

Table 4.12: Comparison of quantitative ^{31}P NMR spectroscopic results for *Pinus radiata* with different extraction procedures.

	C9 units, mmol/g of lignin		
	No extraction	MeOH extraction	C/H/E* extraction
Condensed	1.29	1.39	1.43
Guaiacyl	2.37	2.48	2.52
p-hydroxyphenyl	0.06	0.09	0.10
Total phenolic	3.72	3.96	4.05
% Condensed	35	35	35
* C/H/E = extraction with CH_2Cl_2 followed by H_2O followed by EtOH.			

For *in situ* eucalypt lignin (Table 4.13), quantification of phenolic units after methanol extraction gave results essentially identical to the more complex three-stage extraction. However, quantification performed without extraction, prior to thioacidolysis/^{31}P NMR spectroscopy, led to results quite different from those observed for the methanol and C/H/E extractions.

By not performing any extraction prior to thioacidolysis/^{31}P NMR spectroscopy, quantification of S units was approximately 20% lower *cf.* thioacidolysis/^{31}P NMR spectroscopy performed post methanol extraction. This reduction in observed S concentration, was attributed the presence of β-sitosterol in the hardwood sample. However, similar observations were not made for the condensed G and uncondensed G units. In fact, the concentration of condensed units pre/post extraction was essentially identical. The concentration of G units was actually higher before the methanol extraction than after it. Both these observations were attributed to the presence of phenolic and hydrolysable type extractives in the original eucalypt sample.

Table 4.13: Comparison of quantitative ^{31}P NMR spectroscopic results for an eucalypt sample with different extraction procedures.

	C9 units, mmol/g of lignin		
	No extraction	MeOH extraction	C/H/E* extraction
Condensed	0.59	0.56	0.54
Syringyl	2.10	2.51	2.53
Guaiacyl	0.81	0.64	0.61
p-hydroxyphenyl	-	-	-
Total phenolic	3.50	3.71	3.68
% Condensed	17	15	15

* C/H/E = extraction with CH_2Cl_2 followed by H_2O followed by EtOH.

The results presented above support the use of a single step methanol extraction to remove phenolic extractives.

4.9 Conclusions

- Thioacidolysis softwood lignin, followed by quantitative ^{31}P NMR spectroscopy of the phosphitylated thioacidolysis product is a viable method for the determination of the levels of condensed and uncondensed units in both isolated and *in situ* lignin.

- A significant benefit of this method was that it also enables the determination of levels of individual condensed units such as β-5, 5-5 and 4-O-5 units, in *in situ* wood lignin.

- Isolated and *in situ* wood lignin were found to have similar proportions of condensed and uncondensed units. Both lignin samples contained around 35% condensed units. This tentatively suggested that the ML and SW lignins were more similar than had previously been reported.

- Successful strategies were developed, to deal with issues such as cook time, reproducibility, relaxation delay and the interference of carbohydrates and/or extractives.

I didn't fail ten thousand times.
I successfully eliminated,
ten thousand times,
materials and combinations which wouldn't work.

Thomas Edison

Chapter 5
Technique Application

5.1 Introduction

In Chapter 4, thioacidolysis/^{31}P NMR spectroscopy was shown to be a viable method for determining the proportions of condensed and uncondensed phenylpropane units in both isolated and *in situ* guaiacyl (G) lignin. This Chapter focuses on applying thioacidolysis/^{31}P NMR spectroscopy to various other lignin samples. The lignin samples selected generally reflect a more complex lignin structure than the lignin in radiata pine (*Pinus radiata*).

Lignin samples studied by thioacidolysis/^{31}P NMR spectroscopy in this Chapter include:

- Radiata pine sapwood and heartwood.
- Radiata pine earlywood and latewood.
- Norway spruce.
- Radiata pine compression wood.
- Eucalypt.
- Mechanical and chemimechanical pulps.
- Soluble liquor lignin from kraft pulps.

5.2 Lignin Variation within Radiata Pine

5.2.1 Introduction

The chemical composition of wood varies with position within the tree, both radially and with height [47, 296]. The heartwood of radiata pine typically contains a higher concentration of extractives and lignin than sapwood [39, 40, 47]. Conversely, the

cellulose content of sapwood is typically higher than that of heartwood [296]. While much work has been done in this area, little information is currently available about structural differences in the lignin, in relation to positions within radiata pine. For hardwoods, such results are available. Parameswaran *et al.* [297] amongst others, have reported a higher S unit content in the heartwood of hardwoods, as compared to the corresponding sapwood.

Similarly, the chemical composition of radiata pine earlywood (EW) and latewood (LW) has been thoroughly studied [298]. It has been consistently reported, that EW contains more lignin than LW. This observation has been attributed to cell morphology, with the EW cells having a smaller S2 layer. They therefore, contain a larger proportion of lignin rich ML material than LW. Again, no information is currently available about the structural differences in the lignin in these two regions of the tree.

Lignin-extractive covalent bonds are known to form during heartwood formation. Such covalently bound extractives may interfere with the comparison of heartwood and sapwood lignins. This issue is not of significant concern for softwoods due to their low levels of extractives. However, before comparisons of sapwood and heartwood in hardwoods can be made, the effect of covalent lignin-extractive will need to be adressed.

5.2.2 Lignin variation within radiata pine

Using thioacidolysis/^{31}P NMR spectroscopy, the proportions of condensed G, uncondensed G and H units in the heartwood, sapwood, EW and LW from a 25-27 year old *Pinus radiata*, were determined. The results in *in situ* lignin are presented in Table 5.1.

Table 5.1: ^{31}P NMR spectroscopic results for lignin from different morphological regions of radiata pine.

	C9 units, mmol/g of lignin			
	Earlywood	Latewood	Sapwood	Heartwood
Condensed	1.38	1.37	1.42	1.39
β-5	0.41	0.42	0.39	0.48
4-O-5	0.32	0.33	0.33	0.27
5-5	0.65	0.62	0.70	0.64
Guaiacyl	2.40	2.46	2.48	2.41
p-hydroxyphenyl	0.10	0.11	0.09	0.12
Measured phenolic	3.88	3.94	3.99	3.92
% Condensed	36	35	36	36
Klason lignin, %	27.9	27.2	26.9	28.1

Essentially, no difference in the proportions of condensed G units was observed between the pine wood lignin from different regions of the tree (Table 5.1). In all cases, around 35% of the C9 units were condensed in the C5 position. Also, the proportion of H units was consistent throughout the four *in situ* lignin samples. These results suggest, that although the concentration of lignin in the different regions of the tree varied, the proportions of condensed units present in different regions was rather homogeneous.

These results were not entirely unexpected. For example, heartwood formation in radiata pine occurs through progressive aspiration (closure) of borded pits in the axial EW tracheids of the sapwood [299, 6, 7]. Subsequent to this blocking of the sap flow, the cells die and become enriched in resin, supplied through the horizontal resin canals from the sapwood. This heartwood formation occurs well after lignification of the cell wall is complete. Therefore, aspiration of the borded pits and heartwood formation would not be expected to significantly affect the proportion of condensed structures in the lignin.

Similarly, with EW and LW a difference in SW volume combined with a small difference in lignin content would not be expected to lead to significant changes in the amounts of condensed structures in the lignin.

5.3 *Spruce Lignin*

5.3.1 Spruce MWL

Quantitative ^{31}P NMR spectra for Norway spruce (*Picea abies*) were acquired on derivatised MWL and the derivatised MWL thioacidolysis product. Visually, these spectra were essentially identical to the radiata pine spectra in Figure 4.1. To avoid duplication, the spruce spectra are not shown here. The quantitative spruce results are presented in Table 5.2. As before, the term free phenolic refers to phenolic moieties measured by ^{31}P NMR spectroscopy alone, whereas total lignin refers to phenolic moieties quantified in the MWL thioacidolysate.

Table 5.2: ^{31}P NMR spectroscopic results for spruce and pine MWL's.

	C9 units, mmol/g of lignin					
	Norway Spruce			Radiata Pine*		
	Free phenolic	Etherified C9	Total lignin	Free phenolic	Etherified C9	Total lignin
Condensed	0.66	0.86	1.47	0.36	1.01	1.37
Guaiacyl	1.18	1.45	2.68	0.61	1.87	2.48
p-hydroxyphenyl	0.11	0.01	0.12	0.08	0.01	0.09
Measured phenolic	1.95	2.32	4.27	1.05	2.89	3.94
% Condensed	34	36	34	34	35	35

* From Chapter 4.

The concentrations of free phenolic uncondensed and condensed G units, in the spruce MWL, were nearly twice as high as the same structures in pine MWL. Overall, 1.95 mmol of free phenolic moieties/g of lignin were observed for spruce MWL, equating to about 0.36 phenols/C9 unit. This free phenolic content of the spruce MWL is considerably higher than the 0.20 phenolics/C9 reported for radiata pine MWL (Chapter 4). It is also higher than the typical free phenolic content for spruce MWL, of between 0.2 and 0.26 phenolics/C9, quoted by various investigators [62, 66, 268, 269].

A large range of phenolic hydroxyl contents have however been published. These range from the 0.11-0.12 phenolics/C9, quoted by Lai and Guo [177] for both spruce and pine MWL preparations, to a high value of 0.33 phenolics/C9 by Månsson for spruce MWL [178]. While the production of a consistent MWL between investigators is obviously quite difficult, the MWL used here, contained more free phenolic hydroxyl groups than is typical for a spruce MWL.

Native wood lignins generally have a lower free phenolic content, than the respective MWL [62, 175, 300, 301, 302]. The production of free phenolic groups in the MWL is partially governed by the physical milling of the lignin and partially by the presence of oxygen during the ball milling process [58]. The particularly high level of free phenolic groups in our spruce MWL sample, suggested that this lignin sample may have been exposed to high levels of oxygen during the ball milling process. This may have been due either to incomplete nitrogen flushing prior to pot sealing, or due to a leaky seal on the pot.

For spruce MWL, the proportions of condensed and uncondensed G units in the total lignin (Table 5.2) were very similar to those earlier observed for radiata pine. The only difference between the spruce and radiata pine MWL samples was the slightly higher yield measured for spruce MWL, with around four-fifths of the phenylpropane units measured, *cf.* three-quarters for radiata pine MWL. Overall, there does not appear to be a significant difference in the degree of condensation of these two softwood lignin samples.

5.3.2 *In situ* spruce lignin

Table 5.3 contains the quantitative ^{31}P NMR spectroscopic results for *in situ* spruce lignin. It compares these results with those previously reported for spruce MWL (Table 5.2) and *in situ* radiata pine lignin (Chapter 4).

Table 5.3: ^{31}P NMR spectroscopic results for *in situ* spruce lignin.

	C9 units, mmol/g of lignin		
	Norway spruce		Radiata pine**
	MWL*	*In situ* lignin	*In situ* lignin
Condensed	1.47	1.41	1.43
β-5	0.43	0.41	0.48
4-O-5	0.32	0.30	0.28
5-5	0.71	0.70	0.67
Guaiacyl	2.68	2.58	2.61
p-hydroxyphenyl	0.12	0.09	0.09
Measured phenolic	4.27	4.08	4.04
% Condensed	34	35	35
* from Table 5.2, ** fromChapter 4			

From Table 5.3, a number of conclusions may be drawn:

- There was little difference in the proportions of condensed and uncondensed units for the MWL and the *in situ* lignin from *Picea abies*. This was similar to observations made for radiata pine (Section 4.3).
- The proportions of condensed and uncondensed units in *in situ* spruce and *in situ* radiata pine lignin, were very similar. In both *in situ* lignin samples, around 35% of the phenylpropane units were condensed in the C5 position.

These results, in conjunction with the radiata pine results presented in Sections 4.2 4.3 and 5.2, suggest that the proportions of condensed and uncondensed G units in different softwood lignins are quite homogeneous.

5.4 Compression Wood

5.4.1 Introduction

Compression wood is a vital, structural component in softwoods and typically comprises 10-15% of the xylem tissue in a tree [15]. The presence of compression wood enables the righting of leaning stems or branches by the mechanisms outlined in Sections 1.2 and 1.3. It has been reported that kraft pulps prepared from compression wood contain more residual lignin, are darker in colour and are recovered in a lower yield, compared to comparable pulps prepared from normal

wood [15, 303, 304]. While many of the differences between pulps from compression wood and normal wood may be attributed to microscopic, structural or carbohydrate effects, the high residual lignin content has been attributed to the highly condensed nature of compression wood lignin.

Initially, this study focussed on comparing the isolated MWL from normal radiata pine, with the MWL from EW compression wood and LW compression wood. The samples were collected from a region of mild compression wood, where the EW compression wood had a lignin content of 30.3% and the LW compression wood a lignin content of 34.7%. Following this, the proportions of condensed G units, in *in situ* EW compression wood and LW compression wood, were compared with those in their respective MWL's.

Much work has shown that the EW and LW terminology, as applied to normal wood, is not entirely correct for compression wood [11, 15, 305, 306]. What is usually taken for EW in compression wood, is either normal wood or very mild compression wood, lacking many of the morphological characteristics attributed to compression wood [11, 15, 305, 306]. Conversely, what is generally considered to be LW, is actually pronounced compression wood with anatomical features distinct from the former. For these reasons, the EW/LW terminology is generally not very useful, as pointed out by Timell [307]. Although the author recognises the discrepancy between terminology and anatomical/chemical accuracy, for ease of discussion and identification, the EW/LW terminology has been used for all compression wood discussed in this thesis.

5.4.2 Compression wood MWL

Figure 5.1 shows the ^{31}P NMR spectra of the thioacidolysates from EW compression wood MWL and LW compression wood MWL. The two ^{31}P NMR spectra for these MWL samples were essentially identical, except for an increase in the intensity of signal associated with the H groups, at approximately 138 ppm. The numerical data, generated by integration of the ^{31}P NMR spectra in Figure 5.1, is presented in Table 5.4.

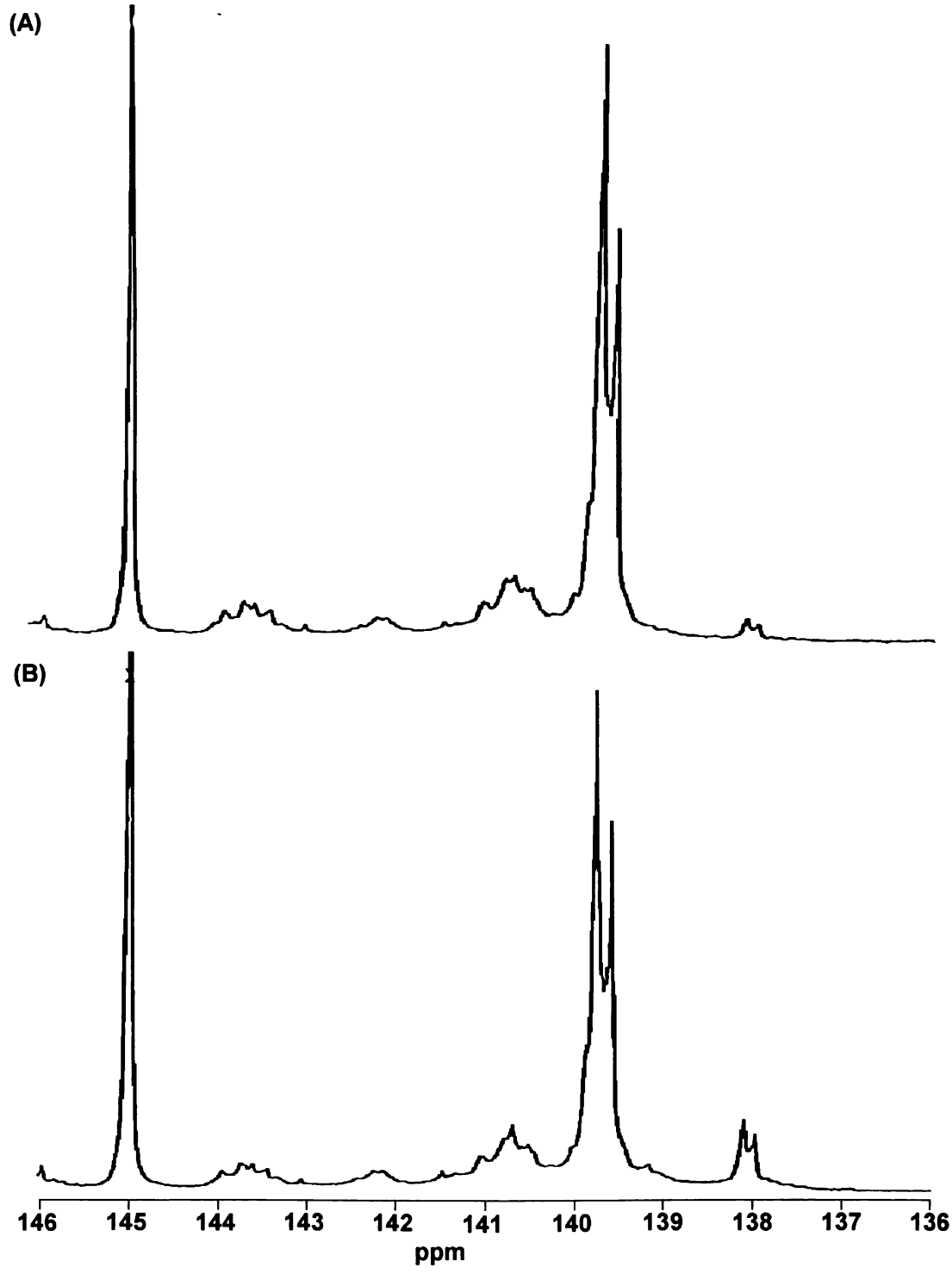

Figure 5.1: ^{31}P NMR spectra of (A) EW compression wood MWL and (B) LW compression wood MWL.

Table 5.4: ^{31}P spectroscopic results for compression wood MWL's

	C9 units, mmol/g of lignin					
	Normal wood*		EW compression wood		LW compression wood	
	Free phenolic	Total lignin	Free phenolic	Total lignin	Free phenolic	Total lignin
Condensed	0.36	1.37	0.38	1.38	0.34	1.31
Guaiacyl	0.61	2.48	0.77	2.53	0.67	2.34
p-hydroxyphenyl	0.08	0.09	0.15	0.16	0.28	0.33
Measured phenolic	1.05	3.94	1.30	4.07	1.29	3.98
% Condensed	34	35	29	34	26	33
* From Chapter 4.						

All three MWL samples exhibited significantly different H unit concentrations, when measured by thioacidolysis/^{31}P NMR spectroscopy (Table 5.4). For EW compression wood, the observed concentration, of 0.16 mmol of H units/g of lignin was significantly higher than the 0.09 mmol/g observed for normal wood. This means, that around 3% of the phenolic units in this EW compression wood MWL were present as uncondensed H moieties. The H unit concentration in LW compression wood MWL was even higher, 0.34 mmol/g lignin, or around 8% of the total C9 units. This compares to around 2% of the phenylpropane units in normal wood MWL being H units.

Literature has shown, that in terms of lignin structure, an increase in H unit concentration is the outstanding difference between normal and compression wood lignins [9, 15, 76, 77, 81]. For example, according to Latif [82] the compression wood lignin of *Pseudotsuga menziesii* was composed of 70% G and 30% H units, compared with 88% and 12% respectively for normal wood lignin.

Our results suggest that LW compression wood MWL contained significantly more compression wood character, than MWL originating from EW compression wood. These findings closely fit with previous anatomical observations and lignin analyses,

which suggest that the compression wood character is predominantly associated with LW regions in compression wood [11, 15, 305, 306].

In the three MWL samples studied, 85-90% of the H units were present as free phenolic moieties. This can be seen from the small number of additional H units released during the thioacidolysis. These results were similar to the 90% free phenolic H units in compression wood lignin, previously reported by Lapierre *et al.* [275] and Lapierre and Rolando [273]. The results were also in line with the reported 80% free phenolic H units in HG and HGS DHP's, regardless of mode of polymerisation [308].

This heterogeneous distribution of H units in compression wood has been attributed to several factors. Firstly, in DHP work by Jacquet *et al.* [308], the observed proportions of free phenolic H units remained unchanged, regardless of the mode or medium of polymerisation. Therefore, the mechanistic control over H unit incorporation during polymerisation was attributed to *p*-coumaryl alcohol chemistry, rather than the matrix. Also, the one electron redox potential of various hydroxycinnamyl alcohol analogues has shown, that addition of methoxyl groups *ortho* to the hydroxyl function renders the substrate more easily oxidised [309]. Hapiot *et al.* [310] also showed, that oligomeric species are difficult to oxidise and that a hydrophobic environment promotes the coupling of phenoxy radicals to phenolate anions. Based on these observations, Jacquet *et al.* [308] speculated, that during copolymerisation of H precursors, with G and/or S monolignols, the G and/or S precursors first polymerise to oligomeric and polymeric compounds. This makes the reaction medium more hydrophobic. The H monolignol is then oxidised, with the subsequent addition of the H monomeric radical to a polymeric GS or G template.

The polymerisation mechanism proposed above, may also explain the observed concentrations of condensed units. In Table 5.4, the concentration of condensed phenylpropane units for normal wood MWL, EW compression wood MWL and LW compression wood MWL were similar at around 1.35 mmol/g. In other words, in all three samples between 33 and 35% of the phenylpropane units were condensed at C5. These findings are in line with recent DHP work by Jacquet *et al.* [308]. They reported that during co-polymerisation of H units with G and/or S monolignols, the

H units were not involved to a high extent in condensed carbon-carbon inter-unit linkages. However, H DHP was severely condensed, compared with HG and HGS co-polymers. A polymerisation mechanism, involving addition of monomeric H radicals to a polymeric G or GS template, may explain this why the concentration of condensed units in compression wood lignin were similar to that in normal pine lignin.

The results presented here and previous findings by Jacquet *et al.* [308] contradict much earlier literature, which indicated that a high proportion of H moieties should be condensed at C5 [64, 82, 111, 112]. The most extensive investigation on the structure of compression wood lignin, is that by Yasuda and Sakakibara [111, 112] on the lignin present in the compression wood of *Larix leptolepis*. On hydrogenolysis, this compression wood lignin gave 26% monomeric degradation products and normal wood lignin 31%, suggesting a higher proportion of carbon-carbon linkages in the former lignin. Fukushima and Terashima [311] used a different approach to determine the proportion of condensed units in compression wood lignin. A *Pinus thunbergii* shoot growing at an angle was administered ferulic acid, randomly labelled with ^{14}C over the benzene ring and, in addition, labelled with ^{3}H at position 5 in the ring. Because condensation involving position 5 will result in the elimination of ^{3}H, the $^{3}H/^{14}C$ ratio may be used as an indication of the degree of condensation. Fukushima and Terashima [311] found a lower $^{3}H/^{14}C$ ratio in the lignin located on the lower side of the shoot than on the upper, indicating a higher degree of condensation in the former. Also, Sarkanen [64] has previously predicted, that compression wood lignin should be more condensed than normal wood lignin, due to bulk, rather than endwise polymerisation. Also, H units have the ability to form two condensed inter-unit linkages, at C3 and C5.

Two factors come into play when considering the differences in proportions of condensed units between the results presented here and those reported previously. Firstly, thioacidolysis/^{31}P NMR spectroscopy is the first technique which can determine the proportions of uncondensed and condensed G units simultaneously in the whole lignin. Therefore, the results presented here may more accurately reflect the actual composition of lignin in compression wood. For example, the monomers measured by Yasuda and Sakakibara [111,112] after hydrogenolysis accounted for only ~30% of the Klason lignin content. Also, the conclusions by Terashima *et al.*

[122] and Tomimura *et al.* [278, 279] were based on a monolignol activity of 8-19%, indicating that the results may not have been representative of the total lignin.

Another consideration is that a portion of the condensed units, containing H units, may be measured incorrectly by thioacidolysis/^{31}P NMR spectroscopy. Normally, condensed G moieties fall in the range 140-144.5 ppm and contain groups at C3 (OCH_3) and C5 (inter-unit linkage). However, condensed H units may contain only one substituent *ortho* to the phenolic group. As an example, two such structures, previously reported by Yasuda and Sakakibara [113, 312, 313], are shown in Figure 5.2.

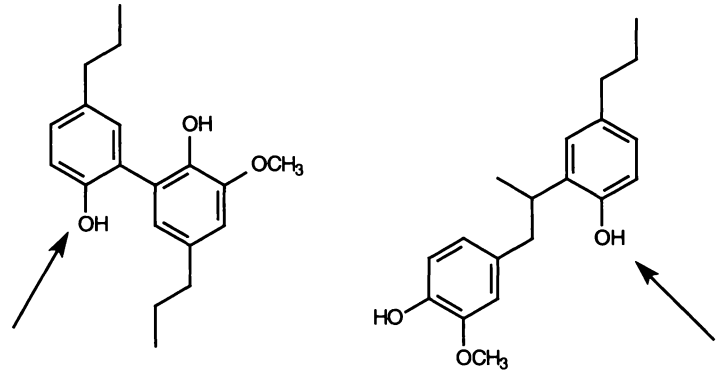

Figure 5.2: Condensed structures containing one H unit.

Model compound data on the ^{31}P NMR spectroscopy chemical shifts of such structures, is not available. However, using the substituent effects published by Jiang *et al.* [194] for G moieties, it is possible to predict chemical shifts of ~139.5-140 ppm for 5-5 coupled H units and 141.5-142 ppm for β-5 coupled H units, after derivatisation with **41**. Whilst β-5 units would still be measured as condensed units, the 5-5 coupled H units would be measured as G units.

5.4.3 *In situ* compression wood lignin

Table 5.5 contains the data collected from thioacidolysis/^{31}P NMR spectroscopy performed on *in situ* lignin from EW compression wood and LW compression wood regions of radiata pine. For comparison, the results for respective MWL samples are also included.

Table 5.5: ^{31}P NMR spectroscopic results for *in situ* radiata pine compression wood.

	C9 units, mmol/g of lignin			
	EW compression wood		LW compression wood	
	MWL	*in situ*	MWL	*in situ*
Condensed	1.38	1.34	1.31	1.27
	0.47	0.46	0.36	0.39
	0.24	0.26	0.28	0.26
	0.67	0.62	0.66	0.62
Guaiacyl	2.53	2.61	2.34	2.27
p-hydroxyphenyl	0.16	0.16	0.33	0.34
Total phenolic	4.07	4.11	3.98	3.88
% Condensed	34	33	33	32
Klason lignin, %		30.0		34.3

The concentrations of condensed G, uncondensed G and H units were remarkably similar for the MWLs, when compared to their matching *in situ* lignins. This suggests that thioacidolysis/^{31}P NMR spectroscopy can readily be applied to *in situ* compression wood lignin, as well as the isolated MWL.

5.5 *Eucalypt*

5.5.1 Introduction

The ease of hardwood kraft pulping relative to softwood kraft pulping, for example lower temperatures, shorter time and lower sulphidity, has been attributed, in part, to structural differences in the respective lignins [108, 109]. Compared with softwoods, hardwoods generally have a lower lignin content and the lignin that is present, contains fewer carbon-carbon inter-unit linkages [54, 63, 76]. This low number of condensed inter-unit linkages is due to the presence of S moieties in the hardwood lignin polymer. Due to the presence of two *ortho* methoxyl groups, these units are unable to form condensed inter-unit linkages through C5.

It is this significantly different lignin structure, which makes application of thioacidolysis/^{31}P NMR spectroscopy particularly interesting. In Section 5.5.2, thioacidolysis/^{31}P NMR spectroscopy was applied to a MWL preparation from a sample of commercial eucalypt chips. Subsequently, in Section 5.5.3, thioacidolysis/^{31}P NMR spectroscopy was applied to *in situ* lignin from the same eucalypt chips to further evaluate the application potential of the technique.

5.5.2 Eucalypt MWL

Figure 5.3 shows the ^{31}P NMR spectra of eucalypt MWL and the MWL thioacidolysate derivatised with the dioxaphospholane **41**. The main difference between these spectra, and those previously observed for radiata pine (Figure 4.1), is the presence of signals at approximately 142.5 ppm, due to the presence of S moieties. The two signals observed in Figure 5.3 (b) were attributed to the *erythro* and *threo* isomerism in the S trithioether **59**, like that observed for G and H moieties.

The intensity of signals associated with condensed units, 140-144.5 ppm (excluding the S peak), was also significantly lower in both eucalypt spectra, than that observed in Figure 4.1. Furthermore, performing thioacidolysis, prior to ^{31}P NMR spectroscopy, clearly caused a significant change in the relative proportions of S (~142.5 ppm) and G (~139.5 ppm) units.

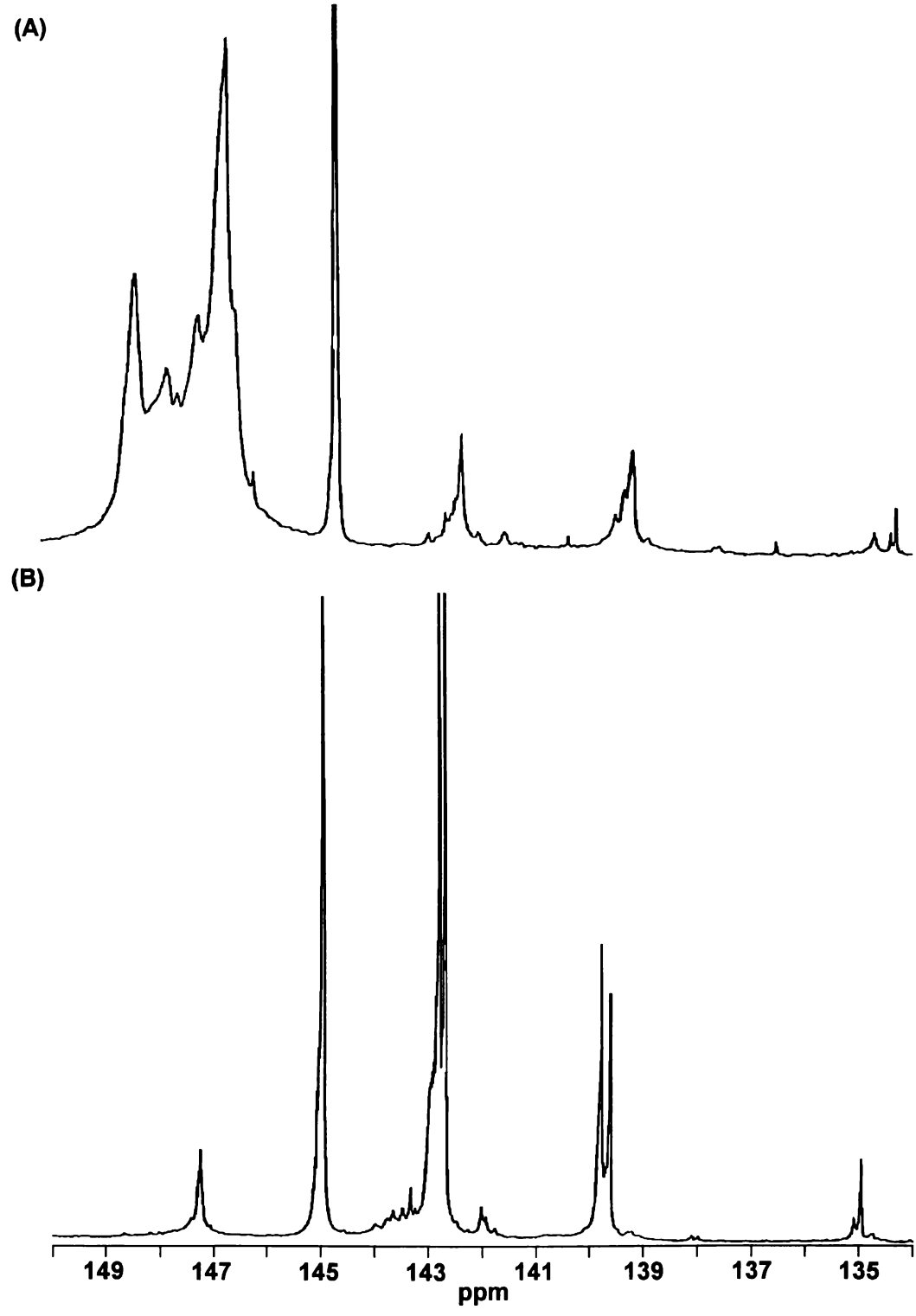

Figure 5.3: ^{31}P NMR spectra of phosphitylated (A) eucalypt MWL and (B) eucalypt MWL thioacidolysate.

Table 5.6: ^{31}P NMR spectroscopic results for eucalypt MWL.

	C9 units, mmol/g of lignin		
	Free phenolic	Etherified C9	Total lignin
Syringyl	0.44	1.81	2.25
Condensed	0.20	0.49	0.69
Guaiacyl	0.51	0.35	0.86
p-hydroxyphenyl	0.04	-	0.04
Total phenolic	1.19	2.65	3.84
% Condensed	17	19	18

Table 5.6 contains the numerical data generated from integration of the spectra in Figure 5.3. The 1.19 mmol of free phenolic units/g of lignin in the MWL is equal to around 25% of the phenylpropane moieties present in the lignin, using a MW of 206 [117, 314]. This amount of free phenolic groups in the MWL is somewhat higher than, but in line with, other hardwood MWL preparations reported earlier [186]. In the total lignin, S units comprise around 60% of the phenylpropane units present. Syringyl concentrations in hardwoods may range from 20% to 60% S units, depending on the species [54, 83].

The proportions of H units present in the total eucalypt lignin was about half that observed in both radiata pine and spruce lignin (0.04 mmol/g *cf.* 0.09 mmol/g). This result fits previous observations, that H unit concentrations in hardwoods are typically lower than in softwoods [63, 78, 79, 83, 212]. As for radiata pine and spruce MWL's, the H units were predominantly present as free phenolic groups.

The proportions of G and S moieties present as free phenolic units, was very different from the proportions of these units in the total lignin. While 60% of the phenylpropane units in the total lignin were S moieties, only about 37% of the free phenolic groups were S units. This marked difference means, that 73% of the etherified phenylpropane units in isolated eucalypt lignin, were S units. The S units were therefore preferentially present as etherified moieties. This compares with the H units in slabwood and compression wood radiata pine MWL, which were

preferentially present as free phenolic units. The results presented for eucalypt MWL above, are in agreement with previous literature for native hardwood lignins [273, 315] and end-wise polymerised HGS DHP's [308], which also report S units as being preferentially present as etherified moieties. The results presented here may therefore be considered as further confirmation for the higher tendency of S units to be etherified at C4, compared with G units.

The results presented above suggest that thioacidolysis/^{31}P NMR spectroscopy, when applied to isolated lignin samples, is an excellent technique for determining the amounts of condensed units present as free phenolic and etherified moeities.

A much lower proportion of condensed units was observed for eucalypt MWL compared with radiata pine MWL, 18 *vs.* 37%. This much lower proportion of condensed units closely fits with the literature description of hardwoods being less condensed [54, 63, 76].

5.5.3 *In situ* eucalypt lignin

Thioacidolysis/^{31}P NMR spectroscopy was next applied to *in situ* eucalypt lignin to see if the technique could be used to compare lignin in the total wood with that isolated as MWL.

In Table 5.7, the overall yield of phenolic material determined in the *in situ* lignin thioacidolysate (3.91 mmol/g) corresponds to a determination of 80% of the phenylpropane units in the original sample. This compares favourably with the 3.84 mmol/g determined for the MWL sample.

Table 5.7: ^{31}P NMR spectroscopic results for *in situ* eucalypt lignin.

	C9 units, mmol/g of lignin	
	MWL Total lignin	*In situ* Total lignin
Syringyl	2.25	2.13
Condensed	0.69	0.77
Guaiacyl	0.86	0.96
p-hydroxyphenyl	0.04	0.05
Total phenolic	3.84	3.91
% Condensed	18	20

The *in situ* lignin contained a slightly higher concentration (1.73 mmol/g) of G units than the MWL sample (1.55 mmol/g). In conjunction with this higher proportion of G units, an increase in the concentration of condensed units was also observed. The *in situ* lignin contained around 20% condensed G units. These results suggest that *in situ* eucalypt lignin was more condensed than the eucalypt MWL. Therefore, unlike the MWL *vs. in situ* lignin results discussed for radiata pine (Section 4.3) and spruce (Section 5.2), the MWL generated from this hardwood sample was not representative of the lignin in the total wood.

5.6 Mechanical Fibres

5.6.1 Lignins from different mechanical pulp fibres

The thioacidolysis/^{31}P NMR spectroscopy technique was next applied to investigate a range of *in situ* mechanical and chemimechanical lignin samples, prepared from *Pinus radiata*. The pulp fibres analysed included MDF, TMP, CTMP, DWS and OPCO fibres (Sections 1.4 and 6.5). Spectra generated from these samples generically looked no different to the spectra for *in situ* radiata pine lignin and are not reproduced here. Table 5.8 shows the numerical data for the thioacidolysis/^{31}P NMR spectra of five different *Pinus radiata* thermomechanical or chemithermomechanical pulp fibre thioacidolysates. Also, Table 5.8 includes some

important production parameters of the analysed fibres, including Klason lignin, sulphur content and refining energy.

Table 5.8: ^{31}P NMR spectroscopic results for radiata pine after various pulping procedures.

	C9 units, mmol/g of lignin					
	Wood*	MDF	TMP	CTMP	DWS	OPCO
Condensed	1.39	1.34	1.49	1.44	1.38	0.45
Guaiacyl	2.51	2.61	2.74	2.18	2.22	0.58
p-hydroxyphenyl	0.09	0.09	0.06	0.13	0.09	-
Total phenolic	3.99	4.04	4.29	3.75	3.69	1.03
% Condensed	35	33	34	38	38	43
Klason lignin (%)	27.8	27.9	27.8	28.2	28.2	24.5
S content (%)	-	-	0.005	0.15	0.17	0.83
Refining energy (KWh/odt)	-	433	3036	2392	2368	1600
* From Chapter 4.						

For both TMP and MDF lignins, the phenolic yields, approximately 75%, were essentially identical to that for *in situ* radiata pine wood. Approximately 35% of the phenolic units, in both TMP and MDF fibre lignin, were condensed at C5, also similar to what was observed in *in situ* radiata pine lignin. These results suggest that mechanical pulp production in the absence of sulphite, even when the fibre was preheated at 170°C for 4 minutes prior to refining, did not lead to the formation of condensed units. Adams and Ede [316] have recently reported little change in the majority of fibre lignin, due to preheating and refining in an MDF process. It is important to remember here, that any condensation reactions at positions other than C5 would not be detected.

For both CTMP and DWS fibres, up to 70% of the C9 units in the *in situ* lignin were determined. This yield is slightly lower than that observed for the radiata pine wood lignin. The proportions of condensed to uncondensed units, in *in situ* CTMP and DWS fibre samples, were different to that in *in situ* wood lignin. In CTMP and DWS, about 38% of the phenolic groups measured were condensed at C5, *cf.* 35% for *in situ* radiata pine lignin.

Initially, these results may suggest that condensation of sulphonated lignin monomers occurred during the chemimechanical pulping. However, much of the increase in the proportions of condensed units may, in part, be attributed to a decrease in the amounts of uncondensed units. The amounts of condensed units in the DWS and CTMP fibre were similar to those in the starting wood (Table 5.8).

It is therefore important to consider the lignin chemistry during and after sulphonation. During sodium sulphite treatment of wood chips or pulp, α-sulphonation of phenolic lignin moieties *via* a quinone methide intermediate is believed to be a major reaction (Figure 5.4) [317, 318].

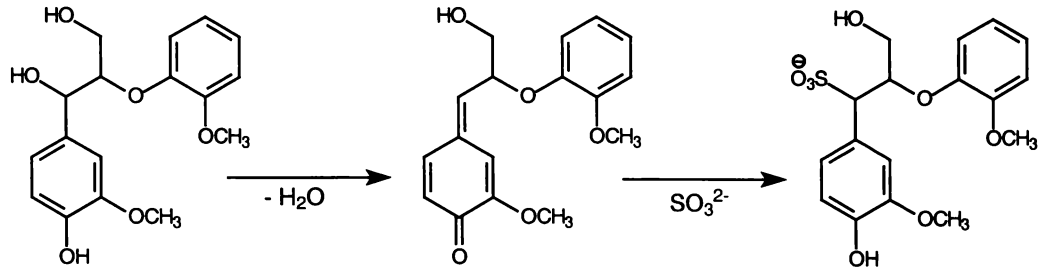

Figure 5.4: Reaction of a phenylpropane-β-aryl ether structure during CTMP pulping.

Such sulphonation at Cα may impede the initial co-ordination of BF_3 to the benzyl alcohol, thus blocking the first step in β-ether cleavage (Figure 5.5). This notion is consistent with previous observations. For example, α-acetylation has been shown to completely repress thioacidolysis when the reagent mixture is composed of BF_3 etherate and EtSH [214]. The repressed thioacidolysis may account for the lowered yield of uncondensed units in CTMP and DWS lignin. Still, around 70% of the C9 units present in the *in situ* CTMP fibre were still being measured, which was only a slight decrease in yield relative to the *in situ* radiata pine lignin.

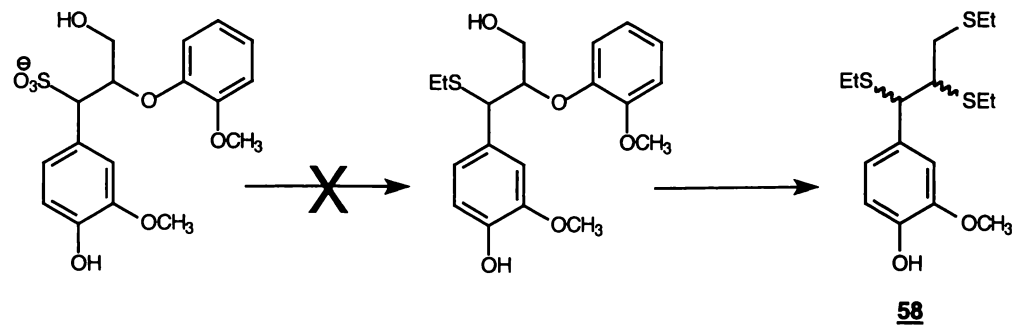

Figure 5.5: Thioacidolysis of an α-sulphonated β-aryl ether.

Interestingly, the lowered yield of uncondensed units recovered from CTMP and DWS lignin suggests possible preferential sulphonation of uncondensed moieties, compared with condensed moieties in the same lignin. Currently, there is little information about the sulphonation rates of uncondensed units compared with condensed ones. Some fundamental work, concerning the formation of quinone methide structures in both condensed and uncondensed units, as well as their subsequent sulphonation, may be useful in answering this question.

For the highly sulphonated OPCO fibre (0.83% S content), the proportion of C9 units analysed was only approximately one-quarter that analysed in the starting wood. The little material that was analysed contained a higher proportion of condensed units (Table 5.8). This fits closely with the repression of thioacidolysis by α-sulphonation.

A contributing side issue to the poor yield may be that sulphonation of the fibre lignin causes, at least part of the lignin to become more hydrophilic [140]. These hydrophilic sulphonated lignin structures are then, less likely to be completely extracted into the dichloromethane layer, during the thioacidolysis work-up.

Thioacidolysis/^{31}P NMR spectroscopy can readily be applied to mechanical pulps to give viable results. However, for mildly sulphonated fibres, the observed yield was affected and questions were raised about the validity of the proportions of condensed units measured. For highly sulphonated lignin samples like OPCO pulps, a significantly lower yield was observed by ^{31}P NMR spectroscopy. This cast some doubt on the application of thioacidolysis/^{31}P NMR spectroscopy to all sulphonated lignins.

5.6.2 Fractionated chemimechanical pulp fibres

In the earlier radiata pine work (Section 4.3), a comparison was made between MWL and *in situ* lignin. From the proportions of ML lignin present in the two different lignin samples, a tentative comparison was made between SW and ML lignin. It was found that the proportions of condensed to uncondensed units in both regions of the cell wall were approximately the same. However, it was noted that the bulk of the lignin in whole wood lignin came from the SW. This may mask any differences in

the proportions of condensed units in the ML and SW, if the differences are only small.

A more robust approach to characterising ML lignin, is to analyse fractions enriched in SW and ML lignin. One common method for achieving this, is to separate the fibres and fines fractions of thermomechanical pulps, as fines fractions have been shown to be considerably enriched in ML lignin [319, 320]. In his work investigating the mechanism of sulphonation for CTMP and DWS chemimechanical pulps, Richardson [153, 154] separated the fines and fibres after different stages of refining (Section 6.5). In summary (Figure 5.6), a primary stage DWS pulp (1° pulp) was screened, to produce a fraction of fibres (1° fibres) and one of fines (1° fines). Subsequent refining of the 1° fibres and separation by the above screens, produced further fractions of fines (2° fines) and fibres (2° fibres). The primary (1°) fines had a significantly higher lignin content (39.6%), than the 1° fibre, and a different carbohydrate composition, both indicating that the 1° fines were indeed, enhanced in ML lignin.

These lignin samples were subjected to thioacidolysis/^{31}P NMR spectroscopy, in order to measure the proportion of condensed units present in the various fractions. The thioacidolysis/^{31}P NMR spectroscopy results for 1° and 2° fibres and fines, are presented below in Table 5.9.

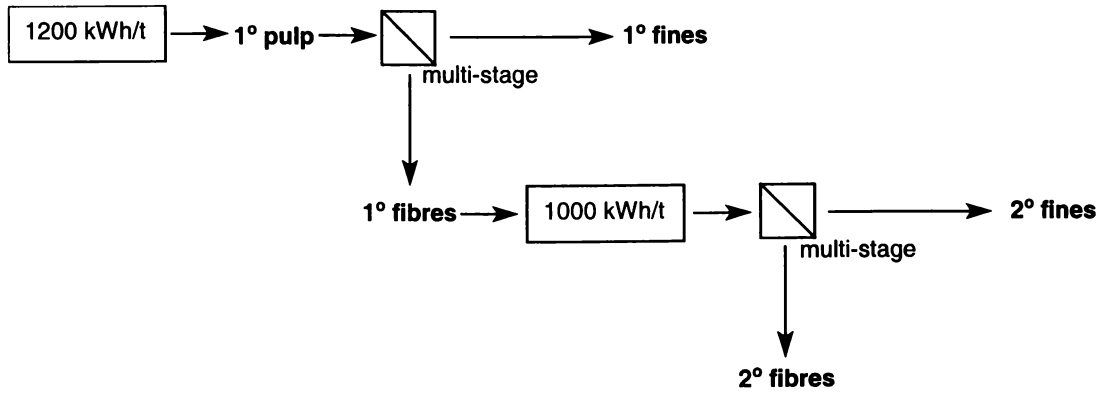

Figure 5.6: Strategy for producing long fibre and fines fractions from a DWS pulp [154].

Table 5.9: ^{31}P NMR spectroscopic results for DWS pulps after selective fractionation.

	C9 units, mmol/g of lignin				
	1° pulp	1° fines	2° fines	1° fibres	2° fibres
Condensed	1.37	1.41	1.42	1.39	1.41
Guaiacyl	2.29	2.20	2.25	2.45	2.42
p-hydroxyphenyl	0.13	0.07	0.09	0.06	0.08
Total phenolic	3.79	3.66	3.76	3.90	3.91
% Condensed	37	39	38	36	36
S content, %	0.10	0.19	0.10	0.07	0.06
Klason lignin, %		39.1	35.8	26.3	25.7

For all five samples in Table 5.9, around 75% of the C9 units in the *in situ* lignin were determined by thioacidolysis/^{31}P NMR spectroscopy. At first glance, the 1° fines lignin did appear to contain a slightly larger proportion of condensed units (39%), than the 1° fibre lignin (36%). However, much of this increase appeared to be due to a decrease in the concentration of uncondensed units, rather than an increase in the condensed ones. The high degree of sulphonation in the 1° fines (0.19%) may, in part, contribute to this increase in proportions of condensed units, through either of the mechanisms outlined above. On the other hand, there was still some difference in the proportions of condensed and uncondensed units, between the 2° fines (38%) and 2° fibres (36%), where the degree of sulphonation was much more similar.

These results suggest that any differences that may exist between the ML lignin and the SW lignin in this sample were masked by the effect of lignin sulphonation. Therefore, future work which attempts to determine the amounts of condensed and uncondensed units in the fibres and fines of thermomechanical pulps and/or MDF fibre, should focus on those samples not modified through sulphonation.

A superficial analysis of the results presented above may suggest a slightly higher proportion of condensed units in the 1° fines than in the 1° fibres. However, due to the concerns raised above and the relatively small difference between samples the differences in the proportions of condensed units do not appear to be very large.

One point to consider, is that the 40% lignin content in the 1° fines implies, that while the fines are enriched in ML lignin, they do not only contain material, and thus lignin, from the ML. Typically, lignin concentrations in the ML are reported around 75-80% [1]. Therefore, the proportions of condensed units in the ML lignin may be higher than the 38% reported here for the 1° fines.

5.7 Kraft Lignins

5.7.1 Application to kraft spent liquor lignin

To evaluate the applicability of the thioacidolysis/^{31}P NMR spectroscopic method to highly modified lignin samples, some isolated kraft spent liquor lignins (KSLL's) were studied. Generically, these KSLL's are released from the wood fibre during kraft pulping and are the lignins residing in the pulping liquor. Their isolation is achieved through acidification of the pulping liquors.

Initially, an "Indulin" kraft lignin was studied, where Indulin is a particular brand name of a commercially produced kraft pulp. This material has been extensively analysed as a sample in the International Energy Agency (IEA) 1991 international "round robin" (IRR) of lignins (Section 6.4.3). Figure 5.7 contains the ^{13}P NMR spectra of the Indulin lignin (5.7(A)) and its thioacidolysate (5.7(B)).

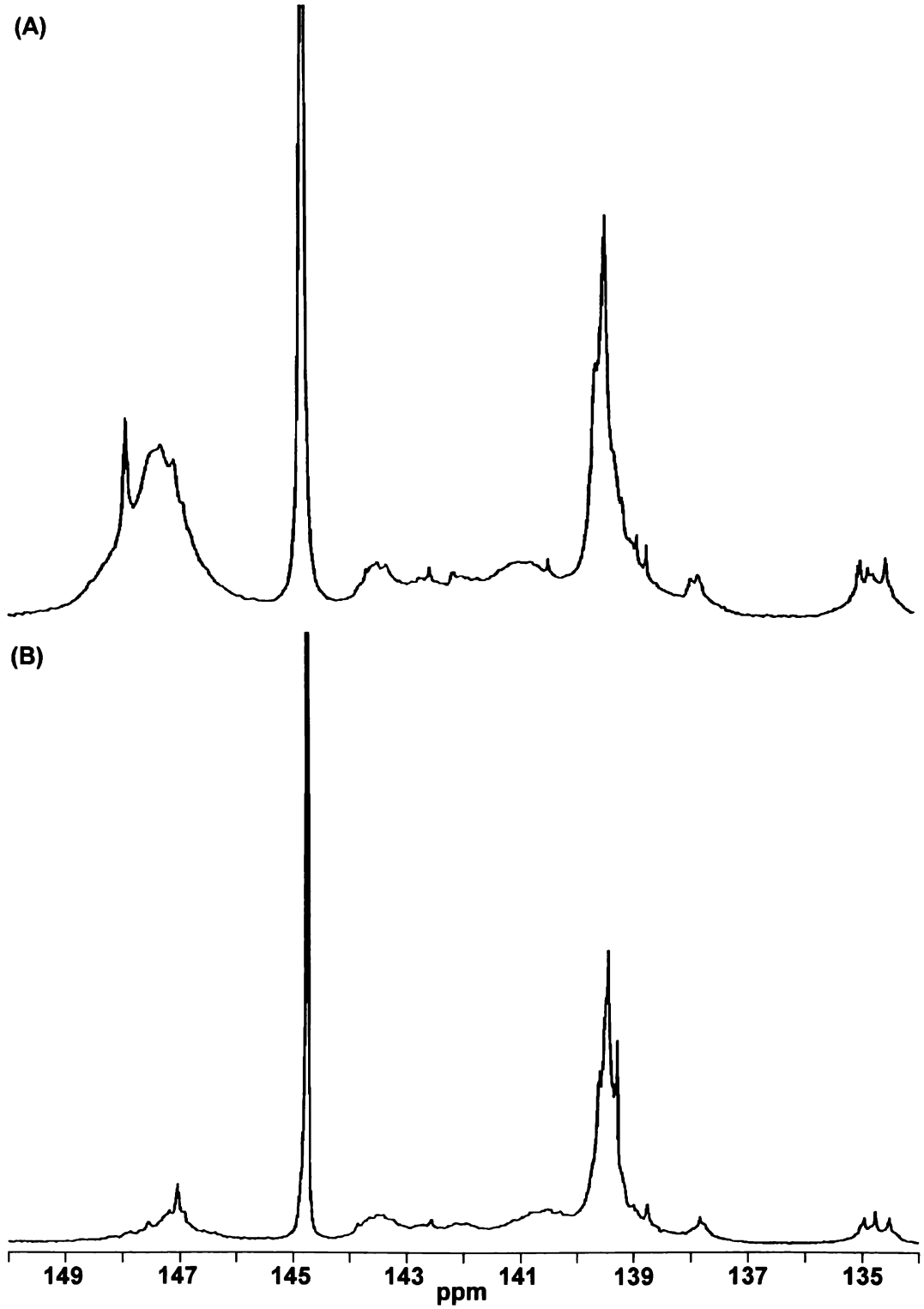

Figure 5.7: ^{31}P NMR spectra of (A) Indulin KSLL and (B) Indulin KSLL thioacidolysate.

In Table 5.10, results from the quantification of the regions of signal in the Indulin lignin spectra are presented. The table compares the distribution of uncondensed and condensed units, as phenolic and etherified moieties, in both radiata pine MWL and Indulin lignin. Also included in Table 5.10 is the term unaccounted material.

This was calculated as the difference, between the observed total phenolic yield and the theoretical maximum yield. Here the theoretical maximum yield describes the total number of C9 units in a lignin sample, and therefore the highest number of phenolic units possible in a thioacidolysis product. The theoretical maximum yield of phenolic units, in mmol/g, was calculated using an assumed MW of 187 g/mol for pine MWL [51, 78, 123] and 178 g/mol for Indulin KSLL [109, 321]. Results for the unaccounted material are discussed later in this Section.

Table 5.10: ^{31}P NMR spectroscopic results for Indulin KSLL.

	C9 units, mmol/g of lignin					
	Pine MWL			Indulin KSLL		
	Free phenolic	Etherified C9	Total lignin	Free phenolic	Etherified C9	Total lignin
Condensed	0.36	1.01	1.37	1.25	0.19	1.44
Guaiacyl	0.61	1.87	2.48	1.45	0.61	2.06
p-hydroxyphenyl	0.08	0.01	0.09	0.16	0.01	0.17
Measured phenolic	1.05	2.89	3.94	2.86	0.81	3.67
Unaccounted material			1.41			1.94
% Condensed	34	35	35	44	23	39

In Indulin kraft lignin, 2.86 mmol/g of phenolic units were measured, indicating that 51% of the C9 units were free phenolic ones. This result compares favourably with the results reported by Faix *et al.* [322] for the same sample. They reported a phenolic hydroxyl concentration of 54 per 100 C9, as an average of three different quantitative NMR spectroscopic techniques. The free phenolic content for Indulin kraft lignin is considerably higher than the ~20 free phenolic units per 100 C9 observed for radiata pine MWL. During the kraft cooking process, β-aryl ether inter-unit linkages are cleaved [109, 128, 132, 133, 134]. This leads to depolymerisation of the lignin and conversion of many etherified units to free phenolic ones. The increase in the level of free phenolic units in kraft spent liquor lignin over that found in MWL, was, therefore, entirely consistent with previous observations.

Over 43% of the free phenolic units in Indulin lignin were condensed moieties. This was considerably higher than the 34% reported for radiata pine MWL. This increase

was consistent with many previous observations, which have indicated that kraft spent liquor lignin contains a higher proportion of condensed units than wood lignins [109, 128, 132, 133, 134, 235]. It has been suggested that formation of these condensed units occurs in part once the lignin has been dissolved out of the wood and is exposed to the pulping chemicals in the bulk solution [220].

After thioacidolysis, the amount of phenolic groups measured in the Indulin lignin was 3.67 mmol/g or about 65% of the C9 units in the lignin. Thioacidolysis of the kraft lignin therefore created fewer new free phenolic groups, than thioacidolysis of MWL (2.86 to 3.67 mmol/g *vs.* 1.05 to 3.94 mmol/g). This was expected, because during the kraft pulping of wood, many β-aryl ether inter-unit linkages, which are also targeted by thioacidolysis, are cleaved. As a result the kraft lignin has fewer β-aryl ether linkages for thioacidolysis to target. Also, the actual yield measured for the kraft lignin thioacidolysate, was lower than the approximately 75%, determined for *in situ* wood lignin.

Indulin lignin contained a higher proportion of condensed units in the total lignin than *in situ* wood lignin, 39% *vs.* 35%. This 39% condensed units in the total Indulin lignin was lower than the 44% condensed units present as free phenolic groups. This is due to the low amount of condensed units released during thioacidolysis of the kraft lignin (0.19 mmol/g).

The ability to quantify different condensed units is one of the major benefits of the thioacidolysis/^{31}P NMR spectroscopy technique. However, little difference in the amounts of β-5, 4-O-5 and 5-5 units, present in the free phenolic and total lignin, was observed. Therefore, a more detailed analysis of the different condensed units in the kraft lignin, was not performed.

Although the proportion of condensed units in the total Indulin lignin was higher, the actual measured amount of condensed units in the total Indulin lignin was similar to that observed in pine MWL (1.44 *vs.* 1.39 mmol/g). Due to the presence of condensation reactions during the kraft pulping, an actual increase in the amounts of the condensed units had been anticipated [109, 132, 133, 134]. In particular, an increase in the signal at 143.5 ppm had been expected. This expectation was due to

the formation of diphenylmethane condensed structures during kraft pulping [161, 235, 323, 324] and the structural similarity between these structures and β-5 ones (that is, a sp^3 hybridised carbon *ortho* to the phenolic hydroxyl). Table 5.11 compares the levels of condensed and uncondensed units in the pine MWL and Indulin lignin, in order to address this issue. For ease of discussion, the results in Table 5.11 have been rounded to 1 decimal place.

Table 5.11: Behaviour of condensed and uncondensed units during kraft pulping.

	C9 units, mmol/g of lignin			
	MWL	Indulin	difference	
Phenolic condensed	0.4	1.3	+ 0.9	
uncondensed	0.6	1.5	+ 0.9	
Etherified condensed	1.0	0.2	- 0.8	
uncondensed	1.9	0.6	- 1.3	
Unaccounted	1.4	1.9	+ 0.5	

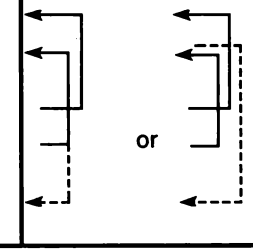

The drop in etherified condensed units on going from the MWL to the Indulin lignin approximately equalled the increase in phenolic condensed units, Table 5.11, suggesting that the phenolic condensed units originate primarily from etherified condensed units in the starting wood. Also the drop in etherified uncondensed units on going from the MWL to the Indulin lignin approximately equalled the increase in phenolic uncondensed and unaccounted material combined. This suggests that few etherified uncondensed units in the *P. radiata* were converted to phenolic condensed units during the action of kraft pulping. Instead, results suggest that etherified uncondensed units were converted to phenolic uncondensed units or, alternatively, to unaccounted material. This increase in unaccounted material was predominantly attributed to material loss during the thioacidolysis work-up. One supporting piece of evidence, was the retention of coloured material in the aqueous layer, during the dichloromethane extraction. It is probable that this dichloromethane-insoluble fraction contains material of a different chemical composition to that of the sample extracted during the work-up, one possibility being that the non-extracted material contains a high proportion of condensed units, thus accounting for the lack of condensed unit formation observed in the lignin thioacidolysate.

During the above comparison, it is important to remember, that 70-75% of the C9 units, in MWL and Indulin lignin, were being measured.

5.7.2 Kraft pulping delignification phases.

In this part of the study, three pulping liquors, kindly supplied by Ms J. Dalgety [325], were studied to determine their proportions of condensed and uncondensed units. This was performed, because the proportion of condensed units in solubilised kraft lignins has been shown to increase, as the degree of pulp delignification increases [189, 301, 326, 327]. For example, using three lignin samples isolated from pine wood at 15, 28 and 37% delignification, Gellerstedt *et al.* [326] showed, by oxidative degradation, that they contained 36.6, 41.1 and 43.5% condensed units.

The three kraft spent liquor lignins used in this study were labelled **A**, **B** and **C**. These were isolated by acidification of liquors, from kraft cooks stopped after differing times [325]. The aim was to isolate lignin from the pulping liquor during the initial (**A**), the bulk (**B**), and the residual (**C**) phases of kraft pulping. This was achieved for the **A** and **C** pulps. However, for the **B** lignin, the transition point from bulk to residual delignification, was passed. Typically, the transition from bulk phase to residual phase delignification is considered to occur around 90% delignification (equal to a kappa number of about 35-40) [108, 109, 128, 136]. However, the **B** lignin was isolated from a Kappa 26 pulp (Section 6.4.4). Therefore, both the **B** and **C** samples were actually isolated during residual phase delignification, just one after more delignification than the other. Table 5.12 summarises some of the pulp parameters associated with the isolated spent liquor lignins.

Table 5.12: Kraft pulping conditions from which spent liquors A, B and C were isolated [325].

Sample label	Cook time (min)	H factor	Pulp yield (%)	Klason lignin of Pulp (%)	Delignification (%)
A	72	6	76.7	28.2	21
B	190	1408	47.3	3.91	93
C	255	2388	45.6	3.27	94

The ^{31}P NMR spectra of the three kraft lignin samples, **A**, **B** and **C**, are shown in Figure 5.8. The quantitative results from these spectra are presented graphically in Figure 5.9 with data in Table 5.13.

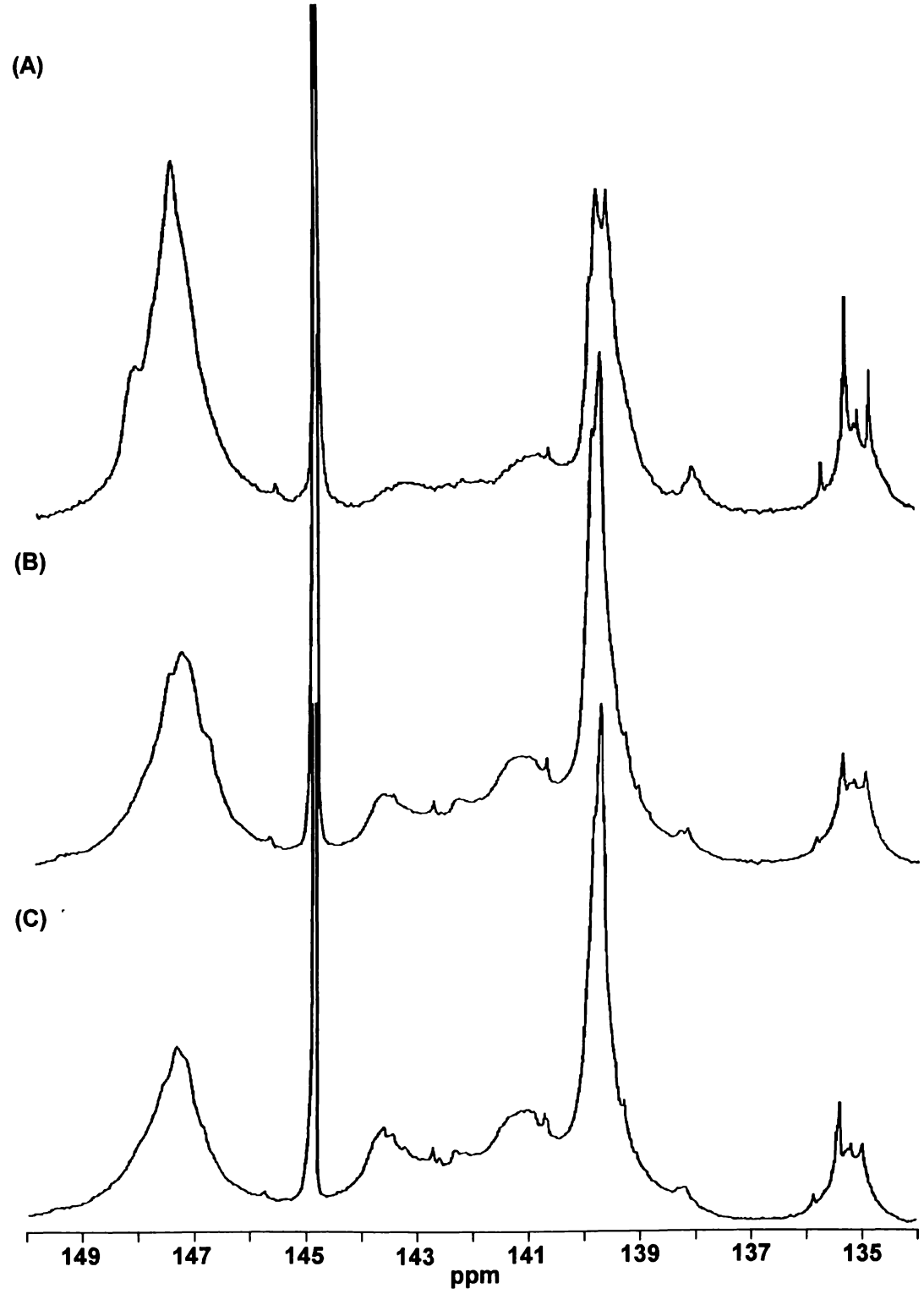

Figure 5.8: ^{31}P NMR spectra of three KSLL's isolated at different stages of the pulping process.

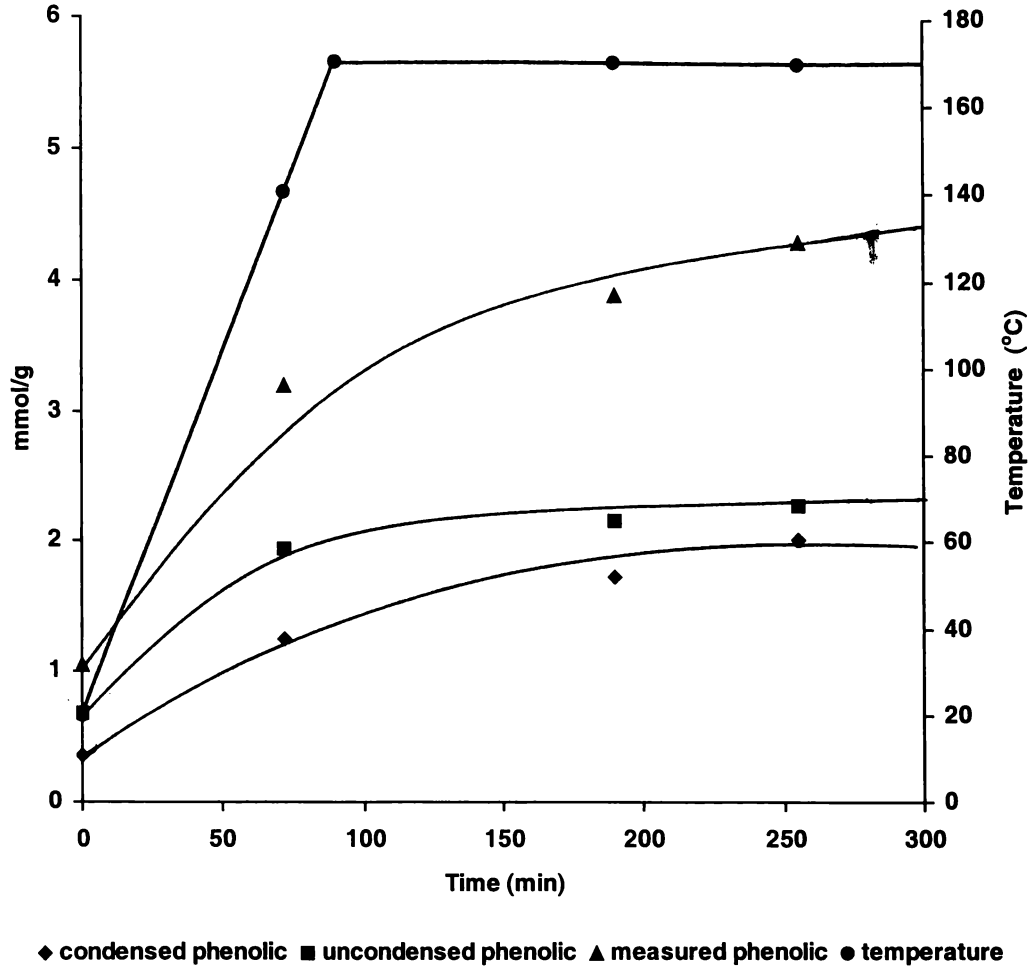

Figure 5.9: ^{31}P NMR spectroscopic yield of condensed and uncondensed units as a function of pulping time.

As the kraft cook time increased, so did the observed amounts of free phenolic units in the lignin. For example, while approximately 20% of the C9 units were free phenolic in MWL, over half the C9 units in the **A** lignin were free phenolic. Also, around three-quarters of the C9 units in the **B** and **C** lignins were free phenolic. As discussed for the Indulin lignin, kraft pulping cleaves β-aryl ether inter-unit linkages [130, 131]. This increase in free phenolic units in spent liquor lignins, as a function of delignification was consistent with previous observations [189, 239, 326]. Furthermore, the actual amounts of free phenolic units determined in **A**, **B** and **C** were reasonably consistent with the amounts of free phenolic units reported by Robert *et al.* [239] for lignins isolated from the liquors of kraft cooking to a similar pulp yield.

Increasing the kraft cook time also increased the proportions of condensed phenolic units, as has previously been observed [108, 109, 132-135]. For radiata pine MWL, 34% of the free phenolic units were present as condensed phenolic moieties (Section 4.2), whereas for sample **A** this had increased to 39%. For the subsequent lignins, **B** and **C**, 44% and 47% respectively of the free phenolic moieties were condensed at C5. This result is in line with the literature suggesting increased pulping leads to higher formation of condensed units [109, 128, 129, 134, 189, 220, 326]. Figure 5.9 shows the amount of free phenolic uncondensed units rises rapidly in the first 72 minutes. After this time there is little further increase in the amount of free phenolic uncondensed units. The amount of condensed G units on the other hand, steadily increases throughout the cook period. Thus at the longer cook times, the increase in total free phenolic units was predominantly due to the production of free phenolic condensed units.

Thioacidolysis/^{31}P NMR spectroscopy was then applied to the different kraft lignins studied above. The ^{31}P NMR spectra of lignin samples **A**, **B** and **C** after thioacidolysis are shown below in Figure 5.10. The numerical data from these spectra is presented in Table 5.13.

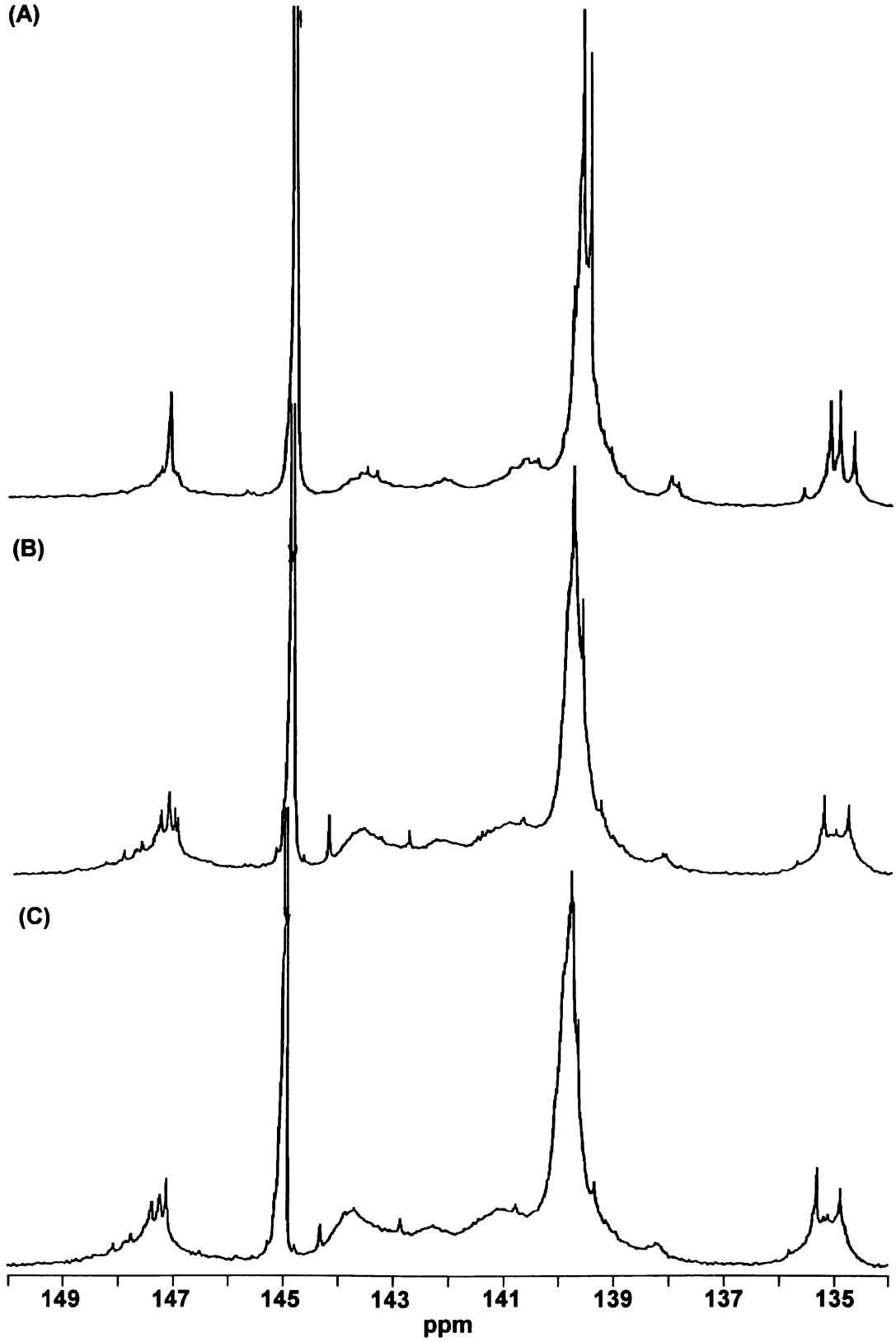

Figure 5.10: ^{31}P NMR spectra of thioacidolysates from three KSLL's isolated at different stages of the pulping process.

Table 5.13: ^{31}P NMR spectroscopic results for KSLL's isolated at different stages of the pulping process.

	C9 units, mmol/g of lignin								
	A			*B*			C		
	Free Phenolic	Etherified C9	Total Lignin	Free Phenolic	Etherified C9	Total Lignin	Free Phenolic	Etherified C9	Total Lignin
Condensed G	1.25	0.03	1.28	1.73	0.06	1.79	2.02	-0.48	1.54
Uncondensed G	1.95	0.84	2.79	2.16	0.42	2.58	2.28	-0.39	1.89
Measured Phenolic	3.20	0.87	4.07	3.89	0.48	4.37	4.30	-0.87	3.44
Unaccounted			1.57			1.24			2.17
% Condensed	39		31	44		41	47	-	45

For the **A** and **B** lignin samples, performing thioacidolysis prior to ^{31}P NMR spectroscopy improved the number of phenylpropane units analysed. For lignin sample **A**, 0.87 mmol of etherified moieties per gram of lignin, were released during thioacidolysis. On the other hand, for lignin sample **B**, 0.48 mmol/g were released. Therefore, as the degree of delignification increases, the incremental benefit of performing thioacidolysis prior to ^{31}P NMR spectroscopy decreased. This was due to the increased cleavage of β-aryl ether inter-unit linkages with increasing depolymerisation, leaving fewer linkages for the thioacidolysis to act on.

The proportion of condensed structures in the total lignin, for samples **A** and **B**, was lower than the proportions present as free phenolic groups. This result mirrors that observed for the Indulin lignin. For both the **A** and **B** lignin samples, this was due to the low amount of etherified condensed structures present, 0.03 and 0.06 mmol/g respectively. These low amounts of etherified condensed units in kraft spent liquor lignins has not, to our knowledge, been previously reported.

Tables 5.14 and 5.15 compare the **A** and **B** lignins with radiata pine MWL, in a similar fashion to the comparison performed for Indulin lignin.

Table 5.14: Comparison of MWL with KSLL A.

	C9 units, mmol/g of lignin			
	MWL	A	difference	
Phenolic condensed	0.4	1.3	+ 0.9	←
uncondensed	0.6	2.0	+ 1.4	←
Etherified condensed	1.0	0.0	- 1.0	
uncondensed	1.9	0.9	- 1.0	
Unaccounted	1.4	1.6	+ 0.2	

Table 5.15: Comparison of MWL with KSLL B.

	C9 units, mmol/g of lignin			
	MWL	B	difference	
Phenolic condensed	0.4	1.7	+ 1.3	←
uncondensed	0.6	2.2	+ 1.6	←
Etherified condensed	1.0	0.1	- 0.9	
uncondensed	1.9	0.4	- 1.5	
Unaccounted	1.4	1.2	- 0.2	

In both the **A** and **B** lignin samples, the increase in the amount of phenolic condensed units is matched by a concomitant decrease in the amount of etherified condensed units. A similar trend was also observed for the uncondensed units. By comparing the differences between the pine MWL and the **A** and **B** lignins, it appears that the phenolic condensed units originate primarily from etherified condensed units in the starting material. Few etherified uncondensed units appear to have been converted to phenolic condensed units during the kraft pulping. For example, the difference between the etherified uncondensed moieties, present in the pine MWL and the **B** lignin sample, was 1.5 mmol/g. This compared with a 1.6 mmol/g difference between the phenolic uncondensed moieties, present in the pine MWL and the **B** lignin sample.

For the **C** lignin fewer C9 units were analysed by ^{31}P NMR spectroscopy, after thioacidolysis than before (Table 5.13). While 76% of the C9 units in the **C** lignin were present as free phenolic units, only 61% of the C9 units contained free phenolic groups in the **C** thioacidolysate. This caused the reporting of negative values for etherified unit content in Table 5.13. The lower C9 yield has tentatively been

attributed to the loss of material during the thioacidolysis work-up. Although the **C** lignin contains only a few percentage points more condensed units than the **B** lignin, the condensed nature may in part account for this material loss. It is possible that some condensed material may not extract into the dichloromethane during the thioacidolysis work-up and thereby lead to the increased amount of unaccounted material reported for the **C** lignin.

Due to β-ether cleavage during kraft pulping, the benefit of performing thioacidolysis prior to ^{31}P NMR spectroscopy for these lignin samples is somewhat limited. Also the observed loss of material during thioacidolysis of the **C** lignin, raises some questions about the reliability of this technique, when applied to highly modified lignins.

5.8 Conclusions

- Thioacidolysis/^{31}P NMR spectroscopy is an excellent technique for determining the proportions of condensed and uncondensed units in isolated and *in situ* lignin. The technique was successfully applied to a range of lignin samples including softwood, hardwood, softwood compression wood and softwood fibre lignin.

- Results suggest that the structure of radiata pine lignin is surprisingly homogeneous. The proportions of condensed and uncondensed units in lignins from different regions within the tree were essentially identical. Also, results from thioacidolysis/^{31}P NMR spectroscopy applied to pine MWL and *in situ* lignin and to DWS fibres and fines suggested little difference in the proportion of condensed units in the ML and the SW, contrary to previous literature.

- The results also highlighed that in eucalypt lignin, S moieties were found to be preferentially present as etherified units. This compared with the work on normal and compression wood radiata pine MWL, which indicated that H units were prefernetially present as free phenolic units. These results were supported by evidence from previously published results. Thioacidolysis/^{31}P NMR

spectroscopy is therefore also an excellent technique for determining the amount of condensed G, uncondensed G, S and H units present as free phenolic and etherified units in a MWL.

- There is significant potential for this technique to be applied as a diagnostic tool to a vast range of lignin samples in future work.

- The proportion of H units in compression wood was significantly higher than in normal wood. Also there was a significant difference in the proportions of H units between the EW and LW in compression wood. In accordance with a polymerisation mechanism earlier proposed by Jaquet *et al.* [308] the proportion of condensed units in compression wood were found to be no higher than the proportions of these units present in toplog radiata pine lignin.

- The method appears to be less applicable to highly modified lignins such as those in heavily sulphonated chemimechanical and kraft pulps. Sulphonation at Cα inhibits thioacidolysis, leading to reduced yields, dependant on extent of sulphonation.

- For kraft lignins, thioacidolysis/^{31}P NMR spectroscopy was also less applicable compared with the original wood lignin. This was due to the cleavage of β-aryl ether inter-unit linkages during the kraft pulping. For these lignins, performing thioacidolysis prior to ^{31}P NMR spectroscopy did not have significant yield advantages.

I seem to have been like a child playing on the seashore,
finding now and then a prettier shell than ordinary,
whilst the great ocean of truth lay undiscovered before me.

Sir Isaac Newton

Chapter 6
Experimental Details

6.1 General Experimental Procedures

Analytical normal phase thin layer chromatography (tlc) was performed using 0.2 mm thick sheets of Merck Kieselgel 60 F_{254}, on aluminium backing. Analytical reverse phase tlc was performed using 0.2 mm thick Whatman $MKC_{18}F$ reverse phased silica, on glass backing. The resultant chromatographs were viewed using either UV fluorescence quenching at 254 nm, I_2 staining, or decomposition by ethanol/sulphuric acid (95/5) followed by heating. Preparative thin layer chromatography (plc) was performed on prepared 1-mm silica gel coated glass plates.

Reverse phased flash column chromatography [260] was performed on LiChroprep RP-18 reverse phase silica gel (particle size 40-63 μm). For phenolic model compounds, 0.1% phosphoric acid was added to reduce tailing. The elution rate was 2 cm min^{-1}, through a column with an internal diameter of 2.5 cm (packing weight was approximately 36g).

Mass spectra were obtained on a Hewlett-Packard HP 5985 spectrometer operating under EI ionisation with probe sample injection. Accelerating EMF was 70 eV and the inlet heated at 20°C min^{-1} from 30°C to 300°C.

Melting points were determined using a Reichert Thermopan melting point microscope and were uncorrected.

Unless otherwise stated, all the solvents used in this thesis were of AR grade and were used without further purification.

BF_3-diethyletherate and 2-chloro-4,4,5,5-tetramethyl-1,3,2-dioxaphospholane **41** were purchased from Aldrich Chemical Co. and used as supplied. Ethanethiol and cholesterol (95%) were purchased from Merck and Ajax Chemical Co's respectively, and used as supplied. 1,4-Dioxane was purchased from BDH Chemical Co and prior to use this was refluxed with Na metal to dryness.

Unless otherwise stated, all *Pinus radiata* used in this study was from the top log of trees aged 22-27 years old. Prior to use, lignocellulosic materials were ground through a Wiley mill with a 60-mesh screen and extracted with MeOH using a Soxhlet extractor.

Isolated and *in situ* lignin samples were analysed for Klason lignin, according to TAPPI 222 om-88, and for acid soluble lignin, according to TAPPI um-250. These analyses were performed by the wood materials test centre, Forest Research, Rotorua.

Elemental analyses were performed by Campbell Microanalytical Laboratory, University of Otago, Dunedin.

For kraft pulping, effective alkali was determined using TAPPI 625 cm-85 and sulphidity according to TAPPI 625 cm-85.

6.2 Spectroscopic Techniques

NMR spectroscopy in this study was performed on a number of NMR spectrometers. In particular, at Forest Research a Bruker AC 200 (later upgraded to a Bruker Avance 200) and a Bruker Avance 400 were used. At The University of Waikato, a Bruker AC 300 was used.

6.2.1 ^{1}H NMR spectroscopy

^{1}H NMR spectra, for all compounds in this thesis, were acquired in chloroform-*d* ($CDCl_3$), acetone-d_6 or dimethyl sulphoxide-d_6. Spectra were acquired using a 5 mm

$^{1}H/^{13}C$ dual probe on a Bruker AC 200 (operating at 200.1 MHz), or using a 5-mm inverse ^{1}H/broadband probe on a Bruker Avance 400 (operating at 400.1 MHz). For the 200 MHz spectra, a 2500 Hz spectral window and 16K data points were used, resulting in peak resolution accurate to 0.3 Hz. Line broadening of 0.1 Hz was used. The 400 MHz spectra were acquired with an 8223 Hz spectral window and 16K data points, resulting in peak resolution accurate to 0.25 Hz. Line broadening of 0.3 Hz was used.

The data is expressed as parts per million (ppm) downfield shift from the tetramethyl silane standard. Each signal is quoted as position (δ), relative integral, multiplicity (s = singlet, d = doublet, t = triplet, q = quartet, m = multiplet). Where applicable, coupling constants (J) are given along with assignment. The labelling used to identify the different atoms in the lignin model compound is shown in Figure 6.1, using β-5 model **89** as an example.

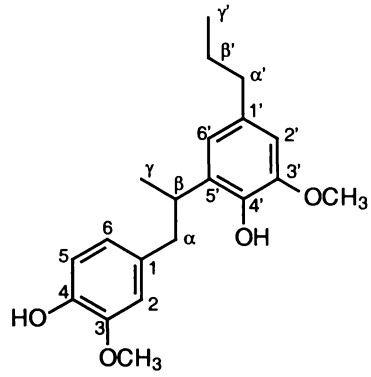

Figure 6.1: Labelling system used in NMR spectroscopic assignments.

6.2.2 ^{13}C NMR spectroscopy

Using a 5 mm $^{1}H/^{13}C$ dual probe on the Bruker AC 200 spectrometer (operating at 50.1 MHz), ^{13}C NMR spectra were acquired in $CDCl_3$, acetone-d_6 or dimethyl sulphoxide-d_6. The ^{1}H decoupled ^{13}C spectra [328] were acquired with a spectral window of 12 kHz and 32K data points, making peak resolution accurate to 0.7 Hz. For quantitative ^{13}C NMR spectra [329], an inverse gated ^{1}H decoupling sequence, with $\theta = 90°$ (14 μs) and a relaxation delay between pulses of 30 seconds, was used. A line broadening of 1 Hz was used.

Some spectral ambiguities were resolved using DEPT (distortionless enhancement via polarisation transfer) pulse sequences [242], with editing pulses of $\theta = 135°$, to give methylene resonance inversion, or $\theta = 45°$, to give methine resonances only.

Alternatively, the ^{13}C NMR spectra were acquired using a 5-mm inverse ^{1}H/broadband probe, on the Bruker Avance 400 spectrometer (operating at 100.6 MHz). The ^{1}H decoupled ^{13}C NMR spectra were acquired with a spectral window of 22 kHz and 32K data points, making the chemical shifts quoted accurate to 0.3 Hz. A line broadening of 1 Hz was used.

6.2.3 ^{1}H-^{1}H COSY

Two dimensional ^{1}H-^{1}H COSY (correlation spectroscopy) NMR spectra [249] were acquired in $CDCl_3$ or acetone-d_6, using a 5 mm inverse ^{1}H/broadband probe, on a Bruker Avance 400 spectrometer. COSY spectra were acquired using the standard Bruker COSY90 (D1-90-1/4J-90-acq) pulse sequence, with a 2048 x 256 data matrix size and using a spectral window of 2796 Hz x 2796 Hz. Spectra were collected using a 90° pulse width of 8.5 μsec and a recycle time of 1 sec.

6.2.4 ^{1}H-^{13}C HMBC

Two dimensional ^{1}H-^{13}C HMBC (heteronuclear multiple bond correlation) NMR spectra [250] were acquired in $CDCl_3$ or acetone-d_6, using a 5 mm inverse ^{1}H/broadband probe, on a Bruker Avance 400 spectrometer. The HMBC spectra were acquired using the standard Bruker inv4lplrnd pulse sequence (in XWIN-NMR), with a 1024 x 256 data matrix size and a spectral window of 3200 x 15000 Hz. The 90° pulse widths were 8.5 μs (^{1}H) and 13.0 μs (^{13}C). A 1-second delay between scans, and a 70 μsec delay to transfer polarisation between the proton and carbon, were also used. The multiple quantum filter used, was 1/4J, where J = 145 Hz.

6.2.5 ^{1}H-^{13}C HMQC

Two dimensional ^{1}H-^{13}C HMQC (heteronuclear multiple quantum coherence) NMR spectra [97, 98] were acquired in $CDCl_3$ or acetone-d_6, using a 5 mm ^{1}H/broadband inverse probe, on a Bruker Avance 400 spectrometer. The HMQC spectra were acquired using the standard Bruker inv4tp pulse sequence, with a 1024 x 128 data

matrix size and a spectral window of 3200 x 15000 Hz. Again, the 90° pulse widths were 8.5 μsec for ^{1}H and 13.0 μsec for ^{13}C. A 1-second delay between scans, and a 70 μsec delay to transfer polarisation between the proton and the carbon, were used.

6.2.6 ^{31}P NMR spectroscopy

Quantitative ^{31}P NMR spectra [189, 282] were acquired using a 10 mm ^{1}H/broadband probe on a Bruker AC 200 NMR spectrometer (operating at 81.0 MHz). Alternatively ^{31}P NMR spectra were acquired using a 5-mm QNP (quad nuclear probe) probe on a Bruker AC 300 NMR spectrometer (operating at 121.1 MHz). In both cases, spectra were acquired using a 90° tip angle and a sweep width of 25 kHz via an inverse gated ^{1}H decoupling sequence. Using a delay of 20 seconds, 750 scans were acquired of each sample. Spectra were processed using a line broadening of 2 Hz.

Qualitative ^{31}P NMR spectra, of lignin model compounds derivatised with **41**, were acquired using conditions essentially identical to those outlined above. In this case, a delay of 2 seconds between pulses was used and 16 scans were collected.

The external reference was 85% H_3PO_4. All downfield shifts from H_3PO_4 were considered positive, with chemical shifts expressed as parts per million (ppm). Chemical shifts were referenced to the reaction product of 2-chloro-4,4,5,5-tetramethyl-1,3,2-dioxaphospholane with water, which has been observed to give a signal in pyridine/$CDCl_3$ at 132.2 ppm [189].

6.2.7 ^{31}P-^{31}P COSY

Two dimensional ^{31}P-^{31}P COSY NMR spectra were acquired in the standard pyridine/$CDCl_3$ phosphorus NMR solution, on a Bruker Avance 400 spectrometer using a 5 mm inverse ^{1}H/broadband probe and operating at 162.0 MHz. The COSY spectra [249] were acquired using the standard Bruker COSY90 pulse sequence, with a 1024 x 256 data matrix and using a spectral window of 1500 Hz x 1500 Hz. A 90° pulse width of 13.5 μsec and a recycle time of 2.0 sec were used.

6.2.8 ^{31}P NMR spectroscopy T_1 calculations

T_1 calculations were performed using a 10-mm broadband probe in a Bruker Avance 200 NMR spectrometer, operating at 81 MHz with 32K data points over a 3200 Hz spectral window. A D1-180°-τ-90°-acq powergate decoupled inversion recovery sequence was used with θ = 90° at 14 μsec. Using a delay of 20 sec between pulses, 4 scans were collected at each τ value of 50, 100, 250, 750, 1000, 2500, 5000 and 10000 msec.

T_1 was calculated using an intensity fit with $I_t = I_o + P \exp(-t/T_1)$.

T_1 calculations were also performed using an inverse ^1H/broadband probe in a Bruker Avance 400 NMR spectrometer, operating at 161 MHz. Generically, the pulse sequence was the same as outlined for the Avance 200 above. However, a pulse time of 13.5 μsec (θ = 90°) was used.

6.3 Model Compound Synthesis

A range of lignin model compounds were prepared, as discussed in Sections 6.3.1-6.3.14. Products were identified by NMR spectroscopy and mass spectrometry performed on pure (single tlc spot) samples. The NMR and mass spectrometry results, presented in each case, were consistent with the model prepared.

6.3.1 Preparation of dehydrodivanillin (54) [330]

To a stirred solution of vanillin **36** (5.00 g, 32.8 mmol) in water (500 mL, 60°C) were added $FeCl_3.6H_2O$ (0.16 g, 0.59 mmol) and $Na_2S_2O_8$ (4.16 g, 17.5 mmol) [330]. A thick, creamy coloured precipitate formed almost instantaneously. The reaction was stirred for 40 minutes, cooled to ambient temperature and the precipitate filtered though a Buchner funnel. A solution of sodium hydroxide (1M, 50 mL) was used to dissolve the collected precipitate. By acidification with H_2SO_4 (1M, 50 mL), the solution was re-precipitated and subsequently filtered. The residue was thoroughly washed with distilled water and dried to give dehydrodivanillin **54** (4.28 g, 85%), as a light brown solid.

^{1}H NMR (200 MHz, d_6-DMSO) δ: 3.90 (6H, ,s -OCH_3); 7.35-7.45 (4H, m, ArH); 9.80 (2H, s, -CHO).

^{13}C NMR (50 MHz, d_6-DMSO) δ: 56.06 (-OCH_3); 109.22 (C2); 124.60 (C6), 127.80 (C5); 128.18 (C1); 148.18 (C4); 150.44 (C3); 191.20 (-CHO).

M/S: m/z = 302 (M^+).

6.3.2 Preparation of dehydrodipropylguaiacol (61) [107]

To a stirred solution of propylguaiacol **88** (2.00 g, 12.2 mmol) in water (500 mL, 60°C) were added $FeCl_3.6H_2O$ (0.16 g, 0.59 mmol) and $Na_2S_2O_8$ (2.08 g, 8.75 mmol) [330, 107]. A thick precipitate formed almost instantaneously. The reaction was stirred for 40 minutes, cooled to ambient temperature and the precipitate filtered through a Buchner funnel. The collected precipitate was purified, as described for dehydrodivanillin (Section 6.3.1), to give dehydrodipropylguaiacol **61** (1.63 g, 82%), as a light brown solid.

^{1}H NMR (200 MHz, $CDCl_3$) δ: 0.96 (3H, t, J = 7.4 Hz, Hγ); 1.65 (2H, m, Hβ); 2.58 (2H, t, J = 8.0 Hz, Hα); 3.89 (3H, s, -OCH_3); 6.01 (1H, s, H6); 6.73 (1H, s, H2).

^{13}C NMR (50 MHz, $CDCl_3$) δ: 13.92 (Cγ); 24.78 (Cβ); 37.90 (Cα); 56.08 (-OCH_3); 110.66 (C2); 123.00 (C6); 126.46 (C5); 134.70 (C1); 141.54 (C4); 147.12 (C3).

M/S: m/z = 330 (M^+).

6.3.3 Preparation of vanillyl alcohol (65)

To a cold (0°C), stirred solution of vanillin **36** (2.00 g, 13.16 mmol) in ethanol (20 mL) and water (20 mL), was added sodium borohydride (0.98 g, 26.48 mmol) [331, 332]. The reaction was allowed to warm to room temperature. After 5 hours, solid NH_4Cl was added until gas evolution stopped. The mixture was stirred for 5 minutes, then filtered and the inorganic residues were washed with dichloromethane. The combined filtrates were diluted with water (100 mL) and extracted with dichloromethane (3x 100 mL). The combined organic extracts were dried ($MgSO_4$) and concentrated under reduced pressure. Recrystallisation, from EtOAc, yielded vanillyl alcohol **65** (0.96 g, 49%), as a white crystalline product.

^{1}H NMR (200 MHz, d_6-acetone) δ: 3.49 (1H, t, α-OH); 3.85 (3H, s, -OCH_3); 5.08 (2H, s, Hα); 6.61-6.97 (3H, m, ArH).

^{13}C NMR (50 MHz, d_6-acetone) δ: 56.76 (-OCH_3); 67.36 (Cα); 113.36 (C2); 119.30 (C5); 123.48 (C6); 132.66 (C1); 147.50 (C4); 149.58 (C3).

M/S: m/z = 154 (M^+).

M.P. = 114-115°C (lit [333] = 115°C).

6.3.4 Preparation of apocynol (66) [334]

Acetovanillone **69** (5 g, 30.1 mmol), 5% palladium on activated carbon (100 mg) and 95% ethanol (300 mL) were placed in a reaction vessel and flushed with N_2. The reaction vessel was placed on a Parr hydrogenator and a H_2 pressure of 35 psi was applied [332, 335, 336]. After 24 hours the reaction mixture was filtered through Celite® 535 and concentrated, under reduced pressure, to approximately 50 mL. Water (150 mL) was added and the aqueous solution extracted with ethyl acetate (3x 100 mL). The combined organic extracts were washed with water (2x 50 mL) and brine (2x 50 mL), then dried ($MgSO_4$), filtered and concentrated under reduced pressure. Recrystallisation, from EtOAc, yielded apocynol **66** (3.96 g, 79%), as a white crystalline product.

^{1}H NMR (200 MHz, $CDCl_3$) δ: 1.47 (3H, d, J = 6.4 Hz, Hβ); 3.90 (3H, s -OCH_3); 4.86 (1H, q, J = 6.4 Hz, Hα); 5.59 (1H, s, α-OH); 6.9-7.4 (3H, m, ArH).

^{13}C NMR (50 MHz, $CDCl_3$) δ: 29.98 (Cβ); 57.62 (-OCH_3); 72.12 (Cα); 112.80 (C2); 119.00 (C5); 121.66 (C6); 132.48 (C1); 147.12 (C4); 149.26 (C3).

M/S: m/z = 168 (M^+).

M.P. = 100-102°C (lit [334] = 101-102°C).

6.3.5 Preparation of dehydrodivanillyl alcohol (72) [107]

Dehydrodivanillin **54** (1.00 g, 3.31 mmol), 5% palladium on activated carbon (150 mg) and NaOH (0.5 N, 120 mL) were placed in a reaction vessel and flushed with N_2. The reaction vessel was placed on a Parr hydrogenator and a H_2 pressure of 35 psi was applied [336, 332, 335]. After 24 hours of shaking, the reaction was stopped and worked up, as described in Section 6.3.4. The collected product was purified by reverse phase flash column chromatography [260] (40% methanol in water), to give dehydrodivanillyl alcohol **72** (0.26 g, 45%), as a brown product.

^{1}H NMR (200 MHz, d_6-DMSO) δ: 3.92 (6H, s, -OCH_3); 4.08 (2H, t, α-OH); 4.65 (4H, d, Hα); 6.93 (2H, s, H6); 7.03 (2H, s, H2).

^{13}C NMR (50 MHz, d_6-DMSO) δ: 56.20 (-OCH_3); 64.78 (Cα); 110.04 (C2); 122.40 (C6); 126.02 (C5); 132.16 (C1); 143.56 (C4); 149.44 (C3).

M/S: m/z = 306 (M^+).

6.3.6 Preparation of dehydrodiapocynol (73) [337]

To a stirred solution of dehydrodiacetovanillone **106** (1.00 g, 3.1 mmol) in NaOH (0.5 M, 100 mL, 25°C) was added sodium borohydride (0.50 g, 13.2 mmol) [331, 332]. After 4 hours the reaction was quenched with solid NH_4Cl, until gas evolution ceased, and was filtered. Then the reaction solution was concentrated under reduced pressure, to 1/4 of its original volume, and extracted with dichloromethane (3x 100 mL). The combined organic fractions were washed with water (2x 20 mL) and brine (2x 20 mL), dried ($MgSO_4$) and concentrated under reduced pressure. The resultant product was purified using reverse phase flash column chromatography [260] (40% methanol in water), to give dehydrodiapocynol **73** (0.42 g, 42%), as a white solid.

^{1}H NMR (200 MHz, d_6-DMSO) δ: 1.50 (6H, d, J = 6.4 Hz, Hβ); 3.94 (6H, s,-OCH_3); 4.86 (2H, q, J = 6.4 Hz, Hα); 5.29 (2H, s, α-OH); 6.09 (2H, s, -OH); 6.90 (2H, s, H6); 6.99 (2H, s, H2).

^{13}C NMR (50 MHz, d_6-DMSO) δ: 26.28 (Cβ); 56.88 (-OCH_3); 72.12 (Cα); 112.04 (C2) 124.00 (C6); 129.72 (C5); 132.68 (C1); 147.18 (C4); 151.44 (C3).

M/S: m/z = 334 (M^+).

6.3.7 Preparation of dehydrodiisoeugenol (77) [338]

To a solution of isoeugenol **63** (10 g, 60 mmol) in ethanol (100 mL) and water (40 mL) was added a freshly prepared solution of $FeCl_3.6H_2O$ (23.2 g, 85 mmol) in water (40 mL) [338]. The reaction was stirred for 30 minutes at room temperature and then stood at 4°C for 24 hours. The resultant pink solid was filtered off and recrystallised from 45% aqueous ethanol to give dehydrodiisoeugenol **77** (5.4 g, 54%), as off white crystals.

^{1}H NMR (200 MHz, $CDCl_3$) δ: 1.41 (3H, d, J = 6.6 Hz, Hγ); 1.86 (3H, dd, J = 6.1 Hz, 0.5 Hz, Hγ'); 3.49 (1H, dq, J = 8.8 Hz, 6.6 Hz, Hβ); 3.88 (3H, s, -OCH_3); 3.91 (3H, s, -OCH_3); 5.11 (1H, d, J = 8.8 Hz, Hα); 5.73 (1H, b, ArOH); 6.11 (1H, dq, J = 16.2 Hz, 6.1 Hz, Hβ'); 6.37 (1H, dd, J = 16.2 Hz, 0.5 Hz, Hα'); 6.7-7.2 (5H, m, ArH).

^{13}C NMR (50 MHz, $CDCl_3$) δ: 17.86 (Cγ); 18.32 (Cγ'); 45.62 (Cβ); 55.98 (OCH_3); 93.70 (Cα); 109.14 (C2); 109.84 (C2'); 113.48 (C6'); 114.22 (C5); 121.02 (C6); 123.42 (Cβ'); 131.38 (Cα'); 132.02 (C1); 132.70 (C1'); 133.38 (C5'); 144.14 (C3'); 145.80 (C4); 146.42 (C4'); 146.96 (C3).

M.P. = 129-131°C (lit [338] = 130°C).

M/S: m/z = 326 (M^+).

6.3.8 Preparation of dehydrodihydrodiisoeugenol (78) [339]

Dehydrodiisoeugenol 77 (0.4 g, 1.23 mmol) and 5% palladium on activated carbon (10 mg) were placed in a reaction vessel with methanol (30 mL) and flushed with N_2 [336, 332, 335]. The reaction vessel was placed on a Parr hydrogenator, under a H_2 pressure of 35 psi, and stirred for 4 hours. The work-up was performed, as described in Section 6.3.4, yielding a colourless oil (3.8 g, 95%). Recrystallisation from petroleum ether (100-120°C) gave dehydrodihydrodiisoeugenol 78 (2.74 g, 68%), as white needles.

^{1}H NMR (200 MHz, $CDCl_3$) δ: 0.97 (3H, t, J = 7.4 Hz, Hγ'); 1.38 (3H, d, J = 6.8 Hz, Hγ); 1.65 (2H, m, Hβ'); 2.55 (2H, t, J = 8.0 Hz, Hα'); 3.45 (1H, dq, J = 9.8 Hz, 6.8 Hz, Hβ); 3.90 (6H, s, OCH_3); 5.08 (1H, d, J = 9.8 Hz, Hα); 5.64 (1H, b, ArOH); 6.55-7.01 (6H, m, ArH).

^{13}C NMR (50 MHz, $CDCl_3$) δ: 13.92 (Cγ'); 17.90 (Cγ); 24.82 (Cβ'); 37.86 (Cα'); 45.68 (Cβ); 55.94 (-OCH_3); 93.72 (Cα); 109.28 (C2); 110.44 (C2'); 113.60 (C6'); 114.22 (C5); 119.84 (C6); 132.06 (C1'); 132.30 (C1); 134.60 (C5'); 144.16 (C3'); 145.88 (C4); 146.58 (C4'); 146.72 (C3).

M.P. = 90-92°C (lit [339] = 89-91°C).

M/S: m/z = 328 (M^+).

6.3.9 Preparation of 4-(2-hydroxyethoxy)-apocynol (86) [340]

To a cold (0°C), stirred solution of 4-(2-hydroxyethoxy)-3-methoxy acetophenone 107 (0.20 g, 0.95 mmol) in ethanol (50 mL), sodium borohydride (0.21 g, 5.55 mmol) was added, and the reaction allowed to warm to room temperature [331, 332]. Tlc after 5 hours indicated, that no starting material remained, so NH_4Cl (solid) was added until gas evolution stopped. The mixture was stirred for 15 minutes, then filtered and the residual inorganic solid was washed with dichloromethane. The filtrate was diluted with water (100 mL) and extracted with dichloromethane (3x 100 mL). The combined organic extracts were dried ($MgSO_4$) and concentrated, under reduced pressure, to give etherified apocynol 86 (1.73 g, 82%), as a colourless oil.

^{1}H NMR (200 MHz, $CDCl_3$) δ: 1.44 (3H, d, J = 6.4, Hβ); 3.86 (3H, s, -OCH_3); 3.93 (2H, t, J = 7.0, -$OCH_2\underline{CH_2}OH$); 4.05 (1H, s, α-OH); 4.10 (2H, t, J = 7.0, -$OCH_2\underline{CH_2}OH$); 4.80 (1H, q, J = 6.4, Hα); 6.83-6.95 (3H, m, ArH).

^{13}C NMR (50 MHz, $CDCl_3$) δ: 24.73 (Cβ); 55.30 (-OCH_3); 60.37 (-$OCH_2\underline{CH_2}OH$); 69.24 (Cα); 70.24 (-$O\underline{CH_2}CH_2OH$); 108.80 (C2); 112.52 (C5); 117.54 (C6); 139.06 (C1); 146.66 (C3); 148.42 (C4).

M/S: m/z = 212 (53, M^+); 197 (51); 153 (100); 135 (11); 125 (55); 93 (85).

6.3.10 Preparation of propylguaiacol (88) [107]

Isoeugenol 63 (5.00 g, 36.5 mmol), 5% palladium on activated carbon (50 mg) and 95% ethanol (300 mL) were placed in a reaction vessel and flushed with N_2 [332, 335, 336]. The reaction vessel was placed on a Parr hydrogenator and a H_2 pressure of 35 psi was applied. After 5 hours, the reaction was stopped and worked up as described in the preparation of apocynol (Section 6.3.4), to yield propylguaiacol 88, (3.41 g, 68%), as an oil.

^{1}H NMR (200 MHz, $CDCl_3$) δ: 0.95 (3H, t, J = 7.4 Hz, Hγ); 1.64 (2H, m, Hβ); 2.56 (2H, t, J = 8.0 Hz, Hα); 3.92 (3H, s, -OCH_3); 6.0-6.6 (3H, m, ArH).

^{13}C NMR (50 MHz, $CDCl_3$) δ: 13.80 (Cγ); 24.58 (Cβ); 37.84 (Cα); 56.18 (-OCH_3) 110.66 (C2); 117.52 (C5); 121.44 (C6); 134.70 (C1); 141.82 (C4); 147.12 (C3).

M/S: m/z = 166 (M^+).

6.3.11 Preparation of β-5 dehydrodipropylguaiacol (89)

Dehydrodiisoeugenol 78 (0.2 g, 0.62 mmol) and 5% palladium on activated carbon (20 mg) were placed in a reaction vessel with methanol (30 mL) and flushed with N_2 [332, 335, 336]. The reaction vessel was placed on a Parr hydrogenator, under a H_2 pressure of 35 psi, and shaken for 48 hours. Work up was performed, as described in Section 6.3.4), to yield β-5 dehydrodipropylguaiacol 89 (0.18 g, 90%), as a colourless oil.

^{1}H NMR (200 MHz, $CDCl_3$) δ: 0.98 (3H, t, J = 7.2 Hz, Hγ'); 1.23 (3H, d, J = 9.4 Hz, Hγ); 1.66 (2H, m, Hβ'); 2.55 (2H, t, J = 7.7 Hz, Hα'); 2.66 (1H, dd, J = 13.4 Hz, 8.7 Hz, $H\alpha_1$); 2.98 (1H, dd, J = 13.4 Hz, 5.9 Hz, $H\alpha_2$); 3.43 (1H, m, Hβ); 3.78 (3H, s, OCH_3); 3.84 (3H, s, OCH_3); 5.49 (1H, b, OH); 5.60 (1H, b, OH); 6.57 (1H, s, H2'); 6.61 (1H, s, H6'); 6.64 (1H, s, H2); 6.69 (1H, d, H6); 6.82 (1H, d, H5).

^{13}C NMR (50 MHz, $CDCl_3$) δ: 14.28 (Cγ'); 19.82 (Cγ); 25.42 (Cβ'); 35.06 (Cβ); 38.48 (Cα'); 43.24 (Cα); 56.22, 56.40 (OCH_3); 108.86 (C2'); 112.20 (C2); 114.28 (C5); 119.62 (C6'); 122.34 (C6); 132.54 (C5'); 133.70 (C1); 134.08 (C1'); 141.28 (C4'), 144.00 (C4); 146.46, 146.52 (C3 and C3').

M/S: m/z = 330 (M^+).

6.3.12 Preparation of dehydrodiacetovanillone (106) [337]

To a stirred solution of acetovanillone 69 (3.00 g, 18.0 mmol) in water (500 mL, 60°C) were added $FeCl_3$ (0.16 g, 0.59 mmol) and $Na_2S_2O_8$ (2.50 g, 10.5 mmol) [330]. A thick, brown precipitate formed immediately. The reaction was stirred for 30 minutes, cooled to ambient temperature and the precipitate filtered off through a Buchner funnel. The collected precipitate was purified, as described for dehydrodivanillin (Section 6.3.1), to give dehydrodiacetovanillone 106 (2.35 g, 79%), as a brown product.

^{1}H NMR (200 MHz, d_6-DMSO) δ: 2.50 (6H, s, Hβ); 3.91 (6H, s, -OCH_3); 7.42-7.65 (4H, m, ArH); 9.55 (2H, s, ArOH).

^{13}C NMR (50.3 MHz, d_6-DMSO) δ: 26.28 (Cβ); 56.00 (-OCH_3); 109.68 (C2); 124.48 (C6); 125.28 (C5); 129.90 (C1); 147.46 (C4); 149.10 (C3); 196.22 (Cα).

M/S: m/z = 330 (M^+).

6.3.13 Preparation of 4-(2-hydroxyethoxy)-3-methoxy acetophenone (107) [340]

A mixture of 4-(2-bromoethoxy)-3-methoxy acetophenone **108** (4.00 g, 16 mmol)and K_2CO_3 (12.00 g, 80 mmol) in water (200 mL) were heated at reflux for 60 hours [340]. The solution was cooled to ambient temperature and extracted with dichloromethane (3x 100 mL). The combined organic extracts were dried ($MgSO_4$) and concentrated under reduced pressure. The product was purified using reverse phase flash column chromatography (25% methanol in water) and recrystallised from dichloromethane/hexane, to give 4-(2-hydroxyethoxy)-3-methoxy acetophenone **107** (2.50 g, 65%), as the product.

^{1}H NMR (200 MHz, $CDCl_3$) δ: 2.56 (3H, s, Hβ); 3.91 (3H, s, $-OCH_3$); 4.05 (2H, t, J = 7.0, $-OCH_2\underline{C}H_2OH$); 4.16 (2H, t, J = 7.0,$-O\underline{C}H_2CH_2OH$); 6.91-7.56 (3H, m, ArH).
^{13}C NMR (50 MHz, $CDCl_3$) δ: 26.04 (Cβ); 55.82 ($-OCH_3$); 60.88 ($-OCH_2\underline{C}H_2OH$); 70.50 ($-O\underline{C}H_2CH_2OH$); 110.44 (C2); 111.74 (C5); 123.06 (C6); 130.72 (C1); 149.12 (C3); 152.38 (C4); 196.66 (Cα).
M.P. = 101.6-101.8°C (lit = 101.5-101.8°C [340]).

6.3.14 Preparation of 4-(2-bromoethoxy)-3-methoxy acetophenone (108) [340]

1,2-dibromoethane (11.2 mL, 120 mmol) was added, at room temperature, to a mixture of acetovanillone **69** (2.00 g, 12.0 mmol), dry K_2CO_3 (16.58 g, 120 mmol) and KI (0.10 g, 0.6 mmol), in acetone (600 mL) [340]. After 8 hours of heating at reflux, the mixture was cooled to ambient temperature and filtered. The filtrate was concentrated, under reduced pressure, to give a yellow solid. The solid was heated in hexane and filtered to remove any excess 1,2-dibromoethane. This yielded 4-(2-bromoethoxy)-3-methoxy acetophenone **108** 2.43 g (73%), as the product.

^{1}H NMR (200 MHz, $CDCl_3$) δ: 2.57 (3H, s, Hβ); 3.96 (2H, t, J = 7.2, $-OCH_2\underline{C}H_2Br$); 3.92 (3H, s, $-OCH_3$); 4.40 (2H, t, J = 7.2,$-O\underline{C}H_2CH_2Br$); 6.91-7.57 (3H, m, ArH).
^{13}C NMR (50 MHz, $CDCl_3$) δ: 26.18 (Cβ); 28.31 ($-OCH_2\underline{C}H_2Br$); 56.08 ($-OCH_3$); 68.82 ($-O\underline{C}H_2CH_2Br$); 111.10 (C2); 112.46 (C5); 122.94 (C6); 131.44 (C1); 149.52 (C3); 151.72 (C4); 196.54 (Cα).

6.4 *Lignin Preparations*

6.4.1 Softwood MWL

Softwood samples were ground to pass 60 mesh on the Wiley mill. This product was then successively extracted with dichloromethane, water and 95% ethanol to remove extractives.

In accordance with the Björkman method [57, 123], the extractive free wood (50 g) was ball milled for 4 days, followed by extraction of the resultant wood meal with 9/1 dioxane/water for 4 days. After filtration through GF filter paper, the product was concentrated under reduced pressure. The residual lignin was dissolved in acetic acid/water (80/3 mL), then precipitated into water (1400 mL). After centrifugation, the residual solid was dissolved in 210 mL of 2/1 CH_2Cl_2/EtOH, which was precipitated into diethylether (400 mL). This precipitate was centrifuged and washed with Et_2O (3 x 300 mL), then 40:60 petroleum ether was added, the material thoroughly stirred and concentrated, under reduced pressure, to yield MWL (1.23 g).

6.4.2 Hardwood MWL

Hardwood milled wood lignins were prepared according to the method by Lundquist *et al.* [341, 342]. Pre-extracted (Section 6.4.1) commercial eucalypt (50 g) was milled and extracted with dioxane-water, as described by Björkman [57, 123]. The extracted product was dissolved in 210 mL pyridine-acetic acid-water (9:1:4). The solution was then extracted with chloroform (540 mL). The chloroform layer was concentrated, under reduced pressure, to about 200 mL and precipitated into stirred diethyl ether (1500 mL). After centrifugation, the precipitate was washed with ether (3 x 300 mL) and concentrated, under reduced pressure, with 40:60 petroleum ether. This yielded the eucalypt MWL (3.08 g).

6.4.3 Kraft lignin

Indulin kraft lignin was sourced from the widely studied International Energy Agency (IEA) 1991 international "round robin" (IRR) of lignins.

6.4.4 Delignification phases

Kraft spent liquor lignins, isolated during different phases of delignification, were prepared by Ms Jacinta Dalgety [325] using a M/K digester. The digester was programmed to increase the temperature of the pulp, from room temperature to 170°C, over 90 minutes (1.7°C/min). The pulp was monitored by H factor.

Initial + Bulk + Residual pulping liquor **(IBR)**
A sample of six hundred grams of *Pinus radiata* chips, was partially pulped, until H factor of 2188 (90 mins to 170°C, 165 mins at 170°C) was reached. The white liquor contained 26.7 g/L (as Na_2O) effective alkali and 30 % sulphidity, with a liquor to wood ratio of 6:1. The liquor was drained from the digester, collected and stored under nitrogen at 4°C. The partially pulped chips were washed for 16 hours with flowing tap water. To remove the excess water, the washed partially pulped chips were centrifuged. These centrifuged chips were oven-dried at 105C for 5 days, in order to determine the yield (45.6%) and moisture content.

Initial + Bulk pulping liquor **(IB)**
A sample of six hundred grams of *Pinus radiata* chips, was partially pulped, until H factor of 1408 was reached (90 mins to 170°C, 100 mins at 170°C). The white liquor contained 26.7 g/L (as Na_2O) effective alkali and 30 % sulphidity, with a liquor to wood ratio of 6:1. The liquor was drained from the digester, collected and stored under nitrogen at 4°C. The partially pulped chips were washed for 16 hours with flowing tap water. To remove the excess water, the partially pulped chips were centrifuged. These centrifuged chips were oven-dried at 105°C for 5 days, in order to determine the yield (47.3%) and the moisture content.

Initial pulping liquor **(I)**
A sample of six hundred grams of *Pinus radiata* chips, was partially pulped until an H factor of 6 (140°C) was reached. The white liquor contained 26.7 g/L (as Na_2O) effective alkali and 30 % sulphidity, with a liquor to wood ratio of 6:1. The liquor was drained from the digester, collected and stored under nitrogen at 4°C. The partially pulped chips were washed for 16 hours with flowing tap water. To remove the excess water, the partially pulped chips, were centrifuged. These centrifuged chips were oven-dried at 105C for 5 days, in order to determine the yield (76%) and moisture content.

6.4.5 Lignin isolation

For the kraft liquors described above, a 100 mL sample of pulping liquor was titrated, to pH 2 at a rate of 1 mL/min, using 1 M HCl. The sample was centrifuged (4500 rpm, 20 minutes) and the supernatant removed. Subsequently, the precipitate was re-suspended in 0.01 M HCl and recovered by centrifuge (4500 rpm, 20 minutes). The precipitate was re-dissolved in 1 M NaOH, with the acidification and centrifuging steps repeated. The precipitate was washed 5 times with 0.01 M HCl and twice with distilled water, centrifuging between each washing. Following freeze drying, the precipitate was extracted for 16 hours with pentane in a Soxhlet™ extractor and dried.

6.4.6 Holocellulose

Holocellulose was prepared according to the method described by Holmes *et al.* [343]. This involved treating *Pinus radiata* wood with chlorine gas, followed by extraction using methanolamine in dioxane. These chlorine/methanolamine treatments were performed 9 times, to yield the holocellulose product.

6.5 Fibre Preparations

6.5.1 Mechanical and chemimechanical pulps

The mechanical pulps were prepared by Dr Ian Suckling and Mrs Maria Pasco in the PAPRO (Pulp and Paper Research Organisation of New Zealand) Fibre Processing Plant. This was equipped with a Jyhla SD 52/36 pressurised refiner, operating at a pressure of 1 bar.

For the TMP (thermomechanical pulp), chips were atmospherically steamed at 86°C for at least 5 minutes. Subsequently, the chips were passed through an empty impregnator and into the preheater, where they were heated with steam at 125°C for 3 minutes, before two stages of pressurised refining.

The DWS (dilution water sulphonation) pulp was prepared in the same way, except that 5.0 g/L sulphite solution (pH 7.7) was added as the dilution water, during the primary refining and the preheater temperature was lowered to 90°C. The two refining stages in DWS pulping required a total mechanical input of approximately 2300 kWh/odt.

For the CTMP (chemithermomechanical pulp) preparation, the atmospherically steamed chips were passed through the impregnator filled with a 10 g/L sulphite solution (pH 7.2), to give a retention time of 5 minutes. Otherwise, the process was run as described for the TMP pulp.

In the OPCO (Ontario Paper Company) simulation, the chips were preheated at 90°C and 6.0 g/L sulphite solution (pH 7.5) was added during primary refining. The refiner was then used as a mixer, to add an additional 11.3 % sodium sulphite and 1.4 % sodium hydroxide to the fibre. After heating at 150°C for 40 minutes, the pulp was given a secondary refining treatment.

6.5.2 MDF

The MDF (medium density fibreboard) fibre was prepared in the same plant, operating at a pressure of 7.5 bar. After preheating at 86°C for 5 minutes, the chips were fed through an empty impregnator and into the preheater. Here, the chips were heated to 172°C for a residence time of 3.6 minutes, prior to single stage refining.

Table 6.1 summarises the total energy applied to the fibre, in the various preparations discussed in Sections 6.5.1 and 6.5.2 above, and the sulphur content of the resultant pulp.

Table 6.1: Summary of pulp fibre production.

	Total Refining Energy	Sulphur Content
	kWh/odt	(%)
MDF	433	
TMP	3036	0.005
CTMP	2392	0.15
DWS	2368	0.17
OPCO	1600	0.83

6.5.3 Fractionation of DWS

In dealing with the separation of pulp into fibres and fines, the term "fibres" shall be used to describe the "fines-free" pulp stream retained by the multi-stage screening system.

The fibres and fines fractions of a DWS pulp were sourced from Mr. John Richardson [344]. The DWS pulp was prepared by atmospherically steaming the chips at 80°C for 5 minutes. The chips were then steamed in the preheater for 3 minutes at 125°C, prior to refining at 1250 kWh/odt. For this pulp, 1.8 % sodium sulphite (pH 7.5) was added to the fibre in the primary stage, with the refiner dilution water. Screening after 1° refining was performed by two Ahlstrom Moduscreen, F1 series, pressure screens. Both screens were fitted with 0.15 mm AHLWIRE™ wedgewire baskets. The accepts from this screening were passed over a 100 μm DSM screen, at approximately 0.5 % consistency. This removed any remaining fibres and provided a sample that was more than 99 % -200 Bauer McNett fines.

"Fibre" from the AHLWIRE™ screening was refined (1000 kWh/odt) in a secondary stage and separated in to fibres and fines as described above.

6.6 *Compression Wood*

Compression wood samples were collected from growth rings 15-17 in a region of medium compression wood, using a disk of *Pinus radiata* wood. From this same region of compression wood, earlywood compresssion wood and latewood compression wood samples were isolated.

6.7 *Thioacidolysis*

6.7.1 Thioacidolysis of model compounds

Model compound (10-15 mg), dry dioxane (9 mL, freshly distilled from sodium/benzophenone), ethanethiol (1 mL) and boron-trifluoride diethyletherate (0.25 mL) were placed in teflon lined, stainless steel vessels, under a nitrogen atmosphere [214]. The lignin depolymerisation was then allowed to proceed at 110°C (oil bath), for 2 hours, with occasional shaking. After rapid cooling in ice water, internal standard (cholesterol, 10 mg) was added to the vessel, contents, where quantification was required. The contents of the reaction vessel together with some water used to rinse the teflon tube (10 mL), was poured over CH_2Cl_2 (20 mL). The pH of the aqueous upper phase was adjusted to 4-5 with $NaHCO_3$ (0.4M), and the whole mixture extracted with CH_2Cl_2 (3 x 20 mL). The combined organic extracts were dried over $MgSO_4$ and concentrated under reduced pressure, at 40°C.

Thioacidolysis products were purified using plc. Analytical results for NMR spectroscopy, mass spectrometry, melting point determinations and gravimetric yields are presented in Section 6.7.2. The exceptions to this presentation of results were thioacidolysis products **79** and **80**, which were analysed without plc, due to their rapid phenylcoumaran reformation. Also, thioacidolysis products **70**, **71** and **76**, did not exhibit a molecular ion during mass spectrometry, M^+-61 being the largest ion observed. The presented NMR spectroscopic and mass spectrometry data accurately fit the proposed structures of the thioacidolysis products.

For ^{31}P NMR spectroscopy, the crude thioacidolysis product was derivatised and analysed.

6.7.2 Thioacidolysis products

6.7.2.1 Product (58) (erythro and threo); thioacidolysis product of 3C guaiacyl β-aryl-ether model (83)

^{1}H NMR (400 MHz, $CDCl_3$) δ: 1.16-1.25 (18H, m, $-SCH_2CH_3$); 2.33-2.61 (12H, m, $-SCH_2CH_3$); 2.73 (1H, dd, J = 9 Hz, 6 Hz, $H\gamma_1$); 2.75 (1H, dd, J = 16 Hz, 9 Hz, $H\gamma_1$); 2.86 (1H, dd, J = 9 Hz, 3 Hz, $H\gamma_2$); 3.05 (2H, m, Hβ and $H\gamma_2$); 3.21 (1H, m, Hβ); 3.93 (3H, s, OCH_3); 3.96 (3H, s, OCH_3); 4.19 (1H, d, J = 4 Hz, Hα); 4.39 (1H, d, J = 4 Hz, Hα); 6.91-7.28 (6H, m, ArH).

^{13}C NMR (100 MHz, $CDCl_3$) δ: 14.46, 14.53, 14.67, 14.71, 14.88, 14.92 (6 x $SCH_2\underline{C}H_3$); 25.93, 26.02, 26.93, 26.96, 26.99, 27.05 (6 x $S\underline{C}H_2CH_3$); 37.04 (Cγ); 37.08 (Cγ); 52.23, 52.63, 53.42, 53.66 (Cα and Cβ); 56.13 (OCH_3); 56.21 (OCH_3); 111.64 (C2); 111.76 (C2); 113.75 (C5); 113.98 (C5); 121.94 (C6); 122.45 (C6); 131.27 (C1); 133.02 (C1); 145.16, 145.22, 146.48, 146.59 (C3 and C4).

M/S: m/z = 346 (2, M^+); 284 (2); 271 (4); 223 (5); 197 (100); 131 (13); 103 (9); 75 (20).

Yield = 90%

6.7.2.2 Product (60) (erythro and threo); thioacidolysis product of 3C p-hydroxyphenyl β-aryl-ether model compound (84)

^{1}H NMR (400 MHz, $CDCl_3$) δ: 1.18-1.28 (18H, m, $-SCH_2CH_3$); 2.34-2.66 (12H, m, $-SCH_2CH_3$); 2.69 (1H, dd, J = 9 Hz, 6 Hz, $H\gamma_1$); 2.74 (1H, dd, J = 16 Hz, 9 Hz, $H\gamma_1$); 2.90 (1H, dd, J = 9 Hz, 3 Hz, $H\gamma_2$); 3.11 (2H, m, Hβ and $H\gamma_2$); 3.24 (1H, m, Hβ); 4.26 (1H, d, J = 4 Hz, Hα); 4.39 (1H, d, J = 4 Hz, Hα); 6.83-7.03 (6H, m, ArH).

^{13}C NMR (100 MHz, $CDCl_3$) δ: 14.48, 14.55, 14.68, 14.75, 14.90, 14.93 (6 x $SCH_2\underline{C}H_3$); 25.91, 26.07, 26.89, 26.96, 26.99, 27.11 ($S\underline{C}H_2CH_3$); 37.07 (Cγ); 37.10 (Cγ); 52.17, 52.71, 53.40, 53.59 (Cα and Cβ); 115.31 (C3 and C5); 115.36 (C3 and C5); 129.22 (C2 and C6); 129.39 (C2 and C6); 135.15 (C1); 135.29 (C1); 153.78 (C4); 153.84 (C4).

M/S: m/z = 316 (3, M^+); 254 (1); 241 (5); 167 (100); 75 (38); 73 (26).

Yield = 97%

6.7.2.3 Product (64); thioacidolysis product of isoeugenol (63)

^{1}H NMR (200 MHz, $CDCl_3$) δ: 0.88 (3H, t, J = 7.3 Hz, Hγ); 1.18 (3H, t, J = 7.4 Hz, $SCH_2C\underline{H}_3$); 1.74-1.91 (2H, m, Hβ); 2.32 (2H, qd, J = 7.4 Hz, J_2 = 2.5 Hz, $SC\underline{H}_2CH_3$); 3.62 (1H, m, Hα); 3.89 (3H, s, OCH_3); 5.76 (1H, b, OH); 6.68-6.95 (3H, m, ArH).

^{13}C NMR (50 MHz, $CDCl_3$) δ: 12.38 (Cγ); 14.52 ($SCH_2\underline{C}H_3$); 24.90 (Cβ); 29.88 ($S\underline{C}H_2CH_3$); 51.18 (Cα); 55.92 (OCH_3); 109.66 (C2); 113.74 (C5); 121.04 (C6); 134.62 (C1); 144.50 (C4); 146.68 (C3).

M/S: m/z = 226 (14); 165 (8); 150 (3); 136 (100); 123 (16).

Yield = 90%

6.7.2.4 Product (67); thioacidolysis product of vanillyl alcohol (65)

^{1}H NMR (200 MHz, $CDCl_3$) δ: 1.24 (3H, t, J = 7.4 Hz, $SCH_2C\underline{H}_3$); 2.47 (2H, q, J = 7.4 Hz, $SC\underline{H}_2CH_3$); 3.69 (2H, s, Hα); 3.86 (3H, s, OCH_3); 5.32 (1H, b, OH); 6.71-6.83 (3H, m, ArH).

^{13}C NMR (50 MHz, $CDCl_3$) d: 14.68 ($SCH_2\underline{C}H_3$); 25.22 ($S\underline{C}H_2CH_3$); 35.86 (Cα); 56.04 (OCH_3); 111.84 (C2); 113.80 (C5); 121.78 (C6); 134.28 (C1); 144.60 (C4); 146.58 (C3).

M/S: m/z = 198 (12, M^+); 137 (100); 123 (11); 77 (2).

Yield = 89%

6.7.2.5 Product (68); thioacidolysis product of apocynol (66)

^{1}H NMR (200 MHz, $CDCl_3$) δ: 1.21 (6H, t, J = 7.4 Hz, $SCH_2C\underline{H}_3$); 1.52 (3H, d, J= 7.3 Hz, Hβ); 2.31 (2H, q, J = 7.4 Hz, $SC\underline{H}_2CH_3$); 3.92 (3H, s, OCH_3); 3.96 (2H, q, J = 7.3 Hz, Hα); 6.78-6.89 (3H, m, ArH).

^{13}C NMR (50 MHz, $CDCl_3$) δ: 15.32 ($SCH_2\underline{C}H_3$); 22.65 (Cβ); 24.94 ($S\underline{C}H_2CH_3$); 43.60 (Cα); 55.96 (OCH_3); 109.62 (C2); 113.62 (C5); 120.44 (C6); 134.48 (C1); 144.82 (C4); 146.78 (C3).

M/S: m/z = 212 (9, M^+); 151 (17); 136 (100); 123 (5).

Yield = 92%

6.7.2.6 Product (70); thioacidolysis product of vanillin (36)

^{1}H NMR (200 MHz, $CDCl_3$) δ: 1.22 (6H, t, J = 7.4 Hz, 2x $SCH_2C\underline{H}_3$); 2.45-2.61 (4H, m, 2x $SC\underline{H}_2CH_3$); 3.85 (3H, s, OCH_3); 4.71 (1H, s, Hα); 5.72 (1H, b, OH); 6.65-6.93 (2H, m, H6 and H5); 7.05 (1H, d, J = 2.5 Hz, H2).

^{13}C NMR (50 MHz, $CDCl_3$) δ: 14.38 ($SCH_2\underline{C}H_3$); 25.94 ($S\underline{C}H_2CH_3$); 52.04 (Cα); 55.98 (OCH_3); 110.20 (C2); 113.62 (C5); 119.74 (C6); 133.74 (C1); 145.30 (C4); 146.70 (C3).

M/S: m/z = 258 (7, M^+); 197 (16); 136 (100); 123 (8).

Yield = 93%

6.7.2.7 Product (71); thioacidolysis product of acetovanillone (72)

^{1}H NMR (200 MHz, $CDCl_3$) δ: 1.20 (6H, t, J = 7.4 Hz, 2x $SCH_2C\underline{H}_3$); 2.11 (3H, s, Hβ); 2.47 (4H, q, J = 7.4 Hz, 2x $SC\underline{H}_2CH_3$); 3.90 (3H, s, OCH_3); 5.21 (1H, b, OH); 6.83 (1H, d, J = 8.7 Hz, H5); 7.16 (1H, dd, J = 8.7 Hz, 2.5 Hz, H6); 7.32 (1H, d, J = 2.5 Hz, H2).

^{13}C NMR (50 MHz, $CDCl_3$) δ: 14.12 ($SCH_2\underline{C}H_3$); 26.00 ($S\underline{C}H_2CH_3$); 30.42 (Cβ); 55.96 (OCH_3); 60.02 (Cα); 110.46 (C2); 113.68 (C5); 119.80 (C6); 135.94 (C1); 144.60 (C4), 146.76 (C3).

M/S: m/z = 211 (15, M^+-61); 150 (100); 123 (18).

Yield = 63%

6.7.2.8 Product (74); thioacidolysis product of dehydrodivanillyl alcohol (72)

^{1}H NMR (200 MHz, $CDCl_3$) δ: 1.21 (6H, t, J = 7.4 Hz, $SCH_2C\underline{H}_3$); 2.50 (4H, q, J = 7.4 Hz, $SC\underline{H}_2CH_3$); 3.69 (4H, s, Hα); 3.91 (6H, s, OCH_3); 5.73 (2H, b, OH); 6.83 (2H, d, J = 2.4 Hz, H6); 6.95 (2H, d, J = 2.4 Hz, H2).

^{13}C NMR (50 MHz, $CDCl_3$) δ: 14.38 ($SCH_2\underline{C}H_3$); 25.16 ($S\underline{C}H_2CH_3$); 34.82 (Cα); 56.08 (OCH_3); 110.76 (C2); 122.92 (C6); 128.60 (C5); 131.24 (C1); 142 04 (C4); 147.30 (C3).

M/S: m/z = 394 (3, M^+); 333 (24); 272 (11); 347 (2); 135 (100).

Yield = 93%

6.7.2.9 Product (75); thioacidolysis product of dehydrodiapocynol (73)

^{1}H NMR (200 MHz, $CDCl_3$) δ: 1.19 (6H, t, J = 7.4 Hz, $SCH_2\underline{C}H_3$); 1.49 (6H, d, J = 7.3 Hz, Hβ); 2.34 (4H, q, J = 7.4 Hz, $SC\underline{H}_2CH_3$); 3.86 (6H, s, OCH_3); 4.01 (4H, q, J = 7.3 Hz, Hα); 6.78 (2H, d, J = 2.4 Hz, H6); 6.90 (2H, d, J = 2.4 Hz, H2).

^{13}C NMR (50 MHz, $CDCl_3$) δ: 14.28 ($SCH_2\underline{C}H_3$); 22.40 (Cβ); 25.26 ($S\underline{C}H_2CH_3$); 44.12 (Cα); 55.90 (OCH_3); 111.32 (C2); 120.54 (C6); 128.70 (C5); 140.92 (C1); 149.62 (C4); 150.78 (C3).

M/S: m/z = 422 (10, M^+); 361 (5); 300 (16); 211 (7); 135 (100).

Yield = 95%

6.7.2.10 Product (76); thioacidolysis product of dehydrodivanillin (54)

^{1}H NMR (200 MHz, $CDCl_3$) δ: 1.25(12H, t, J = 7.4 Hz, 2x $SCH_2\underline{C}H_3$); 2.56-2.74 (8H, m, 2x $SC\underline{H}_2CH_3$); 3.89 (6H, OCH_3); 4.82 (2H, s, Hα); 5.78 (2H, b, OH): 6.93 (2H, d, J = 2.5 Hz, H6); 7.09 (2H, d, J = 2.5 Hz, H2).

^{13}C NMR (50 MHz, $CDCl_3$) δ: 14.38 ($SCH_2\underline{C}H_3$); 25.80 ($S\underline{C}H_2CH_3$); 52.48 (Cα); 55.92 (OCH_3); 109.26 (C2); 122.30 (C6); 124.16 (C5); 132.61 (C1); 142.36 (C4); 147.52 (C3).

M/S: m/z = 453 (2, M^+-61); 392 (19); 331 (5); 270 (8); 257 (3); 135 (100).

Yield = 90%

6.7.2.11 Product (79); thioacidolysis product of dehydrodihydrodiisoeugenol (78)

Enantiomeric Pair 1

^{1}H NMR (400 MHz, $CDCl_3$) δ: 0.85 (3H, t, J = 7.6 Hz, Hγ′); 1.11 (3H, d, J = 6.9 Hz, Hγ); 1.14 (3H, t, J = 7.4 Hz, -$SCH_2\underline{C}H_3$); 1.54 (2H, m, Hβ′); 2.27 (2H, m, -$SC\underline{H}_2CH_3$); 2.43 (2H, t, J = 7.4 Hz, Hα′); 3.52 (1H, m, Hβ); 3.76 (OCH_3′); 3.88 (OCH_3) 4.20 (1H, d, J = 9.2 Hz, Hα); 5.4-5.8 (2H, 2xb, 2x OH) 6.42 (1H, s, H2); 6.52 (1H, s, H6);

^{13}C NMR (100 MHz, $CDCl_3$) δ: 13.99 (Cγ′); 14.88 (-$SCH_2\underline{C}H_3$); 18.84 (Cγ); 25.28 (-$S\underline{C}H_2CH_3$); 25.65 (Cβ′); 38.40 (Cα′); 39.51 (Cβ); 55.69 (Cα); 56.23 (OCH_3); 56.37 (OCH_3′); 108.96 (C2′); 111.02 (C2); 113.93 (C5); 120.37 (C6′); 121.91 (C6); 130.25 (C5′) 133.56 (C1′); 134.87 (C1); 141.10 (C4′); 144.34 (C4); 146.14 (C3); 146.36 (C3′)

Enantiomeric Pair 2

^{1}H NMR (400 MHz, $CDCl_3$) δ: 0.94 (3H, t, J = 7.6 Hz, Hγ'); 1.08 (3H, t, J = 7.4 Hz, -$SCH_2\underline{C}H_3$); 1.47 (3H, d, J = 7.0 Hz, Hγ); 1.61 (2H, m, Hβ'); 2.20 (2H, m, -$SC\underline{H}_2CH_3$); 2.51 (2H, t, J = 7.6 Hz, Hα'); 3.56 (1H, m, Hβ); 3.76 (OCH_3'); 3.90(OCH_3); 4.18 (1H, d, J = 9.2 Hz, Hα); 5.4-5.8 (2H, 2xb, 2x OH) 6.46 (1H, s, H2); 6.60 (1H, s, H6);

^{13}C NMR (100 MHz, $CDCl_3$) δ: 14.22 (Cγ'); 14.80 (-$SCH_2\underline{C}H_3$); 19.19 (Cγ); 25.19 (-$S\underline{C}H_2CH_3$); 25.68 (Cβ'); 38.49 (Cα'); 39.62 (Cβ); 54.78 (Cα); 56.27 (OCH_3); 56.37 (OCH_3'); 109.24 (C2'); 111.02 (C2); 113.57 (C5); 120.63 (C6'); 122.47 (C6); 130.49 (C5') 133.88 (C1'); 134.91 (C1); 141.61 (C4'); 144.25 (C4); 146.25 (C3); 146.47 (C3')

M/S: m/z = 390 (2, M^+); 328 (3); 299 (1); 197 (100).

6.7.2.12 Product (80); thioacidolysis product of dehydrodiisoeugenol (77)

^{1}H NMR (400 MHz, $CDCl_3$) δ: 0.76, 0.77, 0.88,0.90 (3H total, overlapping triplets, J_1 = 7.4 Hz, Hγ'); 1.05-1.50 (9H, overlapping multiplets, 2x $SCH_2\underline{C}H_3$ and Hγ); 1.66-1.85 (2H, m, Hβ'); 2.04-2.26 (4H, overlapping multiplets 2x $SC\underline{H}_2CH_3$); 3.49-3.64 (2H, overlapping multiplets, Hβ and Hα'); 3.76, 3.80, 3.86 (6H total, s, s, s, 2x OCH_3); 4.14-4.20 (1H, m, Hα); 5.55, 5.68, 5.70, 5.84 (2H total, b, b, s, s, 2x OH) 6.39-6.95 (5H, m, ArH)

^{13}C NMR (100 MHz, $CDCl_3$) δ: 12.46, 12.50, 12.70, 12.75 (Cγ'); 14.28-14.31, 14.61-14.63 ($SCH_2\underline{C}H_3$); 18.19, 18.32, 19.18, 19.38 (Cγ); 24.73, 25.08-25.10, 25.32, 25.36, 25.61 ($S\underline{C}H_2CH_3$); 30.14, 30.16, 30.18 (Cβ'); 39.38, 39.66, 39.87, 40.40 (Cβ), 51.42, 51.71, 51.75 (Cα'); 54.53, 54.71, 55.07, 55.37 (Cα); 55.5-55.8 (OCH_3); 55.95-55.99 (OCH_3'); 107.39, 107.65, 107.72 (C2'); 110.34, 110.62, 110.80 (C2); 113.63, 113.69, 114.10 (C5); 120.27, 120.80, 120.92, 121.09 (C6'); 121.13, 121.78, 122.31 (C6); 129.57, 129.65, 130.21, 130.44 (C5'); 133.19, 133.46, 133.50, 133.76 (C1'); 133.42, 133.73, 134.67, 134.96 (C1); 141.78, 141.92, 142.40 (C4'); 144.16, 144.78 (C4); 146.41-146.82 (C3 and C3').

M/S: m/z = 450 (2, M^+); 388 (1); 327 (8); 197 (100); 150 (5); 137 (6).

Table 6.2: Signal assignment for the diastereoisomeric pairs in (80)*.

	Isomer 1		Isomer 2		Isomer 3		Isomer 4	
Position	^{1}H	^{13}C	^{1}H	^{13}C	^{1}H	^{13}C	^{1}H	^{13}C
γ′	0.76	12.46	0.77	12.50	0.88	12.70	0.90	12.75
β′	1.66	30.14	1.8	30.16	1.75	30.16	1.85	30.18
α′	3.50	51.42	3.53	51.42	3.60	51.71	3.64	51.75
$S\underline{CH_2}CH_3'$	*2.04-2.09*	*25.08-25.10*	*2.04-2.09*	*24.73*	*2.04-2.09*	*25.08-25.10*	*2.04-2.09*	*25.08-25.10*
$SCH_2\underline{CH_3}'$	*1.05-1.09*	*14.28-14.31*	*1.05-1.09*	*14.28-14.31*	*1.05-1.09*	*14.28-14.31*	*1.05-1.09*	*14.28-14.31*
1′		133.50		133.19		133.76		133.46
2′	*6.39*	107.65	*6.39*	*107.39*	*6.39*	*107.39*	6.56	107.72
3′		*146.6*		*146.6*		*146.6*		*146.6*
4′		141.92		*142.4*		*142.4*		141.78
5′		130.21		129.57		129.65		130.44
6′	6.56	121.09	6.48	120.92	6.54	120.8	6.61	120.27
OH′	*5.7*		*5.84*		*5.84*		*5.7*	
OCH_3'	*3.8*	*55.95-55.99*	*3.8*	*55.95-55.99*	*3.8*	*55.95-55.99*	*3.8*	*55.95-55.99*
γ	1.13	18.19	1.50	19.18	1.48	19.38	1.11	18.32
β	3.56	39.38	3.49	40.40	3.55	39.87	3.53	39.66
α	4.18	54.53	4.20	55.37	4.14	55.07	4.16	54.71
$S\underline{CH_2}CH_3$	*2.18*	*25.32*	*2.18*	*25.61*	*2.26*	*25.36*	*2.18*	*25.61*
$SCH_2\underline{CH_3}$	*1.11-1.15*	*14.61-14.63*	*1.11-1.15*	*14.61-14.63*	*1.11-1.15*	*14.61-14.63*	*1.11-1.15*	*14.61-14.63*
1		133.42		134.67		134.96		133.73
2	*6.88*	110.8	*6.88*	110.62	*6.88*	110.34	*6.88*	110.8
3		*146.8*		*146.8*		*146.4*		*146.8*
4		144.78		144.16		144.16		144.78
5	6.95	114.1	6.87	113.63	6.87	113.69	6.90	114.1
6	6.74	121.13	*6.59*	*121.78*	*6.59*	*121.78*	6.74	122.31
OH	*5.55 or 5.68*		*5.55 or 5.68*		*5.55 or 5.68*		*5.55 or 5.68*	
OCH_3	*3.76*	*55.5-55.8*	*3.86*	*55.5-55.8*	*3.76*	*55.5-55.8*	*3.76*	*55.5-55.8*

* italics used where assignment ambiguities arose.

6.7.2.13 Product (81); acid catalysed phenylcoumaran reformation of thioacidolysis product (80)

^{1}H NMR (400 MHz, $CDCl_3$) δ: 0.87 (3H, t, J = 7.4, Hγ'); 1.16 (3H, t, J = 7.4 Hz, $SCH_2C\underline{H}_3$); 1.38 (3H, d, J = 6.8, Hγ); 1.85 (2H, m, Hβ'); 2.33 (2H, q, J = 7.4 Hz, $SC\underline{H}_2CH_3$) 3.45 (1H, dq, J = 9.8, 6.8, Hβ); 3.65 (1H, m, Hα'); 3.90 (6H, s, OCH_3); 5.08 (1H, d, J = 9.8, Hα); 5.64 (1H, b, ArOH); 6.55-7.01 (6H, m, ArH).

^{13}C NMR (100 MHz, $CDCl_3$) δ: 12.41 (Cγ'); 17.89 (Cγ); 14.42 ($SCH_2\underline{C}H_3$) 24.81 (Cβ'); 29.76 ($S\underline{C}H_2CH_3$); 45.68 (Cβ); 51.85 (Cα'); 55.93 (-OCH_3); 93.73 (Cα); 109.27 (A2); 110.04 (B2); 113.60 (B6); 114.21 (A5); 119.84 (A6); 132.06 (A1); 132.10 (B1); 134.11 (B5); 144.16 (B3); 145.89 (A4); 146.58 (B4); 146.72 (A3).

M/S: m/z = 388 (3, M^+); 327 (100); 312 (30); 298 (13).

6.7.2.14 Product (85); thioacidolysis product of 2C guaiacyl β-aryl-ether model (82)

^{1}H NMR (400 MHz, $CDCl_3$) δ: 1.18 (3H, t, J = 7.4 Hz, $SCH_2C\underline{H}_3$); 1.20 (3H, t, J = 7.4 Hz, $SCH_2C\underline{H}_3$); 2.38 (2H, q, J = 7.4 Hz, $SC\underline{H}_2CH_3$); 2.45 (2H, q, J = 7.4 Hz $SC\underline{H}_2CH_3$); 2.98 (1H, d, J = 3.7 Hz, $H\beta_1$); 3.00 (1H, s, $H\beta_2$); 3.91 (3H, s, OCH_3); 3.98 (1H, m, Hα); 5.65 (1H, b, OH); 6.70-6.88 (3H, m, ArH).

^{13}C NMR (100 MHz, $CDCl_3$) δ: 14.32 (β-$SCH_2\underline{C}H_3$); 14.45 (α-$SCH_2\underline{C}H_3$); 25.58 (β-$S\underline{C}H_2CH_3$); 26.92 (α-$S\underline{C}H_2CH_3$); 37.96 (Cβ); 49.85 (Cα); 56.13 (OCH_3); 110.08 (C2); 114.17 (C5); 120.86 (C6); 133.22 (C1); 144.89 (C4); 146.27 (C3).

M/S: m/z = 272 (9, M^+); 211 (12); 150 (3); 136 (100); 123 (50).

Yield = 93%

6.7.2.15 Product (87); thioacidolysis product of 4-(2-hydroxyethoxy)-apocynol (86)

^{1}H NMR (200 MHz, $CDCl_3$) δ: 1.14 (3H, t, J = 7.5 Hz, $SCH_2C\underline{H}_3$); 1.51 (3H, d, J = 7.0 Hz, Hβ); 2.30 (2H, q, J = 7.5 Hz, $SC\underline{H}_2CH_3$); 3.85 (3H, s, OCH_3); 3.90 (3H, m, $OCH_2C\underline{H}_2OH$ and Hα with signal overlap); 4.08 (2H, t, J = 4.9 Hz, $OC\underline{H}_2CH_2OH$); 6.70-6.90 (3H, m, ArH).

^{13}C NMR (50 MHz, $CDCl_3$) δ: 14.48 ($SCH_2\underline{C}H_3$); 22.74 (Cβ); 25.22 ($S\underline{C}H_2CH_3$); 43.54 (Cα); 55.84 (OCH_3); 61.24 ($OCH_2\underline{C}H_2OH$); 71.42($O\underline{C}H_2CH_2OH$); 110.50 (C2); 113.46 (C5); 119.64 (C6); 137.96 (C1); 146.90 (C4); 149.78 (C3).

M/S: m/z = 256 (12, M^+); 195 (83); 151 (100); 119 (21); 91 (23).

Yield = 93%

6.7.2.16 Product (98); thioacidolysis product of dibenzodioxocin (97)

^{1}H NMR (400 MHz, $CDCl_3$) δ: 0.72 (3H, t, J = 7.4 Hz, Hγ"); 0.91 (3H, t, J = 7.4 Hz, Hγ'); 1.38 (2H, m, Hβ"); 1.52 (2H, m, Hβ'); 3.36 (2H, t, J = 7.4 Hz, Hα"); 2.50 (1H, m, $Hα_1$'); 2.72 (1H, m, $Hα_2$'); 3.61 (3H, s, OCH_3); 3.75 (overlapping with OCH_3 signal in 1D, $Hγ_1$); 3.78 (3H, s, OCH_3"); 3.90 (overlapping with OCH_3 signal in 1D, $Hγ_2$); 3.93 (3H, s,OCH_3'); 4.36 (1H, br s, Hα); 5.17 (1H, dd, J = 4.9 Hz, 7.3 Hz, Hβ); 5.23 (1H, b, OH); 5.66 (1H, b, OH'); 6.26 (1H, d, overlapping with H2, H6); 6.31 (1H, s, overlapping with H6, H2); 6.43 (1H, s, H2"); 6.48 (1H, d, J = 8.9 Hz, H5); 6.66 (1H, s, H6"); 6.76 (1H, s, H6').

^{13}C NMR (100 MHz, $CDCl_3$) δ: 13.3 (Cγ"); 14.2 (Cγ'); 24.5 (Cβ"); 24.6 (Cβ'); 36.4 (Cα'); 37.9 (Cα"); 43.6 (Cα); 55.6 (OCH_3); 55.9 (OCH_3'); 56.0 (OCH_3"); 65.3 (Cγ); 88.0 (Cβ); 109.2 (C2); 111.3 (C2'); 111.7 (C2"); 113.4 (C5); 119.4 (C6); 122.9 (C6"); 124.2 (C5'); 129.6 (C6') 131.6 (C5"); 133.0 (C1'); 134.1 (C1); 138.5 (C1"); 141.2 (C4'); 141.7 (C4"); 142.7 (C4); 145.4 (C3); 145.8 (C3'); 151.5 (C3").

M/S: m/z = 508 (11, M^+); 477 (1); 447 (1); 405 (3); 342 (25); 341 (100); 325 (2); 297 (2).

Yield = 70%

6.7.2.17 Product (99); acetylated dibenzooxepine (98)

^{1}H NMR (400 MHz, $CDCl_3$) δ: 0.76 (3H, t, J = 7.4 Hz, Hγ"); 0.98 (3H, t, J = 7.4 Hz, Hγ'); 1.39 (2H, m, Hβ"); 1.60 (2H, m, Hβ'); 2.11, 2.15, 2.21 (3 x 3H, s, $COCH_3$); 2.34 (2H, t, J = 7.4 Hz, Hα"); 2.52 (1H, m, Hα'); 2.73 (1H, m, Hα'); 3.61 (3H, s, OCH_3); 3.80 (3H, s, OCH_3"); 3.91 (3H, s, OCH_3) 4.07 (1H, dd, J =11.0 Hz, 7.5 Hz, Hγ); 4.48 (1H, dd, J = 5.4 Hz, 11.0 Hz, Hγ); 4.65 (1H, br s, Hα); 5.44 (1H, dd, J = 5.4 Hz, 7.5 Hz, Hβ); 6.26-6.79 (6H, m, ArH).

^{13}C NMR (100 MHz, $CDCl_3$) δ: 13.5 (Cγ"); 14.4 (Cγ'); 20.8, 21.1 ($CO\underline{C}H_3$); 24.5 (Cβ"); 24.6 (Cβ'); 36.3 (Cα'); 37.9 (Cα"); 43.7 (Cα); 55.7 (OCH_3); 55.9 (OCH_3); 56.1 (OCH_3); 64.9 (Cγ); 84.4 (Cβ); 110.2, 112.1, 112.4, 118.4, 121.6, 121.9, 128.2, 131.6, 133.0, 135.8, 137.2, 138.4, 140.2, 140.5, 141.7, 148.4, 149.8, 151.5 (C arom.).

M/S: m/z = 634 (80, M^+); 574 (24); 532 (45); 490 (49); 329 (100); 285 (21); 269 (12).

MP: 148-149°C (lit [261] = 149°C).

6.7.3 Thioacidolysis of MWL

The general procedure was identical, to that described for the model compounds above. However, 25-35 mg of milled wood lignin was used and the thioacidolysis reagent was scaled up to dioxane (18 mL), ethanethiol (2 mL) and BF_3 (0.5 mL).

6.7.4 Thioacidolysis of wood and pulp samples

Again, the general procedure was followed, as described for the model compounds. For these samples, 100 mg of lignocellulosic material was used and the thioacidolysis reagent was scaled up to dioxane (27 mL), ethanethiol (3 mL) and BF_3 (0.75 mL).

6.8 Phosphorus Derivatisation

6.8.1 Preparation of 2-chloro-4,4,5,5-tetramethyl-1,3,2-dioxaphospholane

Initially the 2-chloro-4,4,5,5-tetramethyl-1,3,2-dioxaphospholane **41** was prepared according to the method described by Zwierzak [345]. During the later work, the tetramethyl dioxaphospholane **41** was available through and obtained from Aldrich.

Pinacol (Aldrich) was dried by azeotropic distillation with benzene (under N_2), using a Dean-Stark apparatus. After cessation of water removal, residual benzene was removed under reduced pressure.

The benzene and triethylamine were dried by refluxing for 12 hours in the presence of calcium hydride, followed by distillation.

Glassware was over dried (105°C) for 18 hours and flushed with nitrogen before use. In order to ensure moisture exclusion, all reactions were performed under nitrogen and solutions were transferred between vessels using syringes.

To a cold (5°C), stirred solution of phosphorus trichloride (3 mL, 34 mmol) in benzene (80 mL), was added drop-wise, a solution of pinacol (4 g, 34 mmol) and triethylamine (9.5 mL, 68 mmol) in benzene (60 mL) over 30 minutes. The reaction mixture was stirred at room temperature for 1 hour.

The reaction mixture was filtered, the residue thoroughly washed with benzene and the combined filtrates concentrated under reduced pressure. The product (Figure 6.2) was then distilled using vacuum distillation at a head temperature of 83-84°C to yield the product.

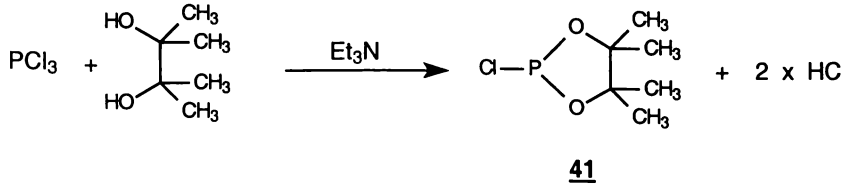

41

Figure 6.2: Preparation of 2-chloro-4,4,5,5-tetramethyl-1,3,2-dioxaphospholane.

Yield: 2.74 g (44.5 %)

^{31}P NMR ($CDCl_3$, 81 MHz) δ: 176.0 ppm (lit: 175.9 ppm)

^{13}C NMR ($CDCl_3$, 50 MHz) δ: 24.47 (CH_3); 25.44 (CH_3); 88.58 (quaternary C).

^{1}H NMR ($CDCl_3$, 200 MHz) δ: 1.33 (CH_3); 1.53 (CH_3).

6.8.2 Preparation of solvent mixture

Pyridine, reagent grade, was further dried by heating it under reflux for 18 hours with potassium hydroxide. It was then distilled at atmospheric pressure and stored over molecular sieves (3A) and under nitrogen.

A solvent mixture, containing dry pyridine and deuterated chloroform (Aldrich) in a 1.6/1 v/v ratio, was prepared [189]. The solution was protected from moisture with molecular sieves (3A) and kept in a sealed container under nitrogen. Solutions of chromium (III) acetylacetonate (5.0 mg/mL) and cholesterol (11.0 mg/mL) were then prepared utilising the solvent described above. These served as the relaxation agent and internal standard, respectively.

6.8.3 Lignin phosphitylation

Lignin or lignin thioacidolysis product (30 mg), previously dried overnight, was accurately weighed into a 1 mL volumetric flask. The sample was then dissolved in the pyridine/deuterochloroform solvent mixture (0.5 mL). The internal standard (100 μL) and the relaxation reagent (100 μL) were then added, followed by 2-chloro-4,4,5,5-tetramethyl-1,3,2-dioxaphospholane **41** (100 μL) [189]. Finally, the solution

was made up to the 1 mL mark with more solvent mixture. The volumetric flask was tightly closed and shaken to ensure thorough mixing and left for 30 minutes, before starting the ^{31}P NMR spectroscopy.

6.9 Acetylation of Lignin

The lignin, or model compound was dissolved in an excess of 1:1 pyridine:acetic anhydride and stirred for 48 hours in a stoppered vessel [346]. The product was taken up in toluene (80 mL) and almost evaporated to dryness under reduced pressure (3x). The product was then suspended in 1:1 EtOH:water (80 mL) and evaporated to dryness under reduced pressure (3x).

6.10 Molecular Modelling

The molecular modelling performed in this thesis used, a Silicon Graphics O_2 workstation, operating a SPARTAN Version 5 programme from Wavefunction.

Conformational analysis, of the 7-membered oxepine ring in **98**, was performed using the Osawa method [347] for flexible rings. Stable confomers were determined by the Mechanics model [348], using a 6-fold axis of rotation and Merck Molecular Force Field (MMFF) [349] parameters.

Through space ^{31}P-^{31}P distances were determined, by first performing a conformational analysis. Stable confomers were determined using the Monte Carlo method [347], using a 3-fold axis of rotation and MMFF parameters. These stable confomers were further analysed, using the semi-empirical [257] AM1 model [255], where total charge was set to 0 and singlet multiplicity used.

It is far better to grasp the Universe as it really is,
than to persist in delusion,
however satisfying and reassuring.

Carl Sagan

References

1 Sjöström E., "Wood Chemistry; Fundamentals and Applications", Academic Press, New York, (1981), p1-20.

2 Parham R.A. and Grey R.L., Formation and Structure of Wood *in* "The Chemistry of Solid Wood", (Rowell R.M. ed.), American Chemical Society, Washington DC, (1984), p3-56.

3 Harada H. and Côté W.A., Structure of Wood *in* "Biosynthesis and Biodegradation of Wood Components", (Higuchi T. ed.), Academic Press, New York, (1985), p1-41.

4 Gray R.L. and Parham R.A., *Chemtech*, (April), (1982), p232.

5 Kininmonth J.A. and Whitehouse L.J., "Properties and Uses of New Zealand Radiata Pine", Ministry of Forestry, Rotorua, (1991), p2,1-2,16.

6 Fengel D. and Wegener G., "Wood; Chemistry, Ultrastructure, Reactions", Walter de Gruyter, Berlin, (1989), p6-23.

7 Kininmonth J.A. and Whitehouse L.J., "Properties and Uses of New Zealand Radiata Pine", Ministry of Forestry, Rotorua, (1991), p3,1-3,18.

8 Côté W.A., *Journal of Coatings Technology*, **55**(699), (1983), p25.

9 Timell T.E., *Wood Science and Technology*, **16**, (1982), p83.

10 Timell T.E., "Compression Wood in Gymnosperms", Volume 1, Springer-Verlag, Berlin, 1986, p1-21.

11 Timell T.E., "Compression Wood in Gymnosperms", Volume 1, Springer-Verlag, Berlin, (1986), p82-267.

12 Bisset I.J.W. and Dadswell H.E., *Australian Forestry*, **14**, (1950), p17.

13 Wardrop A.B. and Dadswell H.E., *Australian Journal of Scientific Research*, **B-3**, (1950), p1.

14 Wardrop A.B., *Australian Journal of Scientific Research*, **B-4**, (1951), p391.

15 Timell T.E., 1st International Symposium on Wood and Pulping Chemistry, (1981), **1**, p99.

16 Banks W.B. and Gibson E.J., *Chemistry in Britain*, June, (1988), p569.

17 Côté W.A., Simson B.W. and Timell T.E., *Svensk Papperstidning*, **69**, (1966), p547.

18 Timell T.E., *Wood Science and Technology*, **12**, (1978), p1.

19 Fengel D. and Wegener G., "Wood; Chemistry, Ultrastructure, Reactions", Walter de Gruyter, Berlin, (1989), p26-59.

20 Kininmonth J.A. and Whitehouse L.J., "Properties and Uses of New Zealand Radiata Pine", Ministry of Forestry, Rotorua, (1991), p4,1-4,45.

21 Sjöström E., "Wood Chemistry; Fundamentals and Applications", Academic Press, New York, (1981), p49-67.

22 Fengel D. and Wegener G., "Wood; Chemistry, Ultrastructure, Reactions", Walter de Gruyter, Berlin, (1989), p66-100.

23 Goring D.A.I. and Timell T.E., *Tappi*, **45**, (1962), p454.

24 Patscheke G. and Poller S., *Cellulose Chemistry and Technology*, **14**, (1980), p3.

25 Sjöström E., "Wood Chemistry; Fundamentals and Applications", Academic Press, New York, (1981), p21-48.

26 Fengel D. and Wegener G., "Wood; Chemistry, Ultrastructure, Reactions", Walter de Gruyter, Berlin, (1989), p268-295.

27 Pfister K. and Sjöström E, *Paperi ja Puu*, **59**, (1977), p711.

28 Teder A. and Tormund D., *Tappi*, **61**, (1978), p59.

29 Fengel D. and Wegener G., "Wood; Chemistry, Ultrastructure, Reactions", Walter de Gruyter, Berlin, (1989), p106-131.

30 Brasch D.D. and Wise L.E., *Tappi*, **39**(11), (1956), p768.

31 Harwood V.D., *Svensk Papperstidning*, **76**(10), (1973), p377.

32 Brasch D.J. and Wise L.E., *Tappi*, **39**(8), (1956), p581.

33 Timell T.E., *Wood Science and Technology*, **1**, (1967), p45.

34 Harwood V.D., *Svensk Papperstidning*, **75**, (1972), p207.

35 Timell T.E., *Advances in Carbohydrate Research*, **19**, (1964), p247.

36 Timell T.E., *Svensk Papperstidning*, **63**, (1960), p472.

37 Fengel D. and Wegener G., "Wood; Chemistry, Ultrastructure, Reactions", Walter de Gruyter, Berlin, (1989), p182-226.

38 Sjöström E., "Wood Chemistry; Fundamentals and Applications", Academic Press, New York, (1981), p83-97.

39 Lloyd J.A., *New Zealand Journal of Forestry Science*, **8**(2), (1978), p288-294.

40 Hemingway R.W. and Hillis W.E., *Appita*, **24**, (1971), p439-443.

41 Hillis W.E., *Appita*, **44**(4), (1991), p239-244.

42 Pettersen R.C., The chemical composition of wood *in* "The Chemistry of Solid Wood", (Rowell R.M. ed.), American Chemical Society, Washington DC, (1984), p57-126.

43 Mutton D.B., Wood Resins *in* "Wood Extractives and their Significance to the Pulp and Paper Industries", (Hillis W.E. ed.), Academic Press, London, (1962), p331-363.

44 Assarsson A. and Åkerlund G., *Svensk Papperstidning*, **69**, (1966), p517.

45 Dahm H.P., *Svensk Papperstidning*, **73**, (1970), p613.

46 Swan B., *Svensk Papperstidning*, **71**, (1968), p436.

47 Uprichard J.M., *Holzforschung*, **25**(4), (1971), p97.

48 Hemingway R.W., Hillis W.E. and Lau L.S., *Svensk Papperstidning*, **76**, (1973), p371.

49 Lindstedt G. and Misiorny A., *Acta Chemica Scandinavica*, **5**, (1951), p121.

50 Wallis A.F.A., "A review of the organic extractives in eucalypt woods for pulp production", National Pulp Mills Technical report 15, (1995).

51 Freudenberg K. and Neish A.C., "Constitution and Biosynthesis of Lignin", Springer-Verlag, Berlin, (1968).

52 Sarkanen K.V. and Ludwig C.H., Definition and nomenclature *in* "Lignins, Occurrence, Formation, Structure and Reactions", (Sarkanen K.V. and Ludwig C.H. eds.), Wiley-Interscience, New York, (1971), p1-17.

53 Sjöström E., "Wood Chemistry; Fundamentals and Applications", Academic Press, New York, (1981), p68-82.

54 Fengel D. and Wegener G., "Wood; Chemistry, Ultrastructure, Reactions", Walter de Gruyter, Berlin, (1989), p132-181.

55 Wardrop A.B., Occurrence and formation in plants *in* "Lignins, Occurrence, Formation, Structure and Reactions", (Sarkanen K.V. and Ludwig C.H. eds.), Wiley-Interscience, New York, (1971), p19-41.

56 Fergus B.J., Procter A.R., Scott J.A.N. and Goring D.A.I., *Wood Science and Technology*, **3**, (1969), p117.

57 Björkman A., *Svensk Papperstidning*, **59**, (1956), p477.

58 Lai Y.Z. and Sarkanen K.V., Isolation and structural studies *in* "Lignins, Occurrence, Formation, Structure and Reactions", (Sarkanen K.V. and Ludwig C.H. eds.), Wiley-Interscience, New York, (1971), p165-240.

59 Goring D.A.I., Polymer properties of lignin and lignin derivatives *in* "Lignins, Occurrence, Formation, Structure and Reactions", (Sarkanen K.V. and Ludwig C.H. eds.), Wiley-Interscience, New York, (1971), p695-768.

60 Glasser W.G. and Barnett C.A. *Tappi*, **62**, (1979), 101.

61 Fengel D., Wegener G. and Feckl J., *Holzforschung*, **35**, (1981), p51.

62 Chang H.M., Cowling E.B., Brown W., Adler E. and Miksche G., *Holzforschung*, **29**, (1975), p153.

63 Adler E., *Wood Science and Technology*, **11**, (1977), p169.

64 Sarkanen K.V., Precursors and their polymerisation *in* "Lignins, Occurrence, Formation, Structure and Reactions", (Sarkanen K.V. and Ludwig C.H. eds.), Wiley-Interscience, New York, (1971), p95-163.

65 Erdtman H., *Industrial Engineering and Chemistry*, **49**, (1957), p1385.

66 Robert D.R. and Brunow G., *Holzforschung*, **38**(2), (1984), p85.

67 Brunow G. and Lundquist K, *Paperi ja Puu*, **11**, (1980), p669.

68 Yamasaki T., Hata K. and Higuchi T., *Mokuzai Gakkaishi*, **18**, (1972), p361.

69 Lai Y.Z. and Sarkanen K.V., *Cellulose Chemistry and Technology*, **9**, (1975), p239.

70 Tanahashi M., Takeuchi H. and Higuchi T., *Wood Research*, **61**, (1976), p44.

71 Tanahashi M. and Higuchi T., *Mokuzai Gakkaishi*, **36**(5), (1990), p424.

72 Terashima N. and Seguchi Y., *Cellulose Chemistry and Technology*, **22**, (1988), p147.

73 Higuchi T., Ogino K. and Tanahashi M., *Wood Research*, **51**, (1971), p1.

74 Freudenberg K., *Science*, **148**(30th April), (1965), p595.

75 Higuchi T., *Wood Science and Technology*, **24**, (1990), p23.

76 Sarkanen K.V. and Hergert H.L., Classification and distribution *in* "Lignins, Occurrence, Formation, Structure and Reactions", (Sarkanen K.V. and Ludwig C.H. eds.), Wiley-Interscience, New York, (1971), p43-94.

77 Nimz H.H., Robert D., Faix O. and Nemr M., *Holzforschung*, **35**, (1981), p16.

78 Glasser W.G. and Glasser H.R., *Paperi ja Puu*, **63**(2), (1981), p71.

79 Sarkanen K.V., Chang H.M. and Allan G.G., *Tappi*, **50**, (1967), p583.

80 Erickson M., Larsson S and Miksche G.E., *Acta Chemica Scandinavica*, **27**, (1973), p903.

81 Bland D.E., *Holzforschung*, **15**, (1961), p102.

82 Latif M.A., "Comparative study of normal and compression wood lignin of Douglas fir (*Pseudotsuga menziesii* Franco), Ph.D. Thesis, University of Washington, Seattle, (1968), p69.

83 Sarkanen K.V., Chang H.M. and Allan G.G., *Tappi*, **50**, (1967), p587.

84 Ralph J., 9th International Symposium on Wood and Pulping Chemistry, Montreal, (1997), proceedings PL2.

85 Ralph J., MacKay J.J., Hatfield R.D., O'Malley D.M., Whetten R.W. and Sederoff R.R., *Science*, **277**(5323), (1997), p235.

86 Ralph J., Hatfield R.D., Martia J.M., Lu F., Peng J., Kim H., Grabber J.H., MacKay J.J., O'Malley D.M., Sederoff R.R., Chapple C., Chiang V. and Boudet A.M., 10th International Symposium on Wood and Pulping Chemistry, Yokohama, (1999), proceedings p138.

87 MacKay J.J., "A mutation in lignin biosynthesis in loblolly pine: genetic, molecular and biochemical analyses", Ph. D. Thesis, NC State, (1997).

88 MacKay J.J., Liu W., Whetten R.W., Sederoff R.R. and O'Malley D.M., *Molecular Genetics*, **247**, (1995), p537.

89 O'Malley D.M., Porter S. and Sederoff R.R., *Plant Physiology*, **98**, (1992), p1364.

90 Sipilä J., Brunow G., Kilpeläinen I., Karlsson O. and Lundquist K., 7th International Symposium on Wood and Pulping Chemistry, Beijing, (1993), proceedings p87.

90b Lewis N.G., *Current Opinion in Plant Biology*, **2**(2), (1999), p153.

90c Ralph J., Peng J., Lu F., Hatfield R.D. and Helm R.F., *Journal of Agriculture and Food Chemistry*, **47**(8), (1999), p2991.

91 Davin L.B., Wang H-B., Crowell A.L., Bedgar D.L., Martin D.M., Sarkanen S. and Lewis N.G., *Science*, **275**, 1997, p362.

91b Lewis N.G. and Davin L.B., *Plant Physiology*, **123**(2), (2000), p453.

92 Lewis N.G., Davin L.B. and Sarkanen S, The Biochemical Control of Monolignol coupling and structure during lignin and lignan biosynthesis *in* "Lignin and Lignan Biosynthesis", (Lewis N.G. and Sarkanen S. eds.), ACS Symposium Series 697, American Chemical Society, Washington DC, (1998), p334-361.

93 Sipilä J. and Brunow G., 6th International Symposium on Wood and Pulping Chemistry, Raleigh, (1991), proceedings p1.

94 Ede R.M., Brunow G., Simola L.K. and Lemmetyinen J., *Holzforschung*, **44**(2), (1990), p95.

95 Lundquist K., *Acta Chemica Scandinavica*, **B35**, (1981), p497.

96 Bax A. and Davis D.G., *Journal of Magnetic Resonance*, **65**(2), (1985), p355.

97 Bax A. and Subramanian S., *Journal of Magnetic Resonance*, **67**(3), (1986), p565.

98 Bax A., Griffey R.H. and Hawkings B.L., *Journal of Magnetic Resonance*, **55**, (1983), p301.

99 Ede R.M. and Kilpeläinen I., 8th International Symposium on Wood and Pulping Chemistry, Helsinki, (1997), proceedings p487.

100 Ede R.M., Ralph J., Torr K.M. and Dawson B.S.W., *Holzforschung*, **50**(2), (1996), p161.

101 Habu N., Matsumoto Y., Ishizu A. and Nakano J., *Holzforschung*, **44**(1), (1990), p67.

102 Gellerstedt G. and Zhang L., *Nordic Pulp and Paper Research Journal*, (3), (1991), p136.

103 Kilpeläinen I., Sipilä J., Brunow G., Lundquist K. and Ede R.M., *Journal of Agriculture and Food Chemistry*, **42**(12), (1994), p2790.

104 Lapierre C., Pollet B. and Monties B., *Phytochemistry*, **30**(2), (1991), p659.

105 Karhunen, P., Rummakko P., Sipilä J. and Brunow G., *Tetrahedron Letters*, **36**(1), (1995), p169.

106 Karhunen, P., Rummakko P., Sipilä J. and Brunow G., *Tetrahedron Letters*, **36**(25), (1995), p4501.

107 Drumond M., Aoyama M., Chen C-L. and Robert D., *Journal of Wood Chemistry and Technology*, **9**(4), (1989), p421.

108 Rydholm S.A., Chemical Pulping *in* "Pulping Processes", Wiley-Interscience, New York, (1965), p439-715.

109 Marton J., Reactions in alkaline pulping *in* "Lignins, Occurrence, Formation, Structure and Reactions", (Sarkanen K.V. and Ludwig C.H. eds.), Wiley-Interscience, New York, (1971), p639-694.

110 Sakakibara A., Degradation products of protolignin and the structure of lignin *in* "The Structure, Biosynthesis and Degradation of Wood", (Loews F.A. and Runeckles V.C. eds.), Plenum Press, New York, (1977), p117-139.

111 Yasuda S. and Sakakibara A., *Mokuzai Gakkaishi*, **21**(6), (1975), p363.

112 Yasuda S. and Sakakibara A., *Mokuzai Gakkaishi*, **21**, (1975), p370.

113 Yasuda S. and Sakakibara A., *Mokuzai Gakkaishi*, **21**, (1975), p639.

114 Lee V.P.F.F., "Structural differences in lignin formation between normal and compression wood of Douglas fir, Ph. D. Thesis, University of Washington, Seattle, (1968), p52.

115 Timell T.E., "Compression Wood in Gymnosperms", Volume 1, Springer-Verlag, Berlin, 1986, p289-409.

116 Sakakibara A., *Wood Science and Technology*, **14**, (1980), p89.

117 Björkman A. and Person B., *Svensk Papperstidning*, **60**, (1957), p158.

118 Fergus B.J. and Goring D.A.I., *Holzforschung*, **24**(4), (1970), p118.

119 Hardell H-L., Leary G.J., Stoll M. and Westermark U., *Svensk Papperstidning*. **83**(2), (1980), p44.

120 Terashima N. and Fukushima K., *Wood Science and Technology*, **22**(3), (1988), p259.

121 Terashima N., Fukushima K., Sano Y. and Takabe K., *Holzforschung*, **42**(6), (1988), p347.

122 Terashima N., Tomimura Y. and Araki H., *Mokuzai Gakkaishi*, **25**(9), (1979), p595.

123 Björkman A., *Svensk Papperstidning*, **60**, (1957), p329.

124 Bland D.E., *Holzforschung*, **20**, (1966), p12.

125 Whiting P. and Goring D.A.I., *Svensk Papperstidning*, **84**, (1981), p120.

126 Maurer A. and Fengel D., *Holzforschung*, **46**(5), (1992), p417.

127 Terashima N., Fukushima K. and Imai T., *Holzforschung*, **46**(4), (1992), p271.

128 Sjöström E., "Wood Chemistry; Fundamentals and Applications", Academic Press, New York, (1981), p104-145.

129 Fengel D. and Wegener G., "Wood; Chemistry, Ultrastructure, Reactions", Walter de Gruyter, Berlin, (1989), p296-318.

130 Gierer J. and Norén I., *Holzforschung*, **34**, (1980), p197.

131 Ljunggren S., *Svensk Papperstidning*, **83**, (1980), p363.

132 Gierer J., *Wood Science and Technology*, **14**, (1980), p241.

133 Gierer J., *Svensk Papperstidning*, **73**, (1970), p571.

134 Gierer J., *Holzforschung*, **36**, (1982), p43.

135 Gierer J., *Holzforschung*, **36**, (1982), p55.

136 Kleppe P.J., *Tappi*, **53**(1), (1970), p35.

137 Åxegard P. and Wiken J.E., *Svensk Papperstidning*, **36**, (1983), p178.

138 Kleinert T.N., *Tappi*, **49**(2), (1966), p53.

139 Teder A. and Olm L., *Papperi ja Puu*, **63**, (1981), p315.

140 Fengel D. and Wegener G., "Wood; Chemistry, Ultrastructure, Reactions", Walter de Gruyter, Berlin, (1989), p414-481.

141 Pew J.C. and Connors W.J., *Tappi*, **54**(2), (1971), p245.

142 Sjöström E., "Wood Chemistry; Fundamentals and Applications", Academic Press, New York, (1981), p146-168.

143 Reeve D.W., Introduction to the principles and practice of pulp bleaching *in* "Pulp Bleaching; Principles and Practice, (Dence C.W. and Reeve D.W. eds.), Tappi Press, Atlanta, (1996), p1-25.

144 MacLeod J.M., *Appita*, **46**, (1993), p445.

145 Outzen P. and van Lee R., 50th Appita annual general conference, Auckland, (1996), proceedings p693.

146 Marcoccia B.S. and Jiang J., *Paper Asia*, **12**, (1996).

147 Johansson B., Mjöberg J., Sandström P and Teder A., *Svensk Papperstidning*, **87**(10), (1984), p30.

148 Sjöblom K., Mjöberg J. and Hartler N., *Paperi ja Puu*, **65**(4), (1983), p227.

149 Rydholm S.A., Mechanical Pulping *in* "Pulping Processes", Wiley-Interscience, New York, (1965), p368-400.

150 Uprichard J.M. and Walker J.C.F., Pulp and paper manufacture *in* Primary Wood Processing, (walker J.C.F. ed.), Chapman and Hall, London, (1993), p481-534.

151 Kurdin J.A., Refiner mechanical and thermomechanical pulping *in* "Pulp and Paper; Chemistry and Technology Vol. 1", (Casey J.P. ed.), Wiley-Interscience, New York, (1980), p197-252.

152 Richardson J.D., Corson S.R. and Murton K.D., *Appita*, **43**(2), (1990), p137.

153 Richardson J.D., *Appita*, **49**(1), (1996), p27.

154 Richardson J.D., *Appita*, **51**(1), (1998), p39.

155 Barnet A.J. and Vihmari P., *Pulp and Paper Canada*, **84**(9), (1983), p52.

156 Walker J.C.F., Wood panels: Particleboards and fibreboards *in* Primary Wood Processing, (walker J.C.F. ed.), Chapman and Hall, London, (1993), p419-480.

157 Suchsland O. and Woodson G.E., Fibreboard Manufacturing Practices in the United States, USDA Forest Service, Agricultural Handbook 640, (1986).

158 Goring D.A.I., *Pulp and Paper Canada*, **64**, (1963), p517.

159 Back E.L. and Salmén N.L., *Tappi*, **65**(7), (1982), p107.

160 Gellerstedt G. and Pettersson E-L., *Svensk Papperstidning*, **77**, (1977), p15.

161 Gierer J., *Wood Science and Technology*, **19**, (1985), p289.

162 Gierer J., *Wood Science and Technology*, **20**, (1986), p1.

163 Browning B.L., Methods of Wood Chemistry, Wiley-Interscience, New York, (1967), 747-784.

164 Sarkanen K. and Schuerch C, *Analytical Chemistry*, **27**, (1955), p1245.

165 Brauns F.E., The Chemistry of Lignin, Academic Press, New York, (1952), p291-308.

166 Brauns F.E., The Chemistry of Lignin, Academic Press, New York, (1952), p270-290.

167 Goldschmid O., Ultraviolet spectra *in* "Lignins, Occurrence, Formation, Structure and Reactions", (Sarkanen K.V. and Ludwig C.H. eds.), Wiley-Interscience, New York, (1971), p241-266.

168 Aulin-Ertdman G., *Svensk Papperstidning*, **57**, (19540, p745.

169 Gärtner A., Gellerstedt G. and Tamminen T., *Nordic Pulp and Paper Research Journal*, **14**(2), (1999), p163.

170 Lin S.Y., Ultraviolet Spectroscopy *in* Methods in Lignin Chemistry, (Lin S.Y and Dence C.W. eds.), Springer-Verlag, Berlin, (1992), p217-232.

171 Milne T.A., Chum H.L., Agblevor F. and Johnson D.K., *Biomass Bioenergy*, **2**(1), (1992), p341.

172 Adler E. and Hernestam S., *Acta Chemica Scandinavica*, **9**(2), (1955), p319.

173 Adler E., Hernestam S. and Walldén I., *Svensk Papperstidning*, **61**(18), (1958), p641.

174 Lai Y.Z., Determination of phenolic hydroxyl groups *in* Methods in Lignin Chemistry, (Lin S.Y and Dence C.W. eds.), Springer-Verlag, Berlin, (1992), p423-434.

175 Lai Y-Z., Guo X-P. and Situ W., *Journal of Wood Chemistry and Technology*, **10**(3), (1990), p365.

176 Francis R.C., Lai Y-Z., Dence C.W. and Alexander T.C., *Tappi Journal*, **74**, (1991), p219.

177 Lai Y-Z. and Guo X-P., *Wood Science and Technology*, **25**, (1991), p467.

178 Månsson P., *Holzforschung*, **37**(3), (1983), p143.

179 Månsson P. and Westfelt L., *Journal of Applied Polymer Science*, **25**, (1980), p1533.

180 Månsson P., *Tetrahedron Letters*, **23**, (1982), p1845.

181 Robert D., Carbon-13 nuclear magnetic resonance spectrometry *in* Methods in Lignin Chemistry, (Lin S.Y and Dence C.W. eds.), Springer-Verlag, Berlin, (1992), p250-273.

182 Landucci L., *Holzforschung*, **39**, (1985), p355.

183 Lundquist K., Proton (^{1}H) NMR spectroscopy *in* Methods in Lignin Chemistry, (Lin S.Y and Dence C.W. eds.), Springer-Verlag, Berlin, (1992), p242-249.

184 Ahvazi B.C. and Argyropoulos D.S., *Journal of Agriculture and Food Chemistry*, **44**(8), (1996), p2167.

185 Argyropoulos D.S., *Journal of Wood Chemistry and Technology*, **14**(1), (1994), p45.

186 Argyropoulos D.S., *Journal of Wood Chemistry and Technology*, **14**(1), (1994), p65.

187 Argyropoulos D.S., Bolker H.I., Heitner C. and Archipov Y, *Journal of Wood Chemistry and Technology*, **13**(2), (1993), p187.

188 Argyropoulos D.S., 7th International Symposium on Wood and Pulping Chemistry, Beijing, (1993), proceedings p776.

189 Granata A. and Argyropoulos D.S., *Journal of Agriculture and Food Chemistry*, **43**(6), (1995), p1538.

190 Gorenstein D.G., Phosphorus-31 chemical shifts: principles and empirical observations *in* Phosphorus-31 NMR; principles and applications, (Gorenstein D.G. ed.), Academic Press, New York, (1984), p7-36.

191 Schiff D.E., Verkade J.G., Metzler R.M., Squires T.G. and Venier C.G., *Applied Spectroscopy*, **40**(3), (1986), p348.

192 Wroblewski A.E., Markuszewski R. and Verkade J.G., *American Chemical Society Division of Fuel Chemistry*, **32**(3), (1987), p202.

193 Archipov Y., Argyropoulos D.S., Bolker H.I. and Heitner C., *Journal of Wood Chemistry and Technology*, **11**(2), (1991), p137.

194 Jiang Z-H., Argyropoulos D.S. and Granata A., *Magnetic Resonance in Chemistry*, **33**, (1995), p375.

195 Sarkanen K., Islam A. and Anderson C.D., Ozonation *in* Methods in Lignin Chemistry, (Lin S.Y and Dence C.W. eds.), Springer-Verlag, Berlin, (1992), p387-406.

196 Sakakibara A., Hydrogenolysis *in* Methods in Lignin Chemistry, (Lin S.Y and Dence C.W. eds.), Springer-Verlag, Berlin, (1992), p350-368.

197 Gellerstedt G., Chemical degradation methods: permanganate oxidation *in* Methods in Lignin Chemistry, (Lin S.Y and Dence C.W. eds.), Springer-Verlag, Berlin, (1992), p322-333.

198 Chang H.M. and Allan G.G., Oxidation *in* "Lignins, Occurrence, Formation, Structure and Reactions", (Sarkanen K.V. and Ludwig C.H. eds.), Wiley-Interscience, New York, (1971), p433-486.

199 Chen C.L., Nitrobenzene and cupric oxide oxidations *in* Methods in Lignin Chemistry, (Lin S.Y and Dence C.W. eds.), Springer-Verlag, Berlin, (1992), p301-321.

200 Schultz T.P. and Templeton M.C., *Holzforschung*, **40**(2), (1986), p93.

201 Funaoka M., Abe I. And Chiang V.L., Nucleus exchange reaction *in* Methods in Lignin Chemistry, (Lin S.Y and Dence C.W. eds.), Springer-Verlag, Berlin, (1992), p369-386.

202 Funaoka M. and Abe I., International Symposium on Wood and Pulping Chemistry, Tsukuba, (1983), proceedings p79.

203 Funaoka M. and Abe I., *Wood Science and Technology*, **21**, (1987), p261.

204 Adler E., Pepper J.M. and Eriksoo E., *Industrial and Engineering Chemistry*, **49**, (1957), p1391.

205 Lundquist K., Acidolysis *in* Methods in Lignin Chemistry, (Lin S.Y and Dence C.W. eds.), Springer-Verlag, Berlin, (1992), p289-300.

206 Lundquist K., *Applied Polymer Symposium*, **28**, (1976), p1393.

207 Lapierre C., Monties B. and Rolando C., *Journal of Wood Chemistry and Technology*, **5**(2), (1985), p277.

208 Lundquist K., *Acta Chemica Scandinavica*, **18**, (1964), p1316.

209 Lundquist K., *Acta Chemica Scandinavica*, **24**, (1970), p889.

210 Lundquist K., Miksche G.E., Ericsson L. and Berndtson L., *Tetrahedron Letters*, (1967), p4587.

211 Lundquist K. and Ericsson L., *Acta Chemica Scandinavica*, **24**, (1970), p3681.

212 Nimz H., *Angewandte Chemie International Edition in English*, **13**, (1974), p313.

213 Nimz H., *Chemische Berichten*, **102**, (1969), p799.

214 Rolando C., Monties B. and Lapierre C., Thioacidolysis *in* Methods in Lignin Chemistry, (Lin S.Y and Dence C.W. eds.), Springer-Verlag, Berlin, (1992), p334-349.

215 Lapierre C., Monties B. and Rolando C., *Holzforschung*, **40**(1), (1986), p47.

216 Lapierre C., Monties B. and Rolando C., 4th International Symposium on Wood and Pulping Chemistry, Paris, (1987), proceedings p431.

217 Lapierre C,. Pollet B. and Rolando C., 3rd European Workshop on Lignocellulosics and Pulp, 1985.

218 Node M., Hori H. and Fujita E., *Journal of the Chemical Society Perkin Transactions 1*, (1976), p2237.

219 Fuji K., Ichikawa K., Node M. and Fujita E., *Journal of Organic Chemistry*, **44**(10), (1979), p1661.

220 Pasco M.F. and Suckling I.D., *Holzforschung*, **48**(6), (1994), p504.

221 Pasco M.F., Suckling I.D. and Allison R.W., 48th Appita Annual Conference, Sydney, (1994), proceedings p219.

222 Suckling I.D., Pasco M.F., Hortling B. and Sundquist J., *Holzforschung*, **48**(6), (1994), p501.

223 Lu F. and Ralph J., 9th International Symposium on Wood and Pulping Chemistry, Montreal, (1997), proceedings L3-1.

224 Lu F. and Ralph J., *Journal of Agriculture and Food Chemistry*, **45**(12), (1997), p4655.

225 Lu F. and Ralph J., *Journal of Agriculture and Food Chemistry*, **46**(2), (1998), p547.

226 Lu F. and Ralph J., *Journal of Agriculture and Food Chemistry*, **45**(7), (1997), p2590.

227 Ralph J. and Lu F., *Journal of Agriculture and Food Chemistry*, **46**(11), (1998), p4616.

228 Adler E. and Lundquist K., *Acta Chemica Scandinavica*, **55**, (1961), p223.

229 Mikawa H., Sato K., Takasaki C. and Ebisawa K., *Bulletin of the Chemical Society of Japan*, **29**, (1956), p259.

230 Lapierre C., Pollet B. and Monties B., 6th International Symposium on Wood and Pulping Chemistry, Raleigh, (1991), p543.

231 Lapierre C., Pollet B. and Monties B., 1st European Workshop on Lignocellulosics and Pulping, Hamburg, (1990), proceedings p1.

232 Lapierre C., Pollet B., Monties B. and Rolando C., *Holzforschung*, **45**(1), (1991), p61.

233 Peng P., Lu F. and Ralph J., *Journal of Agriculture and Food Chemistry*, **46**(2), (1998), p553.

234 Chiang V.L., Stokke D.D. and Funaoka M., *Journal of Wood Chemistry and Technology*, **9**(1), (1989), p61.

235 Chiang V.L. and Funaoka M., *Holzforschung*, **42**(6), (1988), p385.

236 Chan F., Nguyen K.L. and Wallis A.F.A., *Journal of Wood Chemistry and Technology*, **15**, (1995), p473.

237 Tamminen T., Poppius-Levlin K., Aurela B. and Hortling B., *Holzforschung*, **51**(2), (1997), p155.

238 Bose S.K., Wilson K.L., Francis R.C. and Aoyama M., *Holzforschung*, **52**(3), (1998), p297.

239 Robert D.R., Bardet M., Gellerstedt G. and Lindfors E-L., *Journal of Wood Chemistry and Technology*, **4**(3), (1984), p239.

240 Robert D., Gellerstedt G. and Bardet M., *Nordic Pulp and Paper Research Journal*, **3**, (1986), p18.

241 Gellerstedt G. and Robert D., *Acta Chemica Scandinavica*, **B41**, (1987), p541.

242 Doddrell D.M., Pegg D.T. and Bendall M.R., *Journal of Magnetic Resonance*, **48**, (1982), p323.

243 Freudenberg K. and Renner K.C., *Chemische Berichten*, **98**, (1965), p833.

244 Weast R.C. ed., CRC Handbook of Chemistry and Physics, CRC Press, Cleveland, (1975), p C257.

245 Weast R.C. ed., CRC Handbook of Chemistry and Physics, CRC Press, Cleveland, (1975), p C240.

246 Rolando C., Monties B. and Lapierre C., In Methods in Lignin Chemistry, Lin S.Y. and Dence C.W. (Eds), Springer, Heidelberg, (1992), p334.

247 Ede R.M., "The Synthesis and Reactivity of Beta-Aryl Model Quinone Methides", Ph.D. Thesis, University of Waikato, (1987), p71-83.

248 McMurry J., Organic Chemistry, 4th edition, Brooks/Cole Publishing Company, Pacific Grove, (1996), p662-663.

249 Aue W.P., Bartholdi E. and Ernst R.,R., *Journal of Chemical Physics*, **64**, (1976), p2229.

250 Bax A. and Summers M.F., *Journal of the American Chemical Society*, **108**, (1986), p2093.

251 Berndtson L., Hedlund K., Hermå L. and Lundquist K., *Acta Chemica Scandinavica*, **B28**, (1974), p333.

252 Lundquist K. and Olsson T., *Acta Chemica Scandinavica.*, **B31**, (1977).

253 Gorenstein D.G., Phosphorus-31 spin-spin coupling constants: principles and applications *in* Phosphorus-31 NMR; principles and applications, (Gorenstein D.G. ed.), Academic Press, New York, (1984), p37-53.

254 Pastor S.D., Hyun J.L., Odorisio P.A. and Rodebaugh R.K., *Journal of the American Chemical Society*, **110**(19), (1988), p6547.

255 Dewar M.J.S., Zoebisch E.G., Healy E.F. and Stewart J.J.P., *Journal of the American Chemical Society*, **107**, (1985), p3902.

256 Hehre W.J., Radom L., Schleyer P.v.R. and Pople J.A., "Ab Initio Molecular Orbital Theory", Wiley-Interscience, New York, (1986).

257 Stewart J.J.P., *Journal of Computer Aided Molecular Design*, **4**, (1990), p1.

258 Cotton F.A. and Wilkinson G., "Advanced Inorganic Chemistry", 3rd edition, Wiley-Interscience, New York, (1972), p116-122.

259 Szalontai G., Bakos J, Tóth I. And Heil B., *Magnetic Resonance Chemistry*, **25**, (1987), p761.

260 Still W.C., Kahn M. and Mitra A., *Journal of Organic Chemistry*, **43**(14), (1978), p2923.

261 Karhunen P., Rummakko P., Pajunen A. and Brunow G., *Journal of the Chemical Society, Perkin Transaction 1*, (1996), p2303.

262 Karplus M., *Journal of Chemical Physics*, **30**, (1959), p11.

263 Pachler K.G.R., *Journal of the Chemical Society, Perkin Transactions 1*, (1972), p1936.

264 Haasnoot C.A.G., de Leeuw F.A.A.M. and Altona C., *Tetrahedron*, **36**, (1980), p2783.

265 McMurry J., Organic Chemistry, 4th edition, Brooks/Cole Publishing Company, Pacific Grove, (1996), p106-110.

266 McMurry J., Organic Chemistry, 4th edition, Brooks/Cole Publishing Company, Pacific Grove, (1996), p570-585.

267 "Forestry Facts and Figures-1997", New Zealand Forest Owners Association Inc., (1997).

268 Yang J.M. and Goring D.A.I., *Holzforschung*, **32**(6), (1978), p185.

269 Lundquist K., *Acta Chemica Scandinavica*, **B34**, (1980), p21.

270 Chen C.L., Determination of methoxyl groups *in* Methods in Lignin Chemistry, (Lin S.Y and Dence C.W. eds.), Springer-Verlag, Berlin, (1992), p465-472.

271 Robert D., Canadian Wood Chemistry Symposium CIC, (1982), p63.

272 Ralph J. and Grabber J.H., *Holzforschung*, **50**(5), (1996), p425.

273 Lapierre C. and Rolando C., *Holzforschung*, **42**(1), (1988), p1.

274 Lapierre C., Pollet B., Tollier M-T., Chabbert B., Monties B. and Rolando C.,

275 Lapierre C., Monties B. and Rolando C., *Holzforschung*, **42**(6), (1988), p409.

276 Adams T.A., "Isolation and Characterisation of *Pinus radiata* HTMP and TMP Lignins", MSc Thesis, University of Waikato, (1999).

277 Matsukura M. and Sakakibara A, *Mokuzai Gakkaishi*, **15**, (1969), p35.

278 Tomimura Y., Yokoi T. and Terashima N., *Mokuzai Gakkaishi*, **25**(11), (1979), p743.

279 Tomimura Y., Yokoi T. and Terashima N., *Mokuzai Gakkaishi*, **26**(1), (1980), p37.

280 Vold R.L., Waugh J.S., Klein M.P. and Phelps D.E., *Journal of Chemical Physics*, **48**, (1968), p3831.

281 Frye J.S., *Concepts in Magnetic Resonance*, **1**, (1989), p27.

282 Argyropoulos D.S., Bolker H.I., Heitner C. and Archipov Y, *Holzforschung*, **47**(1), (1993), p50.

283 Martin M.L., Martin G.J. and Delpuech J.J., "Practical NMR Spectroscopy", Heyden, London, (1984), p350-376.

284 Kemp W., "Organic Spectroscopy", McMillan Press, London, (1978), p98-99.

285 Walpole R.E., "Introduction to Statistics", 2nd edition, Collier MacMillan, London, (1974), p156-162.

286 Archipov Y., Argyropoulos D.S., Bolker H. and Heitner C., *Carbohydrate Research*, (220), (1991), p49.

287 Holmes G.W. and Kurth E.F., *Tappi*, **42**(10), (1959), p837.

288 Drew J. and Pylant G.D., *Tappi*, **49**, (1966), p430.

289 Snajberk K., Zavarin e. and Bailey D., *Biochemical Systematics and Ecology*, **7**, (1979), p269.

290 Holmbom B. and Ekman R., *Acta Academica Aboensis*, **B38**(3), (1978), p1.

291 Conner A.H. and Rowe J.W., *Journal of the American Oil Chemists' Society*, **52**, (1975), p334.

292 Chen C.L., *Phytochemistry*, **9**, (1970), p1149.

293 Rowe J.W., Seikel M.K., Roy D.N. and Jorgensen E., *Phytochemistry*, **11**, (1972), p2513.

294 Theander O., *Animal Feed Science and Technology*, **32**, (1991), p35.

295 Gardner J.A.F. and Barton G.M., *Forest Products Journal*, **10**(3), (1960), p171.

296 Harwood V.D., *Holzforschung*, **25**, (1971), p73.

297 Parameswaran V.N., Faix O. and Schweers W., *Holzforschung*, **22**(1), (1975), p1.

298 Browning B.L., "The Chemistry of Wood", Wiley-Interscience, New York, (1963).

299 Harris J.M., *New Phytologist*, **53**, (1954), p517.

300 Yang J.M. and Goring D.A.I., *Canadian Journal of Chemistry*, **58**, (1980), p2411.

301 Gellerstedt G. and Lindfors E-L., *Svensk Papperstidning*, (9), (1984), p61.

302 Pew J.C., *Tappi*, **40**, (1957), p553.

303 Timell T.E., "Compression Wood in Gymnosperms", Volume 3, Springer-Verlag, Berlin, (1986), p1855.

304 Watson A.J. and Dadswell H.E., *Appita*, **11**, (1957), p56.

305 Park S., Saiki H. and Harada H., *Mokuzai Gakkaishi*, **25**, (1979), p311.

306 Isebrands J.G. and Hunt C.M., *Wood Fiber*, **7**, (1975), p119.

307 Timell T.E., *IAWA Bulletin*, (4), (1972), p10.

308 Jacquet G., Pollet B., Lapierre C., Francesch C., Rolando C. and Faix O., *Holzforschung*, **51**(4), (1997), p349.

309 Hapiot P., Pinson J., Fancesch C., Mhamdi F., Rolando C. and Schneider S., *Journal of Electroanalytical Chemistry*, **328**, (1992), p327.

310 Hapiot P., Neta P., Pinson J., Rolando C. and Schneider S., *New Journal of Chemistry*, **17**, (1993), p211.

311 Fukushima K. and Terashima N., *Wood Science and Technology*, **25**, (1991), p371.

312 Yasuda S. and Sakakibara A., *Mokuzai Gakkaishi.*, **23**, (1977), p114.

313 Yasuda S. and Sakakibara A., *Mokuzai Gakkaishi*, **22**, (1976), p606.

314 Faix O., Lange W. and Bienhoff O., *Holzforschung*, **34**, (1980), p174.

315 Lai Y-Z. and Funaoka M., *Journal of Wood Chemistry and Technology*, **13**(1), (1993), p43.

316 Adams T. and Ede R.M., 9th International Symposium on Wood and Pulping Chemistry, Montreal, proceedings p1.

317 Gellerstedt G., *Svensk Papperstidning*, **16**, (1976), p537.

318 Gellerstedt G. and Gierer J., *Acta Chemica Scandinavica*, **B31**, (1977), p729.

319 Whiting P., Favis B.D., St-Germain F.G.T. and Goring D.A.I., *Journal of Wood Chemistry and Technology*, **1**(1), (1981), p29.

320 Hardell H-L., Leary G.J., Stoll M. and Westermark U., *Svensk Papperstidning*, (2), (1980), p44.

321 Marton J., *Tappi*, **47**, (1964), p713.

322 Faix O., Argyropoulos D.S., Robert D. and Neirinck V., *Holzforschung*, **48**(5), (1994), p387.

323 Gierer J., Imsgard F. and Pettersson I., *Applied Polymer Symposium*, **28**, (1976), p1195.

324 Brunow G. and Miksche G.E., *Applied Polymer Symposium*, **28**, (1976), p1155.

325 Dalgety J.A., *In* Chemical Composition of Kraft Pulping Liquor, MSc Thesis, University of Waikato, (1999).

326 Gellerstedt G. and Gustafsson K., *Journal of Wood Chemistry and Technology*, 7(1), (1987), p65.

327 Gustavsson C.A-S., Lindgren C.T. and Lindström M.E., *Nordic Pulp and Paper Research Journal*, **12**(4), (1997), p225.

328 Shaka A.J., Keeler J., Frenkiel T. and Freeman R., *Journal of Magnetic Resonance*, **52**, (1983), p335.

329 Robert D.R. and Brunow G., *Holzforschung*, **38**(2), (1984), p85.

330 Elbs K. and Lerch H., *Journal von Praktische Chemika*, **93**, (1916), p1.

331 Hudlický M., Reduction with hydrides and complex hydrides *in* "Reductions in Organic Chemistry", John Wiley & sons, New York, (1984), p13-20.

332 Hudlický M., Procedures *in* "Reductions in Organic Chemistry", John Wiley & sons, New York, (1984), p13-20.

333 Weast R.C. ed., CRC Handbook of Chemistry and Physics, CRC Press, Cleveland, (1975), p C518.

334 Adler E. and Hernestam S., *Acta Chemica Scandinavica*, **B9**, (1955), p319.

335 Brown J.M., *Angewandte Chemie International Edition*, **26**, (1987), p190.

336 Hudlický M., Catalytic hydrogenation *in* "Reductions in Organic Chemistry", John Wiley & sons, New York, (1984), p1-12.

337 Smit R., "A Study Regarding the Cyanamide Activation of Peroxide Bleaching Reactions", MSc Thesis, University of Waikato, (1995).

338 Leopold B., *Acta Chemica Scandinavica*, **4**, (1950), p213.

339 Ede R.M., "The Synthesis and Reactivity of Beta-Aryl Model Quinone Methides", Ph.D. Thesis, University of Waikato, (1987), p39.

340 Robinson M.J., "Reactions of an Iron Phthalocyanine with Lignin Model Compounds", MSc Thesis, University of Auckland, 1994, p31.

341 Lundquist K., Simonson R. and Tingsvik K., *Svensk Papperstidning*, (9) (1979), p272.

342 Lundquist K., Simonson R. and Tingsvik K., *Svensk Papperstidning*, (16) (1980), p452.

343 Holmes G.W. and Kurth E.F., *Tappi*, **42**(10), (1959), p837.

344 Richardson J.D., Sulphonation Mechanism in DWS and CTMP Pulping, 51st APPITA Annual General Conference, May (1997).

345 Zwierzak A., *Canadian Journal of Chemistry*, **45**, (1967), 2501.

346 Labidi A., Robert D. and Pla F., *Holzforschung*, **47**(2), (1993), p133.

347 Hehre W.J., Yu J. and Klunzinger P.E., "A Guide to Molecular Mechanics and Molecular Orbital Calculations in SPARTAN", Wavefunction Inc., Irvine Ca, (1997).

348 Burkert U. and Allinger N.L., "Molecular Mechanics", ACS Monograph 177, ACS, Washington D.C., (1982).

349 Halgren T.A., *Journal of Computational Chemistry*, **17**, (1996), p490.

Advice is like snow –the softer it falls,
the longer it dwells upon,
and the deeper it sinks into the mind.

Samuel Taylor Coleridge

Appendix A

Lignin Composition of Samples

Appendix A.1 Composition of Isolated Lignin Samples

	Lignin content		Lignin composition				
Sample	Klason lignin g/100g	Acid soluble lignin g/100g	C %	H %	O %	OCH_3 %	S %
Pinus radiata	97.4	0.2	56.1	6.1	22.1	14.0	-
Pinus radiata thioacidolysate	-	-	55.1	5.9	7.5	10.5	18.8
Commercial eucalypt	96.3	1.2	56.9	6.3	15.6	21.2	-
Picea abies	96.2	0.1	57.7	6.2	20.6	13.8	1.7
EW/compression wood	96.5	0.2	60.1	6.5	20.5	12.9	-
LW/compression wood	97.1	0.2	60.1	6.3	22.3	11.3	-

Appendix A.2 Preparation and Composition of KSLL samples

Sample label	Pulping conditions, for pulps from which KSLL's A, B and C were isolated				
	Cook time (min)	H factor	Pulp yield (%)	Klason lignin of Pulp (%)	Delignification (%)
A	72	6	76.7	28.2	21
B	190	1408	47.3	3.91	93
C	255	2388	45.6	3.27	94

Samples **A**, **B** and **C** kindly supplied by Ms Jacinta Dalgety [325].

Sample	Lignin content of KSLL's		
	Klason lignin g/100g	Acid soluble lignin g/100g	Total lignin g/100g
A	96.3	1.3	97.6
B	94.7	3.5	98.2
C	93.7	3.6	97.3

Appendix A.3 Lignin Content of in situ Lignin Samples

Sample	Lignin content of wood samples	
	Klason lignin g/100g	Acid soluble lignin g/100g
Pinus radiata	27.8	0.38
Earlywood	27.9	0.37
Latewood	27.2	0.38
Sapwood	26.9	0.35
Heartwood	28.1	0.42
EW/Compression wood	30.0	0.38
LW/Compression wood	34.3	0.41
Eucalypt	23.5	4.78
Picea abies	28.4	0.38

Sample	PAPRO Pulp N°	Lignin content of fibre samples			
		Klason lignin g/100g	Acid soluble lignin g/100g	Total Refining Energy KWh/odt	Sulphur Content (%)
MDF		27.9	0.35	433	-
TMP	951123	27.8	0.39	3036	0.005
CTMP	94532	28.2	0.44	2392	0.15
DWS	94469	28.2	0.50	2368	0.17
OPCO	94432	24.5	3.58	1600	0.83
DWS 1° pulp*	94468			1299	0.10
DWS 1° fines*	94487	39.1	0.54	1276	0.19
DWS 2° fines*	94516	35.8	0.52	2386	0.10
DWS 1° fibres*	94481	26.3	0.38	1276	0.07
DWS 2° fibres*	94513	25.7	0.37	2386	0.06

* DWS fibres and fines kindly supplied by Mr John Richardson, Forest Research [344].

Appendix B
^{31}P NMR Spectroscopy Data

Appendix B.1 Phosphorus-31 NMR Spectroscopy Results for Cook Time

	Thioacidolysis/^{31}P NMR spectroscopic results for varying MWL cook times							
	β-5	4-O-5	5-5	Condensed	Guaiacyl	*p*-hydroxy phenyl	Total phenolic	% Condensed
0 hours								
mmol/g				0.36	0.61	0.08	1.05	34
units/C9				0.07	0.11	0.01	0.20	
1 hour								
mmol/g	0.32	0.26	0.56	1.14	2.07	0.08	3.29	35
units/C9	0.06	0.05	0.10	0.21	0.38	0.01	0.62	
2 hours								
mmol/g	0.35	0.30	0.61	1.27	2.34	0.08	3.69	35
units/C9	0.07	0.06	0.11	0.24	0.44	0.02	0.71	
3 hours								
mmol/g	0.38	0.32	0.68	1.37	2.48	0.09	3.94	35
Units/C9	0.07	0.06	0.13	0.25	0.48	0.02	0.75	
4 hours								
mmol/g	0.38	0.32	0.69	1.39	2.51	0.09	3.99	35
units/C9	0.07	0.06	0.13	0.25	0.48	0.02	0.75	

	Thioacidolysis/^{31}P NMR spectroscopic results for varying *in situ* wood lignin cook times							
	β-5	4-O-5	5-5	Condensed	Guaiacyl	*p*-hydroxy phenyl	Total phenolic	% Condensed
1/2 hour								
mmol/g	0.24	0.12	0.31	0.67	1.27	0.08	1.94	35
units/C9	0.05	0.02	0.06	0.13	0.23	0.01	0.36	
1 hour								
mmol/g	0.25	0.18	0.43	0.86	1.63	0.06	2.49	35
units/C9	0.05	0.03	0.08	0.16	0.31	0.01	0.47	
2 hours								
mmol/g	0.35	0.24	0.55	1.14	2.22	0.09	3.36	34
units/C9	0.07	0.04	0.10	0.21	0.42	0.02	0.62	
3 hours								
mmol/g	0.45	0.26	0.66	1.37	2.47	0.10	3.92	35
Units/C9	0.08	0.05	0.12	0.26	0.46	0.02	0.73	
4 hours								
mmol/g	0.48	0.28	0.67	1.43	2.61	0.09	4.04	35
units/C9	0.09	0.05	0.13	0.27	0.49	0.02	0.76	

Appendix B.2 Phosphorus-31 NMR Spectroscopy Results for Error Calculation

	^{31}P NMR spectroscopic results for the reproducibility of phosphitylation/^{31}P NMR spectroscopy of MWL							
	β-5	4-O-5	5-5	Condensed	Guaiacyl	*p*-hydroxy phenyl	Total phenolic	% Condensed
mmol/g	0.38	0.32	0.68	1.38	2.48	0.09	3.95	35
units/C9	0.07	0.06	0.13	0.26	0.46	0.02	0.74	
mmol/g	0.38	0.31	0.66	1.35	2.39	0.10	3.84	35
units/C9	0.07	0.06	0.12	0.25	0.45	0.02	0.72	
mmol/g	0.37	0.31	0.70	1.38	2.51	0.11	4.00	35
units/C9	0.07	0.06	0.13	0.26	0.47	0.02	0.75	
mmol/g	0.36	0.29	0.65	1.30	2.45	0.09	3.84	34
units/C9	0.07	0.05	0.12	0.24	0.46	0.02	0.72	
mmol/g	0.40	0.32	0.66	1.38	2.59	0.11	4.08	34
units/C9	0.07	0.06	0.12	0.26	0.48	0.02	0.76	
mmol/g	0.37	0.31	0.67	1.35	2.46	0.10	3.91	35
units/C9	0.07	0.06	0.13	0.25	0.46	0.02	0.73	
mmol/g	0.40	0.30	0.72	1.42	2.55	0.09	4.06	35
units/C9	0.07	0.06	0.13	0.27	0.48	0.02	0.76	
mmol/g	0.40	0.31	0.64	1.35	2.46	0.10	3.91	35
units/C9	0.07	0.06	0.12	0.25	0.46	0.02	0.73	
mmol/g	0.39	0.33	0.71	1.43	2.52	0.10	4.05	35
units/C9	0.07	0.06	0.13	0.27	0.47	0.02	0.76	
mmol/g	0.39	0.30	0.69	1.38	2.50	0.11	3.99	35
units/C9	0.07	0.06	0.13	0.26	0.47	0.02	0.75	
mmol/g	0.36	0.33	0.71	1.40	2.49	0.10	3.99	35
units/C9	0.07	0.06	0.13	0.26	0.47	0.02	0.75	
mmol/g	0.39	0.31	0.70	1.40	2.41	0.10	3.91	36
units/C9	0.07	0.06	0.13	0.26	0.45	0.02	0.73	

	^{31}P NMR spectroscopic results for the reproducibility of thioacidolysis/derivatisation/^{31}P NMR spectroscopy of MWL							
	β-5	4-O-5	5-5	Condensed	Guaiacyl	*p*-hydroxy phenyl	Total phenolic	% Condensed
mmol/g	0.41	0.30	0.72	1.43	2.50	0.12	4.05	35
units/C9	0.08	0.06	0.13	0.27	0.47	0.02	0.76	
mmol/g	0.34	0.33	0.63	1.30	2.43	0.10	3.83	34
units/C9	0.06	0.06	0.12	0.24	0.45	0.02	0.72	
mmol/g	0.38	0.29	0.65	1.32	2.39	0.13	3.84	34
units/C9	0.07	0.05	0.12	0.25	0.45	0.02	0.72	
mmol/g	0.35	0.29	0.65	1.29	2.45	0.10	3.84	34
units/C9	0.07	0.05	0.12	0.24	0.46	0.02	0.72	
mmol/g	0.42	0.32	0.66	1.40	2.56	0.12	4.08	34
units/C9	0.08	0.06	0.12	0.26	0.48	0.02	0.76	
mmol/g	0.41	0.34	0.73	1.48	2.67	0.12	4.27	35
units/C9	0.08	0.06	0.14	0.28	0.50	0.02	0.80	
mmol/g	0.39	0.28	0.73	1.40	2.61	0.09	4.10	35
units/C9	0.07	0.05	0.14	0.26	0.49	0.02	0.77	
mmol/g	0.40	0.32	0.62	1.34	2.34	0.09	3.77	35
units/C9	0.07	0.06	0.12	0.25	0.44	0.01	0.70	
mmol/g	0.37	0.31	0.67	1.35	2.45	0.10	3.90	35
units/C9	0.07	0.06	0.13	0.25	0.46	0.02	0.73	
mmol/g	0.36	0.35	0.68	1.39	2.54	0.11	4.04	34
units/C9	0.07	0.07	0.13	0.26	0.47	0.02	0.76	
mmol/g	0.38	0.33	0.76	1.47	2.49	0.10	4.06	36
units/C9	0.07	0.06	0.14	0.27	0.47	0.02	0.76	
mmol/g	0.38	0.31	0.70	1.39	2.50	0.11	4.00	35
units/C9	0.07	0.06	0.13	0.26	0.47	0.02	0.75	

Appendix B.3 Phosphorus-31 NMR Spectroscopy Results for Stability and Relaxation Delay

	Thioacidolysis/^{31}P NMR spectroscopic results for the stability of phosphitylated MWL over time							
	β-5	4-O-5	5-5	Condensed	Guaiacyl	*p*-hydroxy phenyl	Total phenolic	% Condensed
0 hours								
mmol/g	0.38	0.32	0.68	1.37	2.48	0.09	3.94	35
units/C9	0.07	0.06	0.13	0.25	0.47	0.02	0.75	
4 hours								
mmol/g	0.38	0.33	0.70	1.41	2.47	0.13	4.01	35
units/C9	0.07	0.06	0.13	0.26	0.46	0.02	0.75	
8 hours								
mmol/g	0.37	0.31	0.69	1.37	2.50	0.13	4.00	34
units/C9	0.07	0.06	0.13	0.25	0.47	0.02	0.75	
24 hours								
mmol/g	0.39	0.42	0.68	1.49	2.66	0.17	4.32	34
units/C9	0.07	0.08	0.13	0.28	0.50	0.03	0.80	
72 hours								
mmol/g	0.41	0.52	0.72	1.65	2.63	0.21	4.49	37
units/C9	0.08	0.10	0.13	0.31	0.49	0.04	0.84	
2 weeks								
mmol/g	0.46	0.82	0.75	2.03	2.81	0.25	5.09	40
units/C9	0.09	0.15	0.14	0.38	0.53	0.05	0.95	

	Thioacidolysis/^{31}P NMR spectroscopic results for pine MWL spectra collected using different T_1's							
	β-5	4-O-5	5-5	Condensed	Guaiacyl	*p*-hydroxy phenyl	Total phenolic	% Condensed
10 seconds								
mmol/g	0.33	0.28	0.57	1.18	2.22	0.07	3.47	34
units/C9	0.06	0.05	0.11	0.22	0.41	0.01	0.65	
15 seconds								
mmol/g	0.36	0.29	0.63	1.28	2.38	0.09	3.75	34
units/C9	0.07	0.05	0.11	0.23	0.44	0.02	0.69	
20 seconds								
mmol/g	0.38	0.32	0.68	1.37	2.48	0.09	3.94	35
units/C9	0.07	0.06	0.13	0.25	0.47	0.02	0.75	
25 seconds								
mmol/g	0.40	0.31	0.66	1.37	2.50	0.10	3.97	34
units/C9	0.07	0.06	0.12	0.26	0.48	0.02	0.75	
30 seconds								
mmol/g	0.39	0.32	0.68	1.39	2.51	0.09	4.03	35
units/C9	0.07	0.06	0.12	0.27	0.47	0.02	0.75	

Appendix B.4 Phosphorus-31 NMR Spectroscopy Results for Different Extraction Procedures

	Thioacidolysis/^{31}P NMR spectroscopic results for different extraction procedures applied to *Pinus radiata*							
	β-5	4-O-5	5-5	Condensed	Guaiacyl	*p*-hydroxy phenyl	Total phenolic	% Condensed
N-extr								
mmol/g	0.41	0.26	0.62	1.29	2.37	0.06	3.72	35
units/C9	0.07	0.05	0.11	0.23	0.44	0.01	0.70	
CH_2Cl_2								
mmol/g	0.46	0.27	0.66	1.39	2.48	0.09	3.96	35
units/C9	0.09	0.05	0.13	0.25	0.46	0.02	0.74	
C/H/E								
mmol/g	0.48	0.32	0.63	1.43	2.52	0.10	4.05	35
units/C9	0.09	0.06	0.12	0.27	0.47	0.02	0.76	

N-extr = no extraction performed on wood.
CH2Cl2 = Dichloromethane extraction performed on wood.
C/H/E = Sequential extraction with dichloromethane, water and ethanol performed on wood.

	Thioacidolysis/^{31}P NMR spectroscopic results for different extraction procedures applied to Eucalypt					
	Syringyl	Condensed	Guaiacyl	*p*-hydroxy phenyl	Total phenolic	% Condensed
N-extr						
mmol/g	2.10	0.59	0.81	0.05	3.50	27
units/C9	0.45	0.13	0.17	0.01	0.75	
CH_2Cl_2						
mmol/g	2.51	0.56	0.64	0.06	3.71	15
units/C9	0.55	0.13	0.14	0.01	0.80	
C/H/E						
mmol/g	2.53	0.54	0.61	0.05	3.68	14
units/C9	0.53	0.11	0.13	0.01	0.79	

N-extr = no extraction performed on wood.
CH2Cl2 = Dichloromethane extraction performed on wood.
C/H/E = Sequential extraction with dichloromethane, water and ethanol performed on wood.

	Thioacidolysis/^{31}P NMR spectroscopic results for different extraction procedures applied to MDF fibre							
	β-5	4-O-5	5-5	Condensed	Guaiacyl	*p*-hydroxy phenyl	Total phenolic	% Condensed
N-extr								
mmol/g	0.36	0.23	0.71	1.30	2.21	0.06	3.57	36
units/C9	0.07	0.04	0.13	0.24	0.41	0.01	0.67	
CH_2Cl_2								
mmol/g	0.38	0.26	0.70	1.34	2.61	0.07	4.02	34
units/C9	0.07	0.05	0.13	0.25	0.49	0.01	0.75	
C/H/E								
mmol/g	0.39	0.26	0.73	1.38	2.52	0.05	3.95	35
units/C9	0.07	0.05	0.14	0.26	0.47	0.01	0.74	

N-extr = no extraction performed on wood.
CH2Cl2 = Dichloromethane extraction performed on wood.
C/H/E = Sequential extraction with dichloromethane, water and ethanol performed on wood.

Appendix B.5 Phosphorus-31 NMR Spectroscopy Results for Morphological Origin

	Thioacidolysis/^{31}P NMR spectroscopic results for *in situ Pinus radiata* from different morphological origins within a tree							
	β-5	4-O-5	5-5	Condensed	Guaiacyl	*p*-hydroxy phenyl	Total phenolic	% Condensed
Earlywood								
mmol/g	0.41	0.32	0.65	1.38	2.40	0.10	3.88	36
units/C9	0.08	0.06	0.12	0.26	0.45	0.02	0.73	
Latewood								
mmol/g	0.42	0.33	0.62	1.37	2.46	0.11	3.94	35
units/C9	0.08	0.06	0.12	0.26	0.46	0.02	0.74	
Slabwood								
mmol/g	0.39	0.33	0.70	1.42	2.48	0.09	3.99	36
units/C9	0.07	0.06	0.13	0.27	0.46	0.02	0.75	
Corewood								
mmol/g	0.48	0.27	0.64	1.39	2.41	0.12	3.92	36
units/C9	0.09	0.05	0.12	0.26	0.46	0.02	0.73	

Appendix B.6 Phosphorus-31 NMR Spectroscopy Results for Compression Wood

	Thioacidolysis/^{31}P NMR spectroscopic results for *Pinus radiata* EW compression wood							
	β-5	4-O-5	5-5	Condensed	Guaiacyl	*p*-hydroxy phenyl	Total phenolic	% Condensed
MWL								
Free phenolic								
mmol/g				0.38	0.77	0.15	1.30	29
units/C9				0.07	0.14	0.03	0.24	
Total phenolic								
mmol/g	0.47	0.24	0.67	1.38	2.53	0.16	4.07	34
units/C9	0.09	0.04	0.12	0.25	0.46	0.03	0.74	
***in situ* lignin**								
mmol/g	0.46	0.26	0.62	1.34	2.61	0.16	4.11	33
units/C9	0.09	0.04	0.11	0.24	0.48	0.03	0.74	

	Thioacidolysis/^{31}P NMR spectroscopic results for *Pinus radiata* LW compression wood							
	β-5	4-O-5	5-5	Condensed	Guaiacyl	*p*-hydroxy phenyl	Total phenolic	% Condensed
MWL								
Free phenolic								
mmol/g				0.34	0.67	0.28	1.29	26
units/C9				0.06	0.13	0.05	0.24	
Total phenolic								
mmol/g	0.36	0.28	0.67	1.31	2.34	0.33	3.98	33
units/C9	0.07	0.05	0.13	0.25	0.44	0.06	0.69	
***in situ* lignin**								
mmol/g	0.39	0.26	0.62	1.27	2.27	0.34	3.88	32
units/C9	0.07	0.05	0.11	0.22	0.40	0.06	0.68	

Appendix B.7 Phosphorus-31 NMR Spectroscopy Results for Spruce

	Thioacidolysis/^{31}P NMR spectroscopic results for *Picea abies*							
	β-5	4-O-5	5-5	Condensed	Guaiacyl	*p*-hydroxy phenyl	Total phenolic	% Condensed
MWL								
Free phenolic								
mmol/g				0.66	1.18	0.11	1.95	34
units/C9				0.12	0.22	0.02	0.36	
Total phenolic								
mmol/g	0.43	0.32	0.71	1.47	2.68	0.12	4.27	34
units/C9	0.08	0.06	0.13	0.27	0.50	0.02	0.80	
***in situ* lignin**								
mmol/g	0.41	0.30	0.70	1.41	2.58	0.09	4.08	35
units/C9	0.08	0.06	0.13	0.26	0.48	0.02	0.76	

Appendix B.8 Phosphorus-31 NMR Spectroscopy Results for Eucalypt

	Thioacidolysis/^{31}P NMR spectroscopic results for a commercial Eucalypt					
	Syringyl	Condensed	Guaiacyl	*p*-hydroxy phenyl	Total phenolic	% Condensed
MWL						
Free phenolic						
mmol/g	0.44	0.20	0.51	0.04	1.19	17
units/C9	0.09	0.04	0.11	0.01	0.25	
Total phenolic						
mmol/g	2.25	0.69	0.86	0.04	3.84	18
units/C9	0.47	0.15	0.18	0.01	0.80	
***in situ* lignin**						
mmol/g	2.13	0.77	0.96	0.05	3.91	20
units/C9	0.45	0.16	0.20	0.01	0.83	

Appendix B.9 Phosphorus-31 NMR Spectroscopy Results for Mechanical Pulps

	Thioacidolysis/^{31}P NMR spectroscopic results for mechanical pulps							
	β-5	4-O-5	5-5	Condensed	Guaiacyl	*p*-hydroxy phenyl	Total phenolic	% Condensed
MDF								
mmol/g	0.38	0.26	0.70	1.34	2.61	0.09	4.04	0.33
units/C9	0.07	0.05	0.13	0.25	0.49	0.02	0.76	
TMP								
mmol/g	0.44	0.30	0.75	1.49	2.74	0.06	4.29	0.34
units/C9	0.08	0.06	0.14	0.28	0.51	0.01	0.80	
CTMP								
mmol/g	0.38	0.27	0.79	1.44	2.32	0.13	4.13	0.38
units/C9	0.08	0.06	0.17	0.27	0.43	0.02	0.69	
DWS								
mmol/g	0.37	0.23	0.78	1.38	2.29	0.09	3.69	0.38
units/C9	0.07	0.05	0.16	0.26	0.43	0.02	0.68	
OPCO								
mmol/g				0.45	0.58		1.03	
units/C9				0.08	0.11		0.19	

	Thioacidolysis/^{31}P NMR spectroscopic results for fibres and fines from DWS							
	β-5	4-O-5	5-5	Condensed	Guaiacyl	*p*-hydroxy phenyl	Total phenolic	% Condensed
1° pulp								
mmol/g	0.37	0.25	0.76	1.37	2.29	0.13	3.79	37
units/C9	0.07	0.05	0.14	0.25	0.43	0.02	0.70	
1° fines								
mmol/g	0.43	0.29	0.69	1.41	2.20	0.07	3.66	39
units/C9	0.08	0.05	0.13	0.26	0.40	0.01	0.68	
2° fines								
mmol/g	0.41	0.25	0.76	1.42	2.25	0.09	3.76	38
units/C9	0.08	0.05	0.14	0.26	0.42	0.02	0.70	
1° fibres								
mmol/g	0.35	0.32	0.72	1.39	2.45	0.06	3.90	36
units/C9	0.07	0.06	0.13	0.26	0.45	0.01	0.72	
2° fibres								
mmol/g	0.36	0.33	0.72	1.41	2.42	0.08	3.91	36
units/C9	0.07	0.06	0.13	0.26	0.45	0.01	0.73	

Appendix B.10 Phosphorus-31 NMR Spectroscopy Results for Kraft Pulps

	Thioacidolysis/^{31}P NMR spectroscopic results for Indulin kraft lignin							
	β-5	4-O-5	5-5	Condensed	Guaiacyl	*p*-hydroxy phenyl	Total phenolic	% Condensed
Free phenolic								
mmol/g	0.34	0.39	0.52	1.25	1.45	0.16	2.86	44
units/C9	0.06	0.07	0.09	0.22	0.25	0.03	0.49	
Total phenolic								
mmol/g	0.41	0.38	0.64	1.44	2.06	0.17	3.67	0.39
units/C9	0.07	0.07	0.11	0.25	0.35	0.03	0.63	

	^{31}P NMR spectroscopic results for extent of kraft pulping							
	β-5	4-O-5	5-5	Condensed	Guaiacyl	*p*-hydroxy phenyl	Total phenolic	% Condensed
A								
mmol/g				1.25	1.95	-	3.20	39
units/C9				0.21	0.35	-	0.57	
B								
mmol/g				1.73	2.16	-	3.89	44
units/C9				0.31	0.38	-	0.69	
C								
mmol/g				2.02	2.28	-	4.30	47
units/C9				0.34	0.38	-	0.76	

	Thioacidolysis/^{31}P NMR spectroscopy for extent of kraft pulping							
	β-5	4-O-5	5-5	Condensed	Guaiacyl	*p*-hydroxy phenyl	Total phenolic	% Condensed
A								
mmol/g				1.28	2.79	-	4.07	31
units/C9				0.21	0.50	-	0.72	
B								
mmol/g				1.79	2.58	-	4.37	41
units/C9				0.30	0.45	-	0.73	
C								
mmol/g				1.54	1.89	-	3.44	45
units/C9				0.27	0.34	-	0.59	

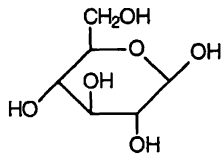

1

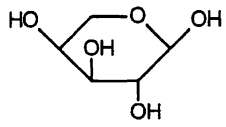

2

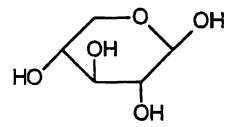

3

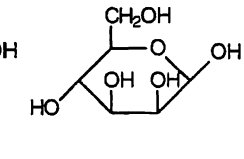

4

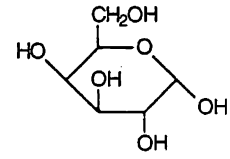

5

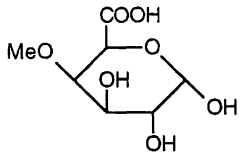

6

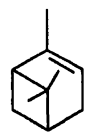

7

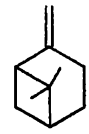

8

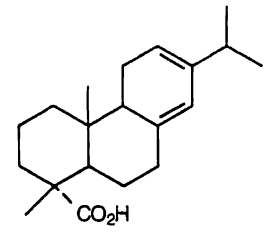

9

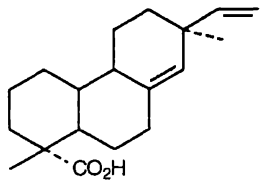

10

CH_3-$(CH_2)_7$-CH=CH-$(CH_2)_7$-CO_2H

11

CH_3-$(CH_2)_7$-CH=CH-CH_2-CH=CH-$(CH_2)_4$-CO_2H

12

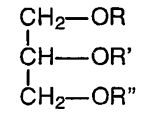

13

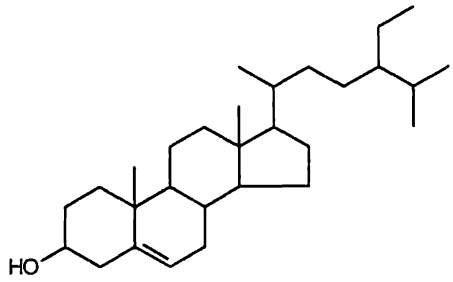

14

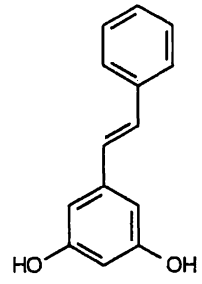

15

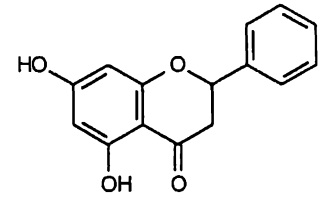

16

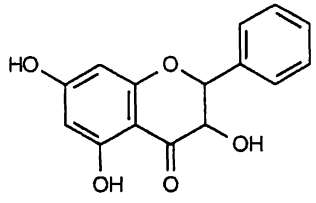

17

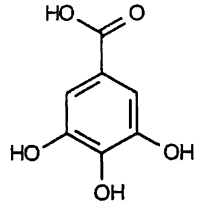

18

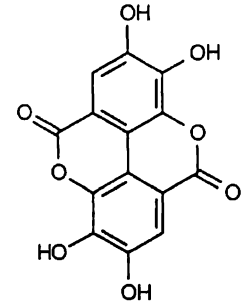

19

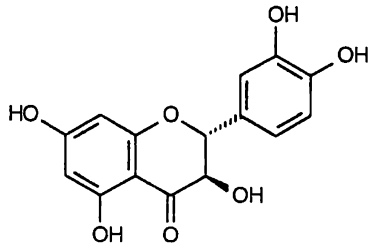

20

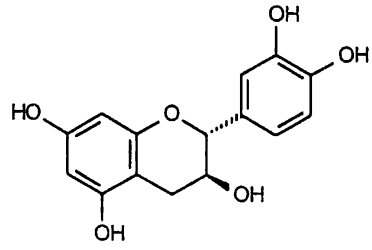

21

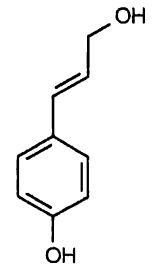

22

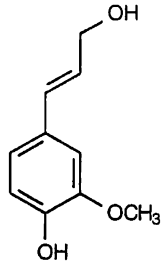

23

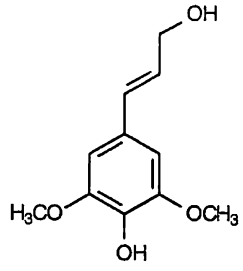

24

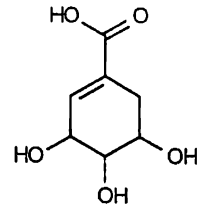

25

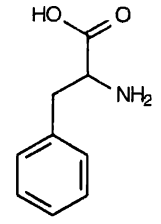

26

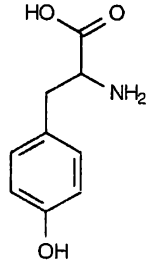

27

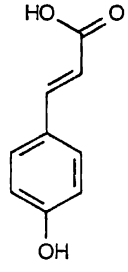

28

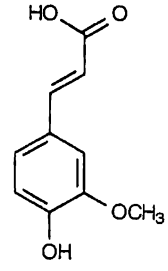

29

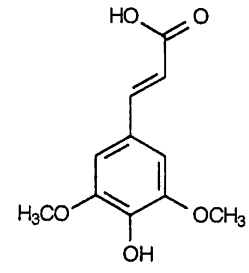

30

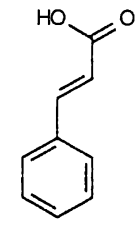

31

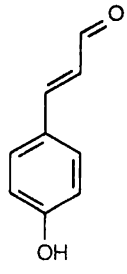

32

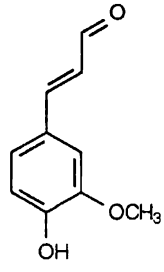

33

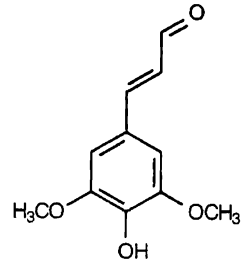

34

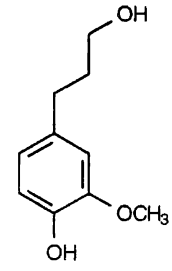

35

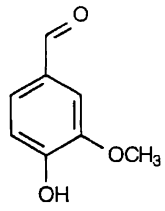

36

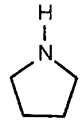

37

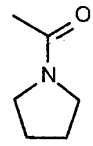

38

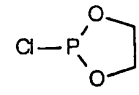

39

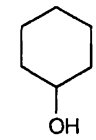

40

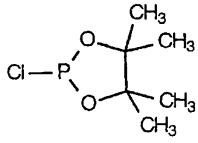

41

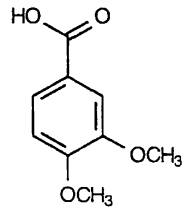

42

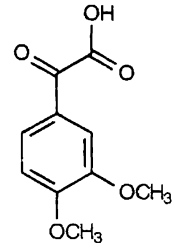

43

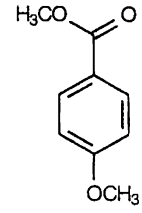

44

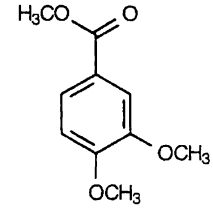

45

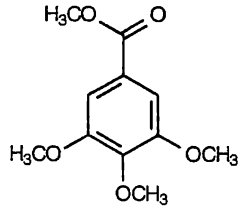

46

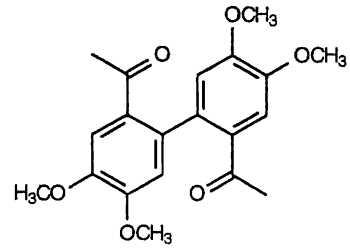

47

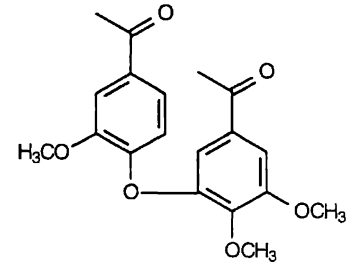

48

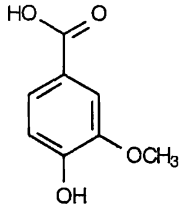

49

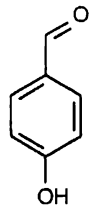

50

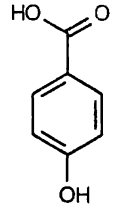

51

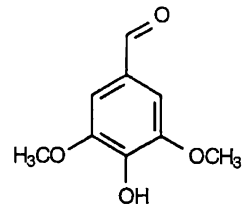

52

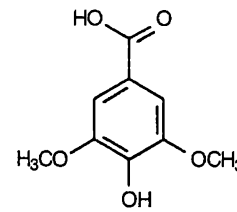

53

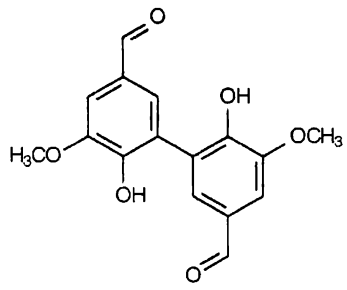

54

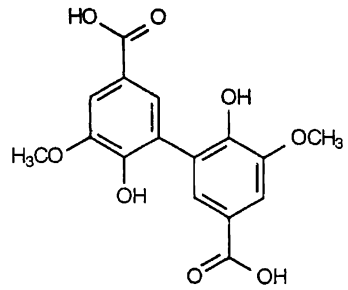

55

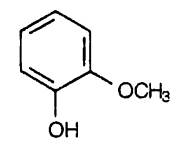

56

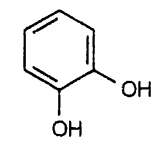

57

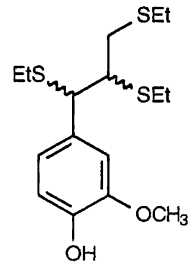

58

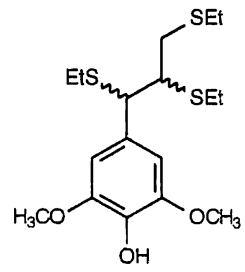

59

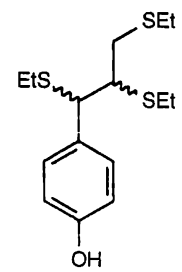

60

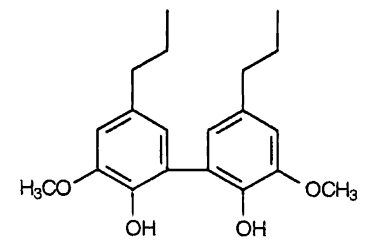

61

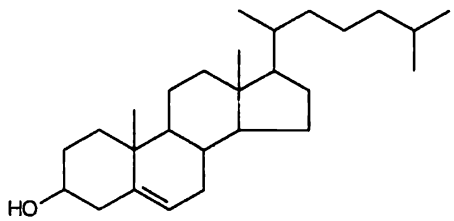

62

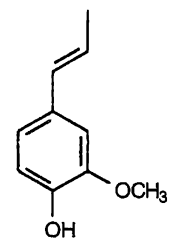

63

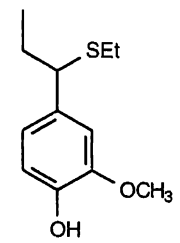

64

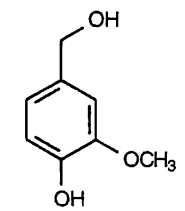

65

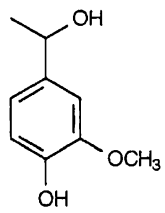

66

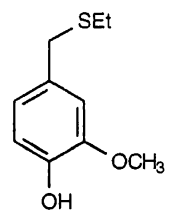

67

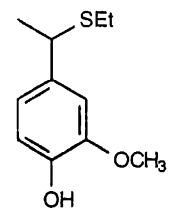

68

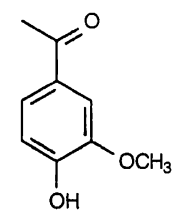

69

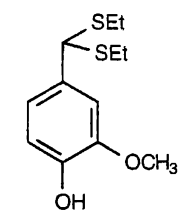

70

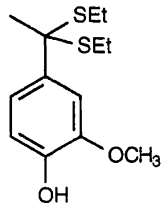

71

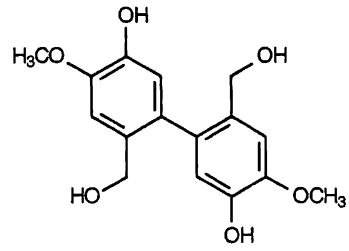

72

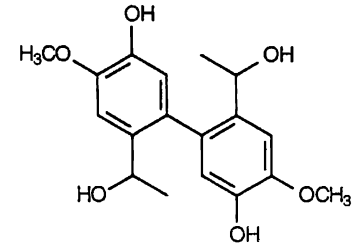

73

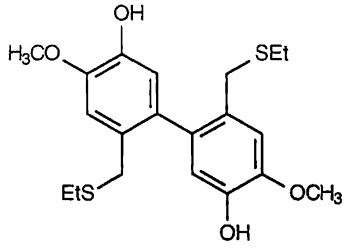

74

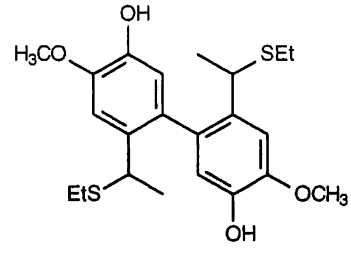

75

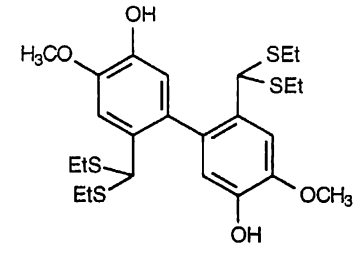

76

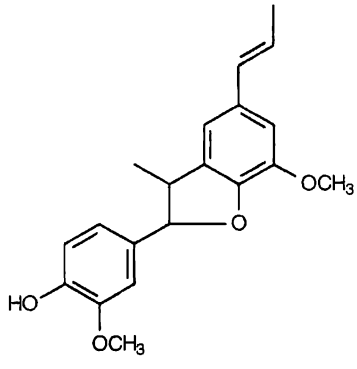

77

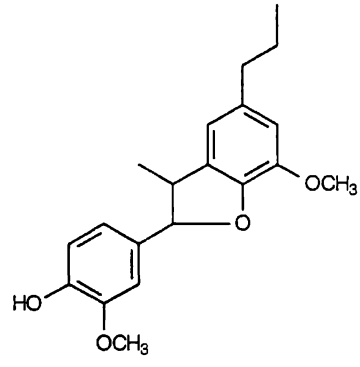

78

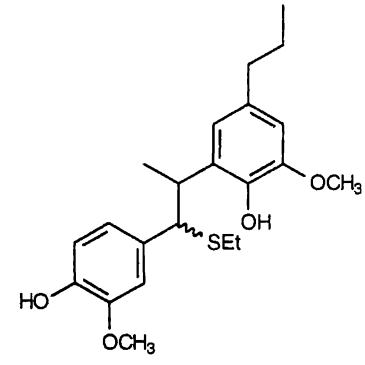

79

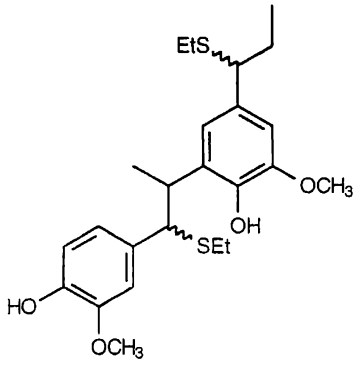

80

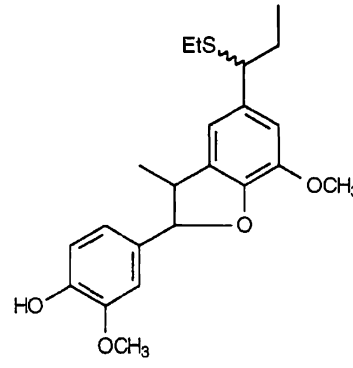

81

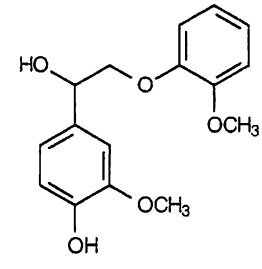

82

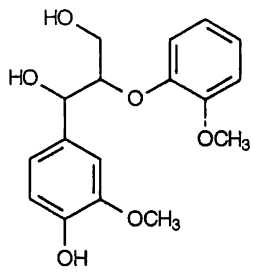

83

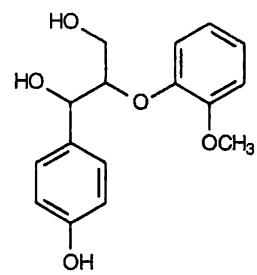

84

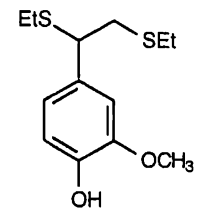

85

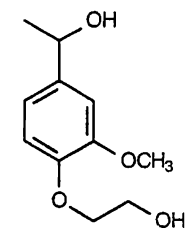

86

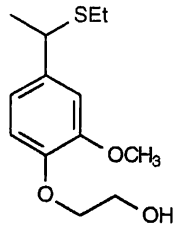

87

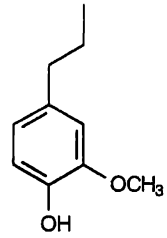

88

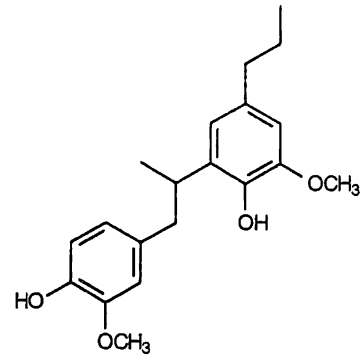

89

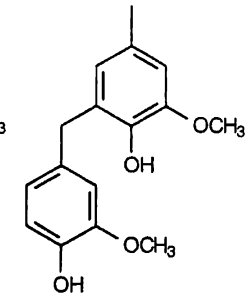

90

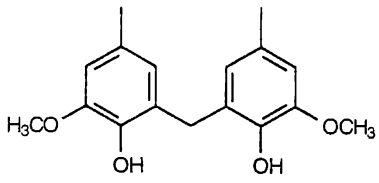

91

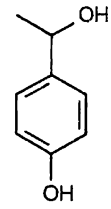

92

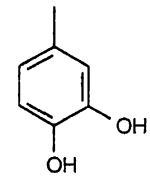

93

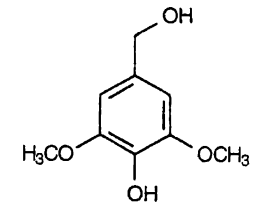

94

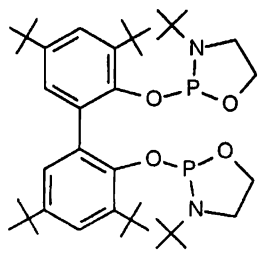

95

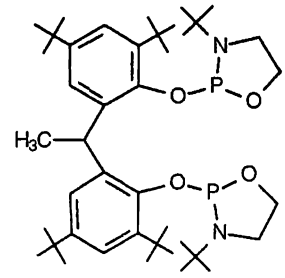

96

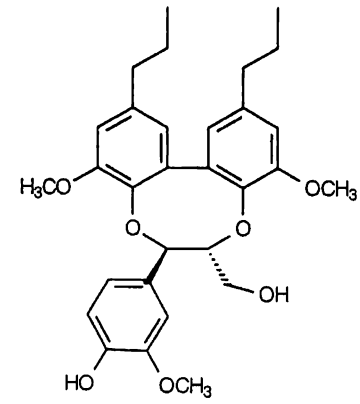

97

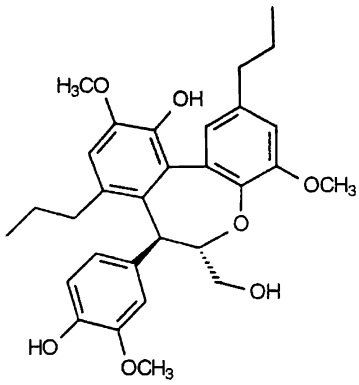

98

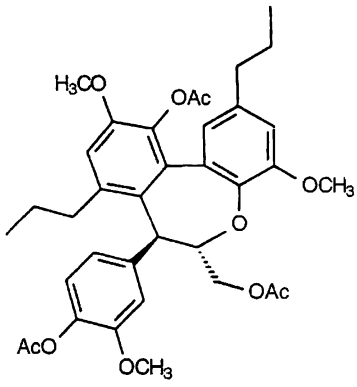

99

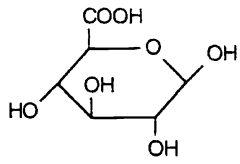

100

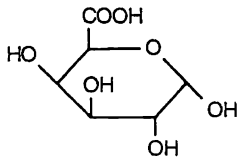

101

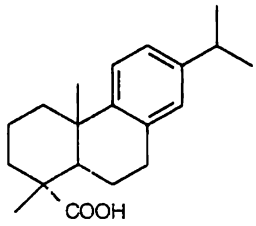

102

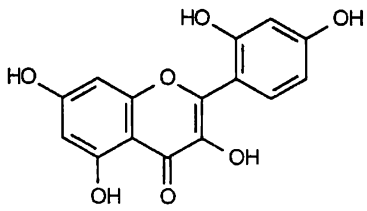

103

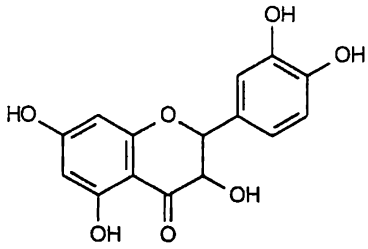

104

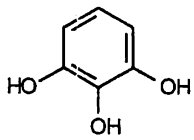

105

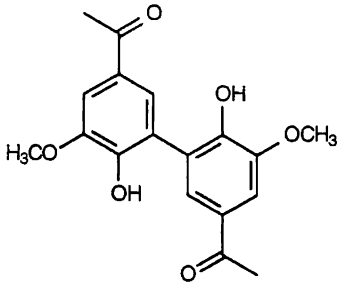

106

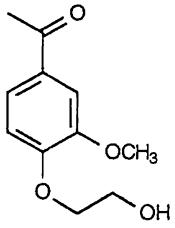

107

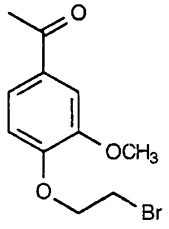

108